UNIVERSITEIT GENT

FACULTY OF SCIENCES

Department Biology
Research unit Protistology and Aquatic ecology

Diversity and dynamics of protist communities in subtidal North Sea sediments in relation to metal pollution and algal bloom deposition

Annelies Pede

Promotor: Prof. Dr. Koen Sabbe

Thesis submitted in partial fulfillment of the requirements for the degree of Doctor (Ph.D.) in Science (Biology)

Academic year 2011-2012

Belgian Federal Science Policy

PROTISTOLOGY AQUATIC ECOLOGY

MICROMET

Members of the examination and reading committee

Prof. Dr. Dominique Adriaens (chairman)
Department of Biology, Ghent University

Prof. Dr. Koen Sabbe (promotor)
Department of Biology, Ghent University

Prof. Markus Weitere (reading committee)
Helmholtz-Zentrum für Umweltforschung (UFZ), Magdeburg, Germany

Prof. Dr. David C. Gillan (reading committee)
Proteomics and Microbiology Lab, Université de Mons

Dr. Jan Vanaverbeke (reading committee)
Department of Biology, Ghent University

Prof. Dr. Wim Vyverman
Department of Biology, Ghent University

Dr. Julie Baré
Department of Veterinary Public Health and Food Safety, Ghent University

CONTENTS

Problem statement, aims and outline

The pollution of marine ecosystems by trace metals is a world-wide problem (Boran & Altinok, 2010). Trace metals (TM) are toxic for many life forms, including humans (a.o. via fisheries). In coastal environments, TM are mainly bound in silty, organically enriched sediments, and changes in the environment can lead to the resuspension of the metals (Eggleton & Thomas, 2004), with the activity of the benthic microbes as one potential factor influencing the release of TM into the water column (Eggleton & Thomas, 2004). Benthic microbial activity and dynamics in turn are regulated by the availability of growth substrates, and sedimentation of algal blooms represents a major source of organic material for the benthic biota in subtidal areas (Boon, *et al.*, 1999). It remains unclear however, how microbial communities, phytodetritus deposition and TM behaviour interact in subtidal sediments.

The overall objective of this thesis is to obtain a better insight in the interactions between microbial communities, metal contaminants and algae-derived organic matter in contaminated marine sediments in the Belgian Coastal Zone (BCZ). The thesis was carried out in the framework of the MICROMET project (**Micro**bial diversity and **Met**al fluxes in contaminated North Sea sediments), supported by funding from the Belgian Federal Science Policy Office (SD/NS/04A & 04B), in the frame of the SDD programme (the 'Biodiversity' & 'Marine Ecosystem' domains). While our project partners focused on prokaryotic communities and sediment biogeochemistry, we focused on the dynamics, role and response of benthic protist communities in the above-mentioned interactions. Protists are eukaryotic unicellular organisms who occupy a central position in benthic food webs, and especially in the microbial loop. We first described the spatial and temporal variation of these communities in relation to the abiotic and biotic subtidal benthic environment (including TM). We then documented how the microbial communities (both pro- and eukaryotic) respond to algal bloom deposition, and how this affects TM mobilization. Finally, we tested the direct effect of high concentrations of the toxic TM arsenic (As) on the protist communities.

This research was performed in two phases:

The first phase of this thesis was based on field observations. We studied the diversity and spatio-temporal variation in benthic protist communities in the BCZ using 18S rDNA-based molecular fingerprinting techniques (DGGE) and clone libraries, and then identified the factors potentially regulating their dynamics using multivariate statistics. In **Chapter 2,**

microeukaryotic community composition was compared between the oxygenated top layer and anoxic bottom layer of sediments from 9 BCZ stations with different granulometries and TM loads, before and after the spring phytoplankton bloom in 2007. In **Chapter 3,** we present a more detailed, monthly analysis of protist community variation with depth (0-10 cm) in one silty, metal-contaminated station, for the period February to July 2008.

The second part of this thesis deals with two separate microcosm experiments in which sediment cores were incubated under various environmental conditions, viz. with and without phytodetritus deposition, and at a range of As concentrations. This not only allowed giving a more detailed picture about the direct response of benthic microbial communities to organic matter enrichment and metal contamination, but also to assess the potential role of microbial communities to metal mobilization. We studied both total and active communities based on SSU rDNA and SSU rRNA respectively. In **Chapter 4** and **Chapter 5**, we performed a microcosm experiment in which the deposition of a phytoplankton bloom was simulated in metal-contaminated sediment cores. Total and active prokaryotic and microeukaryotic communities were studied simultaneously during 7 days, and related to TM dynamics during increased phytodetritus mineralization. The response of microbial activity and community composition are discussed with respect to the microbial loop, the enrichment effect and the metal fluxes. **Chapter 6** focuses on the acute effect of As intoxication after two days of incubation of sediments contaminated with a series of arsenic levels (control, 60, 120, 240, 480 and 960µg L^{-1}). The response of the active protist community was evaluated and compared between two stations with a different granulometry and contamination history: one station with silty sediments and high background As concentrations, and the other station with sandy sediments and low background As concentration.

The main conclusions are summarized and discussed in **Chapter 7**, and perspectives for future research are provided.

All the chapters excluding the introduction (chapter 1), discussion (chapter 7) and summary are manuscripts in preparation. The first author analysed the protist samples and data and wrote the chapters, except when stated otherwise.

1

General Introduction

In this introduction, I first give a description of coastal subtidal marine sediments (biogeochemistry and biota, with special attention to benthic protist communities), then I give an introduction to trace metal (TM) toxicity and factors affecting the release and bioavailability in marine sediments (with emphasis on microbial activity), and finally the study area, i.e. the Belgian Coastal Zone (BCZ) is described in terms of the sediment environment, phytoplankton blooms and TM pollution.

Marine subtidal sediments

Marine subtidal sediments are important as a permanent or temporary (e.g. resting stages; McQuoid, 2002) habitat for many benthic and planktonic organisms. Biogeochemical processes in marine sediments are strongly linked to processes and conditions in the water column (Middelburg & Levin, 2009). Marine coastal areas are often highly productive, which causes high fluxes of organic matter (OM) to the sediment (Boon, *et al.*, 1998). Intense mineralization of this OM takes place in the sediments; as a result, a large part of the coastal carbon and nutrient cycles can take place in the benthic ecosystems (Patterson, *et al.*, 1989, Ehrenhauss, *et al.*, 2004, Lancelot, *et al.*, 2005), making marine subtidal sediments crucial for global biogeochemical cycling (Orcutt, *et al.*, 2011).

Sediment types (sandy vs. silty)

Many coastal areas are characterised by sediments with different grain size composition, mainly resulting from local hydrodynamic conditions. Fine sediments are mainly found in more sheltered sites, since small particles are readily maintained in suspension by turbulence (Fenchel, 1969). The size of the particles influences the porosity, permeability, and capillarity of the sediment. These factors (especially permeability) are important because they determine the behaviour of the interstitial water and thus the availability of oxygen (Fenchel, 1969). Bottom-water oxygen availability is one the main factors governing diagenetic pathways, sediment biogeochemistry and mineralization rates, and sediment-water exchange fluxes, as

well as the biotic communities that influence these processes (Ehrenhauss, *et al.*, 2004, Fenchel & Finlay, 2008, Glud, 2008). Sandy sediments are permeable and permit porewater flows that transport oxygen, as well as dissolved and suspended matter through the interstitial space (Huettel, *et al.*, 1998). As such, sandy sediments are highly oxygenated, rapid OM degradation takes place and no pronounced biogeochemical profiles are established (Ehrenhauss & Huettel, 2004, Ehrenhauss, *et al.*, 2004, Vanaverbeke, *et al.*, 2004). In silty sediments, the interstitial spaces surrounding larger particles are filled by smaller particles. Advection of water is reduced, and the flux of dissolved O_2 into the sediment and CO_2 out of the sediments is restricted. Moreover, the oxygen that diffuses into the sediments is rapidly mineralized by aerobic bacteria and micro- and meiofauna, and as a result silty sediments become anoxic within the first millimeters below the sediment-water interface (Middelburg & Levin, 2009). Anaerobic mineralization dominates in most coastal sediments because of high carbon loading, creating oxygen demands that are not balanced by oxygen supply (Middelburg & Levin, 2009, and references herein). The final non-degraded fraction will be accumulated and preserved under hypoxic and anoxic conditions (Moodley, *et al.*, 2005), and fine grained sediments can have high organic matter contents (Middelburg & Levin, 2009).

Biogeochemistry and redox cycle in anoxic sediments

Anaerobic degradation and related reduction-oxidation reactions in the sediment take place via a complex biogeochemical cascade, as shown in figure 1; a detailed review of sediment biogeochemistry in coastal anoxic sediments is presented by Middelburg & Levin (2009). Briefly, OM deposition from the water column provides energy and matter for heterotrophic consumers inhabiting the sediments. The OM is assimilated by a diverse community of heterotrophic organisms or respired and mineralized in the oxygenated upper sediment layers. As a consequence of high oxygen consumption rates and slow transport of oxygen in silty sediments, oxygen penetration is very limited. This initiates a cascade of alternative electron acceptor use by anaerobic organisms. Following oxygen depletion, anaerobic respiration is sequentially based on nitrate, manganese and iron (hydr)oxides, and sulphates. Dissolved reduced products (ammonium, manganese (II), iron (II) and sulphides) diffuse upwards but are normally efficiently re-oxidized within the sediments. If all oxidants have been consumed, organic matter is anaerobically respired and fermented with the result that methane is generated.

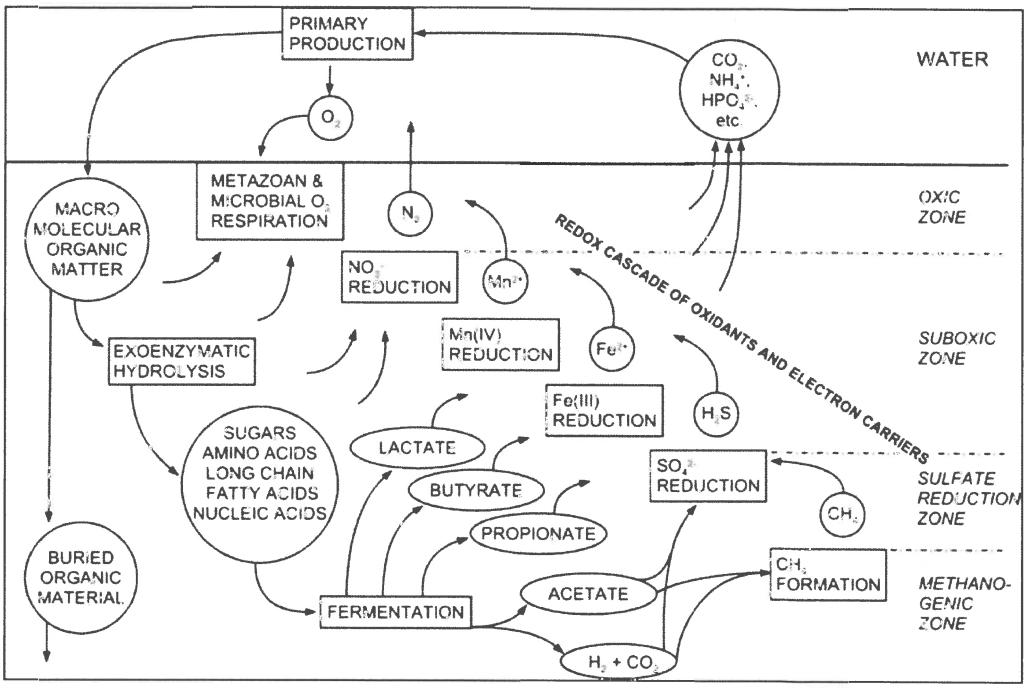

Figure 1: Conceptual model of organic matter (OM) degradation pathways and re-oxidation pathways in marine sediments. Organic matter degradation involves hydrolysis of macromolecular organic matter and fermentation to smaller compounds (from Jørgensen, *et al.*, 2006)

Dependent on sediment depth, different organisms are involved in these degradation processes (Jørgensen, *et al.*, 2006, Middelburg & Levin, 2009). The aerobic food chain consists of organisms of very diverse feeding biology and size. Particulate detritus can be consumed by metazoans, and small organic molecules taken up by aerobic bacteria in the oxic zone may be further fully mineralized through aerobic respiration. Anaerobic respiration is primarily performed by prokaryotic organisms that have a high diversity of metabolic types and use terminal electron acceptors other than oxygen. There are methane-, nitrate, sulphate- and metaloxide reducers that can respire a wide range of monomeric organic substances. It is generally found that oxygen and sulphate play the major role in shelf sediments, where 25-50% of the organic carbon may be mineralized anaerobically by sulphate-reducing bacteria (Jørgensen, 1982).

Various physical, biological and chemical disturbances of sediments can lead to changes in their biogeochemistry. Natural events like storms but also anthropogenic activities, including dredging in coastal areas for example can cause periodical remobilisation of surface

sediments by exposing anoxic sediments to oxic conditions (Glud, 2008). Moreover, biological processes such as bio-irrigation (active or passive burrow flushing as well as pumping to fluidize sediments to facilitate peristaltic burrowing) and bioturbation (sediment reworking by burrowing animals) can results in the enhanced transport of oxygen to deeper anoxic sediments and enhance the rates of aerobic respiration (Meysman, *et al.*, 2008, Braeckman, *et al.*, 2011b). Chemical disturbance can result from contamination of the sediment by organic and/or metal pollutants which can affect the composition and activity of benthic communities.

Sediment biota

Marine benthic organisms play a critical role in the coastal environment due to their role in coastal biogeochemistry (cf. above) and biological interactions with the pelagic food web (by grazing and predation) (Manini, *et al.*, 2003, Meysman, *et al.*, 2006, van Nugteren, *et al.*, 2009, Braeckman, *et al.*, 2011b). Communities inhabiting subtidal marine sediments are composed of complex and highly diverse assemblages of prokaryotic and eukaryotic organisms, often in very high densities (Fenchel, 1969, Tian, *et al.*, 2009, Chariton, *et al.*, 2010, First & Hollibaugh, 2010). Protists (unicellular eukaryotes), together with bacteria, archaea and viruses are the primary drivers of the production, utilization and degradation of most organic matter and the cycling of many elements in these environments (Caron, 2009). Microphytobenthos can be responsible for a significant portion of total primary production and support secondary production in shallow sediments, depending on the turbidity of the overlying water column (Forehead & Thompson, 2010). Prokaryotes are the main mineralisers in the sediments and import carbon, including from sedimented material from the water column, to the benthic food web and as such form an important trophic link between the plankton and the benthos (Kathol, *et al.*, 2011). Protozoa are important grazers on bacteria (Patterson, *et al.*, 1989, Hondeveld, *et al.*, 1995, Epstein, 1997), and by grazing and excretion, release and promote recycling of nutrients essential for the growth of autotrophs (Patterson, *et al.*, 1989). They are also grazed upon by other protozoans and metazoans and as such form a crucial component of the benthic microbial loop (Patterson, *et al.*, 1989). Meio- and macrobenthos are important consumers of protozoans, bacteria and algae (Fenchel, 1969, Vanaverbeke, *et al.*, 2004, Franco, *et al.*, 2008, Caron, 2009) and play a crucial role in sediment biogeochemistry by bioturbation and bio-irrigation (Braeckman, *et al.*, 2011a). Fungi often represent an important fraction of the communities, especially in oxygen-depleted

environments (Stoeck & Epstein, 2003, Luo, *et al.*, 2005, Takishita, *et al.*, 2007, Edgcomb, *et al.*), and play an important role as saprobes and symbionts, but also as pathogens of algae and animals (Kohlmeyer, 1979).

Protists

Protists are unicellular microeukaryotic organisms, having representatives in many different groups in the eukaryotic tree of life (Fig. 2), and form an important component of subtidal benthic ecosystems (e.g. Fenchel, 1969, Patterson, *et al.*, 1989). Many autotrophic protists (= microalgae) can be found in dark sediments (e.g. Shimeta, *et al.*, 2007, Pawlowski, *et al.*, 2011a). They represent deposited, dying individuals or are part of the so called "passive diversity" in the form of viable resting spores (e.g. cyst) or cells (McQuoid, 2002, Veuger & van Oevelen, 2011). Protozoan communities (= heterotrophic protists) are often very diverse in marine sediments, mainly consisting of Alveolata (Ciliata and Dinophyta), Rhizaria (Cercozoa, Acantharea and Foraminifera), Amoebozoa, Euglenozoa and several heterotrophic stramenopiles (Patterson, *et al.*, 1989). Protozoa can be bacterivores and/or algivores but also carnivores, and complex trophic interactions occur; some ciliates have been shown to be consumers of flagellates and smaller ciliates, and flagellates are able to feed on other flagellates (Fenchel, 1969, Sherr & Sherr, 2002). Moreover, previous studies have shown that the decomposition of particulate detritus is accelerated in the presence of protozoan grazers (Taylor, *et al.*, 1985, Sherr & Sherr, 2002).

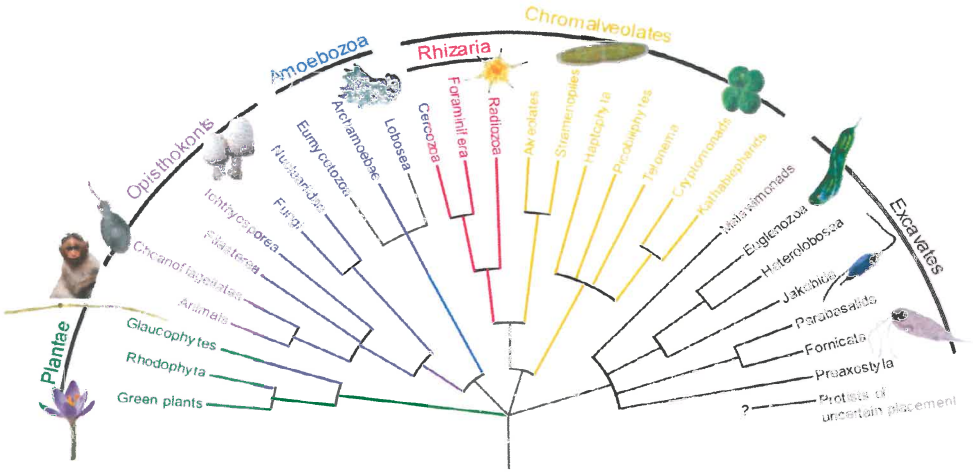

Fig. 2: Eukaryotic tree of life (from Stoeck & Stock, 2010). Protists have representatives in all major evolutionary lineages with the exception of plants and animals. Most lineages are composed entirely of protists.

Our current knowledge of the structure and functioning of protist communities in marine sediments is relatively incomplete, mainly because their identification and quantification is problematic . Traditionally, species were identified on the basis of microscopy, which is time-consuming and difficult due to the general lack of distinct morphological features in smaller cells (e.g. heterotrophic nanoflagellates) or specific groups (e.g. amoebae), and the presence of sediment and/or organic particulate material. Most quantitative studies on benthic protists focused on larger protozoa such as ciliates and large dinoflagellates, since these cells are most conspicuous. Since the development of suitable techniques for efficient extraction of microbes from sediments however (e.g. based on density gradient centrifugation), protistan diversity has become a more active research area. However, major progress in on our knowledge of the diversity and composition of protistan communities has only been made since the advent of molecular technologies (see Epstein & Lopez-Garcia, 2008). These techniques allowed detecting formerly undetected and/or unknown protist up to the highest taxonomic levels in the eukaryotic tree of life (Dawson & Pace, 2002), and uncovered an unexpectedly high richness of protists in even the most extreme habitats surveyed to date (Epstein & Lopez-Garcia, 2008). However, the actual biodiversity in most marine benthic environments is still largely unknown and studies in these habitats are relatively infrequent compared with studies of planktonic communities (e.g. Alexander, *et al.*, 2009, Behnke, *et al.*, 2010). So far, benthic marine environmental studies of protists focused on salt marsh (Stoeck & Epstein, 2003, First & Hollibaugh, 2010), tidal flat (Dawson & Pace, 2002, Hamels, *et al.*, 2004, Wilms, *et al.*, 2006), and subtidal sediments (Garstecki, *et al.*, 2000, Shimeta, *et al.*, 2003, Shimeta, *et al.*, 2007, Park, *et al.*, 2008, Coolen & Shtereva, 2009), including the abyssal sea floor, (Scheckenbach, *et al.*, 2010, Pawlowski, *et al.*, 2011a) and more extreme environments such as hydrothermal vents and cold seeps (Edgcomb, *et al.*, 2002, Lopez-Garcia, *et al.*, 2003, Takishita, *et al.*, 2005, Takishita, *et al.*, 2010) and hyperhaline anoxic basins (Edgcomb, *et al.*, 2009). The most important groups observed in all these environments include Alveolates (mainly ciliates and dinoflagellates), Stramenopila (phototrophic and heterotrophic), Cercozoa, Euglenozoa and Amoeba, but the ratios of different phylogenetic groups differ significantly between these different sites. For an extensive review about the different protistan groups detected in these various environments, see Epstein & Lopez-Garcia (2008).

Light penetration, flow regime, salinity and sediment characteristics (grain size, oxygen content, sulphide levels, pH, Eh, etc.) have been identified as important factors underlying spatial heterogeneity (Fenchel, 1969, Fernandez-Leborans, 2000, Shimeta, *et al.*, 2007,

Fenchel & Finlay, 2008). Protozoans also can show pronounced vertical zonation along the redox gradient (Fenchel & Finlay, 2008).

Trace metals

Trace metals are metals that occur in very small amounts, almost at the molecular level, and that reside or are present in animal and plant cells and tissue (Phipps, 1981). Many TM such as Co, Cu, Cr, Fe, As, Ni and Zn are required and essential nutrients, and play an integral role in the life processes of organisms. Others have no biological role (Al, Cd, Au, Pb and Ag) and are nonessential. Essential trace metals play an important role in regulating gene expression and the activity of biomolecules, often as part of enzymes or cofactors for critical biochemical reactions (Reilly, 2004). In high concentrations however, TM have the potential to become toxic, e.g. Fe, Mg, Zn, Cu, Cr, Ni, Co, V, As, Mo and Se.

Metal sources and accumulation in marine sediments

Trace metals are one of the most important pollutants in natural environments due to their toxicity, persistence and bioaccumulation (Graf, 1992, Chapman, *et al.*, 1998, Middelburg & Levin, 2009). Trace metals are natural constituents of the Earth crust, and are transported along the ecosphere. TM are released from natural as well as anthropogenic sources (Forstner & Wittmann, 1979). Natural emissions include geological sources such as weathering, erosion and volcanic activity. Anthropogenic emissions include point sources such as power plants, metal production facilities, incinerations, and other industrial processes. Especially aquatic environments are vulnerable to the latter source of pollution. TM are released to the aquatic system through discharges including industrial and domestic effluents, urban storm water runoff, landfill leaching, ship traffic, as also through atmospheric deposition (Forstner & Wittmann, 1979, Forstner, 1993, Spokes & Jickells, 1995). Emissions from anthropogenic sources often exceed the flux from natural sources for most metals and pollution by trace metals has gradually become a major concern worldwide. Investigations into metallic contaminants have increased considerably in recent years, due to the growing concern relating to human activities and aquatic environmental quality (Eggleton & Thomas, 2004). As a consequence of their low solubility in seawater and their high persistence, metals are generally deposited in the sediments (complexed by organic matter) and accumulation appears over time. Especially fine-grained sediments tend to accumulate contaminants due to their

sorptive nature, and thus act as an important metal reservoir (Petersen, *et al.*, 1997, Li, *et al.*, 2000a). Variations in the physical and biogeochemical characteristics of the sediment may induce the release of metals back into the water, making sediments important potential sources of TM (Petersen, *et al.*, 1997, Li, *et al.*, 2000a, Eggleton & Thomas, 2004).

Metal speciation and bioavailability

Speciation is of great importance in determining metal behaviour in the environment, its bioavailability, toxicity and remobilization potential (Rivaro, *et al.*, 2011). Within these benthic systems, metals are in dynamic equilibrium, partitioned between dissolved (porewater, overlying water) and solid phase (sediment, suspended particulate matter and biota) (Calmano, *et al.*, 1993, Forstner, 1993). The soluble phase represents the principal source of bioavailable metals (Chapman, *et al.*, 1998). The major pathways of metal partitioning include adsorption-desorption, complexation-redissolution, precipitation-dissolution and biological uptake-organic matter degradation (Forstner, 1993, Baeyens, *et al.*, 1998a, Chapman, *et al.*, 1998, Burton, 2010). Adsorption and desorption are usually the predominant processes because metals have strong affinities for iron and manganese oxyhydroxides, particulate organic matter, and to a lesser extent clay minerals. Reversely, desorption of trace metals occurs when iron and manganese oxyhydroxides are reduced due to changes in redox conditions. TM can complex with ligands or colloids, after which free trace metal ions or small metal particles can grow to become part of the suspended particulate matter, or they can settle on the sediment. Like adsorption-desorption, complexation-redissolution is influenced by chemical composition of aquatic system, such as pH, redox, salinity and so on (Eggleton & Thomas, 2004). Other chemical processes, such as sulphide precipitation with iron, copper and cadmium as a result of high sulphate reducing bacteria activities and calciumcarbonate precipitation as a result of high algal production are important (Braissant, *et al.*, 2007, see also Gao, 2009). As already mentioned, TM are micronutrients and as such are essential for life, so they are taken up by plankton and, inversely, released from the degradation of organic matter. The above biogeochemical processes are not isolated from each other and metals can be transformed from a none or less-toxic form into a very toxic form or vice versa (Forstner, 1993, Baeyens, *et al.*, 1998a, Chapman, *et al.*, 1998). Natural and anthropogenic processes have the capacity to disturb the above-mentioned equilibriums, which can lead to resuspension of the solid phase-metals and the release of dissolved metals from sediment to the water column (upward metal fluxes) (Calmano, *et al.*,

1993, Chapman, *et al.*, 1998, Eggleton & Thomas, 2004). As mentioned before, the benthic environment is a highly dynamic system, characterized by rapidly changing physico-chemical conditions, and factors that influence the general biogeochemical processes of the sediments, like OM deposition, storms, bioturbation, etc. might in turn also influence the remobilisation (and hence the bioavailability) of the metals (Eggleton & Thomas, 2004, Gao, *et al.*, 2009). Especially benthic microorganisms play an important role in the environmental fate of toxic metals with a multiplicity of physicochemical and biological mechanisms effecting transformations between soluble and insoluble phases (Eggleton & Thomas, 2004, Gadd, 2004). Bacterial communities play a pivotal role in the biogeochemistry of marine sediments, and as such influence metal mobility and bioavailability (Ford & Ryan, 1995). It can be expected that these released metals in turn will have an impact on the benthic environment.

Metal toxicity: general

Trace metal intoxication acts upon growth, morphology and metabolism of organisms, through functional disturbance, protein denaturation or the destruction of cell membrane integrity (Chapman, *et al.*, 1998). Consequently, exposed organisms may exhibit increased mortality, reduced growth and fecundity or developmental abnormalities. Scientists have documented the danger from trace metals for humans, such as neurotoxicity from Pb, allergic reactions from Cr, nephrotoxicity from Cd and Hg and cancer from As (Thomas, 1999).

Contaminants are available to aquatic organisms through membrane-facilitated transport (active) or passive diffusion (water dissolved), and from ingestion with food (particle associated). The toxicity depends on several factors: (a) the chemical speciation of the metal, because only bioavailable forms (i.e. the soluble fraction) are toxic for biological systems; (b) the toxicity of the respective metal to the physiological system; (c) the presence of other chemicals that may antagonise or stimulate metal uptake; (d) external factors such as temperature that affect the rate of biological or chemical reactions; (e) the sensitivity of the biological species (Chapman, *et al.*, 1998). Microbes developed several mechanisms against the toxic effects of metals, which can generally be classified into two types: detoxification, i.e. transforming the metal -by oxidation, reduction or methylation- into an innocuous form by production of metal-binding compounds, and dissimilation, i.e. exporting or keeping the metal outside the cell (Ford & Ryan, 1995). Metals that are ingested and assimilated by detoxification strategy can bio-accumulate in the food chain. It has been shown that e.g.

ciliates and Fungi are able to accumulate metals in and outside their cell, and advantage is taken of this particular capacity to use these organisms in bioremediation events (Rehman, *et al.*, 2010b, Srivastava, *et al.*, 2011).

Metal toxicity: effect on marine biota

Especially communities living in or feeding on these contaminated marine sediments or biota will be affected by the presence of these metals. A recent study performed by Chariton, *et al.* (2010) investigated biota (macro- meio and microbenthos) in estuarine sediments, contaminated with trace metals (but also polycyclic aromatic hydrocarbons and total petroleum hydrocarbons), and compared these communities with biota from reference estuaries. They showed that communities were indeed different, for all fractions of the biota but especially for meio- and microfauna, demonstrating that the major ecotoxicological responses can be distinguished in those fractions. Species richness is generally less affected [(Chariton, *et al.*, 2010), but see also (Gillan, *et al.*, 2005) for bacteria]. Several groups (e.g. Bivalvia, Polychaeta, Dinophyceae) were clearly more abundant in contaminated sediments, while other (e.g. Arthropoda, Kinorhyncha, Fungi) were lower, and indicator species only present in the reference locations were found within many groups (especially meio- and microbiota) (Chariton, *et al.*, 2010). The replacement of sensitive species by different resistant species can have serious ecological consequences, as the resistant species can fail to perform specific ecological functions.

Most studies considering metal contamination focused on specific biota. For example, macrofaunal species diversity in Norwegian fjords showed a strong negative correlation with copper concentration (Rygg 1985, Kennish 1998). Many reports have been published on the relationships between metals and bacterial variables such as total biomass, total biodiversity and activity in sediments. However, it is very difficult to draw general conclusions and it seems responses are often idiosyncratic.

Metal toxicity: effect on protists

Virtually nothing is known about the biodiversity, the structure and the physiology of protistan microbial communities in metal contaminated coastal sediments. The few available studies considering protists and trace metals in general (not only marine) focused on the effect of pollutants on individual groups, mainly stramenopiles and ciliates (Gutierrez, *et al.*, 2003, Diaz, *et al.*, 2006, Martin-Gonzalez, *et al.*, 2006, Zhou, *et al.*, 2008, Debelius, *et al.*, 2009,

Rico, *et al.*, 2009). Ciliates appear to be quite resistant to metal contamination, and some ciliate spp. like *Paramecium caudatum*, *Oxytricha fallax* and *Vorticella microstoma* can assimilate/accumulate high concentration of metals in their cell (Rehman, *et al.*, 2010b, a). This can be problematic because toxic metals such as As, Cd, Hg and Pb can be taken up by organisms and bioaccumulate in food chains (Langston, *et al.*, 1999, Twining & Fisher, 2004), producing ecological disturbances and potential human health risks. As a confirmation of this fact, metal levels found in mussels are known to correlate with the metal levels found in the proximate contaminated sediments (Joksimovic, *et al.*, 2011).

Study area: the Belgian Coastal Zone

The Belgian Coastal Zone (BCZ) is situated in the Southern Bight of the North Sea (Fig. 3). This is a region with strong tides, a lack of stratification and a relative shallow water depth. Three distinct water masses are identified (Fig. 3), i.e. (1) Channel water from the English Channel that is the dominant water mass in the region, (2) English Coastal Water along the coast of Southeast England, and (3) continental coastal water which is a band of fresher water which extends from somewhere east of Calais along the Belgian-Dutch coast (Lacroix, *et al.*, 2007b).

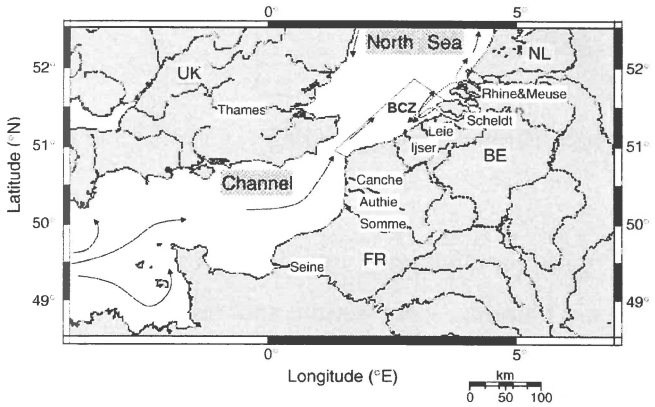

Fig. 3: Map of the Southern Bight of the North Sea, showing the Belgian Coastal Zone (BCZ), adjacent marine areas; the water masses and main rivers.
(from Lacroix, *et al.*, 2007b)

The BCZ has a maximum alongshore width of about 65 km and extends about 87 km offshore with a surface area of about 3600 km^2. Salinity is influenced by continental runoff and results in lower salinities near the mouths of the Scheldt and Rhine/Meuse rivers (Fig. 4B). The average and maximum water depths are approximately 20 m and 45 m respectively (Fig. 4A). The BCZ bathymetry is marked by many large and elongated subtidal sandbanks, the Flemish Banks, which greatly increase habitat heterogeneity, and form a geologically unique area.

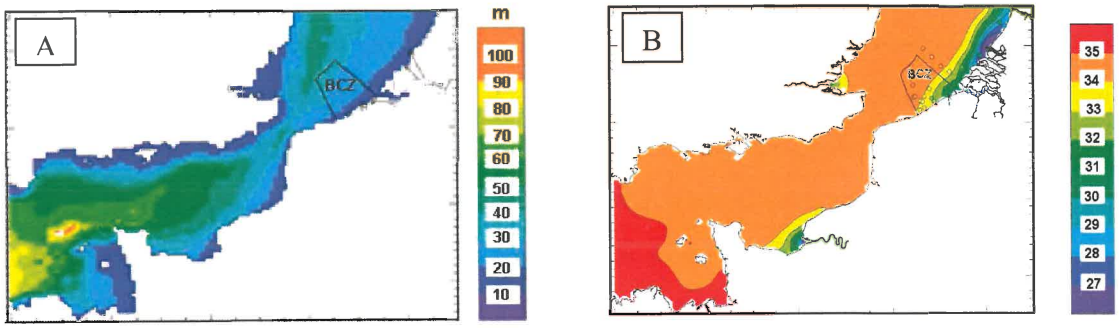

Fig. 4: A, Bathymetry (m) and B, surface salinity (‰) (for the period 1993-2002) of the southern Bight of the North Sea (Ruddick & Lacroix, 2006, Lacroix, *et al.*, 2007b).

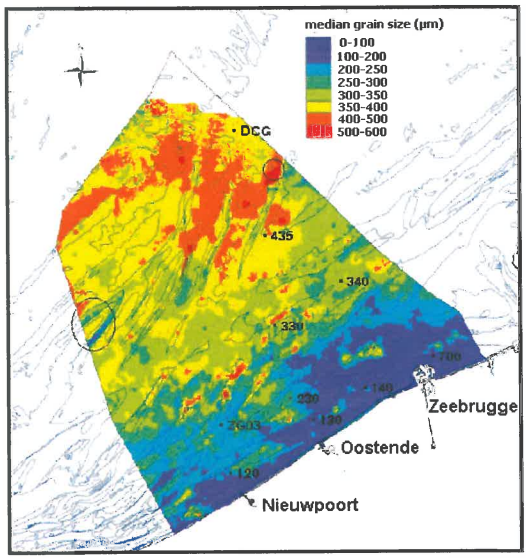

Figure 5: Grain size distribution along the BCZ.

Sediment composition (grain size, organic matter content, etc.) and dynamics in the area are mainly governed by the hydrodynamical circulation, wave action and tidal currents, and sediments vary from fine-grained silty sediments nearby the coast to sandy more offshore sediments with low contents of silt (Fig. 5).

The intensive use of the North Sea, the high population density, as well the economical development of chemical industries result in a high pressure on the marine ecosystem. The main problems in the BCZ, and for the North Sea in general, are caused by pollution by effluents from land containing harmful substances (e.g. metals) and excessive quantities of nutrients (~eutrophication) via the main rivers and other smaller rivers (Baeyens, *et al.*, 1998b, Lacroix, *et al.*, 2007a), and from coastal activities (e.g. fishing).

Phytoplankton blooms in the BCZ

The North Sea is a characterized by a seasonal cycle of phytoplankton blooms, which is reinforced as a consequence of eutrophication (Lancelot, *et al.*, 1987, Lacroix, *et al.*, 2007a). The phytoplankton bloom shows a well-characterized, seasonal cyclicity with the onset of a moderate early-spring diatom bloom (February-March), characterized by a.o. *Skeletonema* ssp. and *Thalassiossira* ssp., followed by a major *Phaeocystis* blooms, generally occurring in April-May (Rousseau, *et al.*, 2000). Anthropogenic eutrophication in the BCZ strongly modify the nutrient balance N:P:Si. This influences the composition of the phytoplankton community characterized by a dominance of opportunistic non-siliceous species (Rousseau, *et al.*, 2002, Lacroix, *et al.*, 2007a).

Sedimentation of phytodetritus derived from the phytoplankton blooms represents a major source of organic matter for the benthic system. It has been reported that in the BCZ about 24% of the phytodetritus is deposited on the sediments (Lancelot, *et al.*, 2005). Bacterial, meio- and macrofaunal communities respond fast to the increased food availability, with the response of the benthic ecosystem depending on the sediment type (Vanaverbeke, *et al.*, 2004, Franco, *et al.*, 2007, Franco, *et al.*, 2008, Rauch & Denis, 2008, Franco, *et al.*, 2010).

TM issues in BCZ

Metals reaching the BCZ mainly accumulate in the fine-grained sediments (see 'metals') along the coast. It has been reported that concentrations of Cd, Cu, Pb and Zn are at or above the level of the Ecotoxicological Assessment Criteria, which are defined as concentration levels above which concern is needed (OSPAR, 2000, Danis, *et al.*, 2004). However, despite the high TM concentrations in the sediments and the potential of metals to remobilise (what can lead to secondary TM pollution; see 'metals'), the importance of benthic fluxes in this area are largely undocumented (Gao, *et al.*, 2009). As increased microbial activity, e.g. as a consequence of algal bloom deposition, can lead to increased bacterial activity, these fluxes are a potential source of contamination to the marine ecosystem of the BCZ

2

MICROBIAL EUKARYOTE DIVERSITY AND COMMUNITY STRUCTURE IN RELATION TO NATURAL STRESSORS AND TRACE METAL POLLUTANTS IN SUBTIDAL COASTAL MARINE SEDIMENTS (NORTH SEA, BELGIUM)

Annelies Pede[1], David C. Gillan[2,5], Yue Gao[3], Gabriel Billon[4], Ludovic Lesven[4], Tine Verstraete[1], Willy Baeyens[3], Wim Vyverman[1] & Koen Sabbe[1]

[1] Protistology & Aquatic Ecology, Department of Biology, Ghent University, 9000 Ghent, Belgium

[2] Proteomics and Microbiology Lab., Mons University, 7000 Mons, Belgium

[3] Dep. of Analytical and Environmental Chemistry, Vrije Universiteit Brussel, 1050 Brussels, Belgium

[4] Université des Sciences et Technologies de Lille, UMR-CNRS 8110, France

[5] Marine Biology Lab., Université libre de Bruxelles, 1050 Brussels, Belgium

Manuscript in preparation

Abstract

Little information is available on the diversity and structure of microbial communities in marine subtidal sediments, especially for microeukaryotes. Using a combination of general and group-specific eukaryotic primers based on the 18S rRNA gene, we characterized benthic microeukaryotic diversity with an emphasis on ciliate and cercozoan diversity in sediments of the Belgian Continental Zone (BCZ). We assessed spatial (9 subtidal stations, top 0-1cm vs. bottom 9-10cm) and seasonal (February vs. July) variation in protist community composition in relation to sediment granulometry, geochemistry and trace metal contamination. Sediments ranged from sandy and well oxygenated to silty and anoxic with high levels of metal contamination. Eukaryotic diversity was dominated by Stramenopila (mainly diatoms), Metazoa and Fungi. Protozoan (Alveolata, Rhizaria, Amoebozoa) sequences were rarely detected using general eukaryotic primers, but 15 unique ciliate and 5 unique cercozoan phylotypes (OTUs) were found using ciliate- and cercozoan-specific primers in the silty sediments. The ciliate clone library was dominated by representatives of the classes Phyllopharyngea and Spirotrichea, followed by Oligohymenophorea, Litostomatea and Karyorelictea, while all cercozoans belonged to the Cryomonadida clade. Many sequences, especially cercozoan, dinophyte and fungal OTUs, were related to as yet uncultured species. While no clear trends in microeukaryotic species richness were found between seasons, community composition showed pronounced differences between sandy and muddy stations. No significant impact of metals on microeukaryotic species richness was observed.

Introduction

Microbial communities inhabiting subtidal marine sediments are composed of complex and highly diverse assemblages of prokaryotic and eukaryotic organisms, often occurring in very high densities (Tian, *et al.*, 2009, First & Hollibaugh, 2010). Protists (unicellular eukaryotes), together with bacteria, archaea and viruses are the primary drivers of the production, utilization and degradation of most organic matter and the cycling of many elements in these environments (Caron, 2009). While previous studies on these communities mainly focused on bacteria (e.g. Gillan, *et al.*, 2005, Sapp, *et al.*, 2010), protists have been much less investigated (but see Patterson, *et al.*, 1989, Fernandez-Leborans, *et al.*, 2001, Shimeta, *et al.*, 2002, Doherty, *et al.*, 2010, Scheckenbach, *et al.*, 2010, Takishita, *et al.*, 2010). Autotrophic

protists (microphytobenthos) can be responsible for a significant portion of total primary production in shallow subtidal sediments, depending on the turbidity of the overlying water column (Forehead & Thompson, 2010). Heterotrophic protists (Protozoa) are major grazers of bacterial, algal and other protozoan production, they facilitate remineralization of detritus deposited from the water column, and at the same time constitute a food source for higher trophic levels (e.g. Hamels, *et al.*, 2001, Dopheide, *et al.*, 2008, Caron, 2009). Investigations on the structure and composition of marine benthic protist communities to date mainly focused on intertidal sediments and the deep sea, including hydrothermal and cold seep vents (Bottcher, *et al.*, 2000, Dawson & Pace, 2002, Stoeck & Epstein, 2003, Hamels, *et al.*, 2004, Wilms, *et al.*, 2006, Takishita, *et al.*, 2007, Park, *et al.*, 2008, Coolen & Shtereva, 2009, Tian, *et al.*, 2009, First & Hollibaugh, 2010). To our knowledge, only two recent studies dealt with the structure of protist communities in subtidal coastal sediments (Garstecki, *et al.*, 2000, Shimeta, *et al.*, 2007), showing that a.o. grain size and flow regime had an important effect on overall community structure (Shimeta, *et al.*, 2007).

The aim of the present study was to document the spatial variation in protist community diversity and structure in subtidal sediments in the Belgian part of the North Sea (hereafter termed the Belgian Coastal Zone or BCZ) before and after the spring phytoplankton bloom, and relate the observed variation patterns to natural factors (physical and biogeochemical sediment characteristics) and anthropogenic pollutants, i.e. trace metals. Specifically, we compared protist community composition between the upper sediment layer (0-1 cm) and the deeper sediments (9-10 cm) at nine stations with different granulometry and metal concentrations, located at different depths and distances from the shore.

The BCZ is a highly productive area due to the input of nutrients and organic matter from adjoining estuaries, which results in intense phytoplankton spring blooms between March and June (Lancelot, *et al.*, 2005). Sedimentation of these blooms represents a major source of organic matter to the benthos; it has been reported that about 24% of the phytodetritus is deposited on the sediments (Lancelot, *et al.*, 2005). The receiving sediment type strongly determines the fate of the freshly deposited organic matter (Graf, 1992, Middelburg & Levin, 2009). In fine-grained sediments, only a shallow (mm's) upper sediment layer is oxygenated (Gao, *et al.*, 2009), and hence mainly anaerobic mineralization takes place (Jørgensen, *et al.*, 2006); resulting in an often slow decomposition of organic matter (Kristensen, *et al.*, 1995, Boon & Duineveld, 1998). Phytodetritus tends to accumulate, resulting in sharp vertical profiles of labile organic matter (OM) after the spring blooms (Steyaert, *et al.*, 1999, Franco,

et al., 2008). In coarser, more permeable sediments, such vertical gradients are usually absent. Here, enhanced porewater flows transport oxygen and dissolved and suspended matter through the interstitial space (Huettel, *et al.*, 1998), resulting in rapid aerobic OM degradation (Ehrenhauss & Huettel, 2004, Ehrenhauss, *et al.*, 2004, Vanaverbeke, *et al.*, 2004). Differences in biogeochemical processes between these contrasting sediments can affect the structure, function and metabolic activity of prokaryote and metazoan communities (Vanaverbeke, *et al.*, 2004, Franco, *et al.*, 2007, Franco, *et al.*, 2010). To date however, nothing is known about the diversity and structure of protist communities in the subtidal sediments of the BCZ.

Subtidal sediments in the BCZ are also characterized by high concentrations of trace metals such as Cd, As, Ni and Pb (OSPAR, 2000, Gillan & Pernet, 2007, Gao, *et al.*, 2009), introduced mostly by riverine input and coastal activity (Baeyens, *et al.*, 1998b, Danis, *et al.*, 2004). Trace metals are serious pollutants because of their toxicity, persistence, and non-degradability in the environment (Eggleton & Thomas, 2004). Their toxic effects mainly result from their interaction with metalloenzymes which impede many metabolic processes (Madoni & Romeo, 2006). Metal speciation is linked to their bioavailability; dissolved trace metals in porewaters are expected to have more biological effects than metals inside mineral particles (Forstner, 1993). However, few studies have focused on porewater metal concentrations, with most studies only considering total metal content of the sediment (e.g. Matthai & Birch, 2001, Zhang, *et al.*, 2008, Thiyagarajan, *et al.*, 2010). Our current view about relationships between metals and microbes in sediments might therefore be biased. During this study, we used the DET (Diffusive equilibration in thin-films; Davison, 1991) and the DGT (Diffusive gradients in thin-films; Davison & Zhang, 1994) approach, two gel-based techniques that allow *in situ* sampling of porewaters by which disturbance of sediments and oxidation artifacts (= a problem in ex-situ sampling) are limited (Davison & Zhang, 1994). A DET probe measures total dissolved metal species (free ions, colloids, organic and inorganic complexes), while a DGT probe mainly measures dissolved labile species which represent the bioavailable metal fraction (Gao, *et al.*, 2009). To our knowledge, it is the first time that *in situ* approaches are used to study the interaction of metals in porewaters and protist communities in sediments. Moreover, very few studies in general are available studying metal impact on marine protist communities; environmental stresses caused by metals may decrease the diversity, density and activity of marine microeukaryotic populations on the short term (Fernandez-Leborans & Novillo, 1994, Leborans, *et al.*, 1998, Fernandez-Leborans, *et al.*,

2007, Jayaraju, *et al.*, 2008, Wang, *et al.*, 2010), however most of these studies were performed in laboratory conditions using high metal concentrations. Long-term exposure to metals can lead to a shift in the microbial population to a more tolerant population, as has been demonstrated for bacterial (and fungal) communities (DiazRavina & Baath, 1996, Bouskill, *et al.*, 2010, Wang, *et al.*, 2010).

For a general assessment of protist community composition and structure, we used denaturing gradient gel electrophoresis (DGGE) with universal eukaryotic primers for the 18S rDNA gene (van Hannen, *et al.*, 1998). DGGE is a relatively fast and inexpensive technique for providing and comparing community fingerprints of large numbers of samples (Muyzer, *et al.*, 1993, Muyzer & Smalla, 1998). However, DGGE using general eukaryotic primers is not free of biases and is known to lead to an underestimation of the diversity due to e.g. primer mismatches, differences in rDNA copy number and PCR biases, often in a highly group-specific way (Stoeck, *et al.*, 2006, Jeon, *et al.*, 2008, Potvin & Lovejoy, 2009, Brate, *et al.*, 2010). It has been shown that universal eukaryotic primers are not optimal for the detection of protozoa (Shimeta, *et al.*, 2007, Dopheide, *et al.*, 2008). We therefore complemented our DGGE analyses by constructing clone libraries using cercozoan- and ciliate-specific 18S rDNA primer sets. Cercozoans are a group of small heterotrophic flagellates (Bass & Cavalier-Smith, 2004, Bass, *et al.*, 2009a), of which recent environmental DNA surveys have revealed a great hidden diversity in marine benthic sediments (Bass & Cavalier-Smith, 2004, Hoppenrath & Leander, 2006, Chantangsi & Leander, 2010). Ciliates are a well-studied group of protozoa and are usually highly diverse in marine sediments (Fernandez-Leborans, *et al.*, 1999, Shimeta, *et al.*, 2002, Hamels, *et al.*, 2005, Shimeta, *et al.*, 2007).

Materials and methods

Sediment sampling

Sediment samples were collected onboard RV 'Zeeleeuw' (cruise numbers 07-051 and 07-451) at nine subtidal stations in the BCZ (Fig. 1) in February and July 2007, before and after the main spring phytoplankton bloom. An overview of the nine stations and their main abiotic characteristics (depth, water temperature and salinity) is given in Table 1. Sediments were sampled for microbiological, chemical and physical analyses using a Reineck corer (diameter 15 cm). In two replicate Reineck cores, subcores were taken for DNA extraction, bacterial

biomass and chlorophyll *a* analysis, using 50 mL polyethylene syringes (diameter 2.8 cm; length 10 cm) with cutoff tips.

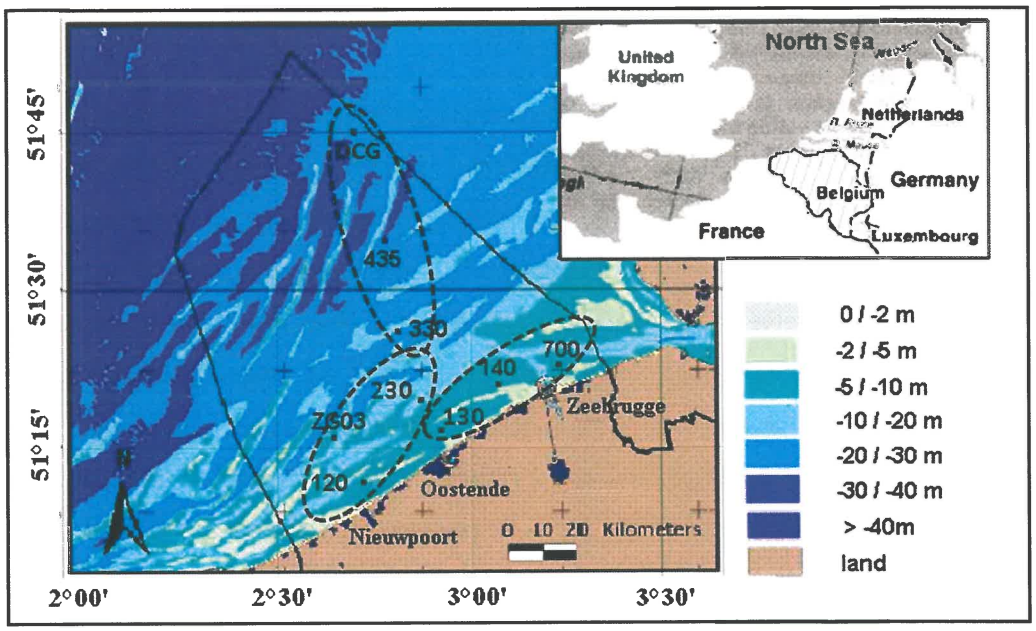

Fig 1: Location of the 9 sampling stations (120, 130, 140, 230, 330, 435, 700, DCG, ZG03) in the Belgian Coastal Zone (BCZ). Bathymetry (m) is indicated. Dotted ellipses indicate the stations grouped according to their sediment characteristics (see Fig. 2).

Each subcore was immediately subsampled for the top 0-1 cm section and the bottom 9-10 cm section. For DNA extraction, sediment samples were placed in cryovials and immediately frozen in liquid nitrogen; in the lab they were stored at -80°C until processing. For bacterial biomass (DAPI counts), sediment samples (2 mL) were fixed overnight in 4% paraformaldehyde, rinsed in sterile seawater and kept in ethanol-sterile seawater (50:50) at -20°C. Sediment samples (0.2-5 g sediment dry weight, SDW) for chlorophyll *a* (CHL *a*) analyses were placed in aluminium vials, frozen in liquid nitrogen and stored at -80°C until processing. Additionally, sediments were analyzed for granulometry, quantity of fine fraction (QFF) and trace metals (see below). Large plastic subcores (ø 7-10 cm) were used for DET/DGT metal analysis and microelectrode analyses. Based on the results of the 2007 sampling campaign, sediment samples were collected in February and July 2008 at 2 metal-contaminated stations (station 130 and 700) to construct clone libraries for ciliates and Cercozoa. Again, top and bottom sections were collected as in 2007.

Table 1: General characteristics of the sampling stations. The stations are arranged per group according to their sediment characteristics (see Fig. 2 and text);. Microeukaryotic species richness (SReuk) in the top (T, 0-1 cm) and bottom (B, 9-10 cm) sediment layer is given. Significant differences for SReuk between February and July 2007 are indicated in boldface (within one station and sediment section). Letters (a, b, c) refer to comparisons between station (within one sediment section and season); stations are not significantly different if at least one letter is shared (t-test/ Dunn's test, $P<0.05$). Fe, February 2007; Jul, July 2007. Nm, not measured.

		700	130	140	120	230	ZG03	330	435	DCG
coordinates		51°22.60 N - 03°13.20 E	51°16.25 N - 02°54.30 E	51°19.57 N - 03°02.93 E	51°18.50 N - 02°51.00 E	51°11.10 N - 02°42.07 E	51°15.70 N – 02°40.00 E	51°26.00 N - 02°48.50 E	51°34.84 N - 02°47.42 E	51°45.00 N - 02°42.00 E
sampling dates	Fe	8/02/2007	9/02/2007	8/02/2007	8/02/2007	9/02/2007	9/02/2007	9/02/2007	7/02/2007	7/02/2007
	Jul	5/07/2007	4/07/2007	5/07/2007	4/07/2007	4/07/2007	4/07/2007	18/07/2007	18/07/2007	18/07/2007
depth (m)		12.70	12.90	10.40	13.50	11.40	19.10	26.20	36.30	37.70
water temperature (°C)	Fe	6.5	6.3	6.3	6.5	6.5	10.0	7.3	8.5	9.1
	Jul	17.0	16.8	nm	16.7	17.0	16.4	17.5	16.9	16.6
water salinity (‰)	Fe	29.30	30.60	29.80	30.00	32.30	34.00	31.90	33.60	34.00
	Jul	32.01	34.28	33.22	34.44	34.26	34.56	34.47	34.88	34.99
sediment pH	Fe	7.02	6.90	7.11	7.81	7.77	7.66	nm	8.53	8.31
	Jul	7.33	7.01	7.79	8.36	7.67	nm	nm	nm	nm
SReuk	Fe-T	35.5 ±0.7 ab	38.0 ±1.4 a	29.5 ±4.9 ab	35.0 ±1.4 ab	**29.5 ±2.1 b**	50.5 ±2.1 c	33.5 ±0.7 ab	36.5 ±3.5 ab	32.0 ±7.1 abc
	Fe-B	33.0 ±0.0 a	**46.0 ±1.4 b**	32.0 ±4.2 ab	31.5 ±3.5 a	**28.0 ±5.7 ab**	46.5 ±7.8 ab	28.0 ±2.8 a	34.0 ±7.1 ab	32.5 ±3.5 a
	Jul-T	36.0 ±2.8 ab	40.5 ±0.7 a	31.5 ±3.5 ab	24.5 ±12.0 ab	**37.0 ±1.4 ab**	48.0 ±5.7 a	34.0 ±14.1 ab	31.0 ±7.1 ab	24.0 ±4.2 b
	Jul-B	30.0 ±2.8 ac	**39.5 ±0.7 b**	35.0 ±0.0 c	28.5 ±2.1 a	**35.5 ±3.5 abc**	47.5 ±5.0 bc	35.5 ±0.7 c	38.5 ±3.5 abc	30.5 ±0.7 a
		GROUP I			**GROUP II**			**GROUP III**		

Physical and chemical parameters

Dissolved oxygen and pH profiles were obtained for all stations as described in Gao, *et al.* (2009), except for stations DCG, 330 and 435 in July. Oxygen profiles were measured every 0.1 cm until the complete depletion of oxygen in the sediments; pH was measured every cm between 0 and 4-16 cm depth. Median grain size (MGS) of the sediments was determined using a Malvern Mastersizer 2000 laser granulometer on a composite sample from the top 10 cm, except for station 140 in July where separate top (0-1 cm) and bottom (9-10) sediments were sampled because the layers were visually very different. The quantity of fine fraction (QFF), i.e. the fraction of particles <150 µm, was measured using 500 mg ± 2 mg of sediments (n=4) separately for top and bottom sediments as described in Gillan *et al.* (subm., see annex 1). CHL *a* in the sediments was extracted in 90% acetone, after freeze-drying of the sediment, and analyzed using HPLC as described in Wright, *et al.* (1991). CHL *a* concentrations were expressed in µg g^{-1} SDW.

Porewater trace metals

High resolution porewater trace metal profiles (Cd, Fe, Mn, Co, As, Cu, Cr and Ni) were obtained to a maximum of 14.5 cm of depth in seven stations in February (130, 140, 230, 435, 700, DCG, ZG03) and three stations in July 2007 (130, 230, 700) by the Diffusive Equilibrium in Thin Films (DET; every 0.2cm) and the Diffusive Gradients in Thin Films (DGT; every 0.5cm) techniques. Concentrations measured by DET and DGT represent the total dissolved respectively the labile (~bioavailable) metal fraction (see introduction). Average values were calculated for top (0-1cm) and bottom (9-10cm) segments. A detailed description of the technique was given in (Gao, *et al.*, 2006, Gao, *et al.*, 2009, Gillan, *et al.*, subm., see suppl. 1).

Eukaryotic DNA extraction and PCR amplification

Genomic DNA was extracted from approximately 3-5 g of sediment using zirconium beads and phenol as described by Zwart, *et al.* (1998). As the extracellular DNA pool is by far the largest DNA fraction in many sediments (Frostegard, *et al.*, 1999), elimination of this DNA before DGGE analysis is recommended. Elimination of extracellular DNA was performed as described by Corinaldesi, *et al.* (2005). After extraction, the DNA was purified on a Wizard column (Promega) and nucleic acid extracts were stored at -20°C until analysis.

The DNA extracted from the sediment was amplified for DGGE analysis using the PCR procedure described in Muyzer, *et al.* (1993). For a broad assessment of the microeukaryotic community, we focused on the 18S rDNA (approximately 210 bp amplicons length) using the universal eukaryotic primers 1427f-GC and 1637r (van Hannen, *et al.*, 1998) (Table 2). Each PCR mixture contained 2 µL of DNA extract, 10 x PCR buffer [Tris/HCl: 100 mM, pH 8.3; KCl: 500 mM; $MgCl_2$: 15 mM; Gelatine: 0.01% (w/v)], 200 µM of each desoxynucleoside triphosphate, 0.5 µM of each primer, 2.5µl U of Taq DNA polymerase (Ampli Taq) and 400 ng of bovine serum albumin (BSA). The mix was adjusted to a final volume of 50 µL with sterile water. PCR was performed with the following thermal protocol: one cycle at 94°C for 5 min, 25 cycles at 94°C for 1min, 65°C for 1min, 72°C for 1min, and a final extension at 72°C for 10min with a hold at 15°C. All PCR products were checked by electrophoresis in 1.5% (w/v) agarose gels and by ethidium bromide staining.

Table 2: Oligonucleotide sequences used in this study for 18S rDNA-DGGE analyses *(DGGE)* and clone library construction *(CL)*.

Primer		Sequence (5'→ 3')	Reference
1427f-GC	*DGGE*	5'-GC-rich clamp-TCTGTGATGCCCTTAGATGTTCTGGG-3'	Van Hannen et al; 1998
1637r	*DGGE*	5'- GCGGTGTGTACAAAGGGCAGGG-3'	Van Hannen et al; 1998
25F	*CL*	5'-CATATGCTTGTCTCAAAGATTAAGCCA-3'	Bass and Cavalier-Smith; 2004
1256R	*CL*	5'-GCACCACCACCCAYAGAATCAAGAAAGAWC-3'	Bass and Cavalier-Smith; 2004
528	*CL*	5'-CGGTAATTCCAGCTCC-3'	Huss et al; 1999
Euk516r-GC	*CL*	5'-ACCAGACTTGCCCTCC-GC-rich clamp-3'	Diez et al; 2001
Cil-315f	*CL*	5'-TGGTAGTGTATTGGACWACCA-3'	Lara et al; 2007
Cil-959r I	*CL*	5'-TCTGATCGTCTTTGATCCCTTA-3'	Lara et al; 2007
Cil-959r II	*CL*	5'-TCTRATCGTCTTTGATCCCCTA-3'	Lara et al; 2007
Cil-959r III	*CL*	5'-TCTGATTGTCTTTGATCCCCTA-3'	Lara et al; 2007
T7	*CL*	5'-TAATACGACTCACTATAGGG-3'	Promega
SP6	*CL*	5'-ATTTAGGTGACACTATAGAA-3'	Promega

DGGE and sequence analysis

DGGE was performed on a Bio-Rad DCode system (Hercules, CA) as described by van Hannen, *et al.* (1998). Gels of 7% (w/v) polyacrylamide were prepared with a linear 30 to 55% denaturant gradient (acrylamide/bisacrylamide ratio, 37,5:1; 100% denaturing polyacrylamide solution contained 7M urea and 40% (v/v) formamide). PCR amplicons were purified on a QiaQuick PCR purification kit (Qiagen) and measured with a Nanodrop 2000 (Thermo scientific). Equal amounts (500 ng) of PCR product were loaded into each well. Electrophoresis conditions were 16h at 100V in 1X Tris-acetate-EDTA (TAE) buffer at 60°C. After electrophoresis, the gels were stained for 30 min in 1X TAE buffer with 1X SybrGold (Molecular probes) and fingerprints were visualized and digitally photodocumented (Kodak Easy Share P880 camera) under UV illumination. For each station and month, DGGE analyses were performed for the top and bottom sections of both two replicates (~ two replicate Reineck cores).

The most prominent bands were excised using plugged micropipette tips; the tips were then immersed in 30 µL 1X TE buffer and incubated overnight at 4°C. A 1 µL subsample was used for PCR, followed by DGGE to check band position and purity. After the purity was ascertained, PCR was performed with the same primer set (cf. above) without GC-clamp, followed by cycle sequencing PCR using primer 1427f (van Hannen, *et al.*, 1998), in accordance with the manufacturer's instructions (BigDye Terminator v3.1 cycle sequencing kit – Applied Biosystems). Sequencing was performed using an ABI 3130XL Genetic Analyzer (Applied Biosystems). Sequences were compared with the NCBI GenBank Database (www.ncbi.nlm.nih.gov) in March 2011, using the nucleotide-nucleotide Basic Local Alignment Search Tool (BLAST), to identify the closest sequence; if the most closely matching sequence was an uncultured organism, the most closely related positively identifed match is also listed. Sometimes a sequence had the same percentage similarity with different organisms; these have been labeled 'various eukaryote' (Table 4). The partial 18S rRNA gene sequences obtained from the universal eukaryotic primers were deposited in the EMBL database under accession numbers HQ830499 to HQ830554.

DGGE fingerprint image analysis

The digital DGGE images were imported and analyzed for fingerprint similarity using BioNumerics 5.10 (Applied Maths BVBA, Belgium). To facilitate fingerprint comparisons, pro- and eukaryotic DNA from previous studies performed in the laboratory was pooled to generate DGGE standards, covering the entire gradient in the DGGE gels (7 different positions). Three standard lanes were included per gel. Fingerprints were normalized using the DGGE markers as an external reference, and bands visually determined to be in common among several fingerprints in the gels were used as internal reference markers. Using both internal and external markers, all fingerprints were aligned (i.e. bands from the same position relative to the position of the marker bands in the gel were grouped into band classes). Sequence information of excised bands was used to check the grouping of bands into the band classes. All digitized DGGE fingerprints are available upon request from the corresponding author.

Each DGGE band class theoretically represents a unique phylotype (hereafter referred to as Operational Taxonomic Unit or OTU) representing a single species in the microbial assemblage (Muyzer & Smalla, 1998). In some cases however, different bands (~ DNA sequences) can co-migrate the same distance on the DGGE gel, and one OTU can yield different phylotypes (referred to as 'mixed OTUs'). These mixed OTUs are a well-known phenomenon for DGGE (Muyzer & Smalla, 1998). The optical density of the DGGE bands within a lane is assumed to be representative of the relative contribution of a phylotype to the overall community composition. Matrices were constructed with the presence/absence and the relative abundance (~ intensity) of the OTUs in each sample. These matrices were then used to determine the OTUs in each profile (= eukaryotic species richness or SReuk) and for the multivariate data analyses (see below) respectively. Very weak bands (<5% of total intensity) were omitted from the analyses.

Eukaryotic 18S clone libraries

Clone libraries were constructed using 18S rDNA group-specific primers for ciliates (Cil-315f; Cil-959r(I-II-III): 600-670bp, Lara, *et al.*, 2007a) and Cercozoa (25F; 1256R: ±1260bp, Bass & Cavalier-Smith, 2004) for two silty stations (130 and 700) (Table 2). Eukaryotic DNA extraction was performed as described above and the 18S rDNA genes were PCR amplified as described in Lara, *et al.* (2007a) and Bass & Cavalier-Smith (2004) respectively. PCR products from eight reactions (February and June 2008, top and bottom, station 700 and 130)

were pooled, cleaned with the Qiagen PCR Purification kit and cloned using the pGem-T vector system kit (Promega). Positive (white and light blue) colonies were picked; 250 colonies for ciliates, 100 colonies for Cercozoa. Presence and size of the 18S rRNA gene insert was checked by PCR using the universal primers T7 and SP6 (Promega) and agarose gel electrophoresis. Clones with the correct insert size were PCR amplified for fast screening by DGGE (to check for duplicates), using a nested PCR approach. The first amplification step used the group-specific primers, while a second amplification used the primer combinations with GC clamp which is required for DGGE: 25F and Euk516r-GC for Cercozoa, and Cil-315f and Euk516r-GC for ciliates. Ciliate PCR products were separated in a denaturing range of 40–65% and cercozoan amplicons in a range of 25-35% (100% denaturant concentration is defined as 7 M urea and 40% deionized formamide). Clones which showed a different DGGE banding pattern were selected for sequencing. Sequencing was performed with forward primer cil-315f and reverse primers cil-959r(I-II-III) for ciliates, and with forward primer 25F, reverse primer 1256R, and internal primers 528 and Euk516r for cercozoans (Table 2). Forward, reverse and internal sequences were assembled in Bionumerics 5.10 (Applied Maths BVBA). SSU DNA sequences were compared with those in GenBank in March 2011 using BLAST analysis to identify the closest sequences (cf. above – DGGE and sequence analysis). The partial 18S rRNA gene sequences obtained in these clone libraries were deposited in the EMBL database under accession numbers HQ696550 to HQ696569.

Bacterial diversity and biomass

PCR amplification and DGGE analysis were performed as described in Gillan, *et al.* (subm.; see annex 1). Bacterial diversity was expressed as the total number of DGGE bands in a sample (= bacterial species richness; SR bact). Bacterial biomass (BM bact) was calculated based on bacterial DAPI counts as described in Gillan, *et al.* (subm., see annex 1).

Statistical analysis

Pearson correlation analysis was performed to assess relations between selected trace metals concentrations, sediment and biological parameters (with Pairwise Deletion). All environmental variables (except salinity) were log-transformed and averaged for replicates prior to the analyses. pH had too many missing values and was not included in the multivariate analyses. The level of significance was set at α=0.01.

Variation in microeukaryotic community structure among the different depths (top vs. bottom), sediment types (groupI-III; see results) and season (February vs. July) was analysed using the software package PRIMER 6 (Clarke & Gorley, 2006) with permutational analysis of variance (PERMANOVA) + add-on (Anderson, *et al.*, 2008). All analyses were based on the relative abundance values of the OTUs (n=97). Data were log (x+1) transformed prior to analyses, and averaged for the two replicates. The July samples for station DCG were not included in any analyses due to their strongly different community composition, resulting in a data set of 34 samples. Differences in community composition between sediment types and seasons were examined according to the two-way crossed design using PERMANOVA based on Bray-Curtis similarities, with 9999 permutations of residuals under a reduced model, followed by PERMANOVA pair-wise comparisons, if significant differences were detected. Patterns in the community structure were visualized by Principal Coordinates Analysis (PCO). PCO is a distance-based ordination method that maximizes the linear correlation between the distances in the distance matrix (based on a Bray-Curtis similarity), and the distances in a space of low dimension (~ the ordination; the 2 main axes are selected and shown). The relationship between the variation patterns in community composition and measured environmental variables were assessed by entering these variables as supplementary variables in the PCO ordinations. The set of environmental variables included MGS, QFF, salinity, microalgal (CHL *a*) and bacterial biomass (BM), bacterial and eukaryotic species richness (SR) and dummy variables for sampling month (February and July) and depth (top and bottom). Only variables that correlated significantly ($p<0.05$) with the first or second axis are shown in the diagrams as supplementary (passive) variables. While the above variables were available for all sampling occasions, metal data were only available for a subset of the sampling occasions (n=15). In order to explore the relationships between the metal data and variation in OTU composition in more detail, we performed a separate PCO on a limited set of samples (n=15) for which DET and DGT data were available.

The variation in the phylotype data set was partitioned over spatial (stations as dummy variables), seasonal (sampling months as dummy variables), environmental (SR bact, BM bact, QFF, MGS, SAL and CHL *a* – SILT was not included) and metal (DET and DGT metal concentrations) components using the DISTLM routine (McArdle & Anderson, 2001). DISTLM is a distance-based multivariate multiple regression tool for analyzing and modeling the relationship between a multivariate data cloud (DGGE relative abundance matrix) described by a resemblance matrix based on Bray-Curtis similarities, and explanatory

Sea (Kuhn, *et al.*, 2000). Many heterotrophic flagellate species (like cercozoans) can be found both in the benthos and the pelagic (Garstecki, *et al.*, 2000). Members of the genus *Protaspis* are a group of gliding biflagellates which are common predators in marine benthic habitats (Hoppenrath & Leander, 2006, Luo, *et al.*, 2009, Chantangsi & Leander, 2010); the genus *Cryothecomonas* comprises both phytoplankton parasites (Tillmann, *et al.*, 1999) and free-living predators (Thomsen, *et al.*, 1991). Most cercozoans found in our study are coastal marine species, but were not related to cercozoans from subtidal sediments (e.g. from Park, *et al.*, 2008, Pawlowski, *et al.*, 2011b). The ciliate clone library was dominated by representatives of the classes Phyllopharyngea and Spirotrichea, followed by Oligohymenophorea, Litostomatea and Karyorelictea. Phyllopharyngea are a group of mainly algivores, Spirotrichea also consume algae and other small-sized food particles, most Oligohymenophorea are bacterivores, Litostomatea are largely predators, often of other ciliates (Taylor & Sanders, 1991), and many Karyorelictea are large omnivores, common in sandy sediments (Hirt, *et al.*, 1995), but also smaller Karyorelictids have been reported, more common in silty sediments (Garstecki, *et al.*, 2000, Shimeta, *et al.*, 2007). The same (except for one group, Nassophorea) ciliate classes were found by Shimeta, *et al.* (2007) in silty subtidal sediments in Buzzards Bay, Massachusetts. Moreover, Shimeta, *et al.* (2007) showed that ciliates have a higher density in silty sediments than in sandy sediments, and especially Karyorelictea and Oligohymenophorea were more abundant in silty sediments. Sequences retrieved from the ciliate libraries were related to sequences from a variety of environments [sediments and water column, freshwater and marine, littoral and subtidal, sea ice, extreme (e.g. water-surrounding chimney) and polluted (polycyclic aromatic hydrocarbon polluted soil) environments, etc., see Table 5 for references]. Many alveolate (Dinophyceae and Marine Alveolates Group I), rhizarian (Acantharea and Dinophyceae) and fungal sequences were also most closely related to uncultured eukaryotes (see Table 4), suggesting that an important part of protistan and fungal diversity in subtidal benthic environments remains to be isolated and sequenced, or is as yet undescribed (Chantangsi, *et al.*, 2008), even in relatively intensively studied groups like the ciliates (Lara, *et al.*, 2007b, Dopheide, *et al.*, 2008).

A significant number of sequences was most closely related to parasitic organisms, belonging to different phylogenetic groups. These include *Duboscquella* sp. (a parasite of other protists – mainly ciliates - belonging to the Marine Alveolates Group I; Harada, *et al.*, 2007), a *Haliphthoros*-like Oomycete parasite (Sekimoto, *et al.*, 2007) known as parasites of a wide range of marine crustaceans and some other marine animals (e.g. Diggles, 2001), the

Rhizarian *Cryothecomonas* (a phytoplankton parasite, Tillmann, *et al.*, 1999), and the dinoflagellate *Pfiesteria shumwayae* which has been implicated in massive fish kills (micropredation vs. toxicity) (Vogelbein, *et al.*, 2002, Shimizu, 2003). Like other recent studies (Kagami, *et al.*, 2007, Gachon, *et al.*, 2009, Mangot, *et al.*, 2011, Rasconi, *et al.*, 2011), our study thus underscores the importance of eukaryotic parasites in marine benthic ecosystems.

Patterns in microeukaryotic community structure

Despite the fact that over ¾ of OTUs are shared between the different sediment types in the BCZ, microeukaryotic community structure is significantly different in sandy and silty sediments; differences in species richness were not significant. Seasonal differences (February vs. July) in community structure were either just (PERMANOVA) or not (PCO, variation partitioning) significant, while no depth-related (top 0-1 cm vs. bottom 9-10 cm sediment layers) variation was observed. Differences in community composition between the sediment types can be attributed to various groups (e.g. alveolates and Fungi), but also diatoms. This may reflect the existence in the BCZ of an on-offshore gradient in phytoplankton species composition (M'Harzi, *et al.*, 1998) or species-specific mineralization and/or preservation of diatom cells in silty and sandy sediments (cf. Kristensen, *et al.*, 1995, Boon, *et al.*, 1999, Harnstrom, *et al.*, 2011).

Differences in community composition between silty and sandy sediments are commonly reported in benthic microeukaryote communities, both in inter- and subtidal habitats (Albrechtsen & Winding, 1992, Vanaverbeke, *et al.*, 2002, Musslewhite, *et al.*, 2003, Hamels, *et al.*, 2005, Shimeta, *et al.*, 2007, First & Hollibaugh, 2010). To our best knowledge however, to date only one study specifically focused on variation in microeukaryotic community structure between different sediment types in subtidal marine sediments (Shimeta, *et al.*, 2007). As in our study, they observed that community structure was strongly related to grain size. The specific factors causing these differences however are difficult to identify, as silty and sandy sediments differ in a suite of environmental stressors, including sediment composition (MGS and QFF), pH, CHL *a* content, oxygen penetration, trace metal concentrations (Figs 2 and 3, Table 2, S1 and S2), and organic matter (OM) and nutrient content (Franco, *et al.*, 2007). In addition, as the silty stations were all situated near the coast, they were characterized by lower salinity (due to the discharge of the Scheldt estuary).

Physical properties of sediments can strongly impact the diversity and biomass of benthic protist communities (Patterson, *et al.*, 1989, Hamels, *et al.*, 2005). In silty sediments, the lack of large interstitial spaces may hamper movement and hence colonization by flagellates and ciliates. As a result, in intertidal sediments, ciliate diversity (but also abundance) can be lower in silty sediments (Hamels, *et al.*, 2005). However, Garstecki, *et al.* (2000) and Shimeta, *et al.* (2007) both found hat ciliates in subtidal sediments have a higher density (but also lower diversity; Shimeta, *et al.*, 2007) in silty sediments than in sandy sediments, and especially Karyorelictea and Oligohymenophorea were more abundant in silty sediments compared to sandy sediments (Shimeta, *et al.*, 2007, see above). They concluded that it is not possible to know whether the differences are specific to certain sites e.g. by higher abundances of food resources for herbivorous and predatory ciliates in silty sediments compared to those at the sandy sites, or if this reflects a fundamental difference between intertidal and subtidal habitats (Shimeta, *et al.*, 2007). General physico-chemical differences between silty and sandy sediments in this study were clear; sedimentation and accumulation of OM (mainly algal bloom-derived phytodetrital matter, cf. CHL *a*) was most pronounced in silty sediments (Boon & Duineveld, 1998, Boon, *et al.*, 1998), and mineralization of this OM leads to steep and shallow (upper mm's) gradient in oxygen penetration (Fig. 3), redox potential and pH (Gao, *et al.*, 2009). This was especially pronounced after the deposition of the spring bloom in late spring/early summer (Fig. 3, cf. also Franco, *et al.*, 2008). In sandy, permeable sediments stronger porewater flows transport oxygen through the interstitial space, resulting in a higher turnover of OM (Dauwe, *et al.*, 2001, Vanaverbeke, *et al.*, 2004), and hence lower CHL *a* values (Fig. 2, Table S1). Oxygen plays a structural role for the distribution of small metazoans in sediments (Levin, *et al.*, 2009). Moreover, In O_2 gradients, many bacteria and protozoa are vertically distributed according to oxygen tension and they show a very limited range of preferred O_2 tension (Berninger & Epstein, 1995, Fenchel & Bernard, 1996, Fenchel & Finlay, 2008). As we did not recover many protozoan (and no ciliate) sequences with the DGGE approach, it is not possible to assess whether the observed differences in community composition between silty and sandy sites could be related to physical constraints. The clone libraries of the silty sediments, however, revealed a considerable diversity of ciliate and cercozoan OTUs. Our data thus do not contradict the findings of (Garstecki, *et al.*, 2000, Shimeta, *et al.*, 2007). Futhermore, we found no indication of a lower microeukaryotic diversity in silty sediments compared to sandy sediments.

Total dissolved (free ions, colloids, organic and inorganic complexes estimated by use of DET) and labile (containing mainly the free hydrated cation, inorganic complexes and to a lesser extent some organic species measured with DGT probes) trace metal concentrations are significantly higher in sandy sediments (Table S2). Other reports have analyzed the relationship between metals and bacterial communities in sediments (e.g. Kandeler, *et al.*, 1996, Gillan, *et al.*, 2005, Gillan & Pernet, 2007, Ogilvie & Grant, 2008, Bouskill, *et al.*, 2010, Pringault, *et al.*, 2010, Nogales, *et al.*, 2011). It is difficult however to draw general conclusions and it seems that each microbial community is unique and reacts in a different way. Trace metal contamination has been shown for example to alter the bacterial community composition (Toes, *et al.*, 2008) and can be negatively (Kandeler, *et al.*, 1996) as well as positively (Bouskill, *et al.*, 2010) related to the diversity of the bacterial sediment-inhabiting organisms. Bacterial SR during this study was lower in the silty contaminated sediments, while bacterial biomass was higher in silty sediments (Fig. S1; see also Gillan, *et al.*, subm., suppl. 1), in contrast to what been reported previously along the metal-contamination gradient in the BCZ (Gillan & Pernet, 2007) and contaminated fjords in Norway (Gillan, *et al.*, 2005). More specifically, bacterial SR was negatively correlated to total dissolved Co (measured by DET), while bacterial biomass was positively correlated to labile Mn (measured by DGT) (see also Gillan *et al.*, subm.; suppl. 1). It should however be noted that most previous studies which have investigated the effects of trace metals on microbial organisms have not measured dissolved metals *in situ* (cf. this study) but have used *ex situ* approaches that are more prone to artefacts (Davison & Zhang, 1994); in addition, they were not focused on pore water concentrations but measured the total HCl extractable metals in the sediment. In our study, no distinct direct negative effects were observed on microeukaryotic SR. However, it is not possible to assess whether the difference in community structure between sandy and silty sediments is directly influenced by metal concentrations, as variation partitioning did not reveal a significant independent effect of trace metals after partialling out the effect of other environmental variables (CHL *a*, bacterial species richness, see Table 7). Our ciliate-specific clone library revealed a high ciliate diversity in the silty, anoxic and metal-contaminated stations 130 and 700 (see above), suggesting that many ciliate species are able to adapt to high metal concentrations. Previous studies indeed showed that ciliates are able to survive a wide range of toxicants including metals (Sauvant, *et al.*, 1999, Diaz, *et al.*, 2006); for As in particular, see (Pede et al., chapter 6), and that e.g. intracellular metal bioaccumulation may occur (Diaz, *et al.*, 2006).

Seasonal variation in the microeukaryote community composition was limited. Diatoms were proportionally more abundant in July than in February, and diatom OTUs differed in relative abundance between February and July (not shown), which can be related to the spring succession in the phytoplankton bloom. However, the lack of a pronounced seasonal signal is surprising given the fact that a pre- and post-bloom situation (February vs. July) was compared, and benthic communities in general tend to strongly respond to changes in OM input resulting from the deposition of the spring bloom (Vanaverbeke, *et al.*, 2004, Franco, *et al.*, 2007, Franco, *et al.*, 2008, Rauch, *et al.*, 2008, Franco, *et al.*, 2010). Moreover, seasonal change was less pronounced in the silty than in the sandy sediments, although CHL *a* input is higher in the former (Fig. 2). Bacterial communities in the same study area displayed stronger seasonal change in silty sediments compared to sandy (Franco, *et al.*, 2007). Strong spatial variation is probably able to mask the seasonal variation effect, as it was shown that spatial variation could still significantly explain as much as 17-30% of the variation after partialling out the environmental and metal-related variation (Table 7). Likewise, the fact that no significant differences in species composition were observed between the top layer of the sediment (0-1cm) and the deeper layers (9-10 cm) may also be due to the strong impact of spatial variation. Indeed, in a study of seasonal and vertical changes in protist communities of a single silty station (cf. Pede, *et al.*, chapter 3), both significant temporal and depth changes in community composition were observed, as was also observed by Park, *et al.* (2008) and Hamels, *et al.* (2005) who found clear vertical gradients in protozoan communities in subtidal respectively intertidal sediments.

Acknowledgements

This research was supported by a Belgian Federal research program (Science for a Sustainable Development, SSD, contract MICROMET n° SD/NS/04A & 04B) and BOF-GOA projects 01GZ0705 and 01G01911 of Ghent University (Belgium). Many thanks to Andre Catrijsse and the crew on the R.V. Zeeleeuw, to Bart Vanelslander for his help during the sampling campaigns, and to Jeroen Van Wichelen and Julie Baré for making corrections and suggestions to the manuscript.

Supplementary

Table S1: General physico-chemical characteristics of the sediments investigated. Stations are arranged per group (GROUP I-III) according to the sediment characteristics; Group I silty stations and Group II and III sandy stations. Fe, February 2007; Jul, July 2007; MGS, median grain size; QFF, quantity of fine fraction in 500 mg sediment (±SD; n=4); CHL *a*, Chlorophyll *a*; T, 0-1cm depth; B, 9-10cm depth; nm, not measured; /, no replicates

		700	130	*140	120	230	ZG03	330	435	DCG
MGS (µm)	Fe	38	28	76	314	228	227	434	460	493
	Jul	52	44	*272(T)-53(B)	233	247	227	351	432	434
QFF (mg)	Fe -T	0,1395 ±0,0112	0,1840 ±0,0419	0,1122 ±0,0675	0,0108 ±0,0080	0,0054 ±0,0073	0,0022 ±0,0020	0,0006 ±0,0005	0,0002 ±0,0000	0,0002 ±0,0000
	Fe -B	0,1613 ±0,0204	0,1929 ±0,0347	0,0795 ±0,0524	0,0148 ±0,0054	0,0435 ±0,0646	0,0032 ±0,0012	0,0060 ±0,0068	0,0003 ±0,0001	0,0016 ±0,0013
	Jul -T	0,1320 ±0,0218	0,1568 ±0,0178	0,0013 ±0,0004	0,0428 ±0,0165	0,0687 ±0,0974	0,0110 ±0,0051	0,0028 ±0,0021	0,0005 ±0,0006	0,0004 ±0,0003
	Jul -B	0,1754 ±0,0538	0,1512 ±0,0348	0,1771 ±0,0345	0,0180 ±0,0099	0,0092 ±0,0092	0,0119 ±0,0054	0,0016 ±0,0011	0,0005 ±0,0003	0,0016 ±0,0012
CHL *a* (µg/g SDW)	Fe -T	11.02 ±3.79	7.07 ±2.25	8.68 ±/	0.20 ±0.09	0.14 ±0.02	0.28 ±0.22	0.10 ±0.04	0.10 ±0.03	0.07 ±0.02
	Fe -B	15.15 ±7.67	13.16 ±10.59	4.24 ±/	0.41 ±0.20	0.11 ±0.03	0.47 ±0.05	0.04 ±0.03	0.03 ±0.02	1,53 ±2.18
	Jul -T	14.06 ±5.82	21.67 ±6.82	0.14 ±0.05	1.93 ±1.05	0.21 ±0.02	0.61 ±0.15	0.04 ±0.01	0.04 ±0.04	0.06 ±0.05
	Jul -B	6.86 ±6.59	10.24 ±1.07	3.17 ±0.21	0.96 ±0.72	0.32 ±0.01	1.00 ±0.39	0.04 ±0.00	0.01 ±0.02	0.05 ±0.04
		GROUP I			GROUP II			GROUP III		

* station 140 received a sandy top layer in July

Table S2: Metal concentrations (μg L^{-1}) in porewaters of seven stations (DCG, 435, 230, 700, 140, 130, ZG03) in the Belgian Coastal Zone as determined by DET and DGT. Average values (± SD) from top (0-1cm) and bottom (9-10cm) sediments are presented (n=5-6 for DET; n=3 for DGT). Fe, February 2007; Jul, July 2007. Significant differences between February and July (within one station and sediment section) are indicated in boldface; t-test, P< 0.05. nm, not measured; I, group I silty stations, II, group II sandy stations; III, group III sandy stations.

	Station	Depth	Group	DET (ppb)										DGT (ppb)									
				Ag	Cd	Sn	Cr	Mn	Fe	Co	Ni	Cu	As	Ag	Cd	Sn	Cr	Mn	Fe	Co	Ni	Cu	As
Fe	130	0-1cm	I	**2,95**	**0,35**	**2,40**	8,87	3259,54	18996,01	**2,77**	6.12	36,18	**58,84**	0.02	**0.03**	0.03	0.32	**255.31**	2230.58	**1.00**	2.47	0.93	1.45
				±0.98	**±0.10**	**±1.05**	±15.26	±973.88	±6349,13	**±0.44**	±2.47	±8.51	**±16.48**	±0.00	**±0.05**	±0.01	±0.39	**±14.79**	±909.58	**±0.31**	±1.15	±0.85	±0.48
	130	9-10cm	I	**13,56**	0,80	2,65	37,37	**5664,94**	19010,52	**3,21**	11,28	46,38	**74,44**	0.04	0.01	0.12	**0.84**	**1158.20**	1626.89	0.21	1.04	**0.74**	**2.95**
				±1.65	±0.73	±0.96	±57.88	**±431.47**	±7454.55	**±0.53**	±6.26	±8.67	**±9.50**	±0.00	±0.01	±0.16	**±0.03**	**±98.80**	±1383.09	±0.03	±0.40	**±0.14**	**±0.34**
	140	0-1cm	I	0,49	0,20	3,96	14,01	742,63	1539,27	1,72	4,79	49,89	13,02	0.03	0.03	0.11	0.30	501.73	147.77	0.24	1.73	0.91	0.15
				±0.58	±0.21	±2.49	±12.23	±436.08	±867.90	±1.97	±5.94	±7.95	±3.53	±0.01	±0.01	±0.01	±0.13	±130.90	±112.62	±0.03	±0.53	±0.21	±0.11
	140	9-10cm	I	2,17	0,66	5,69	7,40	2957.74	8000,58	2,61	22,14	62,62	40,83	0.05	0.01	0.04	0.77	791.89	944.05	0.26	1.34	1.78	1.70
				±1.60	±0.71	±3.66	±3.35	±314.08	±3645.00	±0.42	±6.11	±10.56	±7.53	±0.01	±0.00	±0.01	±0.13	±92.94	±180.67	±0.07	±0.23	±1.06	±0.15
	700	0-1cm	I	1,40	0,40	**0,27**	13,10	**4694,30**	**21760,56**	**3,46**	0,57	64,54	**99,29**	0.02	**0.01**	0.04	0.26	427.46	**5268.6**	0.59	1.29	**0.67**	2.25
				±/	±0.59	**±0.27**	±14.28	**±517.96**	**±4405.93**	**±1.27**	±0.45	±11.80	**±20.81**	±0.00	**±0.02**	±0.01	±0.13	±94.37	**±120.98**	±0.06	±0.43	**±0.12**	±0.88
	700	9-10cm	I	11,92	0,60	6,57	**8,76**	**5862,61**	33566,60	**2,75**	**7,09**	243,09	**101,16**	0.03	**0.00**	0.05	0.70	435.85	**3312.76**	0.36	0.60	**4.88**	2.59
				±15.59	±0.52	±3.77	**±3.45**	**±226.51**	±1307.57	**±0.55**	**±4.46**	±434.85	**±9.26**	±0.01	**±0.00**	±0.02	±0.19	±81.68	**±598.35**	±0.01	±0.13	**±4.93**	±0.21
	230*	0-1cm	II	Nm	**0,10**	0,85	9.09	181.70	3657.44	1,28	20,36	53.29	**12.88**	0.05	0.06	0.02	1.01	54.48	834.26	0.30	11.96	0.85	0.30
					±0.7	±0.95	±9.25	±145.12	±2073.24	±0.60	±19.72	±7.58	**±6.53**	±0.01	±0.04	±0.00	±0.35	±26.54	±593.35	±0.04	±1.67	±0.07	±0.15
	ZG03	0-1cm	II	Nm	1.23	Nm	11,70	9,43	618,90	0,97	10,16	72,60	Nm	0.02	0.05	0.03	0.12	7.60	22.30	0.10	77.00	1.23	0.05
					±1.44		±7.08	±3.84	±225.89	±0.48	±13.14	±58.20		±0.00	±0.01	±00.02	±0.02	±02.92	±10.57	±0.01	±6.41	±0.47	±0.01
	ZG03	9-10cm	II	Nm	0.20	Nm	10,42	747.93	2100,73	2,86	11,76	47,18	Nm	0.04	0.01	0.03	1.68	55.77	1142.07	0.52	19.93	0.96	1.18
					±15		±12.57	±128.57	±284.42	±0.42	±10.75	±4.54		±0.01	±0.01	±0.01	±1.37	±11.34	±838.06	±0.28	±7.05	±0.51	±0.76
	435-	0-1cm	III	1,00	0,37	1,98	1,14	5,73	124.77	0.41	0,98	48,46	2,89	0.01	0.04	0.01	0.12	0.95	32.72	0.03	3.28	0.38	0.06
				±0.49	±0.22	±2.77	±0.71	±3.08	±126.94	±0.32	±0.31	±3.69	±1.55	±0.00	±0.00	±0.01	±0.05	±0.37	±29.90	±0.02	±0.91	±0.06	±0.02
	DCG	0-1cm	III	0,45	1,98	0,80	Nm	12.53	222.70	0,46	17.95	46.16	1.84	0.01	0.06	0.74	0.10	0.38	9.45	0.01	3.03	0.20	0.16
				±0.25	±1.09	±1.18		±8.77	±156.23	±0.07	±29.54	±23.28	±1.11	±0.01	±0.04	±1.23	±0.01	±0.21	±1.41	±0.00	±0.99	±0.09	±0.08
Jul	130	0-1cm	I	**876,28**	**1,63**	**3,72**	7.64	4180.64	22666,14	**0,46**	8,25	Nm	**103,94**	Nm	**0.46**	Nm	0.20	**717.34**	958.92	**0.29**	0.75	0.35	1.30
				±563.57	**±0.98**	**±0.91**	±5.43	±940.40	±14615.65	**±0.26**	±1.32		**±35.01**		**±0.07**		±0.25	**±159.73**	±887.29	**±0.07**	±0.27	±0.43	±0.64
	130	9-10cm	I	**71,27**	0,44	3,36	15,95	**4082,77**	14350,52	**1,24**	16,99	Nm	**88,12**	Nm	0.02	Nm	**0.17**	**882.24**	2587.15	0.15	0.47	**0.12**	**4.24**
				±9.76	±0.18	±1.01	±9.23	**±70.73**	±2088.27	**±0.44**	±17.46		**±5.82**		±0.01		**±0.03**	**±98.69**	±1676.59	±0.05	±0.31	**±0.05**	**±0.17**
	700	0-1cm	I	4,54	0,82	**5,80**	23,25	**3257,77**	**14146,10**	**5,33**	52,61	Nm	**71,82**	Nm	**0.12**	Nm	0.47	284.33	**937.93**	0.69	2.23	**0.24**	0.90
				±3.52	±0.34	**±3.39**	±29.87	**±1206.76**	**±6393.74**	**±1.57**	±71.31		**±6.51**		**±0.01**		±0.10	±67.07	**±194.96**	±0.16	±1.64	**±0.23**	±0.29
	700	9-10cm	I	5,25	0,66	8,99	**52,18**	**3591,15**	30897,24	**10,32**	**30,36**	Nm	**85,71**	Nm	**0.13**	Nm	0.95	379.28	**1806.23**	0.32	0.93	**0.13**	1.49
				±1.65	±0.36	±7.64	**±29.07**	**±609.79**	±14795.75	**±6.03**	**±18.22**		**±10.56**		**±0.2**		±0.19	±42.47	**±207.89**	±0.08	±0.31	**±0.09**	±0.20
	230	0-1cm	II	Nm	**1,16**	11,89	15,86	285,61	2745,20	0,91	45,80	Nm	**5,77**	Nm	Nm	Nm	Nm	Nm	Nm	Nm	Nm	Nm	Nm
					±0.64	±17.59	±19.84	±24.91	±1999.80	±1.02	±51.20		**±1.82**										
	230	9-10cm	II	Nm	0,61	5,04	19,00	1396,91	9605,98	3.07	19,23	Nm	18.82	Nm	Nm	Nm	Nm	Nm	Nm	Nm	Nm	Nm	Nm
					±0.14	±1.37	±7.72	±226.74	±4404.43	±1.21	±13.48		±4.46										

* sandy top layer in February.

Figure S1: Bacterial biomass (BMbact), expressed by the numbers of bacteria counted in 500 mg of sediment (wet weight), and bacterial species richness (SRbact; number of DGGE bands) in Fe, February 2007 (black bars) and Jul, July 2007 (grey bars); T, 0-1cm depth (full bars); B, 9-10cm depth (empty bars); average values ± SD (n=4). Stations are arranged per group (GROUP I-III) according to the sediment characteristics.

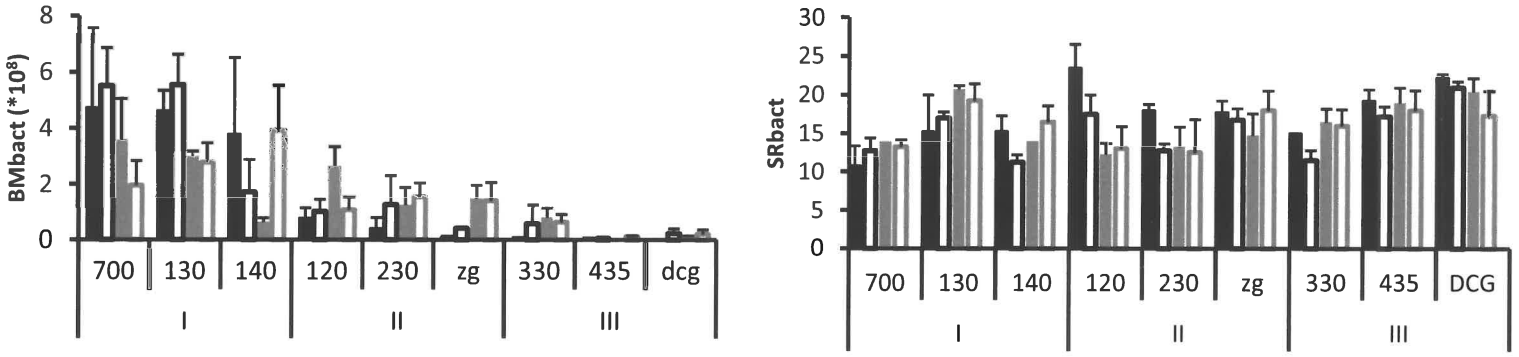

3

EFFECTS OF SPRING PHYTOPLANKTON BLOOM DEPOSITION ON SEASONAL DYNAMICS AND VERTICAL DISTRIBUTION OF MICROBIAL EUKARYOTES IN A SILTY, METAL-CONTAMINATED SEDIMENT IN THE SOUTHERN NORTH SEA

Annelies Pede[1], David Gillan[2;5], Yue Gao[3], Gabriel Billon[4], Ludovic Lesven[4], Martine Leermakers[3], Willy Baeyens[3], Tine Verstraete[1], Wim Vyverman & Koen Sabbe[1]

[1] Lab. Protistology & Aquatic Ecology, Department of Biology, Ghent University, 9000 Ghent, Belgium

[2] Proteomics and Microbiology Lab., Mons University, 5, 7000 Mons, Belgium.

[3] Department of Analytical and Environmental Chemistry, Vrije Universiteit Brussel, 1050 Brussels, Belgium

[4] Université des Sciences et Technologies de Lille, UMR-CNRS 8110, France

[5] Marine Biology Lab., Université libre de Bruxelles, 1050 Brussels, Belgium.

Manuscript in preparation

Abstract

Microbial communities from a subtidal, silty, metal-contaminated sediment in the Belgian Coastal Zone, sampled between February and July 2008, were studied using denaturant gradient gel electrophoresis (DGGE). Seasonal and vertical dynamics in the structure of the microeukaryotic community, and Protozoa in particular, were studied in relation to the sedimentation of the spring phytoplankton bloom and linked to variation in the biogeochemical environment, including trace metal dynamics, as previous research had demonstrated that accumulated metals in sediments are released upon bloom sedimentation and degradation (Gao, *et al.*, 2009). Stramenopila (mainly diatoms) were the dominant group in the sediments, followed by Alveolata (ciliates and dinophytes) and Rhizaria (cercozoans, acanthareans and foraminiferans). Sedimentation of the bloom was reflected in increased levels of chlorophyll *a* and higher abundances of diatoms in the upper sediment layers, and resulted in higher bacterial biomass. Microeukaryote and protozoan community composition changed from February to July, with especially May and July being distinct. Increased microbial mineralization caused pronounced changes in the redox environment and the bioavailable metal concentrations in the sediment, which correlated with the observed seasonal and vertical variation patterns in community structure. Eh and pH were the dominant factors structuring the communities, but trace metals as well had a significant, independent impact on microbial community structure. While no negative effect could be found between the metals and microeukaryotic and protozoan diversity, some taxa, such as a dinoflagellate, appeared to be strongly affected by metal concentrations, while other groups (e.g. ciliates) appeared to be unaffected by higher metal concentrations.

Introduction

The Belgian Coastal Zone (BCZ) is characterized by extensive annual spring phytoplankton blooms (Boon, *et al.*, 1998, Lancelot, *et al.*, 2005), which have intensified as a consequence of anthropogenic eutrophication mainly through input of land-based nutrients via de Scheldt estuary (Lacroix, *et al.*, 2007a). Metal concentrations in the coastal sediments are at or above the Ecotoxicological Assessment Criteria (OSPAR, 2000, Danis, *et al.*, 2004). Metals mainly accumulate in silty, fine-grained sediments due to their tendency to absorb to particulate material (Li, *et al.*, 2000b, Eggleton & Thomas, 2004), while in sandy sediments only low

metal concentrations are detected (Pede, *et al.*, chapter 2, Gillan, *et al.*, subm.). Bioavailability of these contaminants is regulated by biogeochemical processes and environmental conditions (e.g. oxygen, redox and pH) in the sediments (Eggleton & Thomas, 2004). For example, it is known that remineralization of organic matter from the algal blooms can lead to metal remobilization through microbial activity (Ford & Ryan, 1995, Eggleton & Thomas, 2004, Gadd, 2004, Gao, *et al.*, in press, Gillan, *et al.*, subm., chapter 4). Considering the ecotoxicological effects of metals, these metals can in turn influence the benthic and pelagic ecosystem (Ford, 2000, Pede, *et al.*, chapter 5).

Sedimentation of phytoplankton blooms has a strong impact on the benthic ecosystem. The initiation of anaerobic mineralization pathways in anoxic silty sediments causes changes in environmental conditions and biogeochemical processes (redox, pH, organic matter, metals) (Gao, *et al.*, 2009, Middelburg & Levin, 2009), with consequences for the inhabiting communities. Bacterial, nanoflagellate, meio- and macrobenthic communities can respond quickly to the settling of algal blooms, e.g. by increased activity, changes in diversity, density, community structure or vertical distribution (Van Duyl, *et al.*, 1992, Vanaverbeke, *et al.*, 2004, Franco, *et al.*, 2007, Franco, *et al.*, 2008, Franco, *et al.*, 2010). The effect of phytoplankton deposition on microeukaryotic communities (~protists) is to date largely unknown, despite their important role in the benthic ecosystem. Many heterotrophic protists (Protozoa) are major grazers of bacterial, algal and other protozoan production, facilitate remineralization of detritus deposited from the water column by recycling nutrients, and at the same time constitute a food source for higher trophic levels (e.g. Patterson, *et al.*, 1989, Hamels, *et al.*, 2001, Dopheide, *et al.*, 2008, Caron, 2009). In addition, nothing is known about the impact of metal mobilization (as a consequence of phytoplankton deposition) on the structure and diversity of microeukaryotic communities. During a previous study (Pede, *et al.*, chapter 2), we documented microeukaryotic communities from contrasting sediment types (silty contaminated vs. sandy subtidal sediments) in the BCZ. Eukaryotic diversity was dominated by Stramenopila (mainly diatoms), Metazoa and Fungi, and to a lesser degree by Protozoa (Alveolata, Rhizaria, Amoebozoa) when using a PCR-DGGE approach based on general eukaryotic primers. However, using ciliate-specific primers for the construction of a clone library, a high ciliate diversity could be observed in the silty, metal-contaminated sediments, suggesting that the use of general eukaryotic primers seriously underestimates protozoan diversity (Pede, *et al.*, chapter 2). While microeukaryotic community structure was

significantly different between the two sediment types, no independent impact of the metals on the variation in microeukaryotic diversity and community structure could be observed.

Here we focus on seasonal and vertical changes in microeukaryotic communities in a silty, metal-contaminated sediment before, during and after the deposition of a spring phytoplankton bloom, with special emphasis on the impact of trace metal behaviour on their diversity and structure. We use the DGT technique (= Diffusive Gradient in Thin Films) to study the bioavailable metals in the sediment porewaters at high (mm-scale) vertical resolution (Davison & Zhang, 1994, Gao, *et al.*, 2009). We hypothesize that (1) strong seasonal and vertical changes in microeukaryotes can be detected as a consequence of algal bloom deposition, and that (2) mobilization of trace metals and resulting changes in their bioavailability have an independent impact on the microbial communities. A detailed description of the metal profiles and fluxes from February to May 2008 in the study site can be found in Gao, *et al.* (2009). Here, microeukaryotic communities, trace metals and other environmental and biotic variables were monitored between February and July 2008, encompassing a period of intense phytoplankton blooms. The molecular fingerprinting technique Denaturant Gradient Gel Electrophoresis (DGGE) was used, targeting small subunit (SSU) rDNA. DGGE has been proven to be an effective tool for monitoring dynamics and discriminating changes in microbial communities in response to environmental heterogeneity (e.g. Casamayor, *et al.*, 2002), and allows for the processing of large numbers of samples in a cost effective and relatively fast way (Muyzer, *et al.*, 1993, Muyzer & Smalla, 1998).

Materials and methods

Sample collection

On the basis of a previous study (Pede, *et al.*, chapter 2), a silty, trace metal-contaminated subtidal sediment (station 130) in the Belgian Coastal Zone (BCZ) was selected for the present study. The main characteristics of the station are given in table 1. Median grain size (μm) and the quantity of fine fraction (mg) in 500 mg of sediment were obtained from this previous study (see Pede, *et al.*, chapter 2). Sampling was performed monthly between February and July 2008.

Parameters	
Coordinates	51°16.25N-02°54.30E
Water depth (m)	12.90
Water temperature (°C)	7.25 (Fe)- 7.59 (Ma) –8.4 (Apr) 13.82 (May) - 16.48 (Jn)-18.2 (Jl)
MGS (µm)*	36.4 ±10.9
QFF (mg)*	0.17 ± 0.04
Salinity (psu)	31.9 ±7.8

* from Pede, *et al.*, chapter 2

Table 1: General physico-chemical parameters of station 130. MGS: Median Grain Size (± SD); QFF, quantity of fine fraction (< 150 µm) in 500 mg sediment (± SD); Fe, February; Ma, March; Apr, April; Jn, June; Jl, July

Sediments were sampled using a Reineck corer (diameter 30 cm) onboard RV 'Zeeleeuw'. Subcores were obtained using plastic cores (diameter 3 cm; length 11 cm). From each Reineck core (n=2), one subcore was used for molecular analyses (DGGE), and one for pigment analyses (chlorophyll *a*; CHL *a*). Whole cores were immediately frozen in liquid nitrogen and subdivided in 1 cm sections (up to 10 cm depth) in the lab. Sediment samples were stored at -80°C until further analysis. Larger subcores (diameter 7-10 cm) were taken for the determination of metals, sulphides, and microelectrode (oxygen, pH, redox potential Eh) analyses. Metal concentrations were not measured in June. After the micro-electrode analyses, one larger subcore was cut vertically, and sediment for bacterial biomass determination (DAPI counts) was collected every cm down to 10 cm. These subsamples were fixed with an equal volume of 4% paraformaldehyde and stored in darkness at 4°C until further processing.

Water samples for CHL *a* measurements were collected in the surface water layer and near the sediment-water interface to monitor the phytoplankton bloom. A volume of 200 ml was filtered on Whatman GF/F glass microfiber filters (42 mm) using a vacuum pump, and the filters were stored at -20°C until further processing.

Environmental parameters

CHL *a* in the sediments was measured after freeze-drying of the sediment, and expressed in µg g^{-1} sediment dry weight (SDW). Pigments were extracted in 90 % acetone and analyzed using HPLC as described before (Wright, *et al.*, 1991). CHL *a* in the seawater was measured following the protocol described by Aminot & Rey (2000). Filters were thawed, and pigments were extracted with 5 ml of acetone:water (9:1) during 12h. CHL *a* was then measured with a

spectrophotometer (a scan was made between 600-750 nm, without and with HCl), and expressed in $\mu g\ L^{-1}$.

Oxygen, pH and Eh in the sediments were determined using microelectrodes with a resolution of 0.1 cm (oxygen) and 1 cm (pH and Eh); dissolved sulphide concentrations using a DGT-AgI probe (resolution 0.03 cm) and porewater trace metal concentrations using DGT probes (resolution 0.5 cm). For the present study, average values were calculated for every cm section. A detailed description of all these methods is given by Gao, *et al.* (2009). The DGT technique (diffusive gradient in thin films) is a gel-based method that allows *in situ* sampling of porewaters while preventing disturbance of sediments and oxidation artefacts (Davison & Zhang, 1994). In short, it makes use of a diffusive boundary layer backed-up with a resin layer, which functions as a pump and can make a distinction of metal species according to their size (only the species <5nm enter the diffusive gel). In this way, only the labile, bioavailable metal fraction in the sediment porewaters was measured (Davison & Zhang, 1994). Metals measured include Pb, Cr, Mn, Fe, Co, Ni, Cu and As.

Microbial parameters

Bacterial biomass

Bacterial biomass (BM_{bact}) was calculated based on DAPI-stained (4'6-diamidino-2-phenylindole) cell counts, and expressed as the number of bacteria in 500 mg of sediment (wet weight) (see Gillan & Pernet, 2007, and Gillan, et al., suppl. 1 for more details).

Microeukaryotic diversity and composition: Denaturing Gradient Gel Electrophoresis (DGGE)

Genomic DNA was extracted from approximately 2-5 g of sediment using zirconium beads and phenol according to the protocol of Zwart, *et al.* (1998), after elimination of the extracellular DNA by the method of Corinaldesi, *et al.* (2005). Extracted DNA was purified using a Wizard column (Promega) and nucleic acids were stored at -20°C until analysis.

PCR, DGGE and fingerprint analyses were performed as described in Pede, *et al.* (chapter 2). Briefly, the DNA extracted from the sediment was amplified for DGGE analysis using the PCR procedure described in Muyzer, *et al.* (1993) by use of the general eukaryotic primers 1427f-GC and 1637r designed by van Hannen, *et al.* (1998), which amplifies a fragment of the 18S rDNA approximately 210 bp long. Equal amounts (500 ng) of PCR product were

loaded on a 7% (w/v) polyacrylamide gel with a linear 30 to 55% denaturant gradient. After electrophoresis, gels were stained and fingerprints were visualized under UV illumination. Distinct DGGE bands were excised, purified, and sequenced using an ABI 3130XL Genetic Analyzer (Applied Biosystems) and sequences were compared with the NCBI GenBank Database (www.ncbi.nlm.nih.gov) using the nucleotide-nucleotide Basic Local Alignment Search Tool (BLAST), to identify the most closely positively identified phylotype (i.e. higher similarities to e.g. environmental but unidentified sequences are not shown). The partial 18S rRNA sequences of this study are available upon request from the corresponding author.

DGGE fingerprints were digitally photo-documented and further analysed using BioNumerics 5.10 (Applied Maths BVBA, Belgium), as described earlier (Pede, *et al.*, chapter 2). Fingerprints were aligned (i.e. bands from the same position relative to the position of marker bands included in each gel were grouped into band classes). Sequence information of the excised bands was used to check the grouping of bands into the correct band classes. Each band class theoretically represents a unique phylotype, i.e. a single organism in the microbial eukaryotic assemblage (referred to as Operational Taxonomic Unit, OTU). In some cases however, different bands (~DNA sequences) can co-migrate the same distance on the DGGE gel, and one OTU can yield different phylotypes (referred to as 'mixed OTUs'). These mixed OTUs are a well-known phenomenon for DGGE (Muyzer & Smalla, 1998). The intensity of the DGGE bands reflects the relative contribution of the OTU to the overall community composition within a sample; the intensity of each band was expressed as a proportion of the total sample (lane) intensity, thus standardizing any loading differences. A matrix was constructed based on the relative intensities of the OTUs in each lane. This matrix represented the total microeukaryotic community composition. A second, smaller matrix was constructed with only the OTUs representing protozoan sequences (also the mixed OTUs including one or more protozoan sequences), representing the protozoan community. Per sample, protozoan abundance values were rescaled to 100 %. These matrices were used for the data analyses described below.

Microeukaryotic and bacterial diversity

Shannon diversity index (H') was calculated for microeukaryotic (H'_{euk}) and protozoan community (H'_{prot}) based on the relative intensities (~abundances) of the OTUs in the fingerprint profiles, using the following formula: $H' = -\sum_{i=0}^{S} pi * \ln(pi)$, where S is the total number of OTUs in the respective sample (=species richness) and p_i is the relative abundance

of the *i*th OTU. As the index takes into account relative abundances, it provides a better estimate of the diversity than species richness alone.

By analogy, bacterial diversity (H'_{bact}) was determined after DNA extraction, PCR amplification and DGGE analysis as described in Gillan, *et al.* (subm., suppl. 1).

Statistical analysis

Univariate analysis

Two-dimensional plots of selected environmental parameters (CHL *a*, Eh, pH, sulphides, and the metals Co, Pb, Ni, As, Fe, and Mn) and microbial parameters (H'_{bact}, BM_{bact}, H'_{euk} and H'_{prot}) against sampling month were made using SigmaPlot version 11 software. Filled Contour Plots were constructed based on one value [single values for CHL *a*, Eh, pH and the microbial parameters, and average values for dissolved sulphides (n = 33) and metal concentrations (n = 3)] per cm sediment depth for every month.

Pearson correlation analyses were used to assess the relationship between H'_{euk} and H'_{prot}, the relative abundance of selected protozoan OTUs, and the selected environmental variables (trace metals, BM_{bact} and H'_{bact}, Eh, pH and sulphide concentrations). Metal concentrations, BM_{bact} and relative abundances of the protozoan OTUs were log-transformed and dissolved sulphides were square-root transformed prior to analyses.

Multivariate analysis

The computer package PRIMER 6 (Clarke & Gorley, 2006) -with permutational analysis of variance (PERMANOVA) + add-on (Anderson, *et al.*, 2008)- was used for all non-parametric multivariate analyses. Analyses were performed in parallel for microeukaryotic and protozoan communities based on the DNA-based species abundance data matrices (cf. above). Relative species abundances were log (x+1) transformed and averaged for both replicates (n=2) prior to analyses. Bray-Curtis similarity based on these data matrices formed the basis of the multivariate analyses described below. Temporal and vertical differences in microbial community structure were examined according to the two-way crossed design using PERMANOVA, with 9999 permutations of residuals under a reduced model. Patterns in the community structure were visualized by Principal Coordinates Analysis (PCO). PCO is a distance-based ordination method that maximizes the linear correlation between the distances in the distance matrix (based on a Bray-Curtis similarity), and the distances in a space of low

dimension (~ the ordination; the 2 main axes were selected and shown). July samples for 0-1 cm and 1-2 cm of depth formed gross outliers and were not included in the analyses. The relationship between the variation patterns in community composition and measured explanatory (environmental and microbial) parameters were assessed by entering these variables as supplementary variables in the PCO ordinations, using the Spearman correlation coefficient. The set of explanatory variables included Eh, pH, CHL *a* in the sediment, dissolved sulphides, metal concentrations of Mn, Fe, Co, Pb, As, Ni, Cu and Cr, and the bacterial parameters H'_{bact} and BM_{bact}. Trace metals, BM_{bact} and CHL *a* were log-transformed, and sulphides fourth-root-transformed prior to analyses. Only variables that correlated significantly ($p<0.05$) and had R values > 0.5 with one of the first two axes were shown in the diagrams. Month (Julian date) and depth (0 → 10 cm) are introduced as ordinal variables. Note that as no trace metal data were available for June, PCO analyses were first performed for all samples and supplementary explanatory variables except metals, and then again for the selected set of samples for which metal data were available (so excluding June). June sample data were also excluded from all other analyses including the trace metals.

The relationship between the microeukaryotic and protozoan data and explanatory variables was further studied using the DISTLM routine (McArdle & Anderson, 2001). This technique allows partitioning variation in community data into the different components (related to different sets of explanatory variables). This variance partitioning thus allows separating the pure effects of each component and their joint effects. DISTLM is a distance-based multivariate multiple regression modelling tool for analysing and modelling the relationship between a multivariate data cloud (DGGE relative abundance matrix) described by a resemblance matrix based on Bray-Curtis similarities, and the explanatory variables measured for the same set of samples. *P*-values of testing the null-hypothesis (=no relationship between explanatory variables and community composition) were obtained using 9999 permutations of normalized and log-transformed data. Moreover, the DISTLM routine provides a quantitative measure of the variation explained by one or more predictor variables. The marginal test is based on the relationship between the respective variable and the microbial data cloud, while in the sequential test the amount of variance explained by each environmental parameter added to the model is conditional on the variability already in the model (forward selection procedure using the R^2 selection criterion). The predictor variable with the best value for the selection criterion was chosen first, followed by the variable that, together with the first, improves the selection criterion the most, and so on. All above-mentioned transformed

explanatory variables were used in this analysis. The explanatory variables were divided in 2 groups: all explanatory variables except metals, and metals separately. Only a subset of variables, i.e. those variables (per group) which contributed significantly to explaining the variation in the phylotype data based on the forward selection, were used in the DISTLM analyses. Then a series of DISTLM analyses using the all-specified selection procedure were performed to decompose the variance in the community data and partition the variation into the different components (with only the selected variables). This variance partitioning allowed separating the pure effects of each component and their joint effects.

Results

Environmental variables

CHL *a* concentrations in the water column (both surface and above the sediment) showed a small peak in March, followed by a higher peak in May with values up to 105 μg L^{-1} (Fig. 1). CHL *a* in the upper sediment layers roughly followed the same trend but showed a distinct lag with respect to the CHL *a* in the water column, with concentrations being highest during summer (June-July, with up to 23 μg g^{-1} SDW). Relatively high CHL *a* concentrations were also measured in the deeper sediment layers, even during winter (Fig. 1B). The silty sediments were largely anoxic, with the oxic layer becoming more shallow in May (1 mm) then in winter (3 mm) (data not shown, see Gao, *et al.*, 2009; data for June and July are lacking). Eh values peaked in March and especially in June, in the top sediment layer; pH showed a similar pattern but in June, pH values were high across the whole sampled depth, especially in the deeper layers (Fig. 2). Dissolved sulphides were low in spring, but reached peak concentrations up to 400 μM in June and July (Fig. 2), except in the top and bottom sediment layers.

Depth profiles for the trace metals Pb, Mn, Fe, Co, Ni, Cr, Cu and As as measured using the DGT technique are shown in Fig. 3. Porewater concentrations for Cu were relatively stable except for one peak in the deeper sediment layers in April. The other bioavailable metals were generally higher in subsurface sediment layers in winter (February-March), were always low in April, and increased again in the surface and subsurface layers in May (Co, Fe, Mn) and July (Mn). Note that values of Pb, Cr and Ni were also higher in the deeper layers (5-10 cm) in February-March. Pb, Cr and Ni remained low in spring-summer, except for slightly elevated values at 4-5 cm depth in May. Unfortunately, no metal data are available for June.

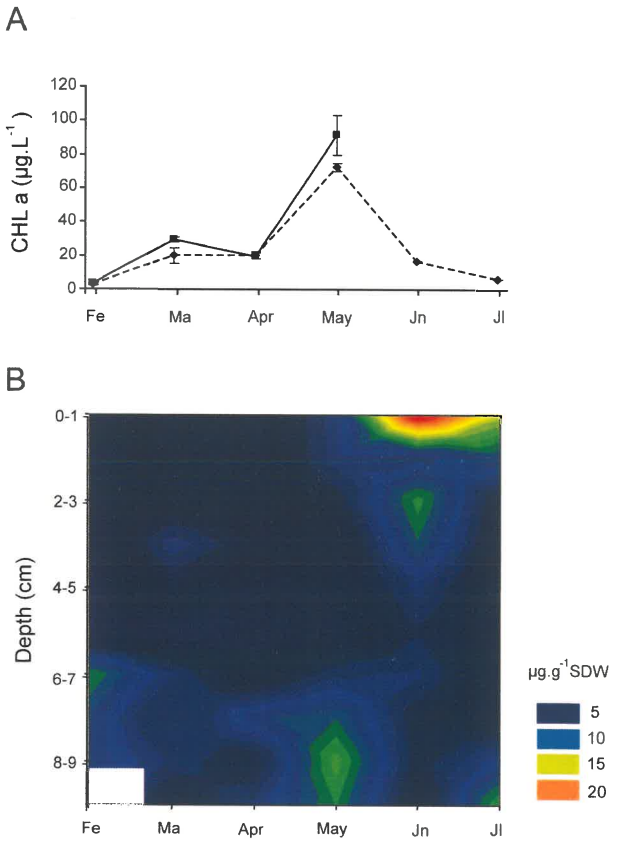

Figure 1: A: CHL *a* concentrations in the water column (±SD, n=3, except Jn and Jl, n=1) in the surface water (full line) and just above the sediment (dotted line), and B: two-dimensional spatio-temporal representation of CHL a concentrations in the sediment in the period February to July 2008. White: missing values. SDW, sediment dry weight

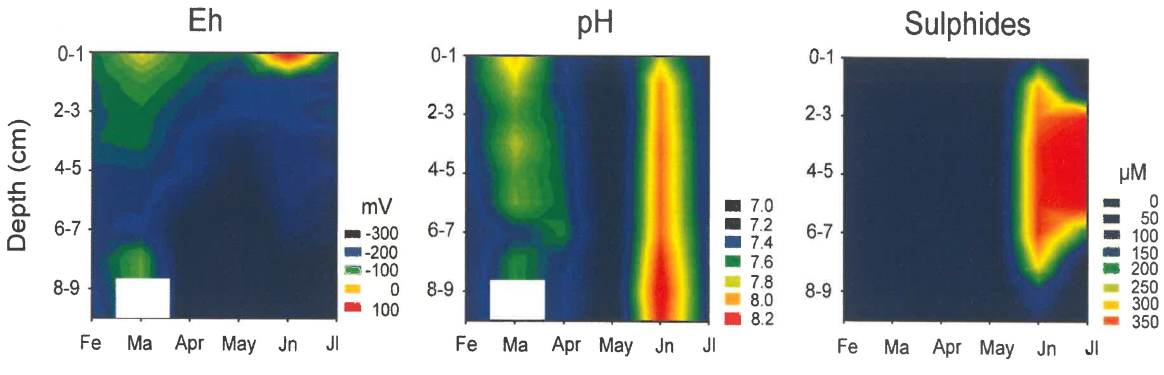

Figure 2: Vertical variation (0-10 cm) in redox potential (Eh), pH and dissolved sulphide concentration in the period February-July 2008 in station 130. White = missing values.

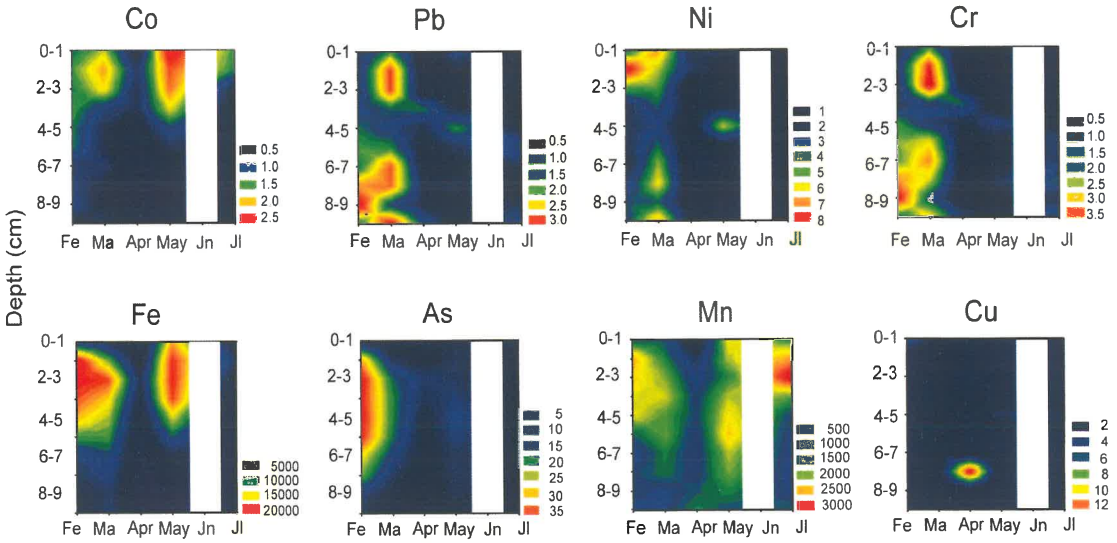

Figure 3: Vertical distribution (0-10 cm) of concentrations (µg L^{-1}) of the trace metals Co, Pb, Ni, As, Mn, Cu, Cr and Fe as measured by the DGT technique in the period February-July 2008 in station 130. White = missing values.

Microbial variables: biomass and diversity

BM_{bact} ranged from 2.31 - 30.3 x 10^7 cells in 500 mg of (wet) sediment and peaked in the upper sediment layer in June (Fig. 4). H'_{bact} ranged between 0.7 - 1.2 (species richness 6-16 OTUs per lane) and was highest in subsurface layers (1-3 cm) in May and July (Fig. 4). The number of OTUs in the microeukaryotic profiles varied between 44 and 66 per lane. H'_{euk} was highest (throughout the sediment core) in February and, to a lesser degree, in June. H'_{prot} resembled the pattern shown by the total microeukaryote diversity, but was also high in the surface (March) and subsurface (April-May) sediment layers. H'_{euk} was significantly correlated with BM_{bact}; H'_{prot} was negatively correlated with H'_{bact} (Table 4). Both H'_{euk} and H'_{prot} were significantly positively correlated with different trace metal concentrations (Pb, Cr, Fe and As, and Cr, Fe, Co, Ni and As respectively) and redox potential (Eh); no correlation was found with sediment CHL *a* concentrations (Table 5). BM_{bact} and H'_{bact} were also not correlated with CHL *a* (data not shown).

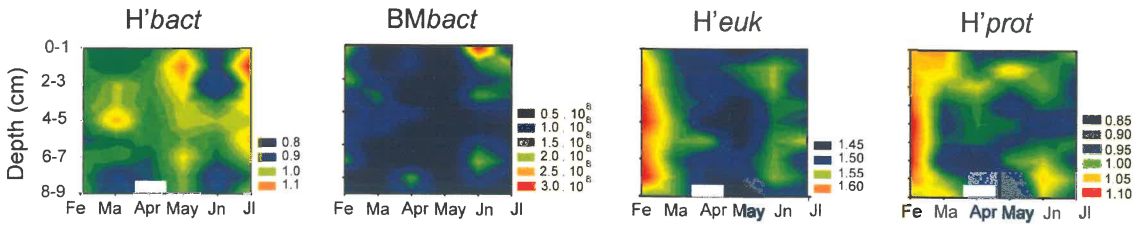

Figure 4: Vertical distribution (0-10 cm) of bacterial diversity (H'_{bact}) and bacterial biomass (BM_{bact}, number of bacteria in 500 mg of sediment; wet weight), and microeukaryotic (H'_{euk}) and protozoan (H'_{prot}) diversity expressed by the Shannon Index, based on DGGE profiles of DNA extracted from sediment sampled in the period February-July 2008 in station 130. White = missing values.

Microeukaryotic community composition

Seventy bands excised from the microeukaryotic DGGE gels were sequenced, resulting in 40 unique sequences (99% similarity cut-off) which represent 46% of the 87 OTUs and account for 71% of total relative abundance in the total DGGE matrix. BLAST analyses of the sequences are listed in Table 2. Relatives of alveolates (ciliates, dinophytes), amoebozoans, Rhizaria (acanthareans, cercozoans, foraminiferans), Stramenopila (diatoms, oomycetes, *Pirsonia*), Chlorophyta, Fungi and metazoans (nematodes and gastrotrichs) were found. throughout the sampling period, Stramenopila (mainly diatoms) were the dominant group in terms of diversity (not shown) and relative abundance (Fig. 5), followed by Alveolata, Rhizaria and Metazoa. When averaged across all depths, no pronounced seasonal in the relative abundances of the higher-level phylogenetic groups could be observed (not shown). However, when only considering the top 0-2 cm, it is clear that diatoms are relatively more important in March and May, and relatively decrease in summer, when Rhizaria and Metazoa become more important (Fig. 5). Fungi decreased from February to July. Amoebozoa abundance was always very limited (<0.5%; but only 1 Amoebozoa-related sequence).

Table 2: Identification of microeukaryotic DGGE bands. Only the first *identified* BLAST match is given. %Sim, percentage of similarity; bp, basepair; ID, identification used in further multivariate analyses. The Protozoa are indicated in grey.

ID	BLAST result (accession number)	Phylogenetic affiliation	%Sim	bp
CIL85	Acineta sp. (AY332718)	Alveolata; Ciliophora; Phyllopharyngea	94	131
CIL106	Acineta sp. (AY332718)	Alveolata; Ciliophora; Phyllopharyngea	90	158
CIL141	Strombidium sp. (AY43564)	Alveolata; Ciliophora; Spirotrichea	98	147
DINO25	Uncultured dinoflagellate clone (GU820002)	Alveolata; Dinophyceae	99	154
DINO39	Amphidinium longum (AF274254)	Alveolata; Dinophyceae; Gymnodiniales	100	149
DINO59	Uncultured dinoflagellate clone (HM103502)	Alveolata; Dinophyceae	100	150
DINO171*	Uncultured dinoflagellate clone (GU820592)	Alveolata; Dinophyceae	99	157
DINO227	Gymnodinium sp. (HQ270473) / Dissodinium sp. (FJ473379)	Alveolata; Dinophyceae	99	158
AMOE187	Paramoeba eilhardi (AY686575)	Amoebozoa; Flabellinea; Dactylopodida	91	159
ACAN84	Uncultured marine acantharean (AF290072)	Rhizaria; Acantharea	94	123
ACAN237	Uncultured marine acantharean (AF290072)	Rhizaria; Acantharea	93	138
CERC58	Protaspis sp. (FJ824124)	Rhizaria; Cercozoa; Silicofilosea	93	146
CER89	Uncultured cercozoan clone (HM103468)	Rhizaria; Cercozoa	100	144
CERC165	Thaumatomastix sp (GQ144681)	Rhizaria; Cercozoa; Silicofilosea	92	143
CERC173	Uncultured cercozoan clone (HM103468)	Rhizaria; Cercozoa	98	145
CERC183	Uncultured cercozoan clone (HM103504)	Rhizaria; Cercozoa	96	155
CERC188	Arachnula sp. (EU853660) / Platyreta sp. (AY941201) / Theratromyxa sp. (GQ377666)	Rhizaria; Cercozoa; Vampyrellidae	92	144
FORA184	Ammonia beccarii (ABU07937)	Rhizaria; Foraminifera; Rotaliina	98	159
FORA234	Ammonia beccarii (ABU07937)	Rhizaria; Foraminifera; Rotaliina	96	103
OOM35	Achlya apiculata (AJ238656)	Stramenopila; Oomycetes; Saprolegniales	90	155
PIRS74*	Pirsonia sp. (AJ561114)	Stramenopila; Pirsonia	96	156
BACI5*	Extubocellulus / Minutocellus / Hyalosira ./e.a.	Stramenopila; Bacillariophyta; Mediophyceae	100	144
BACI6 – 33*	Skeletonema / Thalassiosira / Cyclotella / e.a.	Stramenopila; Bacillariophyta; Coscinodiscophyceae	100	143
BACI7- 164*	Minidiscus / Stephanodiscus / Cyclostephanos/ e.a.	Stramenopila; Bacillariophyta; Coscinodiscophyceae	100	150
BACI8-105	Rhaphoneis sp. (HQ912673) / Delphineis sp. (HQ912629)	Stramenopila; Bacillariophyta; Fragilariophyceae	100	143
BACI9	Skeletonema sp. (AB630061)	Stramenopila; Bacillariophyta; Coscinodiscophyceae	95	152
BACI10*	Thalassiosira sp. (DQ514891)	Stramenopila; Bacillariophyta; Coscinodiscophyceae	100	149
BACI22*	Ditylum brightwellii (FJ266034)	Stramenopila; Bacillariophyta; Mediophyceae	100	151
BACI57*	Odontella aurita (EU818943)	Stramenopila; Bacillariophyta; Mediophyceae	96	155
BACI63	Isthmia sp. (HQ912684)/ Psammoneis sp. (AB433341) / Neofragilaria sp. (AB433340)	Stramenopila; Bacillariophyta; Mediophyceae	95	130
BACI87*	Pleurosira laevis (HQ912585)	Stramenopila; Bacillariophyta; Mediophyceae	94	154
BACI118*	Odontella aurita (AY485522) / Cerataulus smithii (HQ912666)	Stramenopila; Bacillariophyta; Mediophyceae	98	153
CHLOR38	Halosarcinochlamys cherokeensis (DQ009780)	Viridiplantae; Chlorophyta; Chlorophyceae	92	138
CHLOR117*	Choricystis sp. (AY195970) / Nannochloris sp. (AB080306)	Viridiplantae; Chlorophyta; Trebouxiophyceae	99	146
FUNG50*	Uncultured Saccharomycetales isolate (HM449795)	Fungi; Ascomycota	99	145
FUNG115	Urophlyctis sp. (HQ888719)	Fungi; Blastocladiomycota	95	147
FUNG180	Massaria sp. (HQ599458)	Fungi; Ascomycota	94	138
MET51-76-81*	Sabatieria pulchra (FJ040466)	Metazoa; Nematoda; Chromadorea	100	154
MET126	Chaetonotus neptuni (AM231774)	Metazoa; Gastrotricha;Chaetonotida	98	142
MET196*	Chaetonotus neptuni (AM231774)	Metazoa; Gastrotricha; Chaetonotida	97	141
MET111	Procephalothrix sp. (GU227067)	Metazoa; Nemertea; Anopla	100	151

* identical sequences detected during a previous study (Pede, *et al.*, chapter 2)

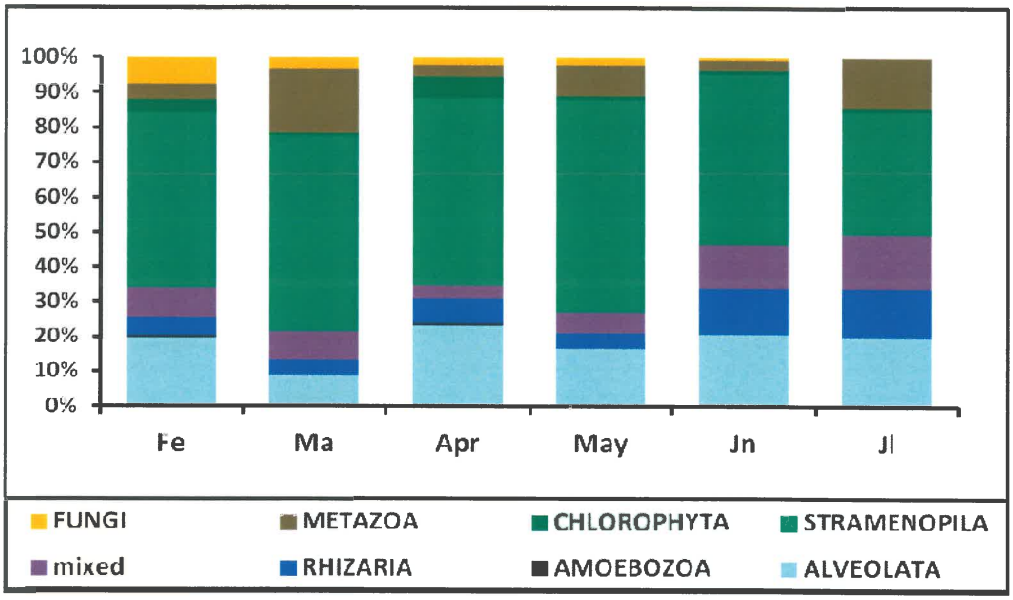

Figure 5: Seasonal variation of the different phylogenetic groups in the top sediment layers (0-2cm depth) in the period February-July 2008, based on relative abundances in the DGGE fingerprint profiles. 'mixed' refers to 3 mixed OTUs.

Microeukaryotic and protozoan community dynamics in relation to measured microbial and environmental variables

Microeukaryotic community structure displayed pronounced variation with sediment depth and month (Fig. 6), with surface samples mainly located in the lower right part of the diagram. Community composition changes from February (top right) to May (bottom left), after which community structure more or less reverts to its spring composition. Variation with both time and depth was significant (2-way PERMANOVA, Fig. 6C; $p<0.001$), and was strongly correlated with Eh (both depth and time) and H'_{bact} (time). The interaction factor 'month x depth' was not significant. Variation with depth was most pronounced for two diatoms (BACI10, BACI5), a dinophyte (DINO171), a Ciliate (CIL85), three Metazoa (MET70, MET81, MET111), etc. (see Fig. 6), while the temporal shift in community structure was mainly driven by the relatively higher abundances of diatoms (e.g. BACI6, BACI7, BACI8, BACI9-33, BACI105, BACI164; Fig. 6B) in late spring/early summer, and also the higher abundances of Fungi (FUNG50, FUNG180), an Amoeba (AMOE187) and a Cercozoa (CERC188). Variation patterns in protozoan community structure were consistent with those of the total microeukaryotic community (Fig. 7, Table 3), with the first axis representing a gradient in OTU composition with depth, and the second axis with time. Note

however that the late winter and spring samples are less distinct, and that communities in June strongly resemble those from spring. Variation with depth was most pronounced for e.g. one ciliate (CIL85), while temporal variation was mainly driven by several Cercozoa (CERC58-59, CERC188), an Amoeba (AMOE187), a Dinophyte (DINO171), etc. (Fig. 7).

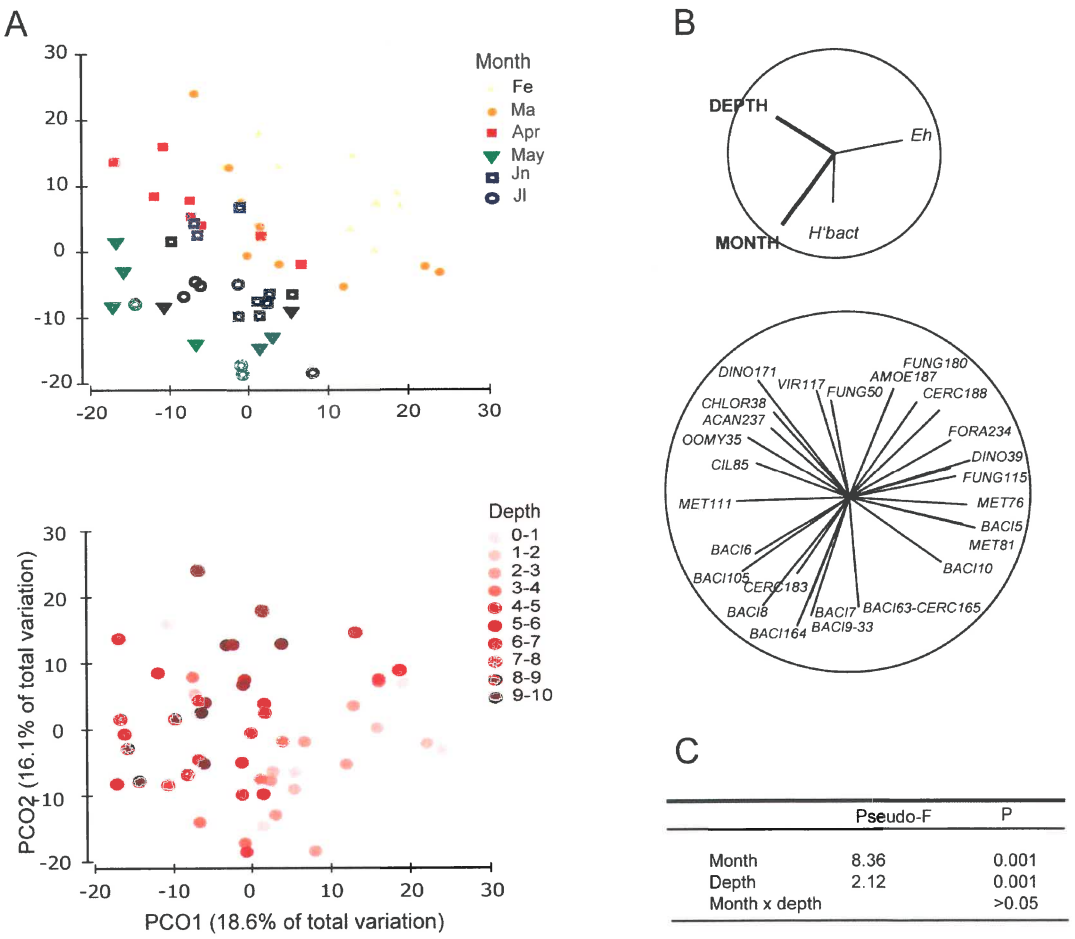

	Pseudo-F	P
Month	8.36	0.001
Depth	2.12	0.001
Month x depth		>0.05

Figure 6: A; Principal Coordinate Analysis (PCO) based on the total microeukaryote data set (the July data for 0-1 and 1-2 cm were omitted due to their outlier position). Percentage of variance explained by individual axes is reported. B; explanatory variables (metals not included) and OTUs (only identified bands; for labels see Table 2) which are significantly ($p < 0.05$) correlated (with $R > 0.5$) to one or both axes. Vectors DEPTH and MONTH (in bold) are based on ordinal variables, 0-10 cm and Julian date respectively. C; p and F-values for 2-way-PERMANOVA results for factor month and depth. H'_{bact}, bacterial diversity expressed by the Shannon Index.

* BACI63-CERC165 is a mixed band classis.

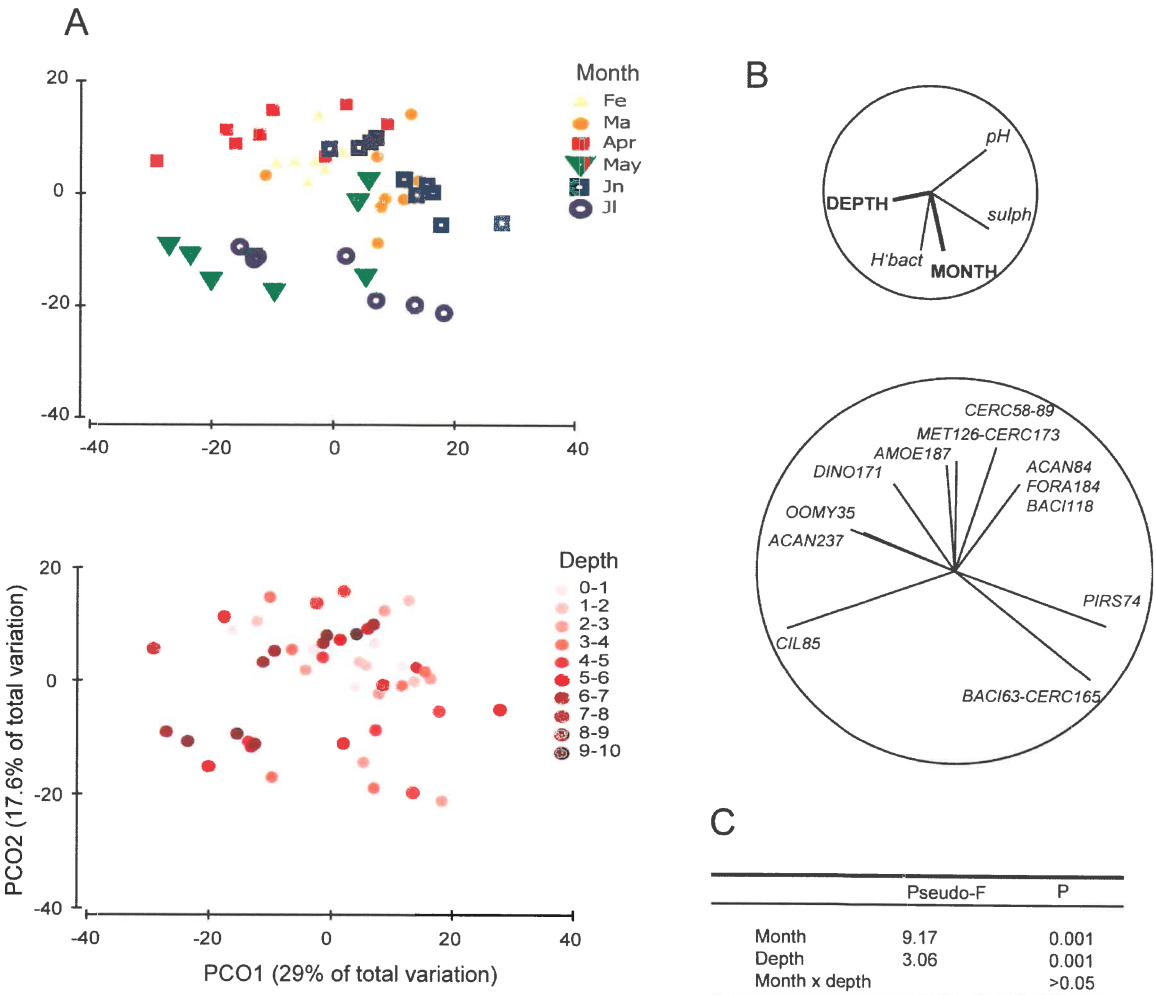

C

	Pseudo-F	P
Month	9.17	0.001
Depth	3.06	0.001
Month x depth		>0.05

Figure 7: A; Principal Coordinate Analysis (PCO) based on the Protozoa data set (the July data for 0-1 and 1-2 cm were omitted due to their outlier position). Percentage of variance explained by individual axes is reported. B; explanatory variables (metals not included) and OTUs (only identified bands; for labels see Table 2) which are significantly ($p < 0.05$) correlated (with $R > 0.5$) to one or both axes. Vectors DEPTH and MONTH (in bold) are based on ordinal variables, 0-10 cm and Julian date respectively. C; p and F-values for 2-way-PERMANOVA results for factor month and depth. H'_{bact}, bacterial diversity expressed by the Shannon Index; sulph, dissolved sulphides

* BACI63-CERC165, MET126-CERC173 and ACAN84-FORA184-BACI118 are mixed band classes.

Results of the DISTLM analyses for total microeukaryotic communities and protozoan communities are shown in Table 3. When considered separately, all explanatory variables, except for CHL *a* and Cu (microeukaryotes), and CHL *a*, BM_{bact}, Ni and Cu (Protozoa) were significantly correlated to the community structure. Eh and Co, and to a lesser degree pH, sulphides and bacterial diversity, showed the strongest relation with community structure, both in the total microeukaryotic as in the protozoan communities. When considering only the top sediments (0-2 cm) of the protozoan communities, CHL *a* could significantly ($p<0.05$) explain as much as 17.4 and 21.7% of the microeukaryotic and protozoan variation respectively (not shown). The forward selection procedure (sequential tests) selected smaller sets of explanatory variables (due to correlation between several variables), which together significantly explained 61.5 and 61.6 % of the variation in the total microeukaryotic and the protozoan communities respectively. Again, Eh, sulphide concentration and Co were the most important variables explaining the variation in community structure.

The PCO's in figure 8 were constructed only with samples for which metal data were available (June excluded). Overall patterns in the microbial communities were consistent with patterns observed in Figs. 6 & 7. These diagrams confirmed that the highest bio-available metal concentrations were observed in the upper sediment layers, and that all metals except Mn were low in summer (July). Metal concentrations (except Mn) covaried with Eh and pH, and BM_{bact}, while Mn covaried with the concentration of dissolved sulphides. H'_{bact} was significantly related ($p < 0.05$) to Cr (-0.32), pH (-0.43) and dissolved sulphides (0.45), while BM_{bact} was related to Co (-0.40) and pH (0.32) (not shown).

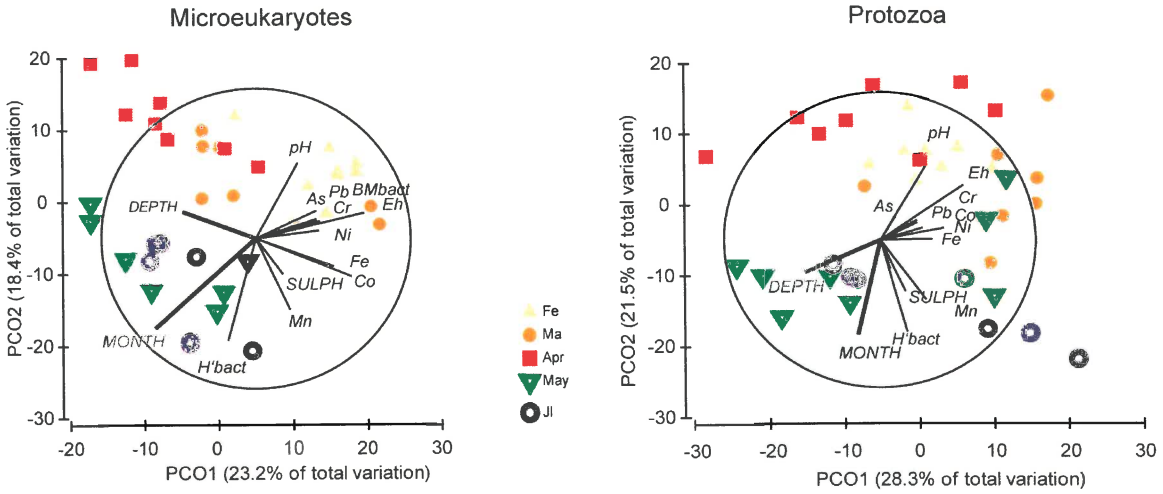

Table 3: Results of DISTLM multiple regression analysis for microeukaryotic and protozoan (June not included) communities: for marginal and sequential tests, see text. H'_{bact}, bacterial diversity expressed by the Shannon Index; BM_{bact}, bacterial biomass; SULPH, dissolved sulphides; CHL *a*, chlorophyll *a*.

Marginal test				Sequential test			
Variable	Pseudo-F	P	Proportion of variance	Variable	P	Proportion of variance	Cumulative variance
Microeukaryotes							
CHL *a*	1.312	0.2045	0.034	Eh	**0.0001**	0.147	0.147
H_{bact}	4.179	**0.0002**	0.101	SULPH	**0.0001**	0.105	0.252
BM_{bact}	3.015	**0.0023**	0.075	Co	**0.0001**	0.115	0.367
Eh	6.398	**0.0001**	0.147	As	**0.0001**	0.070	0.437
pH	4.277	**0.0001**	0.104	Fe	**0.0002**	0.050	0.482
SULPH	4.298	**0.0001**	0.104	pH	**0.0018**	0.039	0.521
				Pb	**0.0008**	0.041	0.562
Pb	2.775	**0.0034**	0.070	H_{bact}	**0.0144**	0.028	0.591
Cr	2.836	**0.0038**	0.071	Ni	**0.0443**	0.023	0.614
Mn	3.059	**0.0004**	0.076	Mn	0.0938	0.020	0.633
Fe	3.950	**0.0007**	0.096	Cu	0.3827	0.014	0.647
Co	5.714	**0.0001**	0.134	CHL *a*	0.7214	0.010	0.657
Ni	2.986	**0.0032**	0.075	Cr	0.9424	0.068	0.664
Cu	1.004	0.4243	0.026	BM_{bact}	/		0.664
As	2.997	**0.004**	0.075				
Protozoa							
CHL *a*	1.13	0.3273	0.030	Eh	**0.0001**	0.146	0.146
H_{bact}	4.99	**0.0001**	0.119	H_{bact}	**0.0001**	0.123	0.268
BM_{bact}	1.73	0.1064	0.045	SULPH	**0.0001**	0.087	0.355
Eh	6.30	**0.0001**	0.146	Co	**0.0001**	0.087	0.442
pH	4.70	**0.0003**	0.113	Pb	**0.0102**	0.039	0.481
SULPH	4.74	**0.0001**	0.114	pH	**0.0073**	0.041	0.523
				Ni	**0.0104**	0.037	0.560
Pb	2.34	**0.0283**	0.060	As	0.0795	0.025	0.584
Cr	2.33	**0.0264**	0.059	Fe	**0.0188**	0.031	0.616
Mn	3.30	**0.002**	0.082	Cu	0.2589	0.017	0.632
Fe	3.52	**0.0017**	0.087	CHL *a*	0.469	0.013	0.645
Co	4.99	**0.0002**	0.119	Cr	0.964	0.035	0.648
Ni	1.57	0.1375	0.041	Mn	0.995	0.081	0.649
Cu	1.47	0.1711	0.038	Fe	/		0.649
As	2.23	**0.0364**	0.057	BM_{bact}	/		0.649

*P-values <0.05 are indicated in bold

Figure 8 (left): Principal coordinates analysis (PCO) of total microeukaryotic and Protozoa data set for which metal data were available (all months except June; July data for 0-1 and 1-2 cm were omitted due to their outlier position). Spearman correlations are shown only for explanatory variables selected in table 3 (significantly correlated to the microbial dataset according to the marginal test). Vectors DEPTH and MONTH (in bold) are based on ordinal variables, 0 → 10 cm and Julian date respectively. Percentage of variance explained by the individual axes is reported. SULPH, dissolved sulphides; H'bact, bacterial diversity; BMbact, bacterial biomass.

Table 4: Partitioning of the variance in the microeukaryotic (MICROEUK) and protozoan (PROTOZOA) dataset (June not included), for explanatory (EXPL, without metals) and metal (METALS) components (predictor variables), based on the selected variables (per component) which contributed significantly to explaining the variance in the data set. The variation was partitioned into the different components, separating the pure effects of each component (highlighted) after removing the other factor as co-variable, and their joint effects (bold). SULPH, dissolved sulphides; H'_{bact}, bacterial diversity

predictor variable	selected variables	Co-variable	% variance explained		*P*
			MICROEUK	PROTOZOA	
EXPL	*H'_{bact} Eh pH SULPH*	-	38.4	41.4	<0.001
		METALS	21.8	26.9	<0.001
METALS	*Cr Mn Fe Co As*	-	35.7	29.1	<0.001
		EXPL	19.1	14.4	<0.001
			57.5	56.0	

Variation partitioning showed that after fitting the significant explanatory variables except metals, the selected metals alone still explained a significant fraction ($p < 0.001$) of respectively 19.1% and 14.6% in the variation of the microeukaryotic and protozoan communities (Table 4). Spearman correlations (Table 5) showed that several species in particular were significantly related to the metal concentrations, e.g. the dinophyte DINO171 was strongly inversely correlated to Mn, Fe and Co, and the *Paramoeba* AMOE187 to Mn. In general, especially dinophytes, cercozoans and foraminiferan OTUs were most strongly correlated (positive or negative) to metal concentrations, while ciliate abundances like e.g. CIL85 and CIL141 where more affected by Eh, pH and concentrations of sulphides. Strikingly, many protozoan OTUs were related to H'_{bact} but not to BM_{bact} (cf. also Table 3). Only one dinophyte (DINO59) was related to CHL *a*.

Table 5: Pearson's correlation analysis between microeukaryotic and Protozoa diversity (H'_{euk}, H'_{prot}), relative abundances of protozoan OTUs and explanatory variables. For identification of the OTUs, see table 2. Only significant correlations ($p < 0.05$) are shown; Bold : $p \leq 0.01$; Underlined, $p \leq 0.001$. SULPH, dissolved sulphides; H'_{bact}, bacterial diversity; BM_{bact}, bacterial biomass.

			ALVEOLATA								RHIZARIA					AMOE	STRAM		MIXED GROUPS		
	H' *euk*	H' *prot*	CIL 106	CIL 85	CIL 141	DINO 171	DINO 227	DINO 25	DINO 39	DINO 59	CERC 188	CERC 183	CERC 58-89	ACAN 237	FORA 234	AMOE 187	PIRS 74	OOMY 35	ACAN84 FORA184 BACI118	BACI63 CERC165	MET126 CERC78
Pb	0.37		-0.37					0.33			**0.56**	-0.36			0.47				0.36		
Cr	**0.43**	0.37						**0.43**			**0.63**	-0.36			**0.51**				0.35		
Mn						**-0.54**							-0.46			**-0.61**		-0.33			
Fe	0.33	0.35				**-0.41**	0.34				0.39	-0.47			0.40				**0.54**		
Co		**0.44**				**-0.54**	0.48		0.40										**0.59**		
Ni		0.34									0.35	-0.39			**0.46**						
As	**0.60**	**0.43**									**0.57**	**0.65**			0.35				0.45		
Cu																					
BM *bact*	**0.50**						-0.40				0.34						0.37				
H*bact*		-0.38	0.38		0.38	-0.49		-0.39			-0.35	0.33			-0.38	-0.36	0.34			**0.51**	**-0.51**
Eh	0.39	**0.48**		**-0.71**				**0.52**	0.39		0.35				**0.50**		0.36		**0.50**		
pH				**-0.52**		0.35		0.32						-0.38			0.38				0.38
SULPH			**0.42**		**051**	-0.35							-0.36				**0.56**	-0.38	-0.38	032	
CHL*a*										0.36											-0.37

Discussion

In dark, subtidal marine sediments, the deposition of seasonal phytoplankton blooms influences the abiotic and biotic status of the benthic ecosystem (e.g. Jørgensen, *et al.*, 2006, Middelburg & Levin, 2009, Franco, *et al.*, 2010). Freshly deposited algal detritus provides a growth substrate for benthic organisms and has been shown to stimulate bacterial growth (Goedkoop, *et al.*, 1997, Gillan, *et al.*, subm., chapter 4), bacterial and protozoan abundance (Van Duyl, *et al.*, 1992, Gillan, *et al.*, subm., chapter 4), and bacterial and metazoan (a.o. nematode) biomass and respiration (Franco, *et al.*, 2010). Increased mineralisation processes lead to changes in the general biogeochemical status of the sediments (Gao, *et al.*, 2009). In metal-contaminated sediments, changes in the redox status of the sediments can lead to the mobilization of toxic trace metals (Gao, *et al.*, 2009, Pede, *et al.*, chapter 5), which can also potentially affect benthic communities. To date, little is known on how algal bloom deposition impacts the seasonal dynamics and the vertical distribution of benthic microeukaryotic communities, and to what degree observed changes can be related to direct (e.g. organic matter mineralization) or indirect (e.g. metal mobilization) consequences of phytodetritus sedimentation.

Phytoplankton bloom development and deposition

Both the early spring diatom bloom (March) and the intense bloom of the colony-forming haptophyte *Phaeocystis* (May) (Boon, *et al.*, 1998, Rousseau, *et al.*, 2000) were observed in spring 2008 (Fig. 1A.), and were followed by accumulation of algal biomass in the surface sediments up to two months after the major bloom event, witness the enhanced CHL *a* concentrations in the surface layers in May-July (Fig. 1B, cf. also Franco, *et al.*, 2007) and the dominance of planktonic diatom sequences in the molecular fingerprints in May (Figs. 5, 6), most of which (e.g. *Thalassiossira* sp., *Odontella* sp., *Skeletonema* sp.) are typical of the spring phytoplankton blooms in the BCZ (M'Harzi, *et al.*, 1998). Higher CHL *a* concentrations were also observed in the deeper sediment layers (below 6 cm, Fig. 1B). This can be related to the burial and incomplete degradation of the pigments due to the anoxic conditions in the deeper sediment layers (Bianchi, *et al.*, 2000). In addition, a recent study by Veuger & van Oevelen (2011) showed that pigments in dark sediments can degrade very slowly, with some having half lives of $\geq$ 1 yr. Furthermore, the formation of resting stages with retention of photosynthetic pigments, during periods of unfavourable conditions is well-

known for diatoms, and could also explain the higher CHL *a* concentrations in the deeper sediment layers (McQuoid & Nordberg, 2006, Sugie & Kuma, 2008, Chen, *et al.*, 2009). Nothing however is known about long-term preservation of diatom resting stages in the BCZ.

Effect of bloom sedimentation on sediment geochemical parameters

Decomposition of the algal material in the silty sediments leads to consumption of oxygen and hence the rise of the oxygenated surface layer in spring, to the top few mm's of the sediment (Gao, *et al.,* 2009). Due to the feeding and bioturbation by benthic invertebrates, the deposited organic matter is gradually buried into the sediment (Jørgensen, *et al.*, 2006), and further degradation of organic matter in deeper layers occurs (predominantly) under anoxic conditions (Middelburg & Levin, 2009). This can explain the increased dissolved sulphide concentrations in June and July, and the maximum pH values in June (Fig. 2), because sulphide is the main end product of anaerobic respiration in anoxic marine sediments (Fenchel, 1969, Middelburg & Levin, 2009), and precipitation of sulphides can increase the pH of interstitial water in anoxic marine sediments (Ben-Yaakov, 1973). The higher pH and Eh especially in the upper sediment layers in March, and also at the sediment surface in June (Eh), can probably also be explained by enhanced oxygenation by bioturbation and bio-irrigation, resulting from increased metazoan activity (see also higher metazoan abundance in the 0-2 cm layer in March; Fig 5) linked with phytodetrital deposition (mainly in June) (Braeckman, *et al.*, 2011b). However, oxygen concentrations were not measured in June during this study.

Variation in trace metal data for the study site were described by Gao, *et al.* (2009) for the period February-May; in the present study, data for July are included as well. Gao documented upward fluxes for the metals Mn, Fe, Co and also for As, Pb, Ni, Cr and Cu, linked to the sedimentation of the spring algal bloom. This can be related to the metal profiles observed in the sediments (Fig. 3); all metals except Cu were generally high in winter in the subsurface layers, while Co, Fe and Mn had a second peak (and As and Pb a smaller increase) at the sediment surface during the period of intense *Phaeocystis* bloom in May (see Fig. 3). Pb, Cr, and Ni were also higher but only in the deeper sediment layers at this time. A recent microcosm experiment which simulated algal blooms deposition on sediments from the same contaminated site revealed similar results, and indicated the link between upward metal fluxes and increased bacterial activity (Gao, *et al.*, in press., suppl.; Gillan, et al., subm., chapter 4). Dissolved oxygen, redox potential in the surface sediment and dissolved sulphide in the

deeper sediment layers were the main physicochemical parameters controlling the vertical metal concentration profiles (Gao, *et al.*, 2009).

Seasonality and effect of bloom sedimentation on benthic microbial communities

General composition of the microeukaryotic community

Microeukaryotic communities in the silty sediments were dominated by Stramenopila (mainly diatoms), Rhizaria (Acantharea, Cercozoa and Foraminifera), Alveolata (Ciliates and Dinophyceae) and Metazoa, and to a lesser degree Fungi, Chlorophyta and Amoebae (Table 2). This corresponds with observations from a previous study in the silty sediments in the same area (Pede, *et al.*, chapter 2), except for the lower number of Fungi and Metazoa in the present study. Fourteen sequences detected in the present study were also observed in 2007 (Table 2, Pede, *et al.*, chapter 2). The number of ciliates detected was low, considering that ciliates are usually reported as a dominant group in marine sediments (e.g. Patterson, *et al.*, 1989, Fernandez-Leborans & de Zaldumbide, 2000, Pawlowski, *et al.*, 2011c). As discussed in Pede, *et al.* (chapter 2), this is probably related to the methodology used, with general eukaryotic primers also detecting inactive or dying organisms (cf. the numerous phototrophic OTUs found in our study), which may potentially 'hide' the presence of the protozoa. This is confirmed by the fact that when rRNA instead of rDNA is targeted (as was done in Pede *et al.*, chapter 5 & 6, for the same study site), which captures only the actively growing part of communities, protozoan OTUs become dominant (cf. Pede et al., chapter 5 & 6, and also Stoeck, *et al.*, 2007a, Coolen & Shtereva, 2009). Likewise, the use of taxon-specific sets of ciliate primers during a previous study in the same sediment (Pede, *et al.*, chapter 2) revealed the presence of 15 unique OTUs representing 5 ciliate classes (dominated by Phyllopharyngea and Spirotrichea, followed by Oligohymenophorea, Litostomatea and Karyorelictea), compared to 3 OTUs representing 2 ciliate classes (1 Spirotrichea and 2 Phyllopharyngea) during this study. We probably only detected representatives of dominant ciliate groups, such as the carnivore *Acineta* spp. and algivore *Strombidium* ssp., two common and ubiquitous marine ciliate genera (Patterson, *et al.*, 1989).

Microbial diversity and bacterial biomass

Bacterial communities are known to respond quickly to the freshly deposited algal material (Franco, *et al.*, 2010). Bacteria import the carbon from the planktonic algae to the benthic

food web and as such form an important trophic link between the plankton and the benthos (Kathol, *et al.*, 2011). Because many protozoa are major bacterial grazers (e.g. Patterson, *et al.*, 1989, Taylor & Sanders, 1991, Epstein, 1997), fluctuations in bacterial diversity and biomass are potentially regulatory factors for microeukaryotic communities (Table 3). In our study, bacterial biomass peaked in June, coinciding with the highest CHL *a* values (Figs. 1, 4) (cf. also Franco, *et al.*, 2010). Bacterial diversity however, was highest before and after the biomass peak in May and again in July; the low values in June may be due to pronounced dominance of one or a few bacterial taxa in response to phytodetrital deposition. Microeukaryote diversity was significantly correlated with bacterial biomass, which could be related to the higher diversity of bloom algae in the microeukaryotic community in the period May-July, when CHL *a* values were highest (Fig. 6). Note also that bacterial diversity contributed significantly to explaining the variation in microeukaryotic and protozoan community structure (Table 3).

Microeukaryotic and protistan diversity were highest in winter and to a smaller degree in May-June beneath the sediment surface. Again (cf. bacterial diversity), the high diversity might be related to overall low abundances in winter (cf. Bak & Nieuwland, 1989; unfortunately no abundance data are available), what can result in the detection of higher diversity, while in periods of high biomass only some species may become more dominant, and the presence of less abundant taxa may be obscured. A recent experiment also showed that heterotrophic nanoflagellate biomass increased in the surface sediment layer after bloom deposition (cf. Gillan, *et al.*, chapter 4, and Pede, *et al.*, chapter 5).

Seasonal and depth variation in microeukaryotic and protozoan community composition

Our results demonstrate distinct and significant temporal and vertical differences in both microeukaryotic (Fig. 6) and protozoan community composition (Fig. 7), with pronounced seasonal change from late winter to summer (Figs. 6-8). Diatoms were clearly more abundant in May (and July), after the phytoplankton bloom. The presence of two nematodes (MET 76, MET 81) in the upper sediment layers is probably related to the increased food availability, lower oxygen penetration in surface layers and the occurrence of sulphide in deeper sediment layers (Brown, *et al.*, 2001, Steyaert, *et al.*, 2003, Vanaverbeke, *et al.*, 2004, Franco, *et al.*, 2008). A ciliate (CIL85), Acantharea (ACAN237), oomycete (OOMY35) and dinophyte (DINO171) in turn were more abundant in the deeper layer. Many ciliates can live in sediments under anaerobic and reducing conditions (Hayward, *et al.*, 2003).

Variation in community structure could be related to pH and Eh, dissolved sulphides, but also to bacterial diversity and biomass (see above) and several metals (see below), significantly explaining almost 62% of the community variation. Fernandez-Leborans (2000) reported that temperature, pH and dissolved sulphides were the main factors explaining seasonal variation in protozoan communities from epibenthic communities from the Cantabrian Sea. Fenchel (1969) showed that benthic protozoa (mainly focused on ciliates) show vertical distribution patterns related to the redox conditions of the sediments, depending on the requirements of oxygen, the tolerance to reduced, toxic compounds (H_2S), and food requirements. This dominant effect of redox potential and pH seems to be confirmed in our study. Higher Eh and pH values in March and June may explain the similarity in microeukaryote and especially protozoan community composition in these months (Figs. 6, 7); For example, CIL85 (which is mainly present in the deeper anoxic sediment layers) showed lower abundances in both March (lowest abundance in the upper sediment layer) and June (0-10cm) compared with the other months (not shown). Alternatively however, as for bacterial diversity (cf. above), the surprising similarity between the March and June communities could be the result of a methodological artefact. At peak algal biomass in June, only a few dominant algal taxa may be detected with the fingerprinting technique, resulting in a lower diversity of algal OTUs and hence a higher similarity with the pre-bloom communities. This could also explain why CHL *a* did not significantly contribute to explaining the variation in microeukaryotic communities, in addition to the fact that refractory chlorophyll in the deeper anoxic sediment layers (Veuger & van Oevelen, 2011) may obscure relations between microeukaryote community structure and CHL *a*.

Biological-metal interactions

Direct relations with *in situ* metal contaminants have rarely been investigated for microeukaryotic communities (but see Pede, *et al.*, chapter 2). Moreover, the fraction measured in this study represents only the bioavailable metals in the porewaters (Gao, *et al.*, 2009). Even though metals are usually strongly correlated to geochemical factors like redox potential, Eh and pH (Calmano, *et al.*, 1993, Eggleton & Thomas, 2004), it was striking that a significant fraction (14-19%) of the variation in the community structure could still independently be explained by Co, Mn, Fe, Pb, Cr, and As concentrations in the sediments (Tables 3, 4). Of course, it cannot be excluded that there are still other factors interfering with metals, not measured during this study, that can explain the observed community pattern. Only positive correlations between microeukaryotic and protistan diversity and the metals Pb,

Cr, Fe, Co, Ni and especially As ($p<0.001$) in the porewaters were measured. Again, this could be related to the method used (cf. above), as it has been shown that metals negatively affect microeukaryotic biomass (not measured during this study, but see e.g. Fernandez-Leborans & Novillo, 1994, Fernandez-Leborans & Herrero, 2000, Fernandez-Leborans, *et al.*, 2007), and hence the observed increase in diversity could be due to lower dominance in the communities. Correlation analyses showed different taxon-specific susceptibilities to different metals (Table 5). Positive correlations observed for individual taxa indicate tolerance to the metal concentrations; e.g. *Ammonia* spp. (FORA234-184) have been reported as indicative of polluted sediments (Jayaraju, *et al.*, 2011). Mainly dinoflagellates- and Rhizaria were affected by metals in the porewaters; e.g. a Syndiniales representative (DINO171) was negatively correlated with Mn, Fe and Co, what could indicate a toxic effect of the metals on this species. The cercozoans (CERC183 and CERC58-89) showed negative correlations to several metals, but either no or positive correlations to As were found. Similarly, a recent laboratory experiment had shown that cercozoans seemed unaffected by the acute As intoxication even at much higher concentrations (Pede, *et al.*, chapter 6). Ciliates and the parasite *Pirsonia* generally seemed less affected by the metals, but appear to be more sensitive to fluctuations in Eh, pH and sulphides (Table 5). Metal tolerance in ciliates was also observed in an As contamination experiment with sediments from the same study area (Pede, et al., chapter 6, Diaz, *et al.*, 2006, Martin-Gonzalez, *et al.*, 2006, Rehman, *et al.*, 2010b, a), and can be related to the metal-resistance mechanisms ciliates possess, e.g. biosynthesis of ciliate-specific metallothioneins (Diaz, *et al.*, 2006), which have unique features compared to metallothioneins from other organisms (Gutierrez, *et al.*, 2009). Due to their high metal-accumulation capacity (Rehman, *et al.*, 2010b), ciliate grazing can lead to metal bioaccumulation in the food chain (Twining & Fisher, 2004), potentially resulting in functional disturbance and health risks to higher trophic levels and humans.

Acknowledgements

This research was supported by a Belgian Federal research program (Science for a Sustainable Development, SSD, contract MICROMET n° SD/NS/04A & 04B) and BOF-GOA projects 01GZ0705 and 01G01911 of Ghent University (Belgium). Many thanks to Andre Catrijsse and the crew on the R.V. Zeeleeuw, and to Bart Vanelslander for his help during the sampling campaigns.

4

EFFECT OF BACTERIAL MINERALISATION OF PHYTOPLANKTON-DERIVED PHYTODETRITUS ON THE RELEASE OF ARSENIC, COBALT AND MANGANESE FROM MUDDY SEDIMENTS IN THE SOUTHERN NORTH SEA

A MICROCOSM STUDY

David C. Gillan[1,5], Annelies Pede[2], Koen Sabbe[2], Yue Gao[3], Martine Leermakers[3], Willy Baeyens[3], Beatriz Louriño Cabana[4,5], Gabriel Billon[4]

[1] Proteomics and Microbiology Lab., Mons University, B-7000 Mons, Belgium

[2] Lab. Protistology & Aquatic Ecology, Department of Biology, Ghent University, 9000 Ghent, Belgium

[3] Department of Analytical and Environmental Chemistry, Vrije Universiteit Brussel, 1050 Brussels, Belgium

[4]Université Lille 1, Sciences et Technologies, Villeneuve d'Ascq, France.

[5]Université libre de Bruxelles, Marine Biology Laboratory, Brussels, Belgium.

Manuscript submitted

I contributed to this chapter by cultivation of *Phaeocystis* and *Skeletonema*, performing analyses during the experiment, delivering the data for chlorophyll *a* in the sediment and heterotrophic flagellate biomass, and by revision of the manuscript.

Abstract

Muddy sediments of the Belgian Continental Zone (BCZ) are contaminated by metals such as Co, As, Cd, Pb, and Ni. Previous studies have suggested that mineralization of phytodetritus accumulating each year on sediments might cause secondary contaminations of the overlying seawater (metal effluxes). The aim of the present research was to investigate these effluxes using a microcosm approach. Muddy sediments were placed in microcosms (diameter: 15 cm) and overlaid by phytodetritus (a mix of *Phaeocystis globosa* with the diatom *Skeletonema costatum*). The final suspension was 130.6 mg L^{-1} (dw) and the final chlorophyll *a* content was 750 ± 35 µg L^{-1} (mean ± SD). Natural seawater was used for controls. Microcosms were then incubated in the dark at 15°C during 7 days. Metals were monitored in overlying waters and microbial communities were followed using bacterial and nanoflagellate DAPI counts, thymidine incorporation, community level physiological profiling (CLPP) and fluorescein diacetate analysis (FDA). Benthic effluxes observed in sediments exposed to phytodetritus were always more elevated than those observed in controls. Large effluxes were observed for Mn, Co and As, reaching 1084 nmol m^{-2} d^{-1} (As), 512 nmol m^{-2} d^{-1} (Co), and 755 µmol m^{-2} d^{-1} (Mn). A clear link was established between heterotrophic microbial activity and metal effluxes. The onset of mineralization was very fast and started within 2h of deposition as revealed by CLPP. An increased bacterial production was observed after two days (8.7 mg C m^{-2} d^{-2}). The bacterial biomass was stable and controlled by heterotrophic nanoflagellates. Calculations suggest that during phytoplankton blooms the microbial activity alone may release substantial amounts of dissolved arsenic in areas of the BCZ covered by muddy sediments.

Introduction

The Belgian Continental Zone (BCZ) is located in the Southern part of the North Sea. As in many coastal areas the delivery of continental nutrients into the BCZ results in large phytoplankton blooms characterized by high biomass levels (Lancelot et al., 1987; Lancelot et al., 2007; Gypens et al., 2007). Strong seasonal patterns are observed in the BCZ with diatom blooms initiating the succession in February-March followed by the main spring bloom composed of diatoms and *Phaeocystis globosa* in April-May (Rousseau et al., 2002; 2008). During the blooms, the biomass of *Phaeocystis* may reach 10 mg C L^{-1} which corresponds to

35 µg L^{-1} of chlorophyll *a* (Schoemann et al., 2005). Phytoplankton is usually a major source of organic matter for coastal sediments and it was estimated for the BCZ that 24% of the phytoplankton production is deposited onto the sediments (Lancelot et al., 2005). After deposition, phytodetritus are actively mineralized by various benthic organisms including microbial communities (Van Duyl et al., 1992).

As a consequence of human activities and the presence of the nearby Scheldt estuary, many areas of the BCZ are contaminated by metals (Danis et al., 2004; Gillan and Pernet, 2007; Gao et al., 2009). Metal concentrations in sediments are frequently above the Ecotoxicological Assessment Criteria (EAC), defined by the OSPAR Commission as concentration levels below which no harm to the environment or biota is expected (OSPAR, 2000). Metals are much more abundant in muddy sediments where concentrations in porewaters can exceed those in overlying waters by several orders of magnitude (Gao et al., 2009). As a consequence, the Fick's first law predicts that benthic effluxes of metals may occur. Such effluxes are well-known phenomena and have been observed in many parts of the world using benthic chambers (Elderfield et al., 1981; Westerlund et al., 1986; Skrabal et al., 1997; Pakhomova et al., 2007). Among the factors that influence metal effluxes we find metal speciation, the presence of Mn and Fe oxide phases, sulfides, organic matter content, salinity gradients, temperature, water advection, bottom currents and thickness of the diffusive boundary layer (DBL), oxygen, and finally microbial communities and bioturbation (Jørgensen and Revsbech, 1985; Ciceri et al., 1992; Skrabal et al., 2000; Iskrenova-Tchoukova et al., 2010; Liu and Cai, 2010).

The influence of microorganisms on metal effluxes, through mineralization of freshly deposited phytodetritus, has been poorly investigated. Organic matter and phytodetritus may influence metal effluxes because they are able to complex metals (Wells et al., 1998; Iskrenova-Tchoukova et al., 2010; Liu and Cai, 2010). The subsequent degradation of phytodetridus by microorganisms may then release complexed metals in bottom waters. Increased oxygen consumption at the water–sediment interface (WSI) may also affect metal speciation in porewaters and promote effluxes. Previous studies have already suggested that mineralization of phytodetritus may cause increased metal effluxes such as for Mn (Aller, 1994; Fones et al., 2004). However, for highly contaminated sediments such as those of the BCZ (containing high levels of Co, As, Cd, Pb, and Ni; Gao et al., 2009; Gillan & Pernet, 2007) and phytodetritus containing *Phaeocystis*, the type of metal released and the importance of the effluxes have, to our best knowledge, never been measured. In addition, on the

microbiological point of view many questions remain to be answered: is there a delay in the onset of mineralization? Will the biomass of bacteria and protozoa increase at the same time? At what moment will change the activity of microorganisms?

The aim of the present research was to investigate dissolved trace metal effluxes during phytodetritus mineralization by microorganisms at the WSI. For that purpose, metal contaminated muddy sediments from the BCZ were placed in microcosms, with or without phytodetritus, and followed during one week in the laboratory. Contrary to the use of benthic chambers deployed *in situ*, our microcosm approach has the advantage to permit easier sediment manipulations like phytodetritus addition, sampling of microorganisms at the interface, Eh/pH measurements and control of temperature. In previous experiments, microcosm approaches have already been used with success for the study of phytodetritus degradation by microorganisms on sandy sediments (Van Duyl et al., 1992).

Materials and methods

Sediment collection

Sediments were collected by a Reineck corer (diameter 15 cm) at station 130 (51°16.25 N - 02°54.30 E; depth: ± 11 m) in March 2010 onboard the "Zeeleeuw" research vessel. Station 130 is one of the most metal-contaminated subtidal stations of the BCZ (Gillan and Pernet, 2007; Gao et al., 2009). Sediments are muddy and have a mean grain size of 12.5 µm. Undisturbed cores were immediately transferred in cylindrical plexiglass microcosms of the same diameter (15 cm) together with 4 cm of overlying seawater. All cores were transported to the laboratory in insulated boxes and stabilized during 10 days in the dark at 15.0 ± 1°C. This stabilization period was necessary because cultivated algae were not fully developped at the time of sediment sampling and it was also necessary to ensure the absence of leaks that would introduce biases in flux calculations. Aerobic conditions were maintained in the overlying water during the stabilization period (oxygen concentration was regularly monitored).

Algal cultures and algal suspension

Two independent 20 liter cultures of unicellular algae were prepared: *Phaeocystis globosa* (a Prymnesiophyte) and *Skeletonema costatum* (an early spring diatom). These algae are naturally present on the BCZ, are dominant members of the phytoplankton and may co-occur in spring (Rousseau et al., 2002). Inocula were obtained from the ESA Lab, ULB, Brussels (both strains were initially isolated from the BCZ). Algae were cultivated in a medium that is composed of natural seawater in which major nutrients, trace metals and vitamins were added. The medium is derived from the medium used by Veldhuis and Admiraal (1987) except for the saline matrix which was composed of natural instead of artificial seawater (*Phaeocystis* cultured in artificial seawater does not form colonies). The natural seawater used was obtained on the BCZ and was filtered through 0.2 µm Sartorius membrane and autoclaved for 20 min at 121 °C before use. Streptomycin (25 and 50 µg mL^{-1}) and Penicillin (75 and 100 µg m L^{-1}) were then added to prevent the development of bacteria (final concentrations, for *Phaeocystis* and *Skeletonema*, respectively). These antibiotics were completely eliminated by the subsequent treatments (centrifugations) and had consequently no effects on sediment bacteria (as demonstrated further by bacterial activity measurements). Cultures were performed at 9-10 °C with an irradiance of 100 µE m^{-2} s^{-1} and a gentle agitation of the culture flasks. After a few days of development cultures reached the stationary phase. At that moment, they were decanted and centrifuged. Cell pellets were kept at -20°C until the start of the experiment. At the start of the experiment (Day-0) cell pellets were thawed and placed into 8 liters of natural BCZ seawater at 15°C (that seawater was not filtered and not autoclaved). This algal suspension was then immediately used for the microcosm experiment. The dry matter content of the final algal suspension was 130.6 mg L^{-1} (dry weight, measured after centrifugation and lyophilisation of three 50 mL samples) and the salinity was 30 ‰. The proportion of the two algae in the algal suspension was 50:50 (w/w), and the final chlorophyll *a* content was 750 ± 35 µg L^{-1} (mean ± SD). Metal concentrations of the algal biomass were as follows (in µg g^{-1} dry weight): Cd, 0.53; Pb 38.6; Cr, 5.1; Mn, 64.5; Fe, 7533; Co, 0.54; Ni, 5.1; Cu, 246; Zn, 381; As, 4.4. Dissolved metal concentrations of the algal suspension (after filtration on 0.45 µm) were as follows (values in µg L^{-1}): Cd, 0.71; Pb, 0.26; Cr, 0.94; Mn, 12.4; Fe, 6.9; Co, 0.28; Ni, 2.1; Cu, 9.9; Zn, 12.0; As, 2.8).

Experimental design

The experimental design featured a total of 18 large microcosms (15 cm ø). These microcosms were used to test two conditions [with and without (controls) phytodetritus]. Samples were taken on three different sampling occasions during the experiment (Day-0, Day-2, Day-7) in triplicate. At the start of the experiment the overlying seawater was slowly removed from all the microcosms and cores without disturbing the sediment-seawater interface. A volume of 710 mL of algal suspension was then slowly deposited on half of the microcosms, the other half were considered as controls and received 710 mL of natural seawater (that seawater was not filtered and not autoclaved). The height of the overlying seawater in all microcosms was 4 cm. After two hours of sedimentation 6 microcosms (3 experimental and 3 controls) were used for the Day-0 analyses. These analyses included microbial and geochemical parameters (see below). After two days (Day-2) and 7 days (Day-7) the same procedure was repeated. Microcosms were kept in the dark throughout the experiment. Salinity variations due to evaporation were avoided by regular MilliQ additions and monitoring by a salinometer. The temperature of the water was maintained at 15.0 ± 1°C during the whole experiment which is the water temperature that may be reached at the end of spring (Hondeveld et al., 1994; Vanaverbeke et al., 2008; Sirjacobs et al., 2011). To allow phytodetritus accumulation at the WSI and prevent their resuspension the overlying water was not agitated. In such a system the DBL is thicker than in the field (Jørgensen and Revsbech, 1985). As a consequence, molecular diffusion completely sustains contaminant transport, as long as chemical activities of the contaminants in the sediment porewater are higher than in the overlying water. For this reason, only a short-term experiment was conducted (7 days). To prevent the development of anaerobic conditions the height of the water was limited to 4 cm and oxygen concentration as well as redox potential were regularly monitored.

Geochemical parameters

Geochemical parameters included Eh and pH profiles in the sediments, oxygen levels at the sediment-water interface, salinity of the overlying seawater, dissolved organic carbon (DOC) in porewaters, chlorophyll *a* in surface sediments, and metals in overlying seawater.

Eh and pH measurements were performed at various depths by potentiometry. For that purpose, a glass electrode (specifically designed for abrasive and hard media, Ingold), and a home made platinum electrode (diameter about 1-2 mm) were used as indicator electrodes to detect pH and Eh, respectively. Both electrodes were combined with an Ag/AgCl, [KCl] =

3M reference electrode with a potential equal to 0.22 V versus a hydrogen normal electrode (HNE). All profiles were determined every 5 mm up to 3 cm into the sediments. Electrodes were fixed on a micromanipulator. All potential values further in this paper, refer to the Ag/AgCl electrode. The pH electrode was calibrated with Merck buffers, type NBS (National Bureau of Standards). In addition, since measurements were carried out in seawater, a correction of the values was made according to Aminot and Kérouel (2004). The salinity and temperature of the overlying water were monitored using a WTW Cond 340i conductivity meter. The dissolved oxygen in the overlying water was measured at ± 5 mm above the sediments using a WTW CellOx 325 galvanic oxygen sensor adapted for measurements in seawater.

For chlorophyll *a*, samples of surface sediments were frozen in liquid nitrogen (immediately after sampling), and kept at -80°C until further analysis. After freeze-drying of the sediment (0.4-2.1 g of sediment dry weight - SDW), pigments were extracted in 90% acetone and analyzed using HPLC with standard protocols (Wright et al., 1991). Chlorophyll *a* concentrations were expressed as $\mu g\ g^{-1}$ SDW.

For dissolved organic carbon (DOC) in porewaters, surface sediments (ca. 20 g of the 0-5 mm layer) were centrifuged and the porewater was collected using a glass syringe. The porewater was then filtered using Whatman GF/F glass fiber filters. Porewaters were preserved with phosphoric acid (5 µL of H_3PO_4 per mL of sample) and stored at 4°C. All glassware and filters were previously treated at 500°C for 4 hours. Before analysis samples were diluted 9 times with MilliQ water. DOC concentrations were measured by a Dohrman Apollo 9000 total organic carbon analyzer in which inorganic carbon is eliminated by bubbling in the presence of phosphoric acid and organic carbon is oxidized at high temperature (680°C). The produced CO_2 was then detected by non-dispersive infra-red (NDIR) analysis. The instrument response was calibrated by the method of standard additions.

For flux calculations, metals in the overlying seawater of the microcosms were determined by HR-ICP-MS as described elsewhere (Gao et al. 2009). For that purpose, a 10 mL water sample was filtered on 0.45 µm and acidified using Suprapur HNO_3. Benthic fluxes were then calculated using dissolved metal concentrations in the overlying waters after 2 and 7 days of exposure (concentrations at Day-0 were subtracted from those at Day-2, and concentrations at Day-2 were subtracted from those at Day-7, respectively). The volume of the overlying water was 710 mL (V) and the surface area (A) of the microcosms was 0.0176

m^2. The efflux can be calculated as $F = C \times V / (A \times T)$. Effluxes were expressed in mol m^{-2} d^{-1}.

Microbial parameters

Microbial parameters included bacterial and nanoflagellate biomass (DAPI counts) as well as three bacterial activity measurements: (i) bacterial production estimated by the tritiated thymidine incorporation, (ii) fluorescein diacetate analysis (FDA), and (iii) community level physiological profiling (CLPP). All analyses were performed on the 0-5 mm layer of the sediments (on the day the analyses were performed, the overlying water was carefully removed and sediment samples were taken with a spatula).

Bacterial DAPI counts were used to evaluate bacterial biomass. Sediment samples (1 mL) were preserved in 8 mL of 4% paraformaldehyde at 4°C. Bacteria were then extracted by sonication and placed on filters as described elsewhere (Gillan and Pernet, 2007). Bacteria in each microscopic field (14 fields per filter) were counted automatically using the ZooImage software v.1.2.2 (http://www.sciviews.org) based on Image J v.1.38r. Image background was first subtracted using a rolling ball radius of 40, and contrast was automatically adjusted. Images were then transformed in 16-bit and the threshold function was used with a lower threshold level of 180, and an upper threshold level of 255. The lower threshold level had to be adapted for each station to avoid the count of mineral particles. This value varied between 140 and 180, and the best value was found by comparing manual counts with automatic counts and outlines generated by ZooImage/Image J. Particles of the size of bacteria were counted automatically with the "Analyse particle" function (size $pixel^2$: 100-2500; circularity: 0). A specific plugin was then developed in ZooImage/ImageJ to process automatically the 2016 pictures generated in this study. For each sediment sample, bacteria counted on the 14 pictures (total area observed = $5.39\ 10^{-8}$ m^2) were summed and the number obtained was compared to the effective filtration area ($1.77\ 10^{-4}$ m^2). Four replicate filters were counted for each type of sediments (n=4) and the mean number of bacteria per field varied between 30 and 60 (the coefficient of variation was 10-30% of the mean). Such a counting scheme guarantees the lowest error in environments with great spatial heterogeneity (Kirchman et al., 1982; Montagna, 1982).

For nanoflagellate DAPI counts, sediment samples (2 mL) were fixed in 4 ml of 2,5% gluteraldehyde at 4°C. Heterotrophic nanoflagellates were isolated within 24h of sampling,

using the Percoll-gradient centrifugation technique of Starink et al. (1994). Upon centrifugation, the supernatant containing the nanoflagellates was decanted from the centrifuge tubes. A subsample was filtered on 0.6 µm pore-size black polycarbonate filters (Whatman) and stained with 4,6-diamino-2-phenylindole (DAPI; 10 µg ml^{-1} final concentration). Filters were mounted on a slide with low fluorescence immersion oil and kept frozen in dark until enumeration. Heterotrophic nanoflagellates were counted manually using epifluorescence microscopy with UV radiation (Zeiss Axioplan2) as described in Hamels et al. (2005). Absence of chlorophyll was checked by switching to blue light excitation. Per filter, at least 20 randomly selected fields were observed (magnification 1000x).

For bacterial production, the tritiated thymidine incorporation approach was used with 1.0 g (ww) of living surface sediments that was suspended in 6 mL of autoclaved sterile seawater. These sediments were collected over a surface of ca 1 cm^2. The sediment suspension was then sonicated for 30 sec to detach bacteria from particles (Gillan and Pernet, 2007). The suspension was then centrifuged 5 min. at 180 g (4°C) to precipitate mineral particles. A volume of 5 mL of supernatant (containing bacteria) was placed in a clean tube with 6.4 µL of a ^{3}H-thymidine stock solution (specific activity, SA : 64 Ci $mmol^{-1}$; 1.0 mCi mL^{-1}) (MP Biomedicals). The final concentration of tritiated thymidine was 0.1 nmol in 5 mL. Tubes were then incubated for 90 min in the dark at 15°C under orbital agitation. The incorporation was stopped using 1.5 mL of 25% cold trichloracetic acid. For the incorporation blanks (controls) the trichloracetic acid was added before the 90 min incubation. All samples were then filtered using Sartorius cellulose acetate filters (0.2 µm). Filters were placed in scintillation vials with 5 mL of scintillation fluid (Filter Count). Radioactivity of the samples was determined using a Packard Tri-Carb scintillation counter. Counts per minute (CPM) were automatically converted to disintegrations per minute (DPM) using a quench curve stored in the counter. Incorporation blanks were then subtracted from the experimental tubes and the rate of incorporation of thymidine was obtained in mg C m^{-2} d^{-1} using the following formulae :

$$[DPM/SA * 2.22x10^{12} * 1000]\,[2x10^{18} * 60/T] * 24 * 10^4 * 2.44x10^{-11}$$

where SA is the specific activity of the added ^{3}H-thymidine (in Ci $mmol^{-1}$), and T is the time

of incubation (min). We considered that 2×10^{18} cells were produced per mol of thymidine incorporated (Moriarty et al., 1985) and that one cell of 0.1 μm^3 contained 2.44×10^{-11} mg C (Servais, 1990).

Community level physiological profiling (CLPP) was determined using living sediments and the Biolog EcoPlate system (Garland and Mills, 1991). Bacteria were first extracted from the sediments. Fresh sediments (2.0 g, wet weight) were placed in 5 mL of autoclaved artificial seawater (Sigma, 40 g L^{-1}). The sediment suspension was sonicated (same protocol as above). The suspension was then centrifuged 5 min. at 180 g (4°C) to precipitate mineral particles. A volume of 150 µL of supernatant (containing bacteria) was placed in each well of an EcoPlate and the microplates were incubated 48 h at 15°C in the dark. The optical density of each well was recorded at 590 nm using a FLUOstar Optima microplate reader (BMG Labtech). The absorbance value of the least utilized substrate (among the 31 substrates) was subtracted from the absorbance value of the remaining wells (Hitzl et al., 1997; Stefanowicz, 2006). Absorbance values obtained with control and experimental microcosms were then compared to each other using the Mann-Whitney U test.

For fluorescein diacetate analysis (FDA), which estimates the total esterase activity of microbial communities (Battin, 1997), sediments (500 mg ww) were placed in sterile 15 mL polypropylene tubes and diluted with 2750 µL of sterile artificial seawater (Sigma, 40 g L^{-1}; autoclaved). Samples were sonicated 30 seconds as explained above. A volume of 250 µL of a FDA working solution (Sigma) in 100% acetone (analytical grade) was then added to the samples to a final concentration of 200 µM. Control tubes were immediately inactivated with acetone 100% to a final concentration of 50% (v/v). Samples were incubated for 60 min in the dark at 15°C. Incubation was stopped with 3 mL of acetone 100%. Absorbance of the supernatant at 490 nm was then measured spectrophotometrically against a water/acetone (50% v/v) blank. A standard curve was prepared with a fluorescein disodium salt (Sigma). FDA hydrolysis was expressed per g of wet weight.

Results

The algal suspension was added on Day-0 in half of the microcosms and samples were taken after 2h (Day-0), 2 days (Day-2) and 7 days (Day-7). A slight but significant acidification was observed at the sediment-seawater interface on Day-2 and Day-7 in the microcosms that received algae: the initial pH values were 7.9 at the beginning of the incubation and dropped

down to 7.7-7.8 after one week (Figure 1). No effects of algae addition were noticed on the redox potential or on the oxygen levels of the overlying waters: Eh values around 200 mV were observed up to -0.5 cm into the sediments for all microcosms, and values dropped to -130 mV at -1.5 cm of depth (not shown). Oxygen levels, measured at 5 mm above the sediments, were maintained at an average of 5 mg L^{-1} throughout the experiment with no significant differences between experimental and control microcosms. Similarly, salinity was stable, with values of 30.0 ± 0.5‰ in all microcosms.

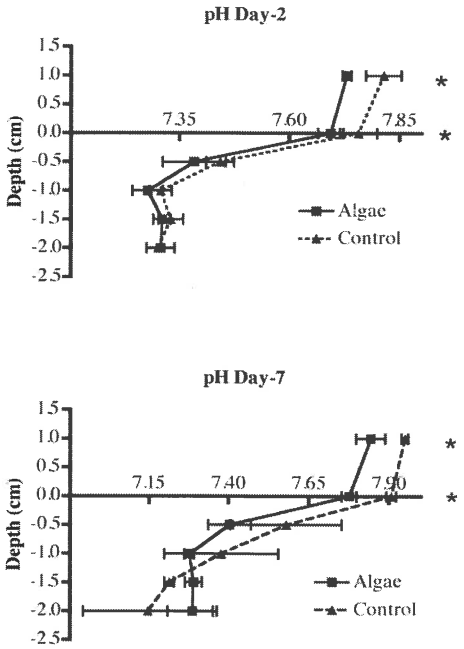

Figure 1. pH profiles measured in sediments of the microcosms on Day-2 and Day-7 (mean ± SD, n=3). Asterisks (*) indicate significant differences (Student T test, $\alpha = 0.05$).

Metals released into the overlying waters were monitored by HR-ICP-MS throughout the experiment (Figure 2). After two hours of exposure to the algal suspension a significant increase of the metal concentration was observed for Cd, Co and As. After two days of exposure (Day-2) the concentrations of four metals were significantly higher in the overlying water of the experimental microcosms when compared to the controls: Cd (x 2.7), Co (x 5.6), Mn (x 13.8), and As (x 1.8) (Figure 2). After 7 days of exposure no differences were observed in the overlying waters between controls and experimental microcosms.

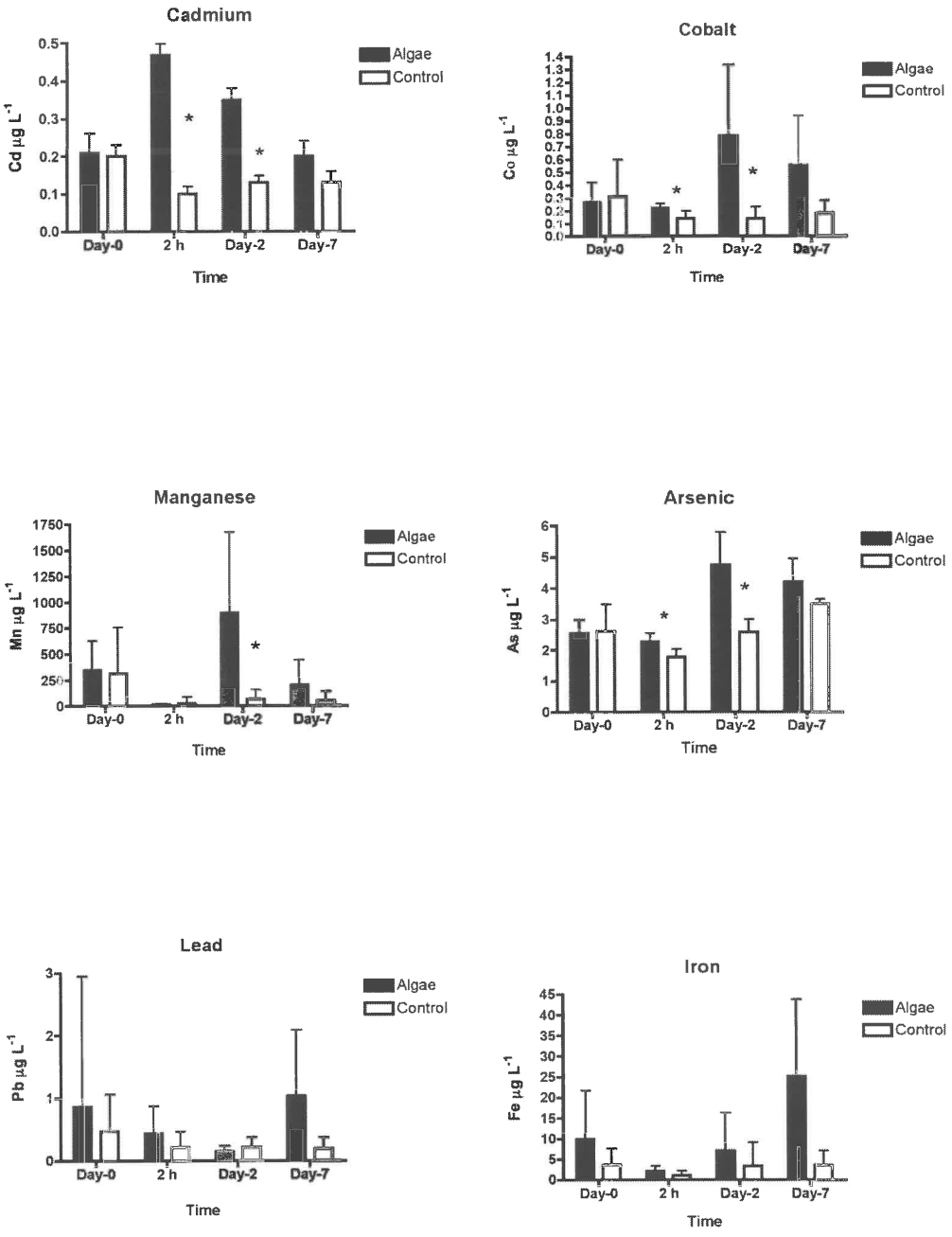

Figure 2. Metals in the overlaying water as measured by ICP-MS (mean ± SD). Significant differences are indicated by an asterisk (Student t-test, $\alpha = 0.05$). Day-0 represents the overlying water at the end of the 10-days stabilization period, i.e. before the start of the experiment; this overlying water was then eliminated and replaced by the algal suspension or fresh seawater for controls.

Exchange fluxes (in mol m^{-2} d^{-1}) were calculated and are presented in Table 1. During the first 48 hours, 4 measured metals in experimental microcosms (As, Cd, Co and Mn) presented fluxes that differed significantly from those observed in the control microcosms. For As, Co and Mn, large negative fluxes (i.e., effluxes, from sediments to overlying water) were observed in the experimental microcosms. These negative fluxes reached –1084 nmol m^{-2} d^{-1} for As, –512 nmol m^{-2} d^{-1} for Co, and –755 µmol m^{-2} d^{-1} for Mn. A positive flux was noticed for Cd (i.e., towards the sediments). For the other metals (Pb, Fe, Ni, Cu and Zn) no differences were observed between control and experimental microcosms and fluxes were either negative or positive (Table 1A). During the last 5 days (Day-2 to Day-7) only 2 measured metals in experimental microcosms (As and Cd) presented fluxes that differed significantly from those measured in the control microcosms (Table 1B). For As in the experimental microcosms, fluxes were less negative than during the first 48 hours and some microcosms displayed large positive fluxes (+262 nmol m^{-2} d^{-1}). For Cd, fluxes were still positive but less elevated than during the first 48 hours.

The chlorophyll *a* content of the sediments was measured at the seawater-sediment interface (Table 2). All sediment cores presented a background chlorophyll *a* concentration around 20 µg g^{-1} (dw). The introduction of phytodetritus into the experimental microcosms was clearly visible; after 2h values of chlorophyll *a* significantly increased to 30 µg g^{-1}. After 2 and 7 days, chlorophyll *a* values were respectively 1.8 and 1.6 more elevated in the experimental microcosms than in the controls. Values of DOC in the 0-5 mm porewaters are shown in Table 3. Although mean DOC values of the experimental microcosms clearly increased with the incubation time, which is indicative of a mineralization process, no significant differences were found (variability between replicate microcosms was particularly high on Day-7). Bacterial DAPI counts are listed in Table 4. Bacterial counts did not evolve during 48h (the differences between controls and experimental microcosms were not significant). At Day-7 bacterial counts were significantly higher (1.3 times) in the experimental microcosms. DAPI counts of nanoflagellates are shown in Table 5. Only on Day-2 these counts were significantly higher (1.4 times) in the experimental microcosms.

Table 1. Exchange fluxes (negative values are from sediments to overlying water) in mol m^{-2} d^{-1} calcultated using metal concentrations in overlying waters. Minimum and maximum values obtained from 6 microcosms (A) or 3 microcosms (B) are indicated. Significant differences between algae and controls are indicated in boldface (Mann-Whitney U test, two-tailed, α=0.05).

	A. Between Day-0 and Day-2			
	Algae		Controls	
	Min	Max	Min	Max
As	**–1084 x 10^{-9}**	**–349 x 10^{-9}**	**–266 x 10^{-9}**	**+ 115 x 10^{-9}**
Cd	**+11 x 10^{-9}**	**+30 x 10^{-9}**	**–12 x 10^{-9}**	**–3.5 x 10^{-9}**
Co	**–512 x 10^{-9}**	**–34 x 10^{-9}**	**–47 x 10^{-9}**	**+51 x 10^{-9}**
Mn	**–755 x 10^{-6}**	**–89.1 x 10^{-6}**	**–77.4 x 10^{-6}**	**+46.2 x 10^{-6}**
Pb	–1.9 x 10^{-9}	+123 x 10^{-9}	–36 x 10^{-9}	+8.7 x 10^{-9}
Fe	–7.1 x 10^{-6}	+0.5 x 10^{-6}	–4.7 x 10^{-6}	+0.1 x 10^{-6}
Ni	–1.0 x 10^{-6}	+0.2 x 10^{-6}	–0.2 x 10^{-6}	–0.1 x 10^{-6}
Cu	–130 x 10^{-9}	+848 x 10^{-9}	–225 x 10^{-9}	+746 x 10^{-9}
Zn	–19 x 10^{-6}	+1.9 x 10^{-6}	–10 x 10^{-6}	+7.0 x 10^{-6}
	B. Between Day-2 and Day-7			
	Algae		Controls	
	Min	Max	Min	Max
As	**–45 x 10^{-9}**	**+262 x 10^{-9}**	**–189 x 10^{-9}**	**–114 x 10^{-9}**
Cd	**+7.8 x 10^{-9}**	**+16 x 10^{-9}**	**–5.0 x 10^{-9}**	**+0.7 x 10^{-9}**
Co	–96 x 10^{-9}	+188 x 10^{-9}	–10 x 10^{-9}	–1.3 x 10^{-9}
Mn	–22 x 10^{-6}	+295 x 10^{-6}	+5.7 x 10^{-6}	+14 x 10^{-6}
Pb	–79 x 10^{-9}	+1.9 x 10^{-9}	–13 x 10^{-9}	+10 x 10^{-9}
Fe	–6.1 x 10^{-6}	–0.3 x 10^{-6}	–0.4 x 10^{-6}	+1.0 x 10^{-6}
Ni	–0.2 x 10^{-6}	–86 x 10^{-9}	–0.1 x 10^{-6}	+1.3 x 10^{-9}
Cu	–614 x 10^{-9}	–281 x 10^{-9}	–759 x 10^{-9}	–49 x 10^{-9}
Zn	–1.4 x 10^{-6}	–0.05 x 10^{-6}	–3.1 x 10^{-6}	+1.1 x 10^{-6}

Table 2. Chlorophyll *a* in 0-5 mm sediments (mean ± SD; µg g^{-1} dw).

	Day-0 (2h)	**Day-2**	**Day-7**
Controls	19.7 ± 1.4 a	22.4 ± 3.6 a	21.9 ± 2.2 a
Algae	30.3 ± 3.1 b	41.6 ± 1.3 b	35.2 ± 4.0 b

Different letters (a, b) indicate significant differences between controls and treatment (Student t-test, α = 0.05).

Table 3. DOC in 0-5 mm sediments (mean ± SD; mg L^{-1}).

	Day-0 (2h)	Day-2	Day-7
Controls	17.3 ± 5.2 a	14.6 ± 2.8 a	17.2 ± 1.3 a
Algae	16.8 ± 0.5 a	18.1 ± 1.5 a	24.1 ± 5.4 a

Different letters (a, b) indicate significant differences between controls and treatment (Student t-test, $\alpha = 0.05$).

Table 4. Bacterial DAPI counts (x 10^9) in 0-5 mm sediments (mean ± SD; cells g^{-1} dw).

	Day-0 (2h)	Day-2	Day-7
Controls	4.0 ± 0.73 a	3.0 ± 0.27 a	2.9 ± 0.31 a
Algae	5.1 ± 1.6 a	4.1 ± 0.85 a	3.8 ± 0.44 b

Different letters (a, b) indicate significant differences between controls and treatment (Student t-test, $\alpha = 0.05$).

Table 5. DAPI counts of nanoflagellates (x 10^6) in 0-5 mm sediments (mean ± SD; cells ml^{-1}).

	Day-0 (2h)	Day-2	Day-7
Controls	8.4 ± 2.7 a	4.5 ± 0.2 a	6.1 ± 1.1 a
Algae	5.6 ± 2.4 a	6.2 ± 0.7 b	5.7 ± 1.4 a

Different letters (a, b) indicate significant differences between controls and treatment (Student t-test, $\alpha = 0.05$).

The mineralization activity of the microbial community was first assessed using the Biolog EcoPlate system (CLPP approach). Mineralization was clearly visible, with a total of 15 enzymatic activities that differed significantly between control and experimental microcosms (Figure 3). The majority of these activities (13 over 15) were more elevated in the experimental microcosms by a factor 1.3 to 15.1 and occurred on Day-2 and Day-7. Only two activities were significantly reduced (on Day-2, by a factor 0.6-0.8). Microbial mineralization already started after 2h of incubation as indicated by the significant increase of three enzymatic activities (Figure 3). The mineralization activity of the microbial community was also studied using the FDA approach. The FDA approach indicated that the esterase activity

progressively increased from Day-0 to Day-7 (Figure 4) with an esterase activity that was 1.9 times more elevated at Day-7 in the experimental microcosms than in the controls.

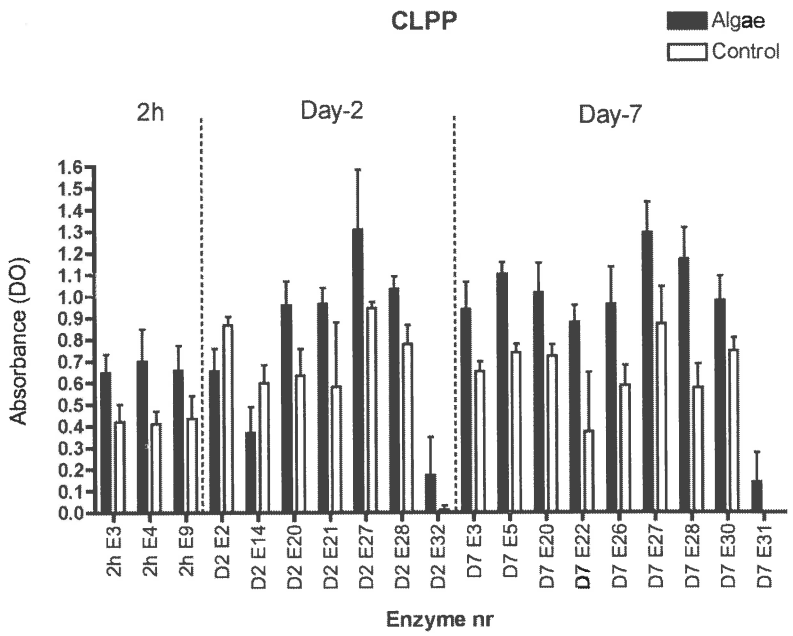

Figure 3. Bacterial activity as measured using Community Level Physiological Profiling (CLPP). The EcoPlate™ system of Biolog was used, which measures the use of 31 carbon sources. Only the carbon sources which produced significant differences between controls and experimental microcosms (Algae) are indicated (Mann-Whitney U test). E2 to E31 refer to the type of carbon source degraded by the microbial community. E2, pyruvic acid methyl ester; E3, Tween 40; E4, Tween 80; E5, α-cyclodextrine; E9, β-methyl-D-glucoside; E14, D-glucosaminic acid; E20, 4-hydroxy-benzoic acid; E21, γ-hydroxybutyric acid; E22, itaconic acid; E26, L-asparagine; E27, L-phenylalanine; E28, L-serine; E30, glycyl-L-glutamic acid; E31, phenylethylamine; E32, putrescine. D2, Day-2; D7, Day-7.

Finally, bacterial production during the incubation of the microcosms was evaluated by the incorporation of tritiated thymidine. Values were stable in the control microcosms and ranged between 0.2 and 0.8 mg C m^{-2} d^{-1} (Figure 5). In the experimental microcosms values were significantly more elevated, especially on Day-2 when a maximum was observed at 8.7 mg C m^{-2} d^{-1}. This value was at least 10 times more elevated than in the controls.

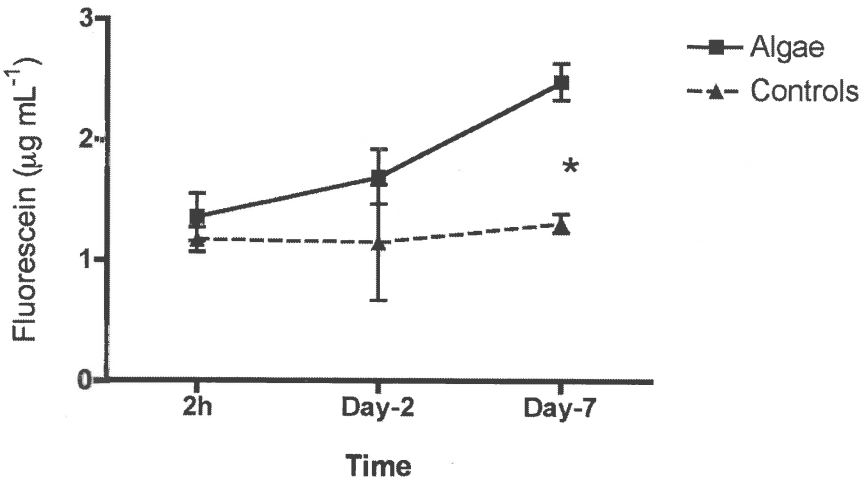

Figure 4. Fluorescein Diacetate Analysis (FDA) which estimates the total esterase activity of the microbial community as the quantity of released fluorescein according to time (mean ± SD). Significant differences are indicated by an asterisk (Student T test, $\alpha = 0.05$).

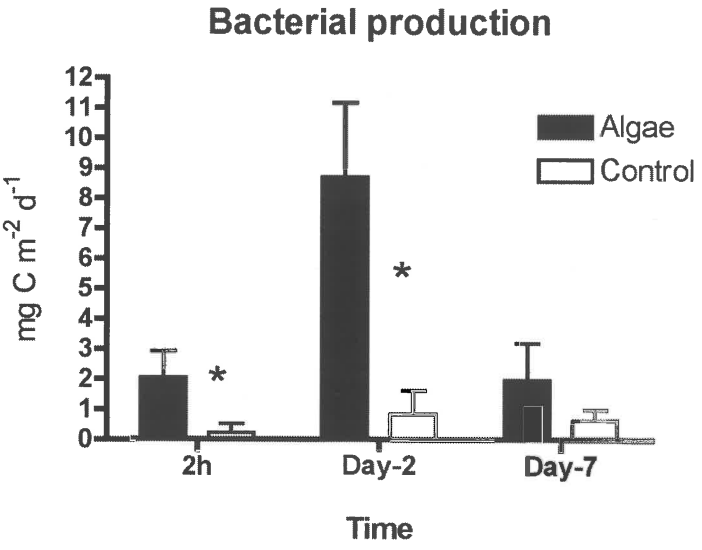

Figure 5. Bacterial production in surface sediments (at the interface) during the incubation of the microcosms as measured by incorporation of tritiated thymidine (mean ± SD). Significant differences are indicated by an asterisk (Student T-test, $\alpha = 0.05$).

Discussion

The experiments performed in this study clearly demonstrate that microbial mineralization of phytoplankton-derived phytodetritus accumulated at the surface of contaminated muddy sediments may lead to an increased efflux of trace elements from these sediments. Several important points must be considered. First, the quantity of phytodetritus used in this experiment was in the range of what can be observed in the field. Although the algal suspension used here was 21.4 times more concentrated than the maximum values observed in the North Sea during a *Phaeocystis* bloom (chlorophyll *a*: 750 µg L^{-1} versus 35 µg L^{-1}) (Schoemann et al., 2005), it should be noted that the height of the water column over the microcosms was only 4 cm, and that station 130 is located at ca. 10 m of depth. Consequently, considering that all phytodetritus may reach sediments, the present experiment was equivalent to an 85 cm column of seawater containing 35 µg L^{-1} of chlorophyll *a* (4 cm × 21.4), or to a 10 m column containing 3 µg L^{-1} of chlorophyll *a* (750 × 0,04 × 10). Such a chlorophyll *a* concentration (3 µg L^{-1}) is exactly the mean concentration observed in spring in coastal areas such as the Bay of Biscay (France), with peaks at 10 µg L^{-1} (Gohin et al. 2003). On the coastal BCZ and the English Channel, mean values are commonly higher than 30 µg L^{-1} (Denis and Desroy 2008). On the BCZ, values of ca. 20 µg L^{-1} at station 130 were observed throughout March and April 2008, with values reaching 100 µg L^{-1} in May (unpublished observations). Lancelot et al., 2005 estimated that 24% of the production may reach sediments, the rest being exported or degraded in the water column. As a result, for the period between March and April on the BCZ, a quantity of 4.8 µg L^{-1} may potentially reach the sediments (24% of 20 µg L^{-1}). Although the actual input of phytodetritus in North Sea sediments is hard to determine, as it depends on currents and wind (Van Duyl et al., 1992; Denis and Desroy, 2008), we may consider that the quantity of phytodetritus used in the present experiment (3 µg L^{-1}) is in the lower range of values that may potentially be observed on sediments during a real phytoplankton bloom.

Another point to consider is the origin of metals appearing in the overlying waters during the experiment. Metals measured after 2h originate mostly from the added algal suspension in itself (clearly our algal suspension was contaminated with Cd) but also from the disturbance of the WSI. Indeed, it can be seen that the increases observed after 2h are of the same range as the dissolved metal concentrations of the algal suspension (see materials and methods). As a consequence, no conclusions can be drawn about effluxes of metals from sediments after 2h

of exposure to phytodetritus. However, this is not the case for Day-2: concentrations of Mn, Co and As in the experimental microcosms were respectively 60 times, 3.6 times and 2.1 times more elevated than the values observed in the same microcosms after 2h. These increases can only be explained by (i) the mineralization of phytodetritus that releases metals directly into the overlying water, and (ii) by an efflux of metals from the sediments. It has been calculated that the complete mineralization of the phytodetritus on Day-2 would only introduce 8.4 (Mn), 0.07 (Co) and 0.58 (As) µg of metals per liter in the overlying water (Appendix A). This means that the complete mineralization of phytodetritus at the interface only represents a maximum of 0.9% (Mn), 12.4% (Co) and 23.3% (As) of the increases observed on Day-2 in the overlying waters. As a result, 99.1% (Mn), 87.6% (Co) and 76.7% (As) of the metals are coming from the sediments.

A third point is the physico-chemical conditions during the experiment. Like with many approaches, the microcosm experiment presented here is not free from biases: (1) Because stagnating water was used oxygen levels were lower than in the field. Low oxygen levels may promote or impede the flux of metals like Fe^{2+}; (2) In the field, hydrodynamics is known to play an important role in the rate of diffusion as it directly influences the thickness of the DBL, which in turn acts as a diffusion barrier; (3) In the sea, currents and waves may cause water advection and sediment resuspension which may influence metal fluxes. For the first bias (1) it must be noted that microcosms were far from anoxia: oxygen levels at 5 mm above the sediments were about 5 mg L^{-1} and increased Fe fluxes were not observed during the experiment (Table 1). Iron effluxes are frequently observed when anoxia is developping (Petersen et al. 1996). For some metals like Mn^{2+} it was shown in other reports that the concentration in porewaters of the top sediment layer (0-5 mm) is not dependent on dissolved oxygen levels of the bottom water, at least on the short term (Pakhomova et al. 2007). Manganese fluxes are therefore not influenced by the redox conditions in the near-bottom water. For the second bias (2) it must be noted that high water flow velocities near the bottom will tend to decrease the DBL thickness and thus increase benthic effluxes (Jørgensen and Des Marais, 1990). Consequently, we may view our measurements in stagnating water as lower estimates of what can be released under high flow velocities. Finally, for the third biases (3), sediment resuspension and water advection are also expected to release more metals into the bottom waters. To sum up, metal fluxes determined in our microcosm approach must be considered as an approximation, probably underestimated, of the real benthic fluxes in muddy sediments of the BCZ (they cannot be applied to the whole BCZ

which also feature coarse and sandy sediments).

Although fluxes determined here are approximations, the most important point of the present research is that mineralization of phytodetritus at the WSI increases effluxes of Mn, Co and As. Flux values obtained in this study are in the range of those observed *in situ* using benthic chambers deployed on other shallow coastal oxic sediments which may be exposed to phytodetritus (Hunt, 1983; Ciceri et al., 1992; Aller, 1994; Thamdrup et al., 1994; Warnken et al., 2001; Pakhomova et al. 2007). For instance, Mn effluxes were found to vary between 70–4450 μmol m^{-2} d^{-1} in the Gulf of Finland and the Vistula Lagoon of the Baltic Sea (Pakhomova et al. 2007), or between 420–2600 μmol m^{-2} d^{-1} in Galveston Bay, Texas (Warnken et al. 2001). The maximum effluxes obtained here for Mn were only 755 μmol m^{-2} d^{-1}. Similarly, for As effluxes, other investigators have observed 0.008–2.5 μmol m^{-2} d^{-1} for Amazon shelf sediments (Sullivan & Aller, 1996) and about 5.1 μmol m^{-2} d^{-1} for Chesapeake Bay sediments (Riedel et al., 1987). In the present study, As effluxes were 0.045–1.084 μmol m^{-2} d^{-1}, exactly in the range of the previous observations.

Another point to consider is the role of the benthic microbial communities. It is clear that the onset of mineralization is very fast and starts within 2h of deposition as revealed by CLPP analyses. Benthic microbial communities were shown in other studies to react quickly to fresh inputs of organic carbon (Turley and Lochte, 1990; Meyer-Reil and Köster, 1992). The increased activity of the microbial heterotrophs results in the consumption of the oxygen (Franco et al., 2007; Rauch et al., 2008) which is known to be responsible for >90% of the organic carbon mineralization at the WSI (Bender and Heggie, 1984). As a consequence, the oxic-anoxic interface [usually located at 3-4 mm into the sediments of that station (Gao et al., 2009)] moves upwards and reduced elements like Fe^{2+}, Mn^{2+}, Co^{2+} and arsenic species, may diffuse out of the sediments. Fe and Mn oxides are important electron acceptors in anaerobic marine sediments (Thamdrup et al., 1994). Mn oxides are reductively dissolved by the action of bacteria that actively mineralize the phytodetritus thereby releasing Mn^{2+} into the porewater (Froelich et al., 1979; Burdige and Gieskes, 1983; van der Zee and van Raaphorst, 2004). This Mn^{2+} is then able to diffuse out of the sediments as it is relatively stable to chemical oxidation. In comparison, Fe^{2+} ions are more reactive and precipitate at the WSI after its re-oxidation in the contact with oxygen (Pakhomova et al., 2007). Consequently, Fe is not expected to accumulate in oxic seawater as observed in the present microcosm experiment. Increased benthic effluxes of Mn, Co and As from sediments may thus be

explained by the development of anaerobic conditions at the WSI which is here a consequence of an increased microbial heterotrophic activity. The effect of anaerobiosis on such metal effluxes was observed in previous microcosm experiments (Petersen et al., 1996) but also *in situ* (Sundby et al., 1986).

The deposition of fresh phytodetritus at the WSI explains the increased bacterial production observed on Day-2 (ca. 4.3 times, from 2.0 to 8.7 mg C m^{-2} d^{-2}). However, this increased bacterial production was not followed by an increased bacterial biomass because the biomass of heterotrophic nanoflagellates immediately increased (6.2×10^6 cells mL^{-1} at Day-2). Nanoflagellates, which are known to be the main bacterial grazers (Hondeveld et al., 1995), were thus able to control the bacterial biomass in the microcosm experiment and were not impeded by high arsenic levels. The total heterotrophic activity increased (bacteria and nanoflagellates) and this resulted in a consumption of oxygen with a lowering of the pH which in turn promoted the reductive dissolution of Fe/Mn oxyhydroxides that release many metals and metalloids. In addition, large quantities of organic acids were probably generated during the mineralization process. Such organic acids are then able to complex many metallic elements and transport them into the overlying water.

During the last 5 days of mineralization (Day-2 to Day-7) effluxes of trace elements were reduced. This is another indication that effluxes are linked to the mineralization of phytodetritus, as the quantity of phytodetritus is decreasing. Although effluxes of trace elements were reduced, the microbial enzymatic activity was still intense, as indicated by the esterase activity and the CLPP profiles on Day-7. These increased bacterial activities were not followed by an increased bacterial production: values on Day-7 were at the level of those observed in the controls (ca. 2 mg C m^{-2} d^{-2}). But the bacterial biomass was now 1.3 times more elevated. This may be explained by a reduced predation by nanoflagellates as these may have been consumed by higher trophic levels (large ciliates, nematodes, etc.). Although the experiment was stopped after 7 days of incubation it is probable that enzymatic activities and bacterial biomass slowly return to pre-exposure values within a few days.

The consequences of arsenic effluxes may be huge in areas covered with contaminated muddy sediments and submitted to an intense rain of phytodetritus. In the microcosm experiment described here the quantity of added phytodetritus was only 5.24 g m^{-2} (dw) (0.092726 g / 0,017670 m^2). It has been calculated that this quantity of deposited phytodetritus has led to the release of 76.4 µg of arsenic per square meter of sediment after only 48h (see Appendix

B). The Belgian Continental Zone (BCZ) is 3600 km^2 and we may estimate that about 20% of that surface area (720 km^2) is composed of muddy contaminated sediments located close to the coast between the cities of Oostende and Zeebrugge (Van den Eynde, 2004; Ruddick and Lacroix, 2008; Gao et al., 2009). These muddy sediments have been monitored in various points and results show that the arsenic content is almost unchanged in the area [the monitored stations include contaminated stations 140 and 700 (Gillan and Pernet, 2007)]. If sediments of the area are considered as equivalent, this means that about 55 kg of arsenic may be released into the seawater of the BCZ, in only two days and as a result of the microbial activity alone, when only 5.24 g (dw) of phytodetritus are mineralized on each square meter of this area. As explained before this quantity of phytodetritus is probably a low estimation of what may be deposited on the BCZ during a real phytoplankton bloom (Schoemann et al., 2005). In addition, arsenic effluxes might even be higher because (1) the metal content of the phytodetritus was not taken into account in the above calculations; (2) hydrodynamic effects which lower the DBL and resuspension events were not taken into account.

These large quantities of arsenic released from sediments in the continental zone may then return to the sediments. Indeed positive fluxes (i.e., towards the sediments) up to +262 nmol m^{-2} d^{-1} have been observed in the present experiment (Table 1). However, during the stay in the overlying water, arsenic species may be accumulated in the biota. The main arsenic compound in oxic seawater is arsenate (AsO_4^{3-}) (Mukhopadhyay et al., 2002). Arsenate is known to be taken up by marine organisms, ranging from phytoplankton, algae, crustaceans, mollusks and fishes (Knowles and Benson, 1983). Fish and marine invertebrates retain 99% of accumulated arsenic in organic form, and crustacean and mollusk tissues are known to contain higher concentrations of arsenic than fishes (Mukhopadhyay et al., 2002). Arsenic, which is now recognized as a carcinogenic element (Pershagen, 1985; Bates et al., 1992), may thus accumulate in marine foodstuffs such as prawns at levels approaching 200 ppm (Nriagu, 1994).

To conclude, measures to limit eutrophication and phytoplankton blooms in contaminated areas are urgently needed for the Belgian Continental Zone. The reason is that upward fluxes of toxic elements like arsenic occur when contaminated muddy sediments are exposed to *Phaeocystis*-derived phytodetritus. A clear link was established here between heterotrophic microbial activity at the sediment-seawater interface and increased effluxes of Mn, As and Co. Calculations have suggested that this microbial activity alone may release substantial amounts of dissolved elements in only 48h when sediments are exposed to large quantities of

phytodetritus, i.e. every year between February and May.

Acknowledgements

This research was supported by a Belgian Federal research program (Science for a Sustainable Development, SSD, contract MICROMET n°SD/NS/04A and SD/NS/04B). AP and KS acknowledge financial support from BOF-GOA projects 01GZ0705 and of Ghent University (Belgium). Contribution of the "Centre Interuniversitaire de Biologie Marine" (CIBIM). We are indebted to Jean-Yves Parents and Dr. Véronique Rousseau (ULB, Brussels) for their help with the cultivation of *Phaeocystis* and *Skeletonema*, to Kevin Denis and Prof. Philippe Grosjean (Mons University) for their help with the automatic counting of bacteria using ZooPhytoImage. Many thanks also to André Cattrijsse and all the crew of the RV Zeeleeuw, and to Mathieu Bauwens for his help in the laboratory.

Appendices

Appendix A :

- The dry matter content of the final algal suspension used as phytodetritus was 130.6 mg L^{-1}.

- Four cm of overlying water in one microcosm of 15 cm of ø = 710 mL.

- A quantity of 92.7 mg (dw) of phytodetritus were deposited in each microcosm (130.6 mg × 710 mL / 1000 ml = 92.7). This corresponds to 0.092726 g.

- The Mn concentration of the phytodetritus was 64.5 µg g^{-1} (dw).

- The Co concentration of the phytodetritus was 0.54 µg g^{-1} (dw).

- The As concentration of the phytodetritus was 4.4 µg g^{-1} (dw).

- The complete mineralization of the 92.7 mg of phytodetritus in one microcosm containing 710 mL of overlying water may thus produce a maximum of 5.98 µg of Mn (0.092726 × 64.5 = 5.98), 0.050 µg of Co (0.092726 × 0.54 = 0.050), and 0.40 µg of As (0.092726 × 4.4 = 0.40).

- If 5.98 µg of Mn are released in 710 mL of water, this corresponds to 8.4 µg L^{-1}.

- If 0.050 µg of Co are released in 710 mL of water, this corresponds to 0.07 µg L^{-1}.

- If 0.40 µg of As are released in 710 mL of water, this corresponds to 0.56 µg L^{-1}.

Appendix B :

- In Fig. 2, the increase observed for arsenic in experimental microcosms, when 2h is compared to Day-2, is 2.49 µg L^{-1} (4.76 – 2.27 µg L^{-1}). For 710 mL (one microcosm) this corresponds to the arrival of 1.76 µg of As (2.49 × 710 / 1000 = 1.76).

- These 1.76 µg of arsenic in one microcosm can only come from the sediments or from the phytodetritus. As 92.7 mg of phytodetritus were deposited in each microcosm (130.6 mg × 710 mL / 1000 ml = 92.7) and that 1 g of phytodetritus (dw) contains 4.44 µg of As, this means that the maximum of As released by the mineralisation of the phytodetritus in one microcosm is 0.41 µg (0.0927 g × 4.44 µg / 1 g = 0.41 µg).

- 0.41 µg is 23.4% of 1.76 µg. This means that the rest (76.6% = 1.35 µg) is coming from the sediments for one microcosm.

- One microcosm is 0.017670 m^2.

- We may conclude that, following the deposition of 92.7 mg of phytodetritus over a surface of 0.017670 m^2 (one microcosm) a quantity of 1.35 µg of As is released from the sediments.

- The quantity of As released from 1 m^2 is thus 76.40067 µg (1.35 / 0.017670 m^2).

- One $km^2 = 10^6$ m^2

- The quantity of As released from 1 km^2 is thus 76.40067 g.

- The quantity of As released from 720 km^2 is thus 55 008,49 g = 55 kg.

5

IMPACT OF PHYTOPLANKTON BLOOM DEPOSITION AND CONCOMITANT METAL FLUXES ON THE COMPOSITION AND ACTIVITY OF BENTHIC MICROBIAL COMMUNITIES IN SUBTIDAL MARINE SEDIMENTS: A MICROCOSM STUDY

Annelies Pede[1], David Gillan[2;5], Yue Gao[3], Gabriel Billon[4], Martine Leermakers[3], Tine Verstraete[1], Wim Vyverman & Koen Sabbe[1]

[1] Lab. Protistology & Aquatic Ecology, Department of Biology, Ghent University, 9000 Ghent, Belgium

[2] Proteomics and Microbiology Lab., Mons University, 5, B-7000 Mons, Belgium

[3] Department of Analytical and Environmental Chemistry, Vrije Universiteit Brussel, 1050 Brussels, Belgium

[4] Université des Sciences et Technologies de Lille, UMR-CNRS 8110, France

[5] Marine Biology Lab., Université libre de Bruxelles, 1050 Brussels, Belgium.

Manuscript in preparation

Abstract

Muddy subtidal sediments in the Belgian Coastal Zone (BCZ, southern North Sea) are characterized by high concentrations of trace metals. During spring, this area is characterized by extensive phytoplankton blooms, which upon sedimentation induce intense remineralization and significant changes in the redox state of the sediments, leading to enhanced trace metal effluxes. We used microcosms to evaluate the interaction between the deposition of moderate concentrations (± 7.1 mg m^{-2} of chlorophyll *a*) of the diatom *Skeletonema* sp. and the haptophyte *Phaeocystis globosa*, metal effluxes and microbial community structure and activity. Sediments were sampled after 0, 2 and 7 days. Changes in composition and activity of both the bacterial and microbial eukaryotic communities (with emphasis on Protozoa) were analyzed using molecular methods (16S and 18S rDNA and rRNA extractions followed by DGGE), and related to bacterial biomass, number of heterotrophic nanoflagellates, dissolved metals and other geochemical variables (redox, O_2, salinity, pH, chlorophyll and DOC). Gamma-Proteobacteria, Bacteroidetes and delta-Proteobacteria were the dominant bacterial members, while Alveolata (ciliates, dinoflagellates and apicomplexans), diatoms, Fungi, and Amoebozoa were dominant in the microeukaryotic communities. DNA- and RNA-based fingerprints of bacteria and Protozoa showed distinct changes in the total and active community structure as a consequence of the algal enrichment, and with time. The enrichment effect was most pronounced after 2 and 7 days for bacteria and Protozoa respectively. Our results suggest that phytodetritus deposition activates and stimulates the microbial loop, via changes in bacterial activity, biomass and community composition, together with subsequent changes in numbers and relative abundance of heterotrophic nanoflagellates and ciliates, and composition and activity of protozoan communities.

Introduction

The Belgian Coastal Zone (BCZ), situated in the Southern part of the North Sea, has received high amounts of metals especially through riverine (Scheldt estuary) input and by local coastal industrial activity (Baeyens, *et al.*, 1998b, Danis, *et al.*, 2004, Gillan & Pernet, 2007). Metals tend to accumulate in silty, organically rich sediments and are non-degradable (Graf, 1992, Middelburg & Levin, 2009), resulting in high concentrations in coastal subtidal

sediments (Gao, *et al.*, 2009, Pede, *et al.*, chapter 2 & 3). The coastal waters are also characterized by recurrent phytoplankton blooms in spring, initiated by a moderate diatom-dominated bloom, followed by a major bloom of the haptophyte *Phaeocystis globosa,* which has intensified by eutrophication of this area (Lancelot, *et al.*, 1987, Boon, *et al.*, 1998, Lancelot, *et al.*, 2005). A considerable amount of the bloom-derived detritus sediments (Lancelot, *et al.*, 2005), resulting in pronounced changes in values and gradients of a.o. redox potential, pH and dissolved sulphides in the sediment (Pede, et al., chapter 3, Gao, *et al.*, 2009, Gillan, *et al.*, subm., chapter 4). These changes have major repercussions for the benthic ecosystem (Pede, *et al.*, chapter 3). Several studies have demonstrated community changes in benthic bacterial, nematode, meio- and macrofaunal communities in relation to algae bloom deposition (Goedkoop, *et al.*, 1997, Vanaverbeke, *et al.*, 2004, Franco, *et al.*, 2007, Franco, *et al.*, 2010). A recent field study in this area also demonstrated temporal changes in benthic microeukaryote community structure in response to algae-derived organic matter (OM) input (Pede, *et al.*, chapter 3). Bacterial benthic communities are primary decomposers of organic matter sedimented from algae blooms (Vanduyl, *et al.*, 1992), and heterotrophic protists (Protozoa) are important consumers of bacteria and other protozoans (Lee & Patterson, 2002, Wey, *et al.*, 2008). In general, there is a coupling between these compartments and a detritus-dependent development of the microbial loop has been described (van Hannen, *et al.*, 1999a); correlations have been demonstrated between phytoplankton biomass and bacterial biomass and community structure (van Hannen, *et al.*, 1999a, Franco, *et al.*, 2007, Franco, *et al.*, 2010), and between protozoan biomass and bacterial biomass and community structure (Tao & Taghon, 1997, van Hannen, *et al.*, 1999a, van Hannen, *et al.*, 1999b). Integrated studies about the effects of algae bloom deposition on benthic microbial community structure and associations between bacterial and protozoan communities remain limited. Moreover, it has been shown that algal OM deposition modifies metal speciation, mobilization and hence bioavailability in sediments (Eggleton & Thomas, 2004). For example, seasonally increased metal effluxes of Mn, Co, Fe and As have been reported from the sediment into the water column after deposition of phytoplankton blooms (Gao, *et al.*, 2009), most probably as a result of increased bacterial respiration affecting oxygen and redox gradients (Eggleton & Thomas, 2004, Gadd, 2004). Increased bioavailability of toxic trace metals can potentially impact the structure and activity of microbial communities and their interactions, causing additional feedbacks on benthic biogeochemistry and hence metal behavior. A better understanding of how microorganisms interact with these fluxes of

contaminants to and from the water column is fundamental to ensure the long-term integrity of these benthic ecosystems and their sustainable exploitation.

During this study, the relationships between OM deposition, structure of the total and active benthic microbial communities and metal dynamics was investigated. To this end, an experimental microcosm setup was used in which natural, undisturbed, metal-contaminated sediments from the BCZ were exposed to algal phytodetritus (*Phaeocystis globosa* and *Skeletonema costatum*, two important members of the spring algae bloom). Microbial community structure was monitored using the molecular fingerprinting technique DGGE (Denaturant Gradient Gel Electrophoresis). This technique allows to simultaneously generate information on both bacterial and microbial eukaryotic communities from the same sample, by PCR amplification with bacterial- and eukaryote-specific primers. We studied community structure of both the total and the metabolically active microbial communities by targeting the small subunit ribosomal DNA and RNA respectively. The effect of bacterial mineralization of the algal phytodetritus on sediment biogeochemistry and metal dynamics is described in detail in Gillan *et al.* (subm., see chapter 4) and Gao *et al.* (in press). Here we focus on changes in microbial (bacteria and microeukaryotes, with emphasis on Protozoa) community structure in relation to variation in biogeochemical variables (O_2, pH, chlorophyll *a*, DOC, …) and trace metals.

Materials and methods

Study site and sampling

The phytoplankton enrichment experiment was performed using sediments from station 130 (51°16.25 N - 02°54.30 E; depth: ± 11 m) located in the Belgian Continental Zone (BCZ). The sampling site was selected based on previous research, as it is one of the most metal-contaminated subtidal stations in the BCZ (Gillan & Pernet, 2007, Gao, *et al.*, 2009). Sediments are muddy and have a mean grain size of 12.5 µm. they were collected in March 2010 aboard RV "Zeeleeuw" using a Reineck corer (ø 30 cm). Undisturbed cores were immediately transferred to cylindrical plexiglass microcosms of the same diameter (ø 30 cm), overlaid by 4 cm of seawater. Smaller subcores (Plexiglass tubes) for trace metal measurements were also prepared (ø 7 cm). All cores were transported to the laboratory in insulated boxes and left for 10 days in the dark at 15.0 ± 1°C.

Experimental setup

Methodologies for preparation of the algae cultures, the experimental microcosm set-up, the biogeochemical and metal analyses and the measurement of microbial biomass have been described in detail in Gillan, *et al.* (subm.; see chapter 4), and Gao, *et al.* (in press). They are briefly summarized below.

Algal cultures and algal suspension

A mixture of the phytoplankton algae *Phaeocystis globosa* (a haptophyte) and *Skeletonema costatum* (an early spring diatom) was prepared. Both algae are naturally present on the BCZ and are dominant members of the phytoplankton bloom in spring (Rousseau, *et al.*, 2002). The strains used were isolated from the BCZ by the ESA Lab, ULB, Brussels. Algae were cultivated in F20 medium that is composed of seawater to which major nutrients, trace metals, minor elements and vitamins were added (Veldhuis & Admiraal, 1987). The proportion of the two algae in the final algal suspension used for the microcosm experiment was 50:50 (w/w). The algal suspension was filtered (GF/F filters; Whatman) and cell pellets were frozen at -20°C until the start of the experiment. At the start of the experiment, cell pellets were thawed and resolved in natural seawater. The final chlorophyll *a* (CHL *a*) content was 750 ± 35 µg L^{-1} (mean ± SD), the dry matter content of the suspension was 130.6 mg L^{-1} (dry weight, measured after centrifugation and lyophilisation of three 50 ml samples).

Microcosm set-up

We used a static setup, i.e. sediments were incubated in the laboratory with stagnant seawater at the surface. Sediments (height ± 7 cm) were not mixed (i.e. the *in situ* stratification was maintained). Eighteen large microcosms were divided in two groups, to test for two conditions (with and without algae) at three different time points (Day-0, Day-2, Day-7) in triplicate. For the measurements of the metals, 6 smaller cores were used. At the start of the experiment the overlying seawater was slowly removed from all the microcosms and cores without disturbing the sediment-seawater interface. A volume of 710 ml of algal suspension was then slowly deposited on half of the microcosms (experimental microcosms), in order to achieve final CHL *a* concentrations of approximately 7.1 mg m^{-2} and a dry matter content of approximately 1.3 g m^{-2} reaching the sediment surface; the other half receiving 710 ml of natural seawater (control microcosms; the same seawater was used for the algal suspension and the control condition; note that the seawater was not sterilized and the cultures were not

axenic). Accordingly, the small cores received 132 ml of algal suspension (experimental cores) or 132 ml of natural seawater (control cores). The height of the overlying seawater in all microcosms and cores was 4 cm. After two hours of sedimentation, 6 microcosms (3 experimental and 3 controls) and two small cores (1 experimental and 1 control) were used for Day-0 analyses (Day-0) of microbial and geochemical parameters. After two days (Day-2) and 7 days (Day-7) the same analyses were repeated. The temperature of the water during the experiment was maintained at 15.0 ± 1°C, a temperature that is reached at the end of spring (Hondeveld, *et al.*, 1994, Pede, et al., chapter 3).

Biogeochemical parameters

Geochemical parameters measured included pH profiles at the sediment-water interface, metals in sediment porewaters, dissolved organic carbon (DOC) in porewaters, CHL *a* in surface sediments, and oxygen levels and salinity of the overlying seawater. Oxygen, salinity and pH were determined using microelectrodes; DOC concentrations were measured by a Dohrman Apollo 9000 total organic carbon analyzer; CHL *a* concentrations (μg g^{-1} sediment dry weight, SDW) were determined by HPLC pigment analysis with standard protocols (Wright, *et al.*, 1991); and metals in porewaters by using DGT probes. The DGT (diffusive gradient in thin films) technique is used for the assessment of the labile metal fraction in the sediment porewaters, which represent the bioavailable metals (Davison & Zhang, 1994). DGT metals were measured for Mn, Fe, Co, As, Pb, Cr, Ni and Cu. The techniques have been descripted in detail in Gillan *et al.* (subm.; see chapter 4), and Gao *et al.* (in press).

Heterotrophic nanoflagellate (HNF) and bacterial biomass (BM_{bact}) in the upper first cm sediment layer was determined using counts of DAPI-stained (4'6-diamidino-2-phenylindole) cells and expressed as the number of cells per ml of sediment, and number of bacteria per gram fine fraction respectively (Gillan *et al.*, subm.; see chapter 4).

Molecular analyses of microbial communities

DNA extraction

Total genomic DNA was extracted from approximately 1g of sediment using zirconium beads and phenol as described by (Zwart, *et al.*, 1998), after elimination of the extracellular DNA (Corinaldesi, *et al.*, 2005). Total extracted DNA was purified on a Wizard column (Promega) and stored at -20°C until further analysis.

RNA extraction and cDNA synthesis

Total RNA was extracted from approximately 0.5g of sediment. 700 µl of pre-warmed (65°C) extraction buffer and 0.5ml of baked 1mm silicon carbide sharp particles were added to the frozen sediment. RNA was isolated using bead-beating, phenol-chloroform extraction, and ethanol precipitation, described by Chang, *et al.* (1993) and adapted by Vannerum, *et al* (2011). RNA was resuspended in 20µl of RNAse-free water and residual DNA was removed from RNA extracts with RNase-free DNase (DNase I; Sigma). Total RNA was transcribed into cDNA using Qiagen OneStep RT-PCR Kit (Qiagen) according to the manufacturer's instructions. RNA and cDNA were stored at -80°C and -20°C respectively.

PCR amplification and Denaturant Gradient Gel Electrophoresis (DGGE)

PCR amplification and DGGE analysis were performed as described elsewhere (Pede, *et al.*, chapter 2, (Gillan, 2004). The same (c-)DNA extract was used for eukaryotic and bacterial communities, using eukaryotic and bacterial-specific primers respectively. The general eukaryotic primers 1427f-GC (5'-GC-rich clamp-TCTGTGATGCCCTTAGATGTTCTGGG-5') and 1637r (5'-GCGGTGTGTACAAA GGGCAGGG-3'), designed by (van Hannen, *et al.*, 1998), amplified a fragment of the 18S rDNA, approximately 210bp long; the general bacterial primers GM5F-GC (5'- GC-rich clamp -CCTACGGGAGGCAGCAG-3') and 518R (5'-ATTACCGCGGCTGCTGG-3'), designed by (Muyzer, *et al.*, 1993, van Hannen, *et al.*, 1998, Gillan, *et al.*, 2005), amplified a fragment of the 16S rDNA, approximately 193bp long. All PCR products were purified with the QiaQuick PCR purification kit (Qiagen) and the concentration of PCR product was determined spectrophotometrically using a Nanodrop 2000 (Thermo scientific). DGGE was performed on a Bio-Rad DCode system. Gels of 7% (w/v) polyacrylamide were prepared with a linear 30-55% (eukaryotic) and 35-60% (bacterial) denaturant gradient (acrylamide/bisacrylamide ratio, 37,5:1; 100% denaturing polyacrylamide solution contained 7M urea 40% (v/v) formamide). Equal amounts, i.e. 500 ng for DNA (except for T0-C2 bacteria: 390ng) and 300 ng for RNA (except for T7-C3 bacteria: 240ng) of PCR product were loaded in each well. DGGE standards were included per gel (minimum 3 lanes), covering the entire gradient in the DGGE gels (see Pede *et al.*, chapter 2). Electrophoresis was performed for 16h at 100V in 1X Tris-acetate-EDTA (TAE) buffer at 60°C. The DGGE gels were stained for 30 min in 1X TAE buffer with SybrGold (Molecular probes) and digitally photo-documented (Kodak Easy Share P880 camera) under UV illumination.

Nucleotide sequences of several bands were obtained by cycle sequencing (BigDye Terminator v3.1 cycle sequencing kit; Applied Biosystems) of DNA and cDNA amplicons (Muyzer, *et al.*, 1993, van Hannen, *et al.*, 1998), without GC-clamp) from excised and purified DGGE bands, as described earlier (Pede, *et al.*, chapter 2). Several bands were excised from the same height in the DGGE gels ('band-classis'; see below). Sequencing was performed using an ABI 3130XL Genetic Analyzer (Applied Biosystems). Nucleotide sequences were compared with the NCBI GenBank Database () using the nucleotide-nucleotide Basic Local Alignment Search Tool (BLAST) to identify their approximate phylogenetic affiliation (closest genbank match) and the most closely positively identified phylotype (i.e. higher similarities to e.g. environmental but unidentified sequences are not shown). Additionally, bacterial sequences were checked in the Ribosomal Database Project (RDP) using the classifier (Wang, *et al.*, 2007) for rapid assignment of the 16S rRNA sequences into the taxonomic group, with confidence threshold $\geq$ 95%. The partial 16S and 18S rRNA sequences of this study are available upon request from the corresponding author.

DGGE fingerprint image analysis

The digital DGGE images were imported and analyzed for fingerprint similarity using Bionumerics 5.10 (Applied Maths BVBA, Belgium), as described earlier (Pede, *et al.*; chapter 2). Fingerprints were normalized using the DGGE markers as an external reference, and bands visually determined to be in common among several fingerprints in the gels were used as internal reference markers. Using both internal and external markers, all fingerprints were aligned (i.e. bands from the same position relative to the position of the marker bands in the gel were grouped into band classes). Sequence information of the excised bands was used to check the grouping of bands into the correct band classes. Each band class theoretically represents a unique phylotype, i.e. a single organism in the microbial eukaryotic assemblage (referred to as Operational Taxonomic Unit, OTU). In some cases however, different bands (~DNA and cDNA sequences) can co-migrate the same distance on the DGGE gel, and one OTU can yield different phylotypes (referred to as 'mixed OTUs'). These mixed OTUs are a well-known phenomenon for DGGE (Muyzer & Smalla, 1998). The intensity of the DGGE bands reflects the relative contribution of the OTU to the overall community composition within a sample; the intensity of each band was expressed as a proportion of the total sample (lane) intensity, thus standardizing any loading differences. Matrices were constructed with the relative abundances of the OTUs in each sample. These matrices represented the microeukaryotic and bacterial composition of the total (DNA) and active (RNA)

communities. For microeukaryotic communities, smaller matrices were constructed with only the OTUs representing heterotrophic microeukaryotes (~Protozoa) (also the mixed band classes including one or more protozoan sequences), representing the total and active protozoan community. Per samples, protozoan abundance values were rescaled to 100 %. The matrices were then used to determine the total number of OTUs in each profile (= species richness or SR) and for the multivariate data analyses (see below). Microeukaryotic SR was calculated for the entire community (based on the total matrices), while further multivariate analyses focused on the protozoan fraction of the community.

Statistical analysis

The effects of treatment (algae addition or control) and time (Day-0, Day-2 and Day-7) on bacterial and eukaryotic SR, and CHL *a* concentrations in the upper sediment layer were tested using factorial ANOVA. Significant differences between groups were analyzed by Tukey HSD test.

Multivariate analyses were performed using the software package PRIMER 6 (Clarke & Gorley, 2006)with the PERMANOVA+ add-on (Anderson, *et al.*, 2008), and Canoco version 4.5 (Ter Braak & Smilauer, 2002). Variation in total and active microbial community structure were examined separately for microeukaryotes and bacteria. The variables analyzed were the relative abundances (~band intensities) of all microbial OTUs derived from the DGGE profiles. Abundance data were log (x+1) transformed prior to analyses, to downweight the influence of the most abundant species. Principal Coordinates Analyses (PCO) based on Bray-Curtis similarities was used to visualize the general patterns in variation in the total and active communities. PCO is a distance-based ordination method that maximizes the linear correlation between the distances in the distance matrix, and the distances in a space of low dimension (~ the ordination; the 2 main axes are selected). Permutational analysis of variance (PERMANOVA; Anderson, 2001, McArdle & Anderson, 2001) was then used on the same data set to statistically test for the effects of extraction method (DNA and RNA), treatment (algae addition and untreated control) and time (Day-0, Day-2 and Day-7). We used a two-way crossed design based on Bray-Curtis similarities with 9999 permutations of residuals under a reduced model. PERMANOVA tests the null hypothesis that there are no differences among a priori defined groups (Anderson, 2001). We additionally performed constrained ordinations by means of the principal response curves (PRC) method (Van den Brink & Ter Braak, 1999) using Canoco (Ter Braak & Smilauer, 2002). The PRC method is especially

suitable for the evaluation of experiments, because PRC extracts information only from this part of the variance, which is explained by the treatment factor (here: algal enrichment) and the time-factor, implemented as a covariable. It focuses on the deviation of the species community in the model ecosystems from that in the untreated controls. The result of the analysis is a diagram (PRC) in which time is displayed on the x-axis and the canonical coefficient relative to the control (or the 'Principal Response') on the y-axis. PRC curves were constructed for the combined set of the DNA and RNA-based data matrices (comparing total and active communities respectively), and for total and active communities separately (comparing the treatment effect vs. control within the respective communities). The canonical coefficients of the enriched communities are shown as deviations from the control at the respective sampling dates. Data from the DNA-derived fingerprints of the control treatment ('dna-c') were used as the reference for the total (=DNA+RNA) and the DNA-based dataset, whereas the control treatment for RNA ('rna-c') was used as the reference for the RNA-based dataset. Together with the PRC, taxon weights are plotted in a second graph. The taxon weight can be interpreted as the weight of a single taxon in the response shown in the diagram. The higher the value, the more the actual response pattern of the species is likely to follow the pattern in the PRC. Taxa with a negative value show an opposite response to the PRC. The taxon weight thus allows evaluating which taxa most respond to the treatments. Monte Carlo permutation tests permuting whole time series were used to compute statistical significance (p-value, F-ratio). The eigenvalue indicates which part of the variance is displayed by this first canonical axis in the ordination.

Relationships between measured biogeochemical and metal variables and changes in total and active microbial community structure were studied by introducing the variables as supplementary (passive; Spearman correlation) variables in the PCO analyses. The variables used were metal concentrations, DOC, oxygen, pH, Eh, CHL *a*, bacterial and eukaryote SR, HNF and BM_{bact}. They were tested for normality and all variables (except pH and Eh) were log-transformed prior to the statistical analyses. Furthermore, the RELATE test (Clarke & Warwick, 2001), which is a non-parametric form of the Mantel test, was performed to define the relationship between community structure of the total and the active communities, between the bacterial and the protozoan communities, and between microbial community structure, CHL *a* concentration and trace metal concentrations. To this end, separate similarity matrices (Euclidean distance) were constructed for the combined set of trace metals measured in porewaters and for CHL *a* concentrations from the upper sediment layer. The RELATE

tool tests for the hypothesis of no relation between the multivariate patterns in two sets of samples, based on the corresponding similarity matrices. The Spearman Rank correlation method (with 9999 permutations) was chosen, by which rho values and significance levels were calculated.

Results

Environmental parameters

As expected, the addition of the algae led to a significant increase in CHL *a* content in the upper sediment layer. Two hours after the start of the experiment, a significantly higher CHL *a* concentration (30.3 ± 3.1 μg g^{-1} SDW) was measured in the sediments where the algae suspension was added compared to the control treatment. The CHL *a* concentration increased to values up to 41.6 ± 1.3 μg g^{-1} SDW after 2 days and decreased slightly after 7 days (35.2 ± 4.0 μg g^{-1} SDW). In the control microcosms, the CHL *a* level was constant throughout the experiment (21.4 ± 2.6 μg g^{-1} SDW) (see also Gillan, *et al.*, subm., chapter 4). Variation in Eh, pH, DOC, concentrations of dissolved labile (bioavailable, DGT) and total dissolved (DET) trace metals, BM_{bact} and HNF in the sediments, and oxygen and salinity in the overlying water, are described and discussed in Gillan; *et al.* (subm.; see chapter 4) and Gao, *et al.* (in press). In the present study, we only considered the concentrations of the bioavailable (DGT) metal fraction.

Microbial diversity and community composition

Microbial SR was based on the total number of band classes (OTUs), i.e. both identified (see below) and unidentified ones, in the DGGE profiles for both the total communities (DNA-based) and the metabolically active communities (RNA-based). The DGGE fingerprint profiles of the bacterial and microeukaryotic communities are shown in Fig. S1. For bacteria (=SRbact), a total of 65 OTUs was detected, 54 and 63 respectively in the total and active communities; 52 OTUs were present in both. For microeukaryotes (=SReuk), a total of 76 OTUs were detected, 64 in the total and 73 in the active communities; 61 of these OTUs were present in both. Bacterial and microeukaryote SR was thus higher in the RNA than in the DNA profiles. Only 2 respectively 3 band classes were unique for total bacterial and microeukaryotic communities, while 11 respectively 12 band classes were unique for the active communities. Changes in SR with time and treatment (algae enrichment vs. controls)

are shown in Fig. 1. Variation in SR was different in the bacterial and microeukaryotic communities: SRbact was constant throughout the experiment in both the total and active communities, except for a small but significant (between day-0 and day-7) decrease in the active communities of the control microcosms. SReuk of the total community was stable in the control microcosms. In the enriched microcosms, a significant increase can be seen 2 days after the algae were added (significantly higher than day-0 and day-7, and the control microcosms). SReuk of the active community on the other hand decreased during the experiment in the control microcosms, and was significantly lower compared to the control and the enriched microcosm on day-7. A decrease was also visible 2 days after the addition of the algae in the enriched microcosms, but this was not significant. Note that although the average diversity during the three sampling periods is equal (bacteria) or lower (protists) in the active compared with the total communities, total SR was higher for both bacteria and microeukaryotes in the active communities, because the OTU overlap between treated and control microcosms was lower (not shown).

One hundred-seventeen bands, representing 47 different sequences (Table S2) in 39 band classes (OTUs) from the bacterial DNA and RNA-based DGGE gel were sequenced and analyzed using BLAST. Overall, the composition of the total and active communities was quite similar (Fig. 3). Retrieved sequences belonged to the Proteobacteria (PB) [Gamma-PB (43-45%), Delta-PB (13-14%), Epsilon-PB (5-6%), Alpha-PB (4-5%) and Beta-PB (2%)], Bacteroidetes (14-15%), Firmicutes (5-6%), Cytophaga (2%), Cyanobacteria (2%), Chloroflexi (2%), and also two marine diatom chloroplast sequences (4-5%). Sixty-nine bands from the microeukaryotic DNA and RNA-based DGGE bands were sequenced, representing 49 different sequences (Table S1) grouped in 39 different OTUs (band classes), due to a number of mixed identities (see materials & methods). Again, the total and active microeukaryotic community compositions (based on presence/absence of the bands) were quite similar (Fig. 2): 32-34% of the sequences belonged to alveolates (ciliates, dinoflagellates and apicomplexans), another 32-34% had best matches with stramenopiles (Bacillariophyta, Labyrinthulida, Chrysophyceae, Pelagophyceae, Bicosoecida, and uncultured stramenopiles), 11% belonged to Fungi, 9% was related to metazoans, 6-9% to amoebozoans, 4-5% to cercozoans and 2% to the haptophyte *Phaeocystis globosa*. The protozoan fraction thus accounted for 55% of all sequences. Ciliates were the dominant members, mainly Spirotrichea but also Phyllopharyngea (Table S1).

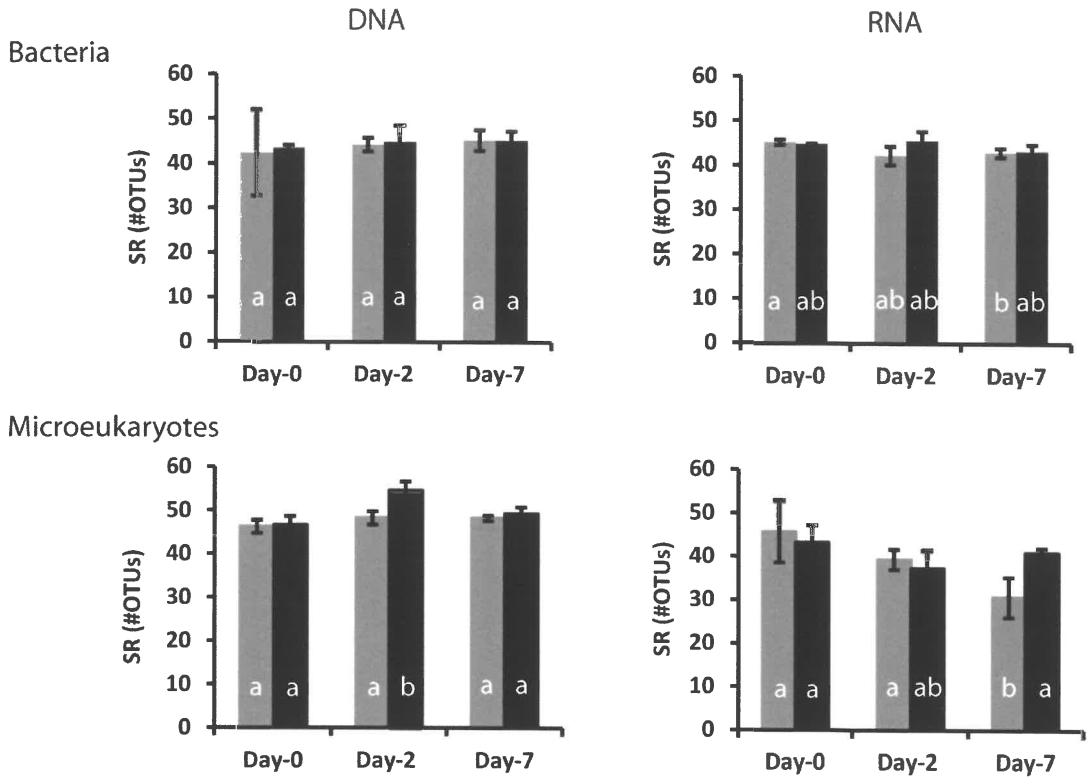

Figure 1: Bacterial and microeukaryotic OTU richness (SR; mean ±SD; n=3) as obtained by DGGE fingerprint analyses of ribosomal DNA and RNA extracted from the surface sediments. Grey, control; black, algae-enriched microcosms. Different letters (a, b) indicate significant differences between SR within each community (Student t-test, $\alpha = 0.05$).

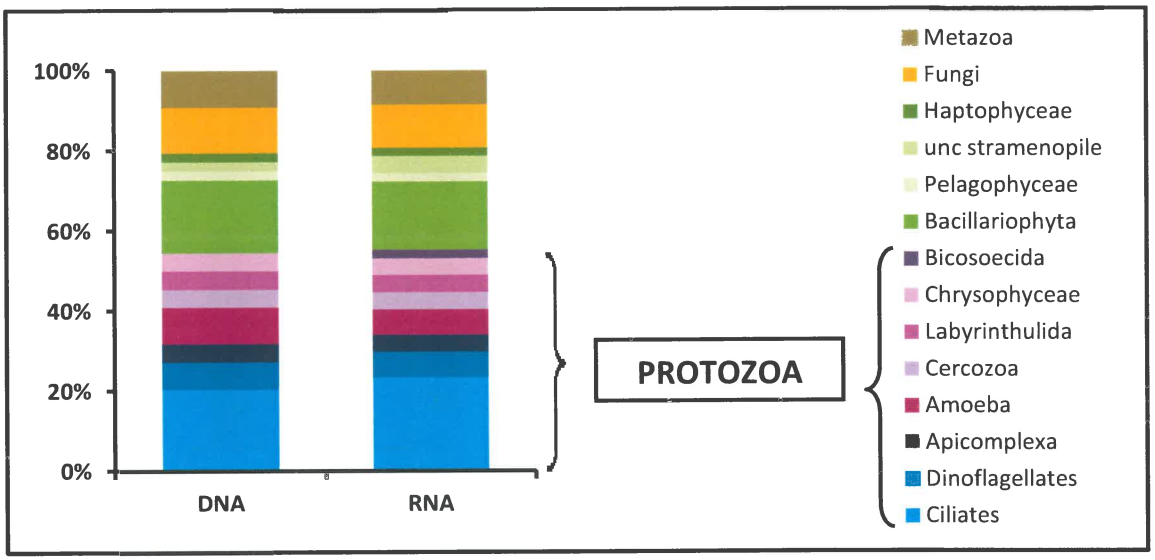

Figure 2: Microeukaryotic community composition for total (DNA) and active (RNA) communities based on the phylogenetic affiliation of the sequenced DGGE bands as retrieved by BLAST analysis. unc, uncultured.

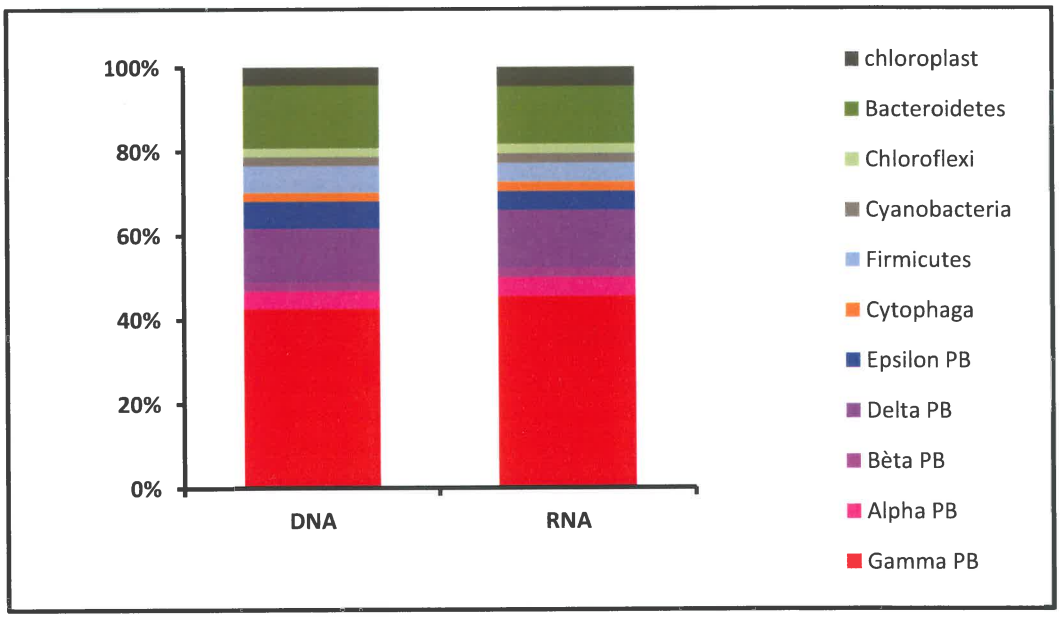

Figure 3: Bacterial community composition for total (DNA) and active (RNA) communities based on the phylogenetic affiliation of the sequenced DGGE bands as retrieved by BLAST analysis. PB, Proteobacteria.

Response of total and active bacterial and protozoan communities to the addition of phytoplankton-derived phytodetritus

PERMANOVA revealed that the difference in community structure between the total and active communities was highly significant ($p<0.001$) for both the bacteria and protozoans (Table 1); they are also clearly separated in the PRC diagrams (Fig. 4).

Both total and active bacterial communities changed significantly in response to the algae enrichment, and also with time; the interaction between treatment and time however was only significant for the total communities (Table 1). Substantial differentiation between the enriched and the control microcosms were already visible 2 hours after the addition of algae (PRC and PCO, Figs. 4, 5, see also below). Divergence was highest 2 days after the start of the experiment, and communities seemed to turn back to their initial (and the control) composition on day 7. For protozoan communities on the other hand, the response of total and active communities to algae enrichment was unmistakably strongest 7 days after the addition of the algae. These shifts were significant for treatment, time and their combined effect for the total communities, whereas the effects were not significant for the active protozoan communities (Table 1), possibly due to the great variation among the replicates (Figs. S1, 5). Monte Carlo permutation tests for the PRC analyses confirmed the PERMANOVA results (Table 2).

Table 1: PERMANOVA F-values (and p-values) for the effect of method of extraction (Method; DNA vs. RNA), treatment (Treatm; control vs. algae enrichment), time (Time; To, T2 and T7) and the combined effect of treatment and time, on the protozoan and bacterial community composition as determined by DGGE. Significant differences ($p<0.05$) are indicated in boldface.

	Method	Treatm	Time	Treatm x Time
Bacteria	**11.9 (0.0001)**			
DNA		**11.77 (0.0001)**	**6.02 (0.0001)**	**1.97 (0.0161)**
RNA		**2.25 (0.0404)**	**2.63 (0.0015)**	1.18 (>0.05)
Protozoa	**20.3 (0.0001)**			
DNA		**3.26 (0.008)**	**5.46 (0.0001)**	**2.52 (0.0038)**
RNA		0.86 (>0.05)	1.54 (>0.05)	0.77 (>0.05)

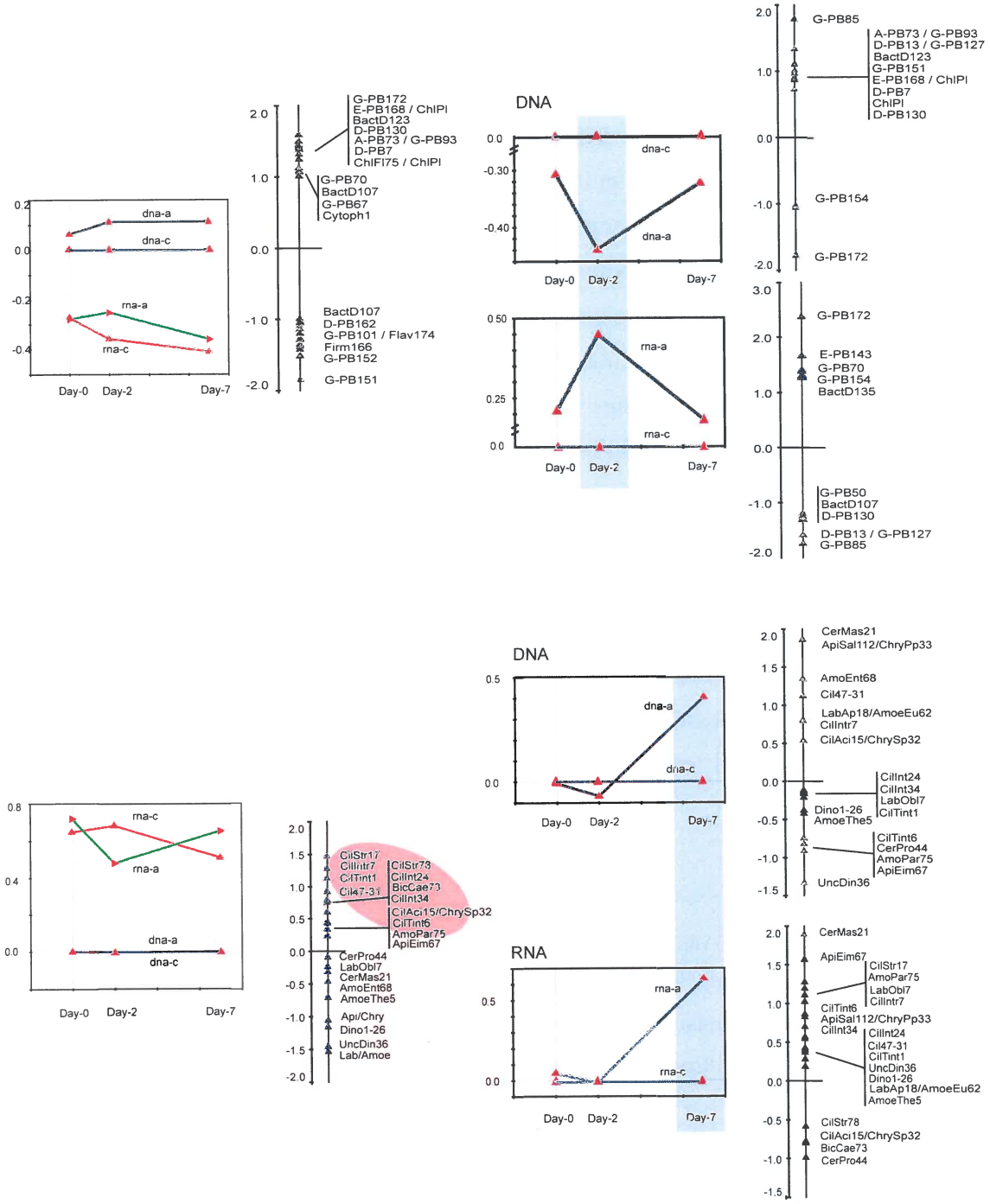

Figure 4: Principal Response Curves (PRC) for the effect of algae enrichment ('-a') on total (DNA) and active (RNA) bacterial and protozoan communities during the microcosms experiment. Presented is the canonical coefficient and the taxon weight for the identified taxa (all protozoan taxa for protozoan communities; lower axis minimum fit 20 for total bacterial communities, and 15 for separate DNA and RNA bacterial profiles). For phylotype labels, see table S2.

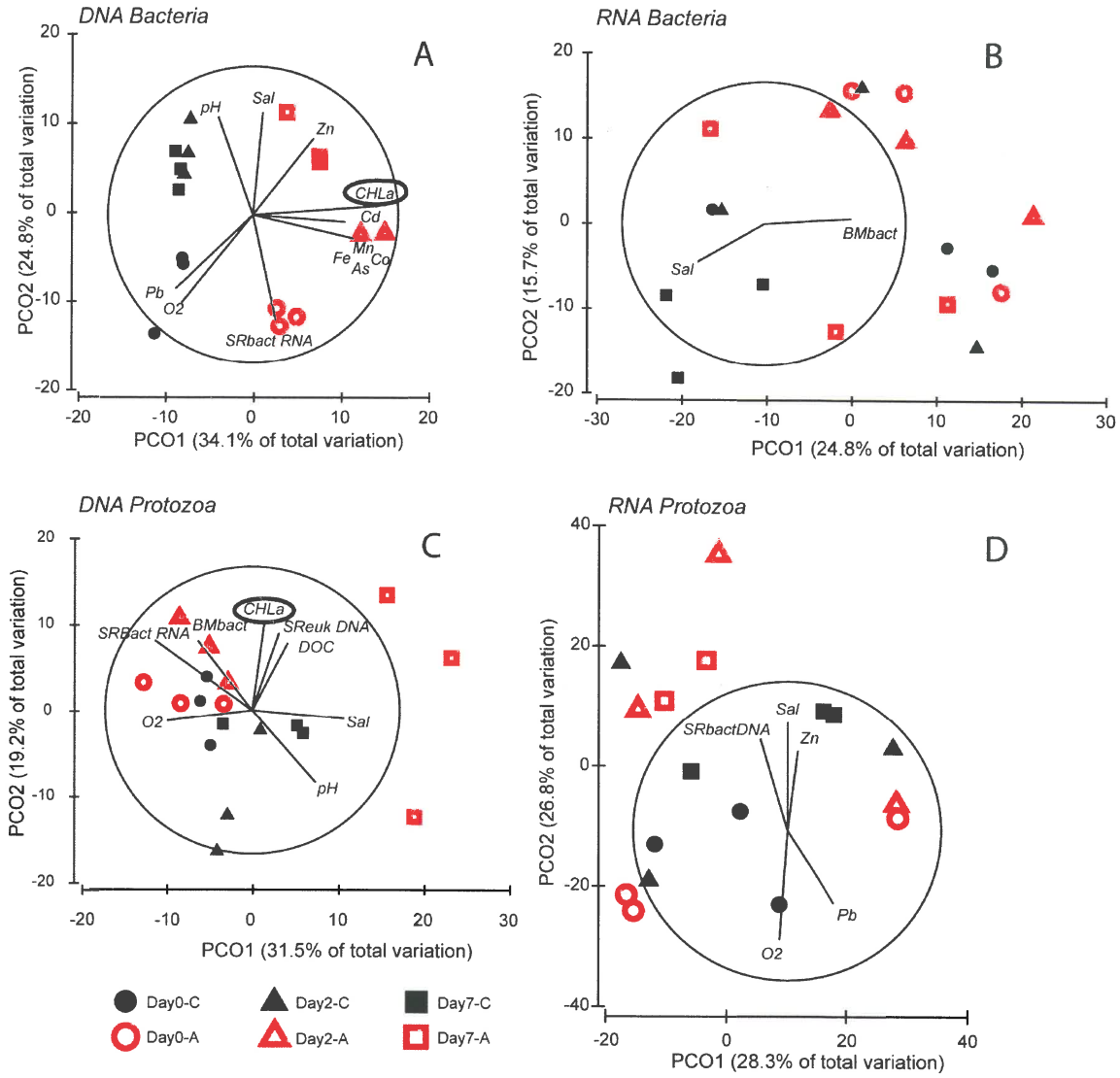

Figure 5: Principal Coordinates Analysis (PCO) based on Bray-Curtis similarities of the relative abundances (log-transformed) for total (DNA) and metabolically active (RNA) bacterial (A & B) and protozoan (C & D) community compositions as obtained by DGGE fingerprint analyses, in the surface sediments of the microcosms after 2 hours (Day-0), 2 days (Day-2) and 7 days (Day-7). Environmental variables significantly correlated ($p<0.05$) to one of both axes with $R>0.5$ are displayed as supplementary variables. Percentages of variation explained by each axis is indicated, C, control (no algae addition); A, algae-enriched sediments; SAL, salinity; DOC, dissolved organic carbon; SR, species richness; BMbact, bacterial biomass.

	eigenvalue	F	p
Bacteria	**0.231**	**8.205**	**0.0020**
DNA	**0.381**	**12.083**	**0.0020**
RNA	**0.168**	**3.179**	**0.004**
Protozoa	**0.326**	**13.218**	**0.002**
DNA	**0.118**	**2.308**	**0.0320**
RNA	0.103	1.683	0.3770

Table 2: PRC statistics:
Eigenvalue, F-ratio and p-value of the Monte Carlo permutation test (999 permutations) on significance of the first canonical axis of the PRC's shown in figure 4.

PCO ordinations showed that the effects of treatment and time are more clear-cut for (a) the total communities compared to the active communities, and (b) bacteria compared to protozoans. The PCO for total bacterial communities (Fig. 5A) showed distinct groups consistent with treatment and time. Variation along the first axis was significantly related to treatment with CHL *a* (evidently) being higher in the algae-enriched microcosms, with values being highest 2 days after the addition of the algae. Likewise, porewater concentrations of the metals Cd, Mn, Co, Fe and As were also higher in the enriched microcosms, and also on day 2 of the experiment. Variation along the second axis mainly reflects variation with time irrespective of treatment: both salinity and pH increased in both the algae-enriched and control treatments. Pb concentrations were higher at the start of the experiment, especially in the controls, while Zn mainly increased towards day 7 (especially in the algae-enriched microcosms). The RELATE test confirmed that CHL *a* and the metal concentrations, and variation in total bacterial community structure, CHL *a* and metals are significantly related (Table 3). Concentrations of Mn, Fe, Co and As are highly correlated in the experiment (Fig. 5A). Variation patterns in active bacterial communities in relation to treatment and time, and the measured environmental variables were less clear-cut, and differences between replicates were much more pronounced (Fig. 5B). The first axis shows a slight shift in structure with time (towards the left, which also explains the significant relation with salinity); BMbact was significantly higher at the beginning of the experiment. Variation patterns in total protozoan communities (Fig. 5C) again showed a change with time (first axis, towards the right, cf. salinity, and the negative relation with oxygen), but this change is clearly more pronounced in the algae-enriched treatment. Algae-enriched and control communities are mainly differentiated along the second axis (especially on day 2 and day 7), witness the relation of CHL *a* and DOC with this axis (note that DOC is highest on day 7 in the algae-enriched

communities). Bacterial biomass and SR of the active bacteria were significantly higher in the communities at the start of the experiment, while SR of the microeukaryotes is higher in the algae-enriched communities, especially on days 2 and 7. Metal concentrations were not significantly related to variation in total microeukaryote community structure (see also Table 3). Like in the active bacterial communities, variations in the active protozoan communities were less clear-cut, with large differences between the replicates (Fig. 5D). The treatment effect is not clear at all, while changes with time are mainly represented along the second axis, which also shows variation in the metals Zn and Pb, salinity and oxygen (cf. above), and SR of the active bacterial communities.

Table 3: Spearman rank correlation coefficients, based on the RELATE routine (Primer, 9999 permutations) calculated on the resemblance matrices (similarity) based on chlorophyll a concentrations in the sediment (CHL *a*), DNA- and RNA-based protozoan (Prot) and bacterial (Bact) community composition, and metals (see text). Only significant correlations ($p<0.05$) are shown; very significant values are indicated in boldface (**$p<0.01$**) and underlined (**$p<0.001$**); -, not significant ($p>0.05$)

	CHL *a*	Prot (DNA)	Prot (RNA)	Bact (DNA)	Bact (RNA)
Prot (DNA)	**0,303**				
Prot (RNA)	-	-			
Bact (DNA)	**0,549**	**0,376**	-		
Bact (RNA)	-	-	**0,257**	-	
Metals	0,257	-	-	**0, 270**	-

Interestingly, the RELATE routine (Table 3) revealed that the variation in community structure of the total prokaryote and protozoan communities are significantly correlated, while the same goes for the active communities of both groups. However, no correlation was detected between total and active bacterial community structure, or between total and active protozoan community structure.

The taxon weights in the PRC diagrams (Fig. 4) allowed to identify which sequenced bacterial and protozoan OTUs are most related to the differentiation in the structure of the total and active bacterial and protozoan communities in response to phytodetritus composition. For bacteria, it can be seen that gamma-Proteobacteria (G-PB172-70-67), delta-

Proteobacteria (D-PB7-130), Bacteroidetes (BactD123-135) etc. were relatively more dominant in the total communities, while different gamma-Proteobacteria (G-PB151-152), Bacteroidetes (BactD107), delta-Proteobacteria (D-PB162), etc. were more abundant in the active communities. We also found several mixed bands, like E-PB168/ChlPl, related to the epsilon-Proteobacteria E-PB168 and a chloroplast (ChlPl). The gamma-Proteobacteria G-PB172 (related to *Alteromonas* sp.) and G-PB154 strongly responded to the algal enrichment, especially on day 2, in both the total and the active community. In the active community, the epsilon-Proteobacterium E-PB143, the gamma-Proteobacterium G-PB70 and the Bacteroidetes BactD135 also showed a strong response on day 2. In contrast, species like the gamma-Proteobacterium G-PB85 and the delta-Proteobacterium D-PB130 (related to an uncultured *Desulfocapsa* sp.) showed strong negative responses to the treatment in both the total and active communities.

The difference between the total and the metabolically active protozoan community was clearly caused by the high abundance of ciliates (*Cil*) in the active communities, while other protozoans (cercozoans, *Cer*; dinophytes, *Dino*; Labyrinthulida, *Lab*; apicomplexans /crysophyceans, *Api, Chry*; Amoeba, *Amo*) dominated the DNA-based profiles. In the total protozoan community, algal enrichment caused an initial (day-2) slight shift in community structure with higher relative abundances of especially an uncultured dinophyte (UncDin36), and then a much stronger change on day-7, when the community was dominated by a *Massisteria* sp. (CerMas21), a mixed OTU (apicomplexan/ chrysophycean), *Entamoeba* sp. (AmoEnt68) and an *Acineta/Aspidisca* sp. (Cil47-31). In the metabolically active protozoan community, we clearly saw an increase in many OTUs in the enriched microcosms towards day 7. A *Massisteria* sp. (CerMas21) increased strongly, as also the apicomplexan Eimeriidae sp (ApiEim67), and seven different ciliates, amongst others (Fig. 6). Species with negative taxon weight like a *Protaspis* sp. (CerPro44) (also in the DNA) and *Caecitellus* sp. (BicCae73) on the other hand were more characteristic for control microcosms and enriched microcosms during the first 2 days of the experiment, and decreased towards day 7. Some taxa increased both in the total and in the active communities, like the cercozoan CerMas21, and the ciliates Cil47-31 and Cil-Intr7.

Discussion

Coastal ecosystems are under pressure from multiple anthropogenic stressors (Danis, *et al.*, 2004, Lancelot, *et al.*, 2005, Boran & Altinok, 2010, Fukunaga, *et al.*, 2010). While these are often studied in isolation, their interaction can exacerbate the consequences for the ecosystem. For example, eutrophication can lead to enhanced algal blooms in marine coastal areas (Lancelot, *et al.*, 2005), and bacterial mineralization of deposited phytodetritus derived from these blooms has been linked to remobilization of toxic trace metals from the sediment to the water column (Fones, *et al.*, 2004). In the BCZ, Gao, *et al.* (2009) recently reported enhanced effluxes of various trace metals (Co, As, Fe and Mn) from metal-contaminated sediments after periods of increased sedimentation of a spring phytoplankton bloom. In order to study the specific role of benthic microbial communities (both bacteria and microeukaryotes) in this process, a microcosm experiment was set-up. In Gillan, *et al.* (subm., see chapter 4), the effect of bacterial mineralization of phytoplankton-derived detritus on the release of bioavailable As, Co and Mn from muddy BCZ sediments is described, while Gao, *et al.* (in press) focus in more detail on the precise dynamics of the total dissolved (DET) and bioavailable (DGT) metals during the same experiment. Both authors reported an increase in chlorophyll *a* and dissolved organic carbon (DOC) in the top sediment layer in the microcosms enriched with algae. The algae-receiving microcosms became more acidified than the controls and redox potential values (Eh) decreased drastically from the sediment water interface (SWI) to reach about 0 mV (*vs* Ag/AgCl) within the first centimeter on Day 2 and Day 7. Benthic microbial communities in the microcosms responded by increased bacterial activity (thymidine incorporation, community level physiological profiling and fluorescein diacetate analysis) immediately after the algal enrichment (2h) with maximum values after 2 and 7 days. This coincided with an increase in microbial biomass, first of heterotrophic nanoflagellates (Day 2) and then of bacteria (Day 7). A clear link was observed between heterotrophic microbial activity and metal effluxes. Significant upward fluxes of the trace metals As, Co and Mn from the sediment into the overlying water column were measured in the microcosms shortly after addition of the algae compared with the control. The upward trend of DOC and the upward and then downward trend of chlorophyll *a* (see Table 2 in Gillan, *et al.*, subm., chapter 4), and the metal concentrations in the algae receiving microcosms reflect the transitory degradation of OM in a short time period, depending on the amount of phytodetritus mineralized at the sediment interface.

In the present paper, we studied the effect of the phytodetritus deposition on the structure of the total and active bacterial and microeukaryotic communities (with focus on Protozoa) in this experiment, and assess how this relates to metal mobilization. Especially the role of microeukaryotic communities in this process has so far been neglected. Moreover, few studies to date have performed a joint analysis of changes in the total and active bacterial and microeukaryotic communities, and linked these with metal fluxes.

Microbial community composition

Most identified Bacteria in the total and active communities belonged to the phyla Proteobacteria, Firmicutes, Bacteroidetes, Cytophaga, Cyanobacteria and Chloroflexi. Gamma-Proteobacteria clearly dominated the communities, followed by Bacteroidetes and delta-Proteobacteria (Fig. 3). These groups are often dominant in marine sediments (Baldi, *et al.*, 2010), including metal-contaminated environments (Gillan, *et al.*, 2005, Akob, *et al.*, 2007). Total and active microeukaryotic communities were dominated by Alveolata (ciliates, dinoflagellates and apicomplexans), diatoms, Fungi, and Amoebozoa; a few Metazoa (including 2 Nematoda, 1 Gastrotricha and 1 Bryozoa) were also detected (Fig. 4). The protozoan component (heterotrophic protists) comprised more than half of the identified taxa, with ciliates as the dominant phylum (cf. Garstecki, *et al.*, 2000). All ciliates belonged to the classes Spirotrichea and Phyllopharyngea, which were clearly the dominant groups in this area, as evidenced by previous field studies from the same sediments (Pede, *et al.*, chapters 2 & 3), and analysis of the active protist community in a study on the effects of As on benthic microeukaryotes, also from the same area (Pede, *et al.*, chapter 6). Other protozoan phylotypes included other Alveolata, Amoebozoa, Cercozoa and several heterotrophic Stramenopila (see Table S2).

There was very little difference in terms of higher taxonomic ranks of the total and active communities of both Bacteria and Protozoa (Figs. 2, 3, Tables S1, S2). If however the relative abundances of the phylotypes were taken into account, total and active communities were significantly different (Tables 1, 2, Fig. 4). While in the bacterial communities, various phylogenetic groups (e.g. alpha-, delta-, gamma- and epsilon-Proteobacteria, Bacteroidetes, etc.) were relatively more important in the active communities, the difference in the protozoan communities was mainly due to the more important contribution of especially ciliates in the active communities (Fig. 4). Dissimilarities in community composition between DNA and RNA-based studies are frequently observed (e.g. Mills, *et al.*, 2005, Akob, *et al.*, 2007, Lillis,

et al., 2009, Edgcomb, *et al.*, 2011). This is not surprising, especially in marine sediments, since DNA profiles theoretically reflect the whole genotypic diversity, and marine sediments form a sink for many organisms from the water column [inactive (e.g. cyst) or dying cells], which can be picked up in DNA-based studies. RNA profiles on the other hand represent only the metabolically active fraction (Stoeck, *et al.*, 2007b, Edgcomb, *et al.*, 2011). Considering the latter however, it is surprising that total diversity (total number of OTUs, including not sequenced ones) was higher in the active than in the total communities of both bacteria and microeukaryotes (in contrary to e.g. Akob, *et al.*, 2007, Lillis, *et al.*, 2009, Lanzen, *et al.*, 2011), and included several sequences (11 and 12 for bacteria and microeukaryotes respectively) unique to the active community. A possible explanation lies with the technique (i.e. DGGE) that was used. An increased proportion of SSU rRNA molecules to rDNA per cell can be observed in highly metabolically active cells (Milner, *et al.*, 2001). Therefore, highly active taxa with low cell counts may be underrepresented or not detected in DNA-derived studies because fingerprinting tools such as DGGE capture the community dynamics of the dominant taxa, and SSU rDNA can be at or below detection limits (Dell'Anno, *et al.*, 1998, Mills, *et al.*, 2005, Nogales, *et al.*, 2011). The opposite would be observed if the cells were numerous (high rDNA) but had low or no metabolic activity (low rRNA), like cysts or other resting stages of e.g. planktonic diatoms and dinoflagellates which can be numerous in marine sediments (McQuoid & Nordberg, 2006, Satta, *et al.*, 2010). Such discrepancies between DNA and rRNA analyses demonstrate the necessity of generating both DNA- and RNA- derived profiles to obtain a more representative analysis of the extant microbial communities (Akob, *et al.*, 2007).

Effects of algal enrichment on diversity and structure of total and active microbial communities

Deposition of phytoplankton-derived detritus did not affect the diversity (~species richness) of the total and active bacterial communities, but had a slight but significant positive impact on the diversity of the total microeukaryotic community (only on day 2 of the experiment, Fig. 1). This was mainly due to appearance of ten sequences related to Metazoa (including Nematoda, cf. Vanaverbeke, *et al.*, 2004), Fungi and non-identified OTUs (not shown). Diversity of the active microeukaryote community significantly decreased by day 7 in the control treatment, resulting in significantly higher species richness in the algae-enriched

active community compared to the control. The organic matter thus is a crucial factor in sustaining the diversity of active microeukaryotes in the experimental benthic system.

While the impact on diversity was low, phytodetritus deposition did have a more pronounced impact on bacterial as well as protozoan community structure (Tables 1-3, Figs. 4, 5), in accordance with other experiments with supplements of phytoplankton (van Hannen, *et al.*, 1999a, Fruh, *et al.*, 2011).

Bacterial community composition showed a distinct change two hours after the addition of the algal suspension, but the bacterial response was most distinct after two days (Fig. 4), and communities shifted back towards initial composition on day 7 (Fig. 4), even though bacterial activity and biomass were still elevated (Gillan, *et al.,* chapter 4). Important OTUs increasing in density in the active communities due to the treatment (e.g. G-PB172, E-PB143, G-PB154, G-PB70) were related to bacteria observed in a carbon source enrichment experiment (HQ836399, HQ836383), from marine hydrocarbon seep sediments (GU584838), and to epiphytic bacteria (HM437298, GU451667), suggesting that they belong to groups that prefer organically enriched conditions. OTU G-PB85, related to sequences obtained from marine polluted sediments, e.g. hydrocarbon-polluted areas after the Prestige oil spill in Spain (JF344624), and hydrocarbons and heavy metal contaminated sediments from the BCZ (HM598555) most strongly decreased after algal enrichment (Fig. 4). Apart from this evidence that part of the change in bacterial community composition is related to the organic enrichment, it is unclear to what degree other factors, such as changes in oxygen concentration, the increase in salinity and pH in the microcosms (Fig. 5) (Fernandez-Leborans, 2000, Fenchel & Finlay, 2008), the efflux of toxic trace metals, or changes in grazing intensity (cf. below, see also Gillan, *et al.*, subm., chapter 4) impact the communities.

The effect of algal enrichment on total and active protozoan community structure was most pronounced on day 7 (Fig. 4), confirming literature reports (Bick, 1973, Fruh, *et al.*, 2011). This is related to increases of bacterivore flagellates (e.g. *Massisteria* sp. - CerMas21), but also to pronounced increases of ciliates (Patterson, *et al.*, 1989, Taylor & Sanders, 1991, Fruh, *et al.*, 2011). The exact feeding habits of the latter are not well known, and could include algivores (e.g. *Strombidium* sp.), bacterivores and/or species feeding on other protozoa [including HNF whose biomass increased on day 2 (cf. Gillan, *et a.l,* subm., chapter 4), or other organisms which decreased towards day 7, such as e.g. *Protaspis* sp. (CercPro44), *Oblongichytrium* sp. (LabObl17) and *Caecitellus* sp. (BicCae73), a dinophyte (UncDin36), or

other ciliates (see Fig. 4)]. In the active ciliate community at least seven ciliates increased in (relative) abundance after seven days (cf. Fruh, *et al.*, 2011), while other ciliates became less abundant (DNA) at that time (Fig. 4). This could be the result of complex interactions taking place within the microbial loop, even within ciliate communities, e.g. competition between algivores (Fruh, *et al.*, 2011) like *Aspidisca* sp. (CilAsp31) and *Tintinnopsis* sp. (CilTint66), or predation by the carnivore *Acineta* sp. (Cil47, CilAci5). As for the bacterial communities (cf. above), it is not clear to what degree other factors impact the structure of the protozoan communities.

Overall, our results (this study and Gillan, *et al.* subm., chapter 4) suggest that the addition of phytodetritus stimulates the development of the microbial loop. Phytodetritus deposition causes a rapid response in bacterial production (Gillan, *et al.* subm., chapter 4, Fig. 5). This increase in activity however does not lead to higher bacterial biomass (Gillan, *et al.* subm., chapter 4, Table 4). This could be due to grazing control by HNF and/or ciliates, which become relatively more abundant by day 7 (Fig. 4). HNF biomass increases by day 2 (but this is not significant, data not shown), which together with the absence of an increase in HNF biomass by day 7 (Gillan, *et al.* subm., chapter 4, Table 5) suggests grazing control by ciliates or other grazers (Wey, *et al.*, 2008). Unfortunately, no biomass data are available for ciliates. Bak & Nieuwland (1989) studied seasonal fluctuations in benthic protozoan communities in marine sediments, and observed a positive relation between protist numbers and bacterial productivity (see also Hondeveld, *et al.*, 1994). In contrast to what our data suggest however, they propose that under conditions of high organic input only an insignificant fraction of the bacterial biomass is consumed (Bak & Nieuwland, 1989).

Dynamics of bacteria, nanoflagellates and ciliates are strongly coupled in the microbial loop (van Hannen, *et al.*, 1999a, Wey, *et al.*, 2008). In our study, total bacterial and protozoan communities were significantly correlated to one another, and the same was observed for the metabolically active communities, while total and active communities of the same group were, surprisingly, not correlated (Table 3). This suggests that common factors structure total respectively active microeukaryotic and bacterial communities, and/or that they exert a structuring influence on one another. The lack of correlation between the total and active communities suggests that community structure and activity are regulated by different processes, or that they are not in sync with one another.

Interestingly, changes in bacterial and protozoan communities during the experiment were much more clear-cut and pronounced for the total than for the active communities, where the effect was only slightly (Bacteria) or not significant (Protozoa). DNA-based approaches are generally used for microbial community analyses. Previous studies however had indicated that DNA-based fingerprints do not always accurately reflect environmental changes (Ellis, *et al.*, 2003, Kowalchuk, *et al.*, 2003, Hoshino & Matsumoto, 2007). A more direct response would be expected by using RNA-based approaches (Nicol, *et al.*, 2003, Noll, *et al.*, 2005, Not, *et al.*, 2009), because RNA has a more rapid turnover within the cell than DNA (i.e. rare species would become active before they start dividing), as was observed by Hoshino & Matsumoto (2007) for soil bacterial communities in response to fumigation. The high variation between replicates in the active communities in our study may explain the lack of a significant signal in the RNA data. Nevertheless, PRC data (Fig. 4) showed that the community response of active communities for the Bacteria and Protozoa was also visible 2 and 7 days respectively after the algal enrichment, similar to total communities.

Metal remobilization and microbial-metal interactions

The metal effluxes for Mn, Co and As observed during this experiment were linked to the algae enrichment of the contaminated sediments (Gao, et al., in press; Gillan, et al., subm., chapter 4, but see also Fones, *et al.*, 2004). It was found that bacteria were activated by the increased food supply (chapter 4), and this result, combined with the observation that bacterial communities and metal profiles were strongly correlated to each other, and to the CHL *a* concentration (Table 3), indicates that bacteria are involved in the release of the metals as a consequence of the increased food availability (Gao, *et al.*, in press, Gillan, *et al.*, subm., chapter 4). The metals measured during this study represented the bioavailable (dissolved) metals in the porewaters, and an increase of these toxic trace metals could potentially influence the microbial inhabitants. We found that changes in total bacterial and active protozoan community composition could indeed be significantly related to many of the measured trace metals (Cd, Fe, As, Co, Zn and Pb) (Fig. 5). Even though no direct negative correlation was measured (for microbial species richness and biomass) that could be linked to a toxic effect of these metals (cf. Pede, *et al.*, chapters 2 & 3), it remains unclear to what degree the released trace metals have a structuring impact on the communities. During a field study in 2008, a significant, independent influence of the metals on the microeukaryotic community composition was observed (Pede, *et al.*, chapter 3). Metal behaviour/ speciation/bioavailability however is strongly linked to the dynamics of other biogeochemical

factors (O_2, Eh, OM, salinity, etc.) (Calmano, *et al.*, 1993, Eggleton & Thomas, 2004), which may hide an effect of the trace metals on the bacterial and protozoan community composition. In order to gain a better insight in the direct effect of the metals *per se*, dedicated experiments, in which metals are added while controlling for the other environmental factors, should be set up (see chapter 6).

Acknowledgements

This research was supported by a Belgian Federal research program (Science for a Sustainable Development, SSD, contract MICROMET n°SD/NS/04A and SD/NS/04B) and BOF-GOA projects 01GZ0705 and 01G01911 of Ghent University (Belgium). We are indebted to Jean-Yves Parents and Dr. Véronique Rousseau (ULB, Brussels) for their help with the cultivation of *Phaeocystis* and *Skeletonema*. Many thanks also to André Cattrijsse and all the crew of the RV Zeeleeuw.

Supplementary

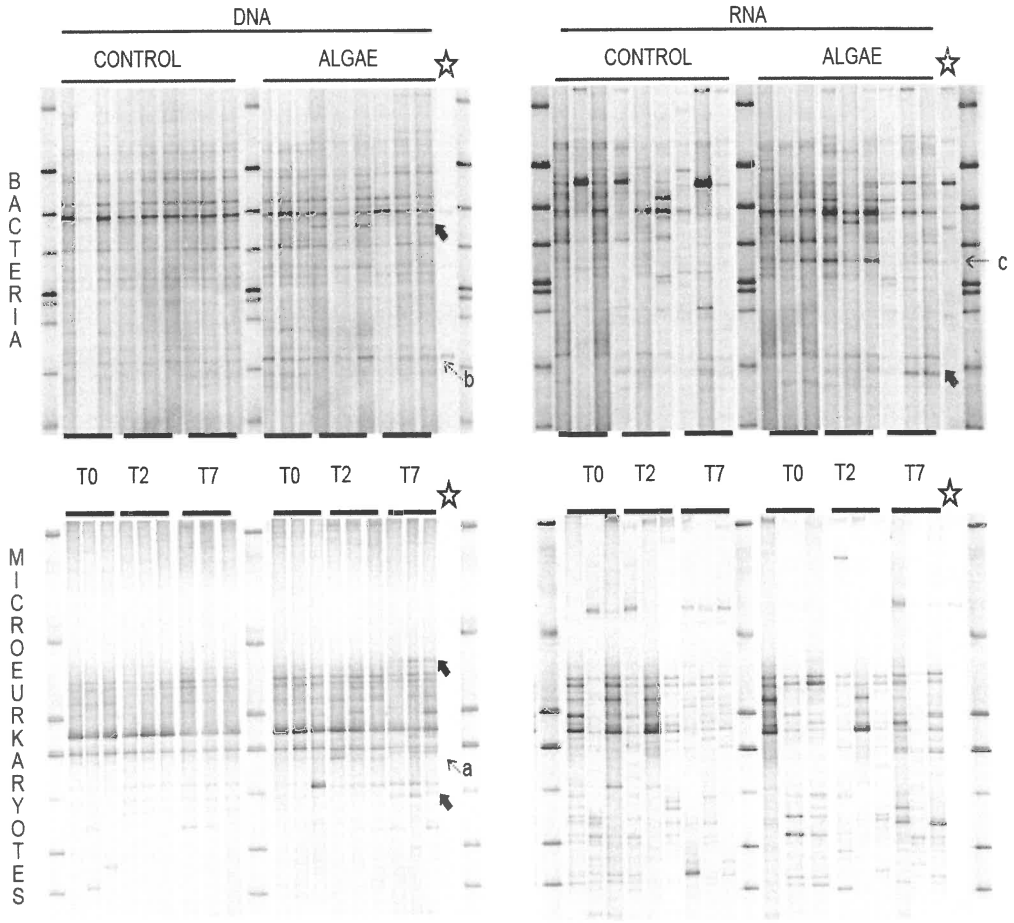

Figure S1: DGGE fingerprint profiles of the microbial communities, based on 16S rDNA and rRNA (bacteria) and 18SrDNA and rRNA (microeukaryotes) extracted from the sediments during the microcosm experiment, two hours (T0), 2 days (T2) and 7 days (T7) after the start of the experiment. Control microcosms ('control') received seawater, while experimental microcosms ('algae') received seawater enriched with algae. There are 3 replicates for each treatment. Visible inspection of the DGGE gels clearly showed –for both bacterial and microeukaryotic fingerprints- that (1) DNA profiles were more homogeneous than RNA profiles, (2) the 2 different extraction techniques resulted in distinctly different fingerprint profiles, especially in de lower half of the DGGE gels, and (3) there was variation among replicates in the RNA-based profiles. DNA and RNA extractions of the algal mixture; their DGGE profiles are indicated with an asterix. Some of the bands (a and b) from the algal mixture are clearly more abundant in the DNA-based profiles of the enriched microcosms ('algae') compared with the control microcosms, especially at T0 and T2 (bacteria), and at T2 (eukaryotes) after the addition of the algae. This is less obvious in the RNA profiles (except for band c). Furthermore, an intensification of some bands can be observed after the enrichment of microcosms with the algal suspension; for example the bands indicated by grey arrows.

Table S1: Identification of microeukaryotic DGGE bands. Only the first *identified* BLAST match is given. %Sim, percentage of similarity; bp, basepair; LAB, label of the phylotype used in multivariate analyses (only protozoan sequences, indicated in grey). The last columns show the presence of the phylotypes in the DNA and RNA-based DGGEs.

ID	Taxonomic classification	Closest BLAST match (accession number)	% Sim (bp)	DNA	RNA
CilAci15	Alveolata; Ciliophora; Phyllopharyngea	Acineta sp. (AY332718)	90 (167)	x	x
CilAci47	Alveolata; Ciliophora; Phyllopharyngea	Acineta sp. (AY332718)	90 (167)	x	x
CilAsp31	Alveolata; Ciliophora; Spirotrichea	Aspidisca aculeata (EF123704)	97 (143)	x	x
CilStr17	Alveolata; Ciliophora; Spirotrichea	Strombidium sp. (AY143564)	100 (155)	0	x
CilStr78	Alveolata; Ciliophora; Spirotrichea	Strombidium sp (AY143564)	98 (166)	0	x
CilInt72	Alveolata; Ciliophora; Spirotrichea	Salpingella sp. (EU399536)/ Parastrombidinopsis sp. (DQ393786)	98 (138)	x	x
CilInt24	Alveolata; Ciliophora; Spirotrichea	Steenstrupiella sp. (EU399537)/Amphorellopsis sp .(EU399530)	94 (149)	x	x
CilInt34	Alveolata; Ciliophora; Spirotrichea	Steenstrupiella sp. (EU399537)/Amphorellopsis sp .(EU399530)	95 (149)	x	x
CilInt79	Alveolata; Ciliophora; Spirotrichea	Stenosemella sp. (FJ96074) / Favella sp. (FJ196073)/ a.o.	100 (85)	x	x
CilTint16	Alveolata; Ciliophora; Spirotrichea	Tintinnopsis sp. (DQ487200)	95 (156)	x	x
CilTint66	Alveolata; Ciliophora; Spirotrichea	Tintinnopsis beroidea (EF123709)	95 (165)	x	x
ApiSel12	Alveolata; Apicomplexa	Selenidium serpulae (DQ683562)	98 (161)	x	x
ApiEim67	Alveolata; Apicomplexa	Eimeriidae sp. (EF024716)	90 (169)	x	x
Dino26	Alveolata; Dinophyceae	Protoperidinium punctulatum (AB181906)	100 (154)	x	x
Dino1	Alveolata; Dinophyceae	uncultured dinoflagellate (GU820543 a.o.)	99 (156)	x	x
uncDino36	Alveolata; Dinophyceae	uncultured dinoflagellate (GU820592 a.o.)	95 (168)	x	x
AmoEnt68	Amoebozoa; Archamoeba	Entamoeba histolytica (X89636)	84 (101)	x	0
AmoeTh5	Amoebozoa; Flabellinea	Thecamoalgivore eba sp. (EF455775)	89 (167)	x	x
AmoPar75	Amoebozoa; Flabellinea	Paramoeba eihardi (AY6865 75)	90 (173)	x	x
AmoeEu62	Amoebozoa; Tubulinea	uncultured Euamoebida (AB520727)	83 (127)	x	x
CerMas21	Rhizaria; Cercozoa	Massisteria Marina (AF174374)	98 (165)	x	x
CerPro44	Rhizaria; Cercozoa	Protaspis grandis (DQ303924)	97 (168)	x	x
LabObl7	Stramenopila; Labyrinthulida	Oblongichytrium sp. (FJ821481 a.o.)	98 (149)	x	x
LabApl8	Stramenopila; Labyrinthulida	Aplanochytrium sp. (FJ799799 a.o.)	97 (145)	x	x
BicCae73	Stramenopiles; Bicosoecida	Caecitellus parvulus (AY520457)	95 (169)	0	x
ChrySp32	Stramenopiles; Chrysophyceae	Spumella-like flagellate (EF043285)	100 (159)	x	x
ChryPp33	Stramenopiles; Chrysophyceae	Paraphysomonas butcheri (AF109326)	98 (161)	x	x
				x	x
				x	x
	Haptophyceae	Phaeocystis globosa (JF698771)	96 (170)	x	x
	Stramenopila; Bacillariophyta	Cyclotella sp. / Skeletonema sp. / Thalassiossira sp./ a.o.	100 (142)	x	x
	Stramenopila; Bacillariophyta	Baccilariophyta sp. / Fragilariopsis sp. / Stauroneis sp. / a.o.	96 (166)	x	x
	Stramenopila; Bacillariophyta	Minutocellus sp. / extubocellules sp. / Hyalosira sp. / a.o.	99 (165)	x	x
	Stramenopila; Bacillariophyta	Dytilum brightwelli (FJ266034)	99 (167)	x	x
	Stramenopila; Bacillariophyta	Skeletonema sp. / Thalassiossira sp.	100 (168)	x	x
	Stramenopila; Bacillariophyta	Cyclotella sp. / Skeletonema sp. / Thalassiossira sp./ a.o.	100 (142)	x	x
	Stramenopila; Bacillariophyta	Thalassiossira sp. (HM991699 a.o.)	99 (186)	x	x
	Stramenopila; Pelagophyceae	Aureoumbra lagunensis (U40258)	88 (156)	x	x
	Stramenopila	Uncultured stramenopile (GU823367)	98 (168)	0	x
	Stramenopila	Uncultured stramenopile (GU823367)	98 (168)	x	x
	Fungi; Dikarya	Gibberella sp. / Fusarium sp.	100 (159)	x	0
	Fungi; Dikarya	uncultured Auriculariaceae (EF024776)	96 (152)	x	x
	Fungi; Dikarya	Botryobasidium sp. / Paulia sp. / Tremelia sp. / a.o.	89 (160)	0	x
	Fungi; Dikarya	Kazachstania sp. /Saccharomyces sp.	89 (168)0	x	x
	Fungi; Dikarya	uncultured Auriculariaceae (EF024776)	90 (162)	x	x
	Fungi; Chytridiomycota	Gonapodya sp. (AF164329S2)	90 (162)	x	x
	Metaoza; Nematoda	Uncultured Plathyhelminthes (EU910607)	88 (121)	x	x
	Metaoza; Nematoda	Sabatiera pulchra (FJ040466)	100 (155)	x	x
	Metazoa; Gastrotricha	Chaetonotus neptuni (AM231774)	98 (156)	x	x
	Metazoa; Bryozoa	Eucratea sp. / Securflustra sp. / a.o.	83 (102)	x	x

Table S2: Identification of the DGGE bands related to bacterial sequences based on BLAST analyses. The most important species, i.e. the species with high taxon weight (lower axis minimum fit 20) in the PRC curves, are indicated in grey. These sequences were checked in the RDP database and the most detailed affiliations with a confidence threshold ≥ 95% is given. Their presence in DNA and RNA-based DGGE profiles is indicated Unc, uncultured; ID, label of taxon used in analyses.

ID	Tax classification	RDP (≥ 95%)	Closest BLAST match	Accession nb	% Sim (bp)	DNA	RNA
A-PB73	alpha PB	Hyphomonadaceae	Hyphomonas sp	HQ441213	100 (127)	x	x
D-PB7	delta PB	Desulfobulbaceae	unc bacterium clone	EF028998	95 (150)	x	x
D-PB13	delta PB	Desulfobulbaceae	unc bacterium clone	EU362299	100 (151)	x	x
D-PB130	delta PB	Desulfobulbaceae	unc Desulfocapsa sp (ao)	AY177798	100 (150)	x	x
D-PB162	delta PB	Bacteria	Desulfuromonadaceae bacterium	JF806815	99 (153)	x	x
G-PB101	gamma PB	Gamma PB	unc gamma PB	AM980554	96 (151)	x	x
G-PB127	gamma PB	Bacteria	unc sediment bacterium	HQ191085	98 (149)	x	x
			unc gamma PB	AY515465	97 (149)		
G-PB151	gamma PB	Gamma PB	unc gamma PB	FJ497551	97 (156)	x	x
G-PB152	gamma PB	proteobacteria	unc gamma PB	AM501834	96 (149)	x	x
G-PB93	gamma PB	/	unc bacterium	HQ852437	88 (150)	x	x
G-PB154	gamma PB	Proteobacteria	unc marine bacterium	HM437298	98 (152)	x	x
			Microbulbifer sp	FM200853	95 (152)		
G-PB85	gamma PB	Gamma PB	unc gamma PB	JF344501	99 (152)	x	x
G-PB172	gamma PB	Alteromonas	Alteromonas sp	HQ836399	99 (150)	x	x
G-PB50	gamma PB	Gamma PB	unc gamma PB	JF344624	97 (152)	x	x
G-PB70	gamma PB	Bacteria	unc gamma PB	EF215728	97 (152)	x	x
G-PB67	gamma PB	/	unc gamma PB	FM211775	85 (157)	x	x
E-PB143	epsilon PB	Epsilon PB	unc epsilon PB	HQ836383	98 (128)	0	x
			Arcobacter defluvii	HQ115597	98 (128)		
E-PB168	epsilon PB	Campylobacterales	unc epsilon PB	FM879047	100 (123)	x	x
			Sulfurospirillum sp	FR774809	99 (123)		
BactD174	Bacteroidetes	Bacteria	unc bacterium clone Belgica	DQ351752	100 (144)	x	x
BactD135	Bacteroidetes	Flavobacteriaceae	unc Flavobacteriaceae bacterium	EU600467	99 (146)	x	x
BactD107	Bacteroidetes	Bacteria	unc Bacteroidetes bacterium	EU642016	99 (146)	0	x
BactD123	Bacteroidetes	Bacteria	unc Bacteroidetes bacterium	EU702829	97 (144)	x	x
Cytoph1	Cytophaga	Bacteroidetes	uncultured marine bacterium	FR683721	99 (147)	x	x
			Cytophaga sp	AJ786088	99 (147)		
Firm166	Firmicutes	Bacillales	unc Staphylococcus sp	FJ384491	100 (148)	0	x
ChlF75	Chloroflexi	Bacteria	unc Chloroflexi bacterium	AB448848	82 (126)	x	x
ChlPl92	Chloroplast	Bacillariophyta	Thalassiosira/Ditylum	GU323224	99 (129)	x	x
ChlPl106	chloroplast	Bacillariophyta	unc bacterium DGGE band	FJ159132	100 (129)	x	x
			chloroplast	GQ342163	99 (129)	x	x
	alpha PB		Mesorhizobium sp.	FN546876	100 (127)	x	x
	Beta PB		Schlegelella sp.	AM501745	98 (120)	x	x
	delta PB		unc delta PB	AY771981	99 (150)	x	x
	delta PB		unc bacterium clone	GU292252	99 (150)	x	x
	gamma PB		Vibrio vulnificus	HM996966	86 (155)	x	x
	gamma PB		unc gamma PB	AB015250	98 (152)	x	x
	gamma PB		Colwellia sp	FJ889666	98 (148)	x	x
	gamma PB		unc gamma PB	AM882569	96 (149)	x	x
	gamma PB		unc bacterium clone	GQ246429	99 (152)	x	x
	gamma PB		unc gamma PB	JF344501	96 (152)	x	x
	gamma PB		unc gamma PB	AY711817	98 (120)	x	x
	gamma PB		Rickettsiella symbiont	AM490939	96 (146)	x	x
	gamma PB		unc bacterium clone	HM598620	99 (153)	x	x
	epsilon PB		Arcobacter defluvii	HQ115597	98 (128)	x	x
	Bacteroidetes		unc Tenacibaculum	HQ727499	97 (147)	x	x
	Bacteroidetes		unc Flavobacteriales bacterium	EU640712	98 (147)	x	x
	Bacteroidetes		unc bacteriodetes bacterium	DQ351763	99 (147)	x	x
	Firmicutes		unc bacterium clone	HM192389	98 (126)	x	x
	Firmicutes		Staphylococcus sp	GU595377	95 (154)	x	x
	cyanobacteria		Cyabobacterium sp.	HQ724771	99 (126)	x	x
			Desulfurobacteraceae	HQ400799	96 (126)		

6

SHORT-TERM RESPONSE OF ACTIVE MICROEUKARYOTIC COMMUNITIES TO ARSENIC CONTAMINATION IN SILTY AND SANDY SUBTIDAL COASTAL MARINE SEDIMENTS

Annelies Pede[1], David Gillan[2], Tine Verstraete[1], Julie Baré[3], Wim Vyverman[1] & Koen Sabbe[1]

[1] Protistology & Aquatic Ecology, Department of Biology, Ghent University, 9000 Ghent, Belgium

[2] Proteomics and Microbiology Lab, Mons University, 7000 Mons, Belgium

[3] Department of Veterinary Public Health and Food Safety, Ghent University, 9820 Merelbeke, Belgium

Manuscript in preparation

Abstract

We used an experimental approach to assess the effect of acute arsenic (As) contamination on active microeukaryotic communities in two subtidal marine sediment types. Silty sediments from a chronically metal-contaminated marine station and sandy sediments from a reference station were spiked with a range of As levels (KH_2ASO_4; 0-960µg L^{-1}) and incubated in the dark for 2 days. The response of the microeukaryotic communities to the different As contamination levels was analysed by 18S rRNA-based DGGE analysis. We hypothesized that communities from silty sediments would be more resistant to acute metal intoxication due to their contamination history. Ciliates (from 6 different classes), which occurred together with representatives of Cercozoa, Bacillariophyta, Amoebozoa, Euglenozoa, Fungi and Metazoa (2 nematodes) were the dominant active component of the microeukaryotic communities. We detected distinct effects of As contamination on the diversity and composition of these communities. Diversity (~number of DGGE bands) significantly decreased at contamination levels ≥ 480 µg As L^{-1} in both sediment types, but the decrease was more pronounced in the sandy (43%) than in the silty sediment (32%), suggesting higher tolerance to As contamination in the silty sediment. In addition, a significant shift in community composition occurred at contamination level ≥ 120 µg As L^{-1} and again at ≥ 480 µg As L^{-1} in silty sediment. Surprisingly, the effect of As on protist community composition was not significant in the sandy sediment. Fungi responded most sensitively to high As concentrations, while only some ciliates increased in relative abundance with higher As levels. These included representatives from various classes such as the *Phyllopharyngea, Spirotrichea, Litostomatea* and *Colpodea.*

Introduction

Coastal areas worldwide are contaminated by trace metals, mainly through atmospheric and riverine input (Forstner & Wittmann, 1979). They accumulate in sediments due to their generally low solubility and tendency to adsorb onto particles (Li, *et al.*, 2000b), and as such remain available for uptake by living organisms (Eggleton & Thomas, 2004). In microorganisms, trace metal intoxication affects growth, morphology and metabolism through functional disturbance, protein denaturation or the destruction of cell membrane integrity (Chapman, *et al.*, 1998, Bruins, *et al.*, 2000, Zhou, *et al.*, 2008). Trace metal toxicity depends on its concentration and chemical speciation. Several metals are essential for living organisms

at very low concentrations, but most are toxic at high concentrations (Bruins, *et al.*, 2000). Metals in sediments are in a dynamic equilibrium between a dissolved (pore water, overlying water) and solid phase (sediment, suspended particulate matter and biota) (Calmano, *et al.*, 1993). The soluble phase represents the principal source of bioavailable metals, and only these forms are toxic for biological systems (Eggleton & Thomas, 2004). The partitioning behaviour and spatial distribution of these contaminants in marine sediments is regulated by hydrodynamical and biogeochemical processes, and environmental conditions (oxygen concentration, redox potential, pH, salinity and temperature) in interstitial water and sediment (Calmano, *et al.*, 1993, Forstner, 1993, Huettel, *et al.*, 1998, Gao, *et al.*, 2009, Hong, *et al.*, 2011). For example, mobilization and resuspension of bioavailable metals into the water column can occur in polluted sediments due to benthic microbial remineralization of phytodetritus deposited from algal blooms (Pede, et al., chapter 3, 4 & 5, Gao, *et al.*, 2009). Marine sediments thus constitute potential reservoirs and sources of metal contamination for the benthic and pelagic ecosystem. Moreover, trace metals can biomagnify throughout the food chain, resulting in serious ecological disturbance for coastal ecosystems and potential health risks for animals and humans (de Mora, *et al.*, 2004, Fratini, *et al.*, 2008, Piola & Johnston, 2008, McKinley, *et al.*, 2011). Observing the toxic effects on microbial communities following their exposure to trace metals can provide data on their biological effects, which may be extended to other more complex living systems (Gutierrez, *et al.*, 2003).

Microbial communities inhabiting marine sediments are composed of complex and highly diverse assemblages of prokaryotic and eukaryotic organisms, often in very high densities (Tian, *et al.*, 2009, First & Hollibaugh, 2010). Benthic microorganisms are the primary drivers of the production, utilization and degradation of most organic matter and the cycling of many elements (Caron, 2009). Many of these communities are highly sensitive to the presence of pollutants in the environment (Cheung, *et al.*, 1997, Boran & Altinok, 2010). Previous studies considering metal contamination mainly focused on bacterial (e.g. Gillan, 2004, Gillan & Pernet, 2007, Bouskill, *et al.*, 2010, Wang, *et al.*, 2011), fungal (Wang, *et al.*, 2010, Wang, *et al.*, 2011) or metazoan communities (Hermi, *et al.*, 2009, Boufahja, *et al.*, 2010, Fukunaga, *et al.*, 2010, Vashchenko, *et al.*, 2010). Despite their ecological importance in marine sediments (see Patterson, *et al.*, 1989), microeukaryotic communities have been less investigated in this context (but see Pede, *et al.*, chapters 2, 3, 5). It has been shown that acute intoxication with high metal concentrations of e.g. Pb (1 mg L^{-1}) and Cd (1000 mg Cd dm^{-3})

can cause a decrease in the diversity and biomass of marine (benthic) microbial communities (Fernandez-Leborans & Novillo, 1994, Fernandez-Leborans, *et al.*, 2007). Most available studies in this context however mainly focused on a limited number of microeukaryotic species, mainly for bioremediation events in waste water treatment plants, and bio-indicators and test organisms in ecological risk assessments (Leborans, *et al.*, 1998, Sauvant, *et al.*, 1999, Diaz, *et al.*, 2006, Martin-Gonzalez, *et al.*, 2006, Fernandez-Leborans, *et al.*, 2007, Araujo, *et al.*, 2010, Rehman, *et al.*, 2010b, a, Jayaraju, *et al.*, 2011).

In the present study, we focus on the effects of the trace metal arsenic (As) on total microbial eukaryotic communities in subtidal coastal marine sediments from the Belgian Coastal Zone (BCZ). As is a semi-metallic element which is ubiquitous in natural environments due to natural processes (e.g. from volcanic eruptions or forest fires) (Spencer, 2002). Concentrations of As in open ocean seawater are typically low (1–2 µg As L^{-1}) (ICPS 2001). In rivers and lakes, concentrations are somewhat higher but generally below 10 µg As L^{-1} (ICPS 2001). Exceptions are near man-made sources such as pesticide manufacturing or mining, where concentrations in surface waters may be 1000 times higher (up to 5000 µg As L^{-1}) (ICPS 2001). Marine sediments are often heavily polluted as a consequence of anthropogenic activities (e.g. ore mining and smelting, preservatives in wood products, pesticides, herbicides, burning of fossil fuels) (Lee, *et al.*, 2010a, Lee, *et al.*, 2010b), and concentrations range between 4.8-113 mg As kg^{-1} (Reimann, *et al.*, 2009). As toxicity is strongly dependent on the chemical species (Irvin & Irgolic, 1995). Immobile As forms in sediments such as arsenosugars are considered non-toxic, but as mentioned before, metals can remobilize in the seawater and As can be easily transformed into bioavailable and toxic inorganic forms (III and V) as a consequence of environmental changes (Gao, *et al.*, 2009). As(V) has a structural similarity to phosphate, and can easily enter microbial cells via phosphate-uptake systems; As(III) has a high affinity for thiols, which, in the form of cysteine residues, are situated in the active sites of many important enzymes (Speir, *et al.*, 1999).

The aim of this study was to assess the response of benthic microeukaryotes to As contamination in two sediments with different granulometry and As contamination levels in the BCZ. More specifically, we wanted to assess whether communities of chronically highly contaminated sediments are more tolerant against acute As pollution than communities from non-contaminated sediments. Previous studies in this area demonstrated that natural microeukaryotic diversity in contaminated sediments was not lower compared to uncontaminated sediments (Pede et al., chapter 2; see also Chariton, *et al.*, 2010), and it is

suggested that long-term exposure to a trace metal contamination can select for a population of opportunistic and metal-tolerant taxa (Bouskill, *et al.*, 2010). Two BCZ stations were selected on the basis of previous research: sediments of station 130 are silty and contain high concentrations of trace metals and metalloids (including arsenic), while sediments of station 230 are sandy and contain relatively low arsenic concentrations (Pede, *et al.*, chapter 2). The stations differ in microbial eukaryotic community structure (Pede, *et al.*, chapter 2). We used microcosms to evaluate the short-term response (48h) of the microbial eukaryotic community from both stations to different levels of As pollution. Changes in the structure of the active community were analyzed by rRNA extractions from the sediments followed by denaturing gradient gel electrophoresis (DGGE). rRNA serves as a phylogenetic marker for the identification and relative abundance of metabolically active members within complex microbial communities, as the number of cellular ribosomes, and thus also the rRNA content, increases with growth rate and decreases with starvation (Kerkhof & Ward, 1993, Milner, *et al.*, 2001). DGGE allows rapid and easy comparison of communities between different treatments and sediment types and has been widely used to evaluate the effects of pollutants on soil and sediment microbial communities (e.g. Liu, *et al.*, 2010).

Materials and methods

Sediment sampling

Sediment samples for the microcosm experiments were collected in May 2010 from two subtidal stations situated in the Belgian Continental Zone (BCZ; Fig. 1), aboard RV 'Zeeleeuw'. Three replicate sediment samples were taken at both sites using a Reineck corer (diameter 30 cm). The top centimeter of the sediments was collected, homogenized and transported to the laboratory for the experiments.

Average values (of two sampling occasions) for the pH of the bottom waters (n= 4), the quantity of fine fraction (QFF; n= 8) and chlorophyll *a* concentrations (CHL *a*; n=5) in the upper sediment layer (0-1cm), and median grain size (MGS) in the 0-10 cm sediment layer (n=6) of the stations as obtained during previous field studies in 2007 and 2008 (Pede, *et al.*, chapter 2 & 3) are shown in table 1. The range [minimum-maximum, based on two sampling dates (2007) and 6 sampling dates (2008); measurements on mm-scale] of arsenic concentrations (As), as measured by the Diffusive Equilibrium and Diffusive Gradient in Thin

films technique (DET and DGT; see Chapter 2 and Gao, *et al.*, 2009, for a detailed description) in the porewaters of the upper sediment layer (0-1cm), are also shown.

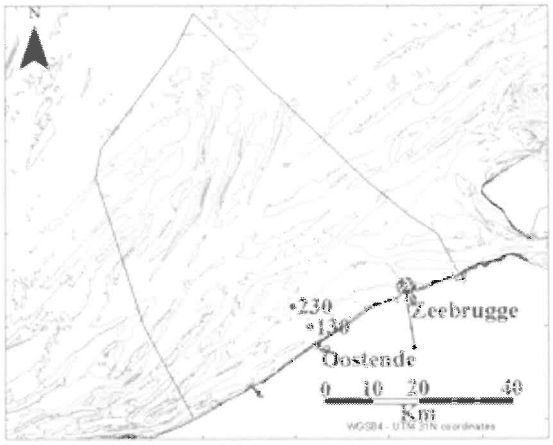

Fig. 1: Location of sampling stations in the Belgian Continental Zone

Table 1: Physico-chemical parameters of the sediments as measured in 2007 and 2008 (Pede, *et al.*, chapters 2 & 3). pH, QFF and CHL *a* are average values (n= 4, 8 and 5 respectively) calculated for the upper sediment layer (0-1cm), and MGS are average values (n=6) calculated for the 0-10cm sediment depth. MGS, median grain size; QFF, quantity of fine fraction in 500 mg sediment; CHL *a*, Chlorophyll *a*; dw, dry weight. [As], range of concentration of arsenic in the sediment porewaters in the upper sediment layer (0-1 cm) for two (chapter 2) and five sampling occasions (chapter 3). The bioavailable fraction (DGT) and the total soluble fraction (DET) are given.

		Station 130 *silty*	**Station 230** *sandy*
Depth (m)		12.9	11.4
pH		7.04	8.18
MGS (µm)		36.4	237.5
QFF (mg)		0.170	0.037
CHL *a* (µg g^{-1} dw)		12.91	0.17
[As] (µg L^{-1})	**DGT**	0.85-2.03 (2007)	0.15-0.45 (2007)
		0.95-8.02 (2008)	
	DET	27.02-149.81 (2007)	3.66-21.14 (2007)
		2.10-63.99 (2008)	

Station 130 (51°16.25 N - 02°54.30 E) is located near the harbor outlet of Ostend and is closer to the mouth of the Scheldt estuary, and as such receives high loads of anthropogenic pollutants, including trace metals (Gillan & Pernet, 2007, Gao, *et al.*, 2009). On the basis of MGS and QFF, its sediment can be defined as silty (see also Pede et al., chapter 2; Table 1). Station 230 (51°18.50 N - 02°51.00 E) is situated more offshore and has sandy sediments (Table 1). As a result, much lower amounts of trace metals are present in station 230 than in station 130 (Table 1). For more information about the sampling stations and methodology of granulometry, QFF and CHL *a* determination, see Pede, *et al.* (chapter 2); for methodology of As determination, see (Gao, *et al.*, 2009).

As solution and microcosm set-up

Microcosms, i.e. 50 ml falcon tubes consisting of 5g of sediment and 25 ml of filtered (0.2 µm polycarbonate membrane filter, Nucleopore) seawater, were exposed to six different arsenic concentrations. To this end, a stock solution of the arsenic salt KH_2AsO_4 (1g L^{-1} KH_2AsO_4 in filtered seawater) was serially diluted to 0, 150, 300, 600, 1200 and 2400 µg L^{-1}, which approximately corresponds to 0, 60, 120, 240, 480 and 960 µg L^{-1} final arsenic concentration in the microcosms. The arsenic stock solution was added to the falcon tubes by pipetting into the water column in the correct concentration, and falcon tubes were stirred gently to evenly distribute the toxicant. All doses for both stations were tested in triplicate, totaling 36 microcosms (2 sediment types x 6 concentrations x 3 replicates). Microcosms were incubated at 12°C in the dark for 46-48h. After this incubation period, water was removed by decantation and pipetting, and 0.5 ml of sediment was immediately frozen on dry ice and stored at -80°C until RNA extraction.

The chemical form of the metal is important with respect to the toxicity to microbes (Forstner, 1993), and we used arsenate (KH_2AsO_4; oxidation state +5), the highly bioavailable form of arsenic that can be found in oxidized environments. This form is very toxic, as it has a structural similarity to phosphate and as such can easily enter microbial cells (Speir, *et al.*, 1999, Niegel & Matysik, 2010).

Molecular community profiling of eukaryotic microcosm assemblages

RNA was extracted from the sediments according to the protocol of (Chang, *et al.*, 1993)and adapted by Vannerum, *et al.* (in press), and total RNA was transcribed into cDNA using Qiagen OneStep RT-PCR Kit (Qiagen) according to the manufacturer's instructions. A more

detailed description of the procedure can be found in (Pede, *et al.*, chapter 5). PCR and DGGE analysis were performed as described in Pede *et al.* (chapter 2). General eukaryotic primers 1427f (5'-GC-rich clamp-TCTGTGATGCCCTTAGATGTTCTGGG-3') and 1637r (5'-GCGGTGTGTACAAAGGGCAGGG-3'), designed by van Hannen, *et al.* (1998), which amplify a 210 bp fragment of the 18S rRNA., were used. Gels of 7% (w/v) polyacrylamide were prepared with a linear 30 to 55% denaturant gradient [acrylamide/bisacrylamide ratio, 37,5:1; 100% denaturing polyacrylamide solution containing 7M urea 40% (v/v) formamide]. Equal amounts (300 ng) of PCR product were loaded in each well (except for replicate c of the control treatment in station 230 where not enough PCR product could be retrieved). Electrophoresis was performed for 16h at 100V in 1X Tris-acetate-EDTA (TAE) buffer at 60°C. The DGGE gels were stained for 30 min in 1X TAE buffer with SybrGold (Molecular probes) and digitally photo-documented (Kodak Easy Share P880 camera) under UV illumination.

Nucleotide sequences of DGGE bands were obtained by cycle sequencing (BigDye Terminator v3.1 cycle sequencing kit; Applied Biosystems) of cDNA amplicons (van Hannen, *et al.*, 1998), without GC-clamp) from excised and purified DGGE bands, as described earlier (Pede et al., chapter 2). Several bands were excised from the same height ('band-classis') in the DGGE gels, to facilitate the comparison between different samples, and between different gels (see below). Sequencing was performed using an ABI 3130XL Genetic Analyzer (Applied Biosystems). Nucleotide sequences were compared with the NCBI GenBank Database (www.ncbi.nlm.nih.gov) using the nucleotide-nucleotide Basic Local Alignment Search Tool (BLAST) to identify the closest, positively identified phylotype (i.e. higher similarities to e.g. environmental but unidentified sequences are not shown). The partial 18S rRNA sequences of this study are available upon request from the corresponding author.

The digital DGGE images were imported and analyzed for fingerprint similarity using BioNumerics 5.10 (Applied Maths BVBA, Belgium). To facilitate fingerprint comparisons, pro- and eukaryotic DNA from previous studies performed in the laboratory was pooled to generate DGGE standards, covering the entire gradient in the DGGE gels (7 different positions). Three standard lanes were included per gel. Fingerprints were normalized using the DGGE markers as an external reference, and bands visually determined to occur in several fingerprints in the gels were used as internal reference markers. Using both internal and external markers, all fingerprints were aligned (i.e. bands from the same position relative to

the position of the marker bands in the gel were grouped into band classes). Moreover, sequence information of the excised bands was used to check the grouping of bands into the band classes. Each band class theoretically represents a unique phylotype, i.e. a single organism in the microbial eukaryotic assemblage (referred to as Operational Taxonomic Unit, OTU). In some cases however, different bands (~ cDNA sequences) can co-migrate the same distance on the DGGE gel, and one OTU can yield different phylotypes (referred to as 'mixed OTUs'). These mixed OTUs are a well-known phenomenon for DGGE (Muyzer & Smalla, 1998). The intensity of the DGGE bands reflects the relative contribution of a phylotype to the overall community composition within a sample. Matrices were constructed with the presence/absence and the relative abundances of the OTUs in each sample. These matrices were then used to determine the number of OTUs in each profile (= eukaryotic species richness or SR) and for the multivariate data analyses (see below) respectively. Very weak bands which represented less than 5% of the total band signal in a sample were omitted from further analyses.

Statistical analysis

The experimental design consisted of 2 factors: treatment (fixed with 6 levels: 0, 60, 120, 240, 480 and 960 µg As L^{-1}) and station/sediment type (fixed with 2 levels: 130= silty/contaminated, and 230= sandy/non-contaminated). The design was balanced, with n= 3 replicate microcosms, in each of the 6x2= 12 combinations of the 2 factors for a total of 12x3= 36 microcosms in the experiment.

Factorial ANOVA was used to test for the effect of treatment and station on microeukaryotic SR. Significant differences between groups were analyzed by post hoc Tukey honest significant different (HSD) tests.

Variations in the structure of the active microeukaryotic communities were analyzed using the software package PRIMER 6 (Clarke & Gorley, 2006) with the PERMANOVA+ add-on (Anderson, *et al.*, 2008). Differences in microeukaryotic assemblages were analyzed according to the two-way crossed design for the factors station and treatment using permutational analysis of variance (PERMANOVA; Anderson, 2001, McArdle & Anderson, 2001) based on Bray-Curtis similarities with 9999 permutations of residuals under a reduced model, followed by PERMANOVA pairwise comparisons, including Monte-Carlo tests, if significant differences were detected among the treatments. The variables analyzed were relative abundance values of all OTUs as detected by RNA-based DGGE. Abundance data

were fourth-root transformed prior to analyses. Group average Hierarchical Cluster analysis was performed in order to visualize relationships among samples in terms of community structure, and variation patterns in the OTU community composition were investigated by Principal Coordinate Analyses (PCO). PCO is a distance-based ordination method that maximizes the linear correlation between the distances in the distance matrix, and the distances in a space of low dimension (~ the ordination; typically, 2 or 3 axes are selected). PCO based on Bray-Curtis similarity was performed for all samples, and for samples of both stations separately. Only positively identified (i.e. sequenced) OTUs which were significantly ($p<0.001$) correlated and had R values > 0.5 (Spearman) with one of the first two PCO axes are shown in the PCO diagrams.

Additionally, the occurrence and relative abundances of the identified OTUs detected in the sediments from both stations were calculated for the different As levels. Visualization was performed based on a grey intensity scale reflecting abundance (average for 3 replicates), varying from white (absence), to light grey (indicating minimum abundance), to black (indicating the highest abundance). OTUs are ordered according to the taxonomic group.

Results

Community profiling by DGGE

The PCR-DGGE fingerprints from the various microcosms are shown in Figure 2. The DGGE profiles from station 130 showed more or less similar band patterns across all treatments for all replicates. Patterns for station 230 were more variable, and more variation among the replicates was observed. Replicate c of this station consistently showed lighter band patterns, and the control treatment for this replicate was excluded from further analyses. Replicate a was consistently different from replicate b and c. In both stations, the number of bands decreased with increasing As concentration, especially for the bands in the lower half of the DGGE gel. In station 130, some bands remained very intense irrespective of As concentration, in contrast to station 230, where the most intense bands (except for one) disappear at As concentrations above 240 $\mu g\ L^{-1}$. A small number of bands appeared or intensified at higher arsenic concentrations (see e.g. the arrowed band in Fig. 2).

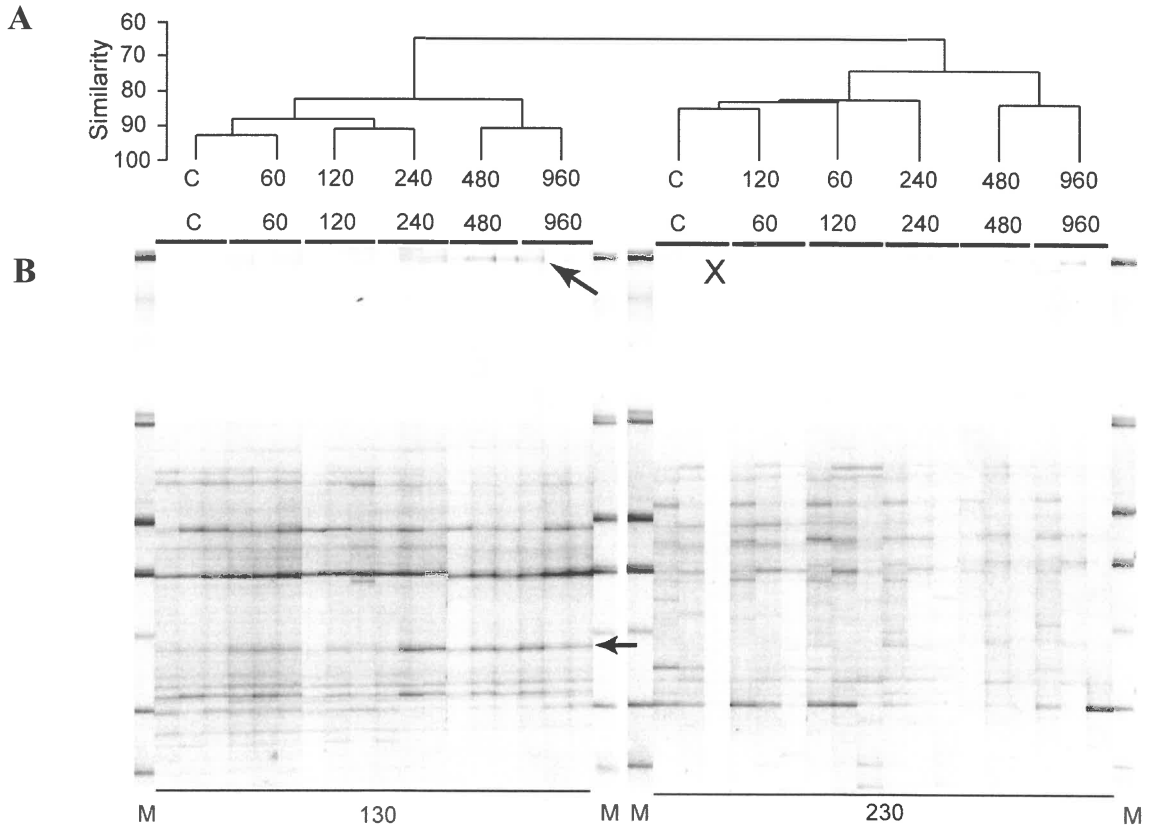

Fig. 2: A: Cluster Analysis of Bray-Curtis similarity of microeukaryotic communities from the 2 different sediment types (130 and 230), exposed to 5 different levels of arsenic contamination. Mean values (n=3) of relative abundances (band intensities) were used; B: DGGE profiles of these samples. The letter (a, b, c) above each lane represents the three replicates, and the number from the cluster corresponds to the respective treatment. M; DGGE Markers used to normalize band positions between different DGGE gels; C, control. See Table 3 for the phylogenetic identities of these bands. Replicate c of the control treatment for station 230 (X) was excluded for further analyses

Effect of As contamination on microeukaryotic SR

A total of 89 OTUs were observed in the 36 microcosms, 62 (=75.6%) of which were present in both stations. Station 230 was more diverse (83 OTUs) than station 130 (68 OTUs). Microeukaryotic species richness (SR) within one sample varied between 29 and 60 0TUs, and significantly decreased at the highest As concentrations (480 and 960 $\mu g\ L^{-1}$, Fig. 2). The decrease in SReuk was 32% (treatment 60 vs. 480 $\mu g\ As\ L^{-1}$) and 43% (control vs. 480 $\mu g\ As\ L^{-1}$) for station 130 and station 230 respectively. Both treatment (ANOVA, $F= 15.93$; $p< 0.001$) and station ($F= 13.16$; $p<0.01$) showed independent, significant effects on species

richness, but no significant interactions between the two factors were observed (treatment x station, F= 2.23; p= 0.086). SR was slightly but significantly higher at 60µg As L^{-1} than in the control treatment (=0µg L^{-1}) in station 130. Note that while the total number of OTUs in station 230 was higher, the average SR within the different treatment levels was similar or lower compared to station 130.

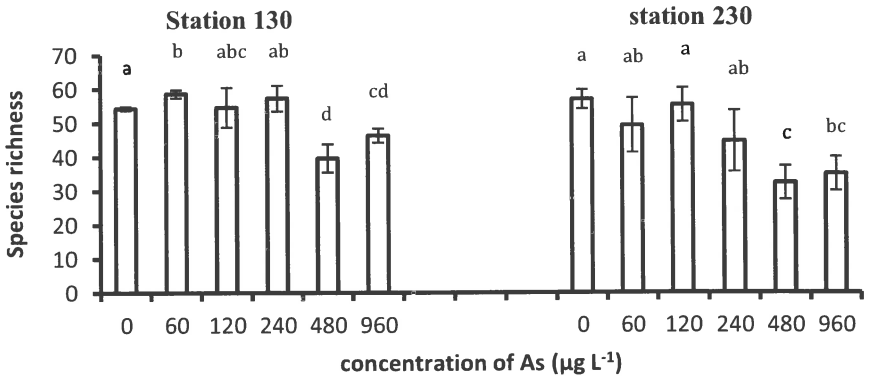

Fig. 3: Microeukaryotic species richness (Nb of DGGE bands) as obtained by DGGE fingerprint analyses of ribosomal RNA extracted from the surface sediments (mean ± SD; n=3). Different letters (a, b, c, d) indicate significant differences between different treatments (arsenic concentrations) within each station (Student t-test, $\alpha = 0.05$)

Microeukaryotic community response to As contamination

The structure of the microeukaryotic community was significantly influenced by sediment type and by As level (station: F= 29,81; p<0.001, and treatment: F= 2,65; p<0.001). The combined effect station x treatment however was not significant (p> 0.05). Cluster Analysis and PCO ordinations (Fig. 2 and 4a) both showed a clear separation between assemblages from both stations. Separate PCO analyses for both stations (Fig. 4 B, C) revealed a substantial shift in community structure from low to high As concentrations, from left to right along the first axis in station 130, and from bottom to top along the second axis in station 230. Note that variation along the first axis in station 230 is mainly related to the divergent position of the "a" replicates, which are all situated on the right side of the diagram. In station 130, three groups of samples can be distinguished: control and 60µg L^{-1}, 120 and 240 µg L^{-1}, and 480 and 960 µg As L^{-1}. In station 230, only two clusters (with respect to As concentration) are

visible, viz. the control and three lowest concentrations vs. the two highest concentrations. Omitting the "a" replicates from the analysis did not change this pattern (not shown). Similarly, the same pattern (three clusters in station 130, only two in station 230) can also be seen in the cluster analysis (Fig. 1). For station 130, we found an overall significant effect of the As treatments on microeukaryotic community structure ($F=7.44$; $p=0.0001$). The control and 60 µg As L^{-1} treatment differed significantly from the treatments with higher concentrations, while the 120 and 240 µg As L^{-1} also significantly differed from the 480-960 µg As L^{-1} treatments, confirming the distinctness of the three groups observed in the PCO's and the cluster analysis (Table 2). The treatment effect was not significant for station 230, even not when repeating the analyses without the diverging replicate "a" (but $p = 0.0669$!), and pairwise comparisons revealed no significant differences (not shown). We identified OTUs (correlation > 0.5 and significant correlated to one of both axes for $p< 0.001$) for the silty or the sandy sediments (fig. 4A), for the different As concentrations along the first ordination axis in station 130 (fig. 4 B), and for replicates along the first axis, and As concentration along the second ordination axis for station 230 (fig. 4 C). Note that no arrow points in the direction of the highest As concentrations for station 230. Identification of the OTU numbers in Fig. 4 is given in table 3.

Table 2: Matrix of Bray-Curtis similarity between and within (diagonal; between replicates) groups (concentration of As; µg L^{-1}) and PERMANOVA pairwise comparison (t; p), calculated from the relative abundance data (fourth-root transformed) in station 130. Significant differences between groups are indicated in boldface

	control	60	120	240	480	960
control	90,571					
60	88,971 t=1.69 p= 0.0615	92,265				
120	**84,23** t=1.93 p= 0.0404	**83,852** **t=2.21** p= 0.0316	87,17			
240	**83,639** t=2.35 p= 0.0214	**85,53** t=2.16 p= 0.0292	86,512 t=1.35 p= 0.1868	88,691		
480	**73,748** t=4.24 p= 0.0022	**76,075** t=4.17 p= 0.0030	**76,029** t=3.14 p= 0.0092	**79,607** t=2.88 p= 0.0124	89,42	
960	**79,037** t=3.62 p= 0.0053	**81,683** t=3.43 p= 0.0042	**80,844** t=2.56 p= 0.0179	**83,4** t=2.38 p= 0.0190	87,422 t=1.73 p= 0.0845	90,901

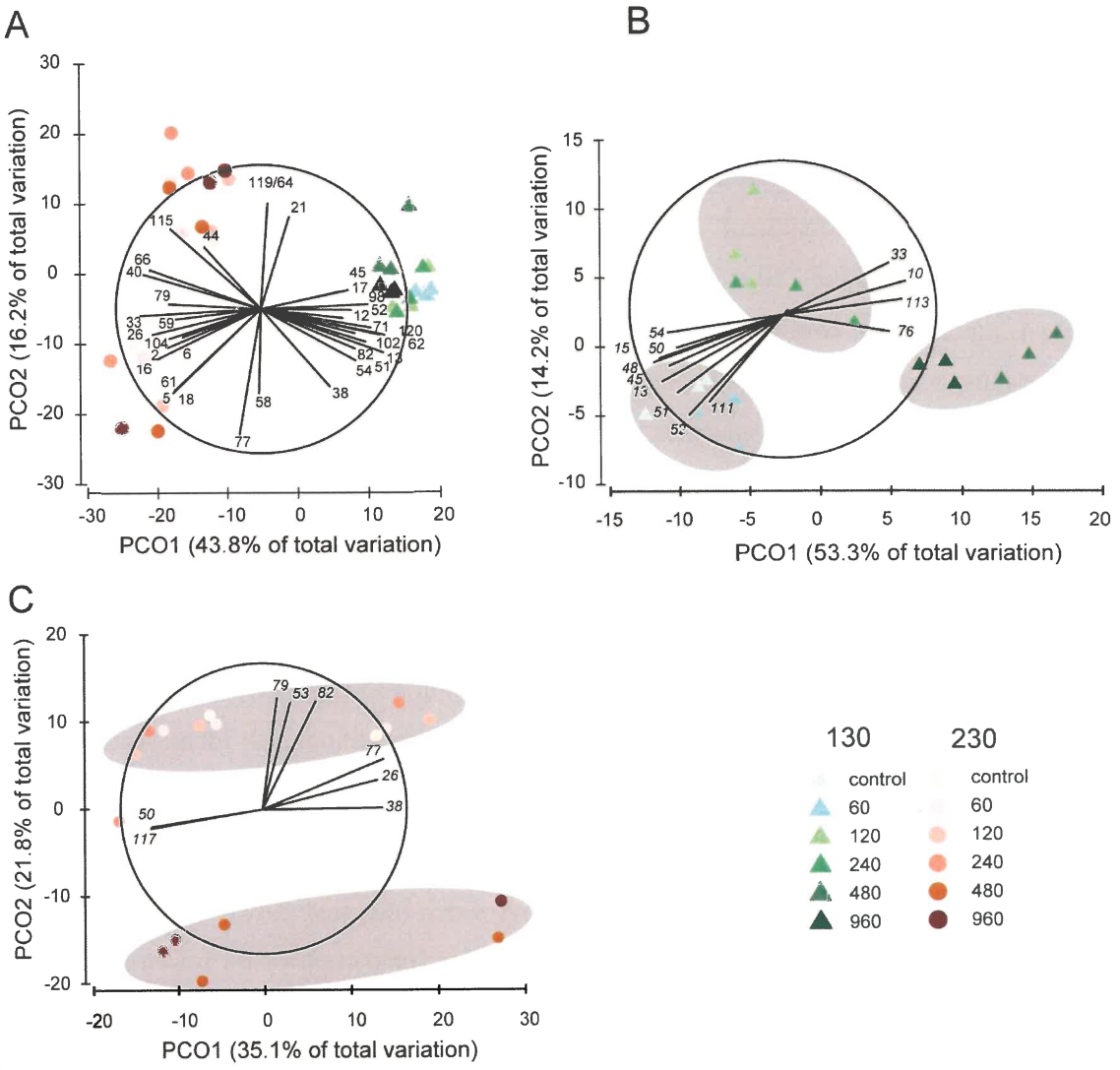

Fig. 4: Principal Coordinates Analyses (PCO) based on Bray-Curtis similarities for all samples (A), and samples from station 130 (B) and station 230 (C) separately. Species (DGGE band nr –for identification see table 3) with a correlation >0.5 and significantly correlated ($p<0.001$) to one of both axes are given in the diagram (Spearman correlation type). Percentage of variation explained by the individual axes is given. Replicate C for the control is excluded for station 230 due to an outlier position.

Composition of the active microeukaryotic communities

The most important OTUs (n=64) representing a total 81% of relative abundance were identified by sequencing and BLAST analysis (Table 3). Similarities ranged between 72 - 99% to positively identified sequences in the databases. Six sequences gave ambiguous BLAST results (VAR) either from within a phylogenetic group (numbers 53 and 58), or from different groups (50, 54, 115, 117). For some sequences, only low sequence homology (around 75%) to a known sequence was found (53, 79, 104, 120). More than half (54 %) of all sequences were ciliates (Fig. 5A). The most dominant ciliate class was the Phyllopharyngea, followed by the Spirotrichea and Litostomatea, and to a lesser degree the Nassophorea, Colpodea, Karyorelictea and Prostomatea (Fig. 5B). Furthermore, several sequences matching with Fungi (11%) and stramenopiles (Bacillariophyceae, 8%; and others including the heterotrophic Labyrinthulida and Oomycetes, 3%), and a few sequences matching to Rhizaria (6%), amoebozoans (5%), dinophytes (2%), metazoans (3%; nematodes) and Euglenozoa (2%) were retrieved.

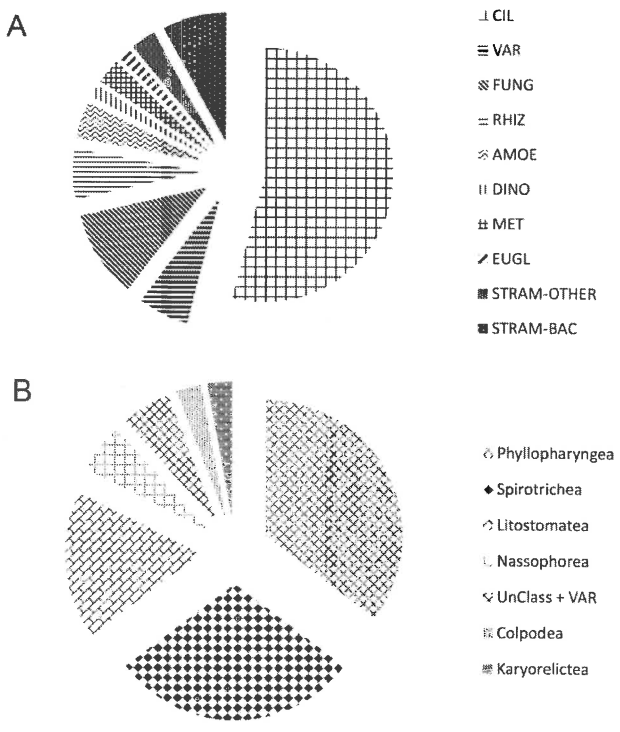

Fig. 5: General microeukaryotic (A) and ciliate (B) diversity based on sequencing of DGGE bands from silty and sandy sediments

Nr	LABEL	Taxonomic group	BLAST (accession no of GenBank match)	%Sim (bp)
2	*AMOE-PLATYAMOEBA-2*	Amoebozoa - Flabellinea	Platyamoeba oblongata (DQ229955)	96 (171)
3	*CIL-LITONOTUS-3*	Alveolata; Ciliophora; Litostomatea	Epiphyllum shenzhenense (GU574809) Litonotus paracygnus (EU242509)	97 (132)
5	*CIL-LOXOPHYLUM/ LITONOTUS-5*	Alveolata; Ciliophora; Litostomatea	Loxophyllum sp. (EU242511) Litonotus paracygnus (DQ190464)	97 (158)
6	*CIL-DYSTERIA-6*	Alveolata; Ciliophora; Phyllopharyngea	Dysteria derouxi (AY378112)	91 (135)
7	*CIL-ENCHELYS-7*	Alveolata; Ciliophora; Litostomatea	Enchelys polynucleata (DQ411861)	94 (127)
12	*CIL-PHIALINA-12*	Alveolata; Ciliophora; Litostomatea	Phialina salinarum (EU242508)	95 (169)
10	*EUGL-DIPLONEMA-10*	Euglenozoa; Diplonemida	Diplonema sp. (AY425012)	80 (116)
13	*CIL-PHIALINA-13*	Alveolata; Ciliophora; Litostomatea	Phialina salinarum (EU242508)	98 (168)
14	*BAC-VAR-14*	Stramenopila; Bacillariophyta	Cyclotella sp. / Skeletonema sp. / Thalassiossira sp./ e. a.	99 (169)
15	*BAC-MINIDISCUS-15*	Stramenopila; Bacillariophyta	Minidiscus trioculatus (FJ590769)	99 (169)
16	*CIL-CHILODONELLA-16*	Alveolata; Ciliophora; Phyllopharyngea	Chilodonella uncinata (AF300283)	94 (169)
17	*BAC-RHAPHONEIS/ DELPHINEIS-17*	Stramenopila; Bacillariophyta	Rhaphoneis amphiceros (AB433337) Delphineis sp. (AY485465)	99 (167)
18	*CERC-CYPHODERAI-18*	Rhizaria; Cercozoa; Silicofilosea	Cyphoderai compressa (GU228867)	97 (169)
21	*BAC-LEPTOCYLINDRICUS-21*	Stramenopila; Bacillariophyta	Leptocylindricus danicus (AJ535175)	86 (175)
22	*BACI/OOM22*	Stramenopila; Bacillariophyta Stramenopila; Oomycetes	Ardissonea sp. (AM746973) Apodachlya sp. (AJ238663)/ Haliphtoraos sp. (AB178865)	86 (176)
26	*CERC-AURANTICORDIS-26*	Rhizaria; Cercozoa; Novel Clade I	Auranticordis quadriverberis (EU484394)	94 (161)
29	*FUNG-AURICULARIACEAE-29*	Fungi; Dikarya; Basiodiomycota	Uncultured Auriculariaceae (Ef24776)	90 (150)
33	*CIL-DYSTERIA-33*	Alveolata; Ciliophora; Phyllopharyngea	Dysteria derouxi (AY378112)	93 (168)
89	*CIL-PRODISCOPHRYA-89*	Alveolata; Ciliophora; Phyllopharyngea	Prodiscophrya sp. (AY372787)	89 (167)
35	*CIL-DYSTERIA-35*	Alveolata; Ciliophora; Phyllopharyngea	Dysteria derouxi (AY378112)	92 (168)
36	*CIL-COLPODIDIUM-36*	Alveolata; Ciliophora; Nassophorea	Colpodidium caudatum (EU264560)	91 (169)
38	*CIL-PLATYOPHRYA-38*	Alveolata; Ciliophora; Colpodea	Platyophrya bromelicola (EU039905)	90 (169)
40	*CIL-PHIALINA-40*	Alveolata; Ciliophora; Litostomatea	Phialina salinarum (EU242508)	95 (169)
42	*CERC-ALLAS-42*	Rhizaria; Cercozoa; Silicofilosea	Allas sp. (AY268040)	95 (170)
44	*CIL-TRACHELOCERCA-44*	Alveolata; Ciliophora; Karyorelictea	Trachelocerca ditis (GQ167153)	98 (162)
45	*FUNG-GONAPODYA-45*	Fungi; Chytridiomycota	Gonapodya sp. (AF164330)	89 (165)
48	*CIL-STROMBIDIUM-48*	Alveolata; Ciliophora; Spirotrichea	Strombidium sp. (AY143564)	99 (167)
49	*MET-ASTOMONEMA-49*	Metazoa; Nematoda	Astomonema sp. (DQ408759)	93 (166)
50	*VAR50*	Fungi/Metaoza/Stramenopila/ e.a.	VAR	/ (165)
51	*CIL-TINTINNOPSIS-51*	Alveolata; Ciliophora; Spirotrichea	Tintinnopsis sp. (DQ487200)	93 (166)
52	*FUNG-MYCOARTHRIS-52*	Fungi; Dikarya; Ascomycota	Mycoarthris corallinus (AF128439)	97 (78)
53	*FUNG-VAR-53*	Fungi; Dikarya	Fungus (VAR)	76 (156)
54	*VAR-54*	Fungi/Apusozoa/Stramenopila/ e.a.	VAR	80-88 (166)
56	*FUNG-VAR-56*	Fungi; Dikarya; Basidiomycota	Kriegeria sp/ Mycogloea sp. / Zymoxenogloea sp	88 (166)
57	*CERC-VAR-57*	Rhizaria; Cercozoa	Hedriocystis sp. /Clathrulina sp. / Gymnophrys sp.	81 (165)
58	*CIL-VAR-58*	Alveolata; Ciliophora; Intramacronucleata	VAR ciliates	85 (118)
61	*CIL-HOLOSTICHA-61*	Alveolata; Ciliophora; Spirotrichea	Holosticha bradburyae (EF123706)	98 (167)
62	*AMOE-PARAMOEBA-62*	Amoebozoa; Flabellinea	Paramoeba eihardi (AY686575)	97 (172)
64	*CIL-EUTINTINNUS-64*	Alveolata; Ciliophora; Spirotrichea	Eutintinnus pectinis (AY143570	96 (166)
66	*CIL-TINTINNOPSIS-66*	Alveolata; Ciliophora; Spirotrichea	Tintinnopsis tubulosoides (AF399110)	98 (167)
70	*BAC-ODONTELLA-70*	Stramenopila; Bacillariophyta	Odontella aurita (AY485522)	97 (171)
73	*CIL-ISOCHONA-73*	Alveolata; Ciliophora; Phyllopharyngea	Isochona sp. (AY242119)	88 (173)
76	*CIL-TINTINNOPSIS-76*	Alveolata; Ciliophora; Spirotrichea	Tintinnopsis beroidea (EF 123709)	95 (166)
77	*CIL-ASPENDISCA-77*	Alveolata; Ciliophora; Spirotrichea	Aspendisca leptaspis (EU880597)	93 (165)
78	*CIL-ISOCHONA-78*	Alveolata; Ciliophora; Phyllopharyngea	Isochona sp. (AY242119)	90 (172)
79	*FUNG-CHYTRIDIOMYCOTA-79*	Fungi; Chytridiomycota	Uncultured Chytridiomycota clone (HQ191373)	77 (171)
83	*CIL-CRYPTOCARPUS-83*	Alveolata; Ciliophora; Prostomatea	Cryptocaryon irritans (AF351579)	96 (171)
82	*CIL-ACINETA-82*	Alveolata; Ciliophora; Phyllopharyngea	Acineta sp. (AY332718)	89 (165)
87	*CIL-PRODISCOPHRYA-87*	Alveolata; Ciliophora; Phyllopharyngea	Prodiscophrya sp. (AY331803)	86 (167)
89	*CIL-PRODISCOPHRYA-89*	Alveolata; Ciliophora; Phyllopharyngea	Prodiscophrya sp. (AY331803)	89 (167)
92	*LABY-OBLONGICHYTRICHUM-92*	Stramenopila; Labyrinthulida	Oblongichytrichum sp. (FJ799794)	91 (173)
98	*CIL-ACINETA-98*	Alveolata; Ciliophora; Phyllopharyngea	Acineta sp. (AY332718)	91 (164)
100	*CIL-ORTHODONELLA-100*	Alveolata; Ciliophora; Nassophorea	Orthodonella sp. (EU 286809)	91 (169)
101	*AMOE-THECAMOEBA-101*	Amoebozoa; Flabellinea	Thecamoeba sp. (EF455775)	84 (167)
102	*CIL-ACINETA-102*	Alveolata; Ciliophora; Phyllopharyngea	Acineta sp. (AY332718)	91 (164)
104	*HAPT/VIRI-VAR-104*	Haptophyceae; Syracosphaerales / Viridiplantae	Syracosphaera sp. (AM490987)/ Dictyosphaerium sp. e.a.	74 (157)
105	*MET-STILBONA-105*	Metazoa; Nematoda	Stilbona majum (Y16922)	91 (163)
108	*CIL-ASPIDISCA-108*	Alveolata; Ciliophora; Spirotrichea	Aspidisca steini (AF305625)	86 (165)
111	*CIL-PROTOGASTROSTYLA-111*	Alveolata; Ciliophora; Spirotrichea	Protogastrostyla pulchra (EF194082)	83 (168)
113	*CIL-ASPIDISCA-113*	Alveolata; Ciliophora; Spirotrichea	Aspidisca leptaspis (EU880597)	84 (175)
115	*VAR-115*	*Metazoa/ Alveolata / Amoebozoa*	*VAR*	
117	*VAR-117*	*Viridiplantae/ Alveolata/ Amoebozoa*	*VAR*	
119	*DINO-UNC-119*	Alveolata; Dinophyceae	Uncultured dinoflagellate (GU820396)	84 (166)
120	*FUNG-CHYTRIDIOMYCOTA-120*	Fungi; Chytridiomycota	Uncultured Chytridiomycota clone (HQ191373)	72 (145)

Table 3: Identification of microeukaryotic DGGE bands. Only the first identified BLAST match is given. %Sim, percentage of similarity; bp, basepair; Nr, number of taxa as used in PCO (Fig. 4); LABEL, label of the phylotype used in Fig. 7; VAR, various.

Diversity, based on presence/absence of OTUs and relative abundance (~ band intensities) of the different phylogenetic groups, for the different As treatment levels are shown in Fig. 6A and B respectively. The diversity of the different groups was more or less stable at all As concentrations in both stations, except for a slight decrease in the number of Fungi. Changes in the relative abundances of the phylogenetic groups were more pronounced (Fig. 6B). The relative contribution of ciliates, Amoebae and stramenopiles was generally higher in station 130 than in station 230, while Rhizaria were generally more important in station 230. The proportion of ciliates relatively increased with arsenic level in station 130, while Amoebae, stramenopiles and Fungi decreased. The relative abundance of Fungi also decreased in station 230, but in these sandy sediments the proportion of ciliates first increased at 60 µg As L^{-1}, and then more or less decreased, to be lowest at the highest contamination level. The proportion of mixed OTUs ('mixID') also increased with contamination level.

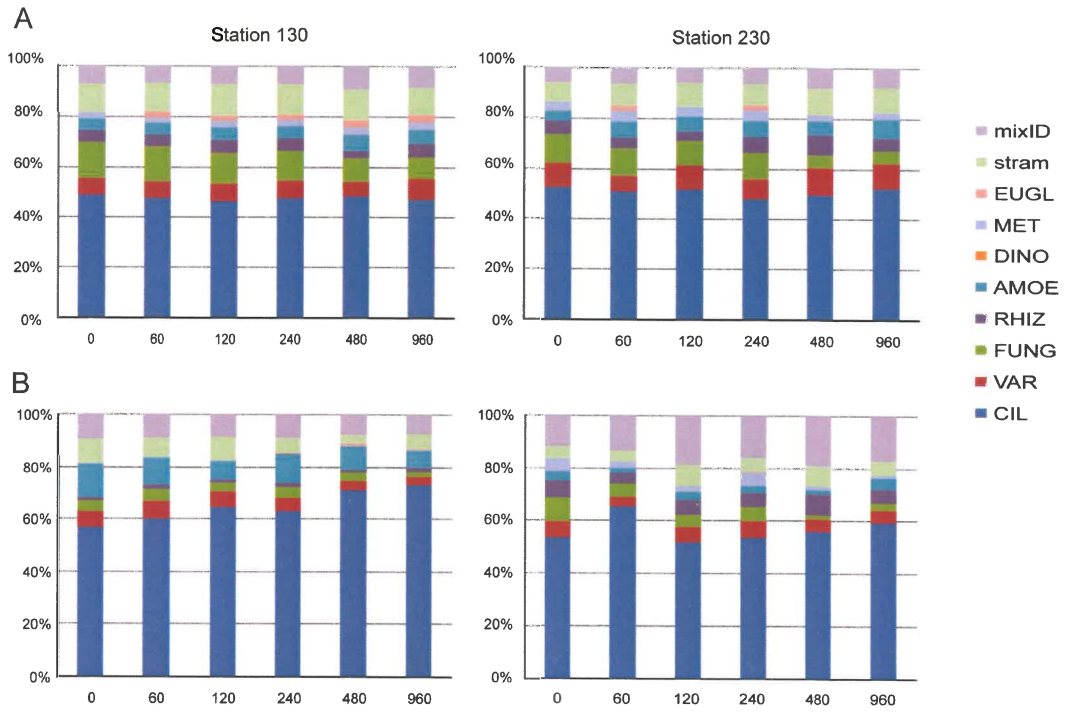

Fig. 6: Relative contribution of different taxonomic groups from 18S rRNA sequences obtained from the sediments from the microcosms after the treatments with different arsenic levels, for both stations. (A) microeukaryotic diversity based on presence/absence, and (B) on relative abundances. mixID, mixed OTU (see text).

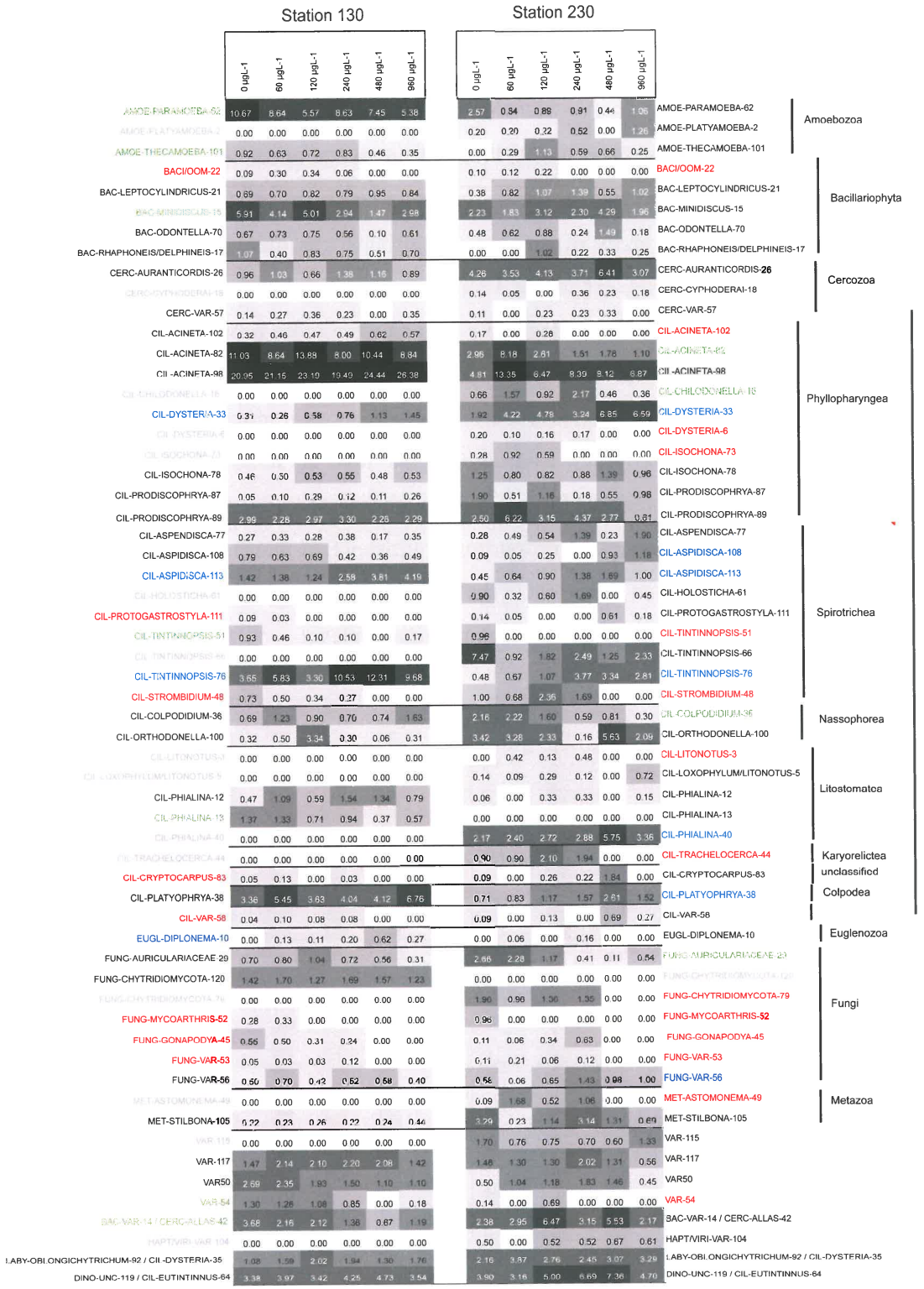
Station 130
Station 230
0 µgL-1
60 µgL-1
120 µgL-1
240 µgL-1
480 µgL-1
960 µgL-1
AMOE-PARAMOEBA-62 10.67 8.64 5.57 8.63 7.45 5.38 2.57 0.54 0.88 0.91 0.44 1.06 AMOE-PARAMOEBA-62
AMOE-PLATYAMOEBA-2 0.00 0.00 0.00 0.00 0.00 0.00 0.20 0.20 0.22 0.52 0.00 1.26 AMOE-PLATYAMOEBA-2
AMOE-THECAMOEBA-101 0.92 0.63 0.72 0.83 0.46 0.35 0.00 0.29 1.13 0.59 0.66 0.25 AMOE-THECAMOEBA-101
Amoebozoa
BACI/OOM-22 0.09 0.30 0.34 0.06 0.00 0.00 0.10 0.12 0.22 0.00 0.00 0.00 BACI/OOM-22
BAC-LEPTOCYLINDRICUS-21 0.69 0.70 0.82 0.79 0.95 0.84 0.38 0.82 1.07 1.39 0.55 1.02 BAC-LEPTOCYLINDRICUS-21
BAC-MINIDISCUS-15 5.91 4.14 5.01 2.94 1.47 2.98 2.23 1.83 3.12 2.30 4.29 1.96 BAC-MINIDISCUS-15
BAC-ODONTELLA-70 0.67 0.73 0.75 0.56 0.10 0.61 0.48 0.62 0.88 0.24 1.49 0.18 BAC-ODONTELLA-70
BAC-RHAPHONEIS/DELPHINEIS-17 1.07 0.40 0.83 0.75 0.51 0.70 0.00 0.00 1.02 0.22 0.33 0.25 BAC-RHAPHONEIS/DELPHINEIS-17
Bacillariophyta
CERC-AURANTICORDIS-26 0.96 1.03 0.66 1.38 1.16 0.89 4.26 3.53 4.13 3.71 6.41 3.07 CERC-AURANTICORDIS-26
CERC-CYPHODERAI-18 0.00 0.00 0.00 0.00 0.00 0.00 0.14 0.05 0.00 0.36 0.23 0.18 CERC-CYPHODERAI-18
Cercozoa
CERC-VAR-57 0.14 0.27 0.36 0.23 0.00 0.35 0.11 0.00 0.23 0.23 0.33 0.00 CERC-VAR-57
CIL-ACINETA-102 0.32 0.46 0.47 0.49 0.62 0.57 0.17 0.00 0.28 0.00 0.00 0.00 CIL-ACINETA-102
CIL-ACINETA-82 11.03 8.64 13.88 8.00 10.44 8.84 2.96 8.18 2.61 1.51 1.78 1.10 CIL-ACINETA-82
CIl -ACINFTA-98 20.95 21.15 23.19 19.49 24.44 26.38 4.81 13.35 6.47 8.39 8.12 6.87 CIl -ACINFTA-98
CIL-CHILODONELLA-16 0.00 0.00 0.00 0.00 0.00 0.00 0.66 1.57 0.92 2.17 0.46 0.36 CIL-CHILODONELLA-16
CIL-DYSTERIA-33 0.31 0.26 0.58 0.76 1.13 1.45 1.92 4.22 4.78 3.24 6.85 6.59 CIL-DYSTERIA-33
CIL-DYSTERIA-6 0.00 0.00 0.00 0.00 0.00 0.00 0.20 0.10 0.16 0.17 0.00 0.00 CIL-DYSTERIA-6
CIL-ISOCHONA-73 0.00 0.00 0.00 0.00 0.00 0.00 0.28 0.92 0.59 0.00 0.00 0.00 CIL-ISOCHONA-73
CIL-ISOCHONA-78 0.46 0.50 0.53 0.55 0.48 0.53 1.25 0.80 0.82 0.88 1.39 0.96 CIL-ISOCHONA-78
CIL-PRODISCOPHRYA-87 0.05 0.10 0.29 0.12 0.11 0.26 1.90 0.51 1.16 0.18 0.55 0.98 CIL-PRODISCOPHRYA-87
CIL-PRODISCOPHRYA-89 2.99 2.28 2.97 3.30 2.26 2.29 2.50 6.22 3.15 4.37 2.77 0.61 CIL-PRODISCOPHRYA-89
Phyllopharyngea
CIL-ASPENDISCA-77 0.27 0.33 0.28 0.38 0.17 0.35 0.28 0.49 0.54 1.39 0.23 1.90 CIL-ASPENDISCA-77
CIL-ASPIDISCA-108 0.79 0.63 0.69 0.42 0.36 0.49 0.09 0.05 0.25 0.00 0.93 1.18 CIL-ASPIDISCA-108
CIL-ASPIDISCA-113 1.42 1.38 1.24 2.58 3.81 4.19 0.45 0.64 0.90 1.38 1.69 1.00 CIL-ASPIDISCA-113
CIL-HOLOSTICHA-61 0.00 0.00 0.00 0.00 0.00 0.00 0.90 0.32 0.60 1.69 0.00 0.45 CIL-HOLOSTICHA-61
CIL-PROTOGASTROSTYLA-111 0.09 0.03 0.00 0.00 0.00 0.00 0.14 0.05 0.00 0.00 0.61 0.18 CIL-PROTOGASTROSTYLA-111
CIL-TINTINNOPSIS-51 0.93 0.46 0.10 0.10 0.00 0.17 0.96 0.00 0.00 0.00 0.00 0.00 CIL-TINTINNOPSIS-51
CIL-TINTINNOPSIS-66 0.00 0.00 0.00 0.00 0.00 0.00 7.47 0.92 1.82 2.49 1.25 2.33 CIL-TINTINNOPSIS-66
CIL-TINTINNOPSIS-76 3.65 5.83 3.30 10.53 12.31 9.68 0.48 0.67 1.07 3.77 3.34 2.81 CIL-TINTINNOPSIS-76
CIL-STROMBIDIUM-48 0.73 0.50 0.34 0.27 0.00 0.00 1.00 0.68 2.36 1.69 0.00 0.00 CIL-STROMBIDIUM-48
Spirotrichea
CIL-COLPODIDIUM-36 0.69 1.23 0.90 0.70 0.74 1.63 2.16 2.22 1.60 0.59 0.81 0.30 CIL-COLPODIDIUM-36
CIL-ORTHODONELLA-100 0.32 0.50 3.34 0.30 0.06 0.31 3.42 3.28 2.33 0.16 5.63 2.09 CIL-ORTHODONELLA-100
Nassophorea
CIL-LITONOTUS-3 0.00 0.00 0.00 0.00 0.00 0.00 0.00 0.42 0.13 0.48 0.00 0.00 CIL-LITONOTUS-3
CIL-LOXOPHYLUM/LITONOTUS-5 0.00 0.00 0.00 0.00 0.00 0.00 0.14 0.09 0.29 0.12 0.00 0.72 CIL-LOXOPHYLUM/LITONOTUS-5
CIL-PHIALINA-12 0.47 1.09 0.59 1.54 1.34 0.79 0.06 0.00 0.33 0.33 0.00 0.15 CIL-PHIALINA-12
CIL-PHIALINA-13 1.37 1.33 0.71 0.94 0.37 0.57 0.00 0.00 0.00 0.00 0.00 0.00 CIL-PHIALINA-13
CIL-PHIALINA-40 0.00 0.00 0.00 0.00 0.00 0.00 2.17 2.40 2.72 2.88 5.75 3.36 CIL-PHIALINA-40
Litostomatea
CIL-TRACHELOCERCA-44 0.00 0.00 0.00 0.00 0.00 0.00 0.90 0.90 2.10 1.94 0.00 0.00 CIL-TRACHELOCERCA-44
Karyorelictea
CIL-CRYPTOCARPUS-83 0.05 0.13 0.00 0.03 0.00 0.00 0.09 0.00 0.26 0.22 1.84 0.00 CIL-CRYPTOCARPUS-83
unclassified
CIL-PLATYOPHRYA-38 3.36 5.45 3.83 4.04 4.12 6.76 0.71 0.83 1.17 1.57 2.61 1.52 CIL-PLATYOPHRYA-38
Colpodea
CIL-VAR-58 0.04 0.10 0.08 0.08 0.00 0.00 0.09 0.00 0.13 0.00 0.69 0.27 CIL-VAR-58
Ciliates
EUGL-DIPLONEMA-10 0.00 0.13 0.11 0.20 0.62 0.27 0.00 0.06 0.00 0.16 0.00 0.00 EUGL-DIPLONEMA-10
Euglenozoa
FUNG-AURICULARIACEAE-29 0.70 0.80 1.04 0.72 0.56 0.31 2.66 2.28 1.17 0.41 0.11 0.54 FUNG-AURICULARIACEAE-29
FUNG-CHYTRIDIOMYCOTA-120 1.42 1.70 1.27 1.69 1.57 1.23 0.00 0.00 0.00 0.00 0.00 0.00 FUNG-CHYTRIDIOMYCOTA-120
FUNG-CHYTRIDIOMYCOTA-79 0.00 0.00 0.00 0.00 0.00 0.00 1.90 0.96 1.36 1.35 0.00 0.00 FUNG-CHYTRIDIOMYCOTA-79
FUNG-MYCOARTHRIS-52 0.28 0.33 0.00 0.00 0.00 0.00 0.96 0.00 0.00 0.00 0.00 0.00 FUNG-MYCOARTHRIS-52
FUNG-GONAPODYA-45 0.56 0.50 0.31 0.24 0.00 0.00 0.11 0.06 0.34 0.63 0.00 0.00 FUNG-GONAPODYA-45
FUNG-VAR-53 0.05 0.03 0.03 0.12 0.00 0.00 0.11 0.21 0.06 0.12 0.00 0.00 FUNG-VAR-53
FUNG-VAR-56 0.50 0.70 0.42 0.52 0.58 0.40 0.56 0.06 0.65 1.43 0.98 1.00 FUNG-VAR-56
Fungi
MET-ASTOMONEMA-49 0.00 0.00 0.00 0.00 0.00 0.00 0.09 1.68 0.52 1.06 0.00 0.00 MET-ASTOMONEMA-49
MET-STILBONA-105 0.22 0.23 0.26 0.22 0.24 0.44 3.29 0.23 1.14 3.14 1.31 0.69 MET-STILBONA-105
Metazoa
VAR-115 0.00 0.00 0.00 0.00 0.00 0.00 1.70 0.76 0.75 0.70 0.60 1.33 VAR-115
VAR-117 1.47 2.14 2.10 2.20 2.08 1.42 1.46 1.30 1.30 2.02 1.31 0.56 VAR-117
VAR50 2.69 2.35 1.93 1.50 1.10 1.10 0.50 1.04 1.18 1.83 1.46 0.45 VAR50
VAR-54 1.30 1.26 1.08 0.85 0.00 0.18 0.14 0.00 0.69 0.00 0.00 0.00 VAR-54
BAC-VAR-14 / CERC-ALLAS-42 3.68 2.16 2.12 1.38 0.87 1.19 2.38 2.95 6.47 3.15 5.53 2.17 BAC-VAR-14 / CERC-ALLAS-42
HAPT/VIRI-VAR-104 0.00 0.00 0.00 0.00 0.00 0.00 0.50 0.00 0.52 0.52 0.67 0.61 HAPT/VIRI-VAR-104
LABY-OBI.ONGICHYTRICHUM-92 / CIL-DYSTERIA-35 1.08 1.59 2.02 1.94 1.30 1.76 2.16 3.87 2.76 2.45 3.07 3.29 LABY-OBI.ONGICHYTRICHUM-92 / CIL-DYSTERIA-35
DINO-UNC-119 / CIL-EUTINTINNUS-64 3.38 3.97 3.42 4.25 4.73 3.54 3.90 3.16 5.00 6.69 7.36 4.70 DINO-UNC-119 / CIL-EUTINTINNUS-64

Fig. 7 (left): Incidence and relative abundances of the identified OTUs detected in the sediments from both stations 130 and 230 for the different As levels. Columns represent the 6 different As treatments (0, 60, 120, 240, 480 and 960 μg L^{-1}) and rows show the OTU [group (abbreviated) – species – nr. (for more information; see table 3)]. OTUs are ordered per taxonomic group. The color intensity reflects the relative abundance (average for 3 replicates), with white indicating absence, and grey scales reflecting increasing relative abundances (0-0.5%, 0.5-1%, 1-2%, 2-5%, 5-10%, >10). Grey OTU labels = absent; red = disappearance at higher As levels; green = decrease with increasing As levels; black = no distinct pattern; blue = increase with increasing As levels.

Individual OTU patterns

The changes in relative abundances of the identified OTUs in both stations for the different treatments (Fig. 7) are generally in accordance with the patterns of OTUs (numbers) observed in the PCO's (Fig. 4). Several patterns can be extracted from figure 7: (A) it confirms the difference in species composition between station 130 and 230 as seen in fig. 4A; for example the OTUs related to a chytridiomycote fungus (120), a *Paramoeba* sp. (62) and some ciliates (12, 13, 102) were more characteristic for station 130, while ciliates in general were more diverse in station 230 (e.g. 3, 4, 5, 13, 16, 40, 41, 44 and 73 can only be found in station 230); (B) with increasing As levels 16 OTUs disappeared (indicated in red), 11 decreased (indicated in green), 7 increased (indicated in blue) and the remaining OTUs remained relatively stable (indicated in black); (C) often similar patterns can be observed in both station 130 and 230, for example a decrease of the OTUs related to a *Paramoeba* sp. (62), the stramenopile BACI/OOM-22, *Strombidium* sp. (48), *Gonapodya* sp. (45), etc., and an increase of the OTUs related to *Dysteria* sp. (33), *Aspidisca* sp. (113), *Tintinnopsis* sp. (76); (D) Several OTUs absent from station 130 seemed to be sensitive to increasing As levels in station 230, for example nematode sp. 49, the fungus sp. 79 and the ciliate sp. 44; (E) Generally, OTUs that disappeared in one station, never showed a distinct increase in the other; (F) It seemed that especially relatively less abundant species tend to disappear at higher arsenic concentrations, while more dominant taxa only decreased or remained stable in one or both sediments.

The OTUs are ordered according to their affiliation, and it can be seen that e.g. Fungi reacted very sensitively to increasing As levels, which also confirms our previous findings in Fig. 6; 57% of the OTUs related to Fungi in both stations disappeared (45, 52, 53 and 79), the others remained stable (120) or decreased (29) and no OTU increased. Metazoans (only 2 nematode OTUs) reacted differently in both stations; in station 230, one disappeared (49) and the other

one decreased (105) while in station 130 the latter remained stable. Cercozoans were relatively unaffected, Euglenozoa (10) increased and amoebozoans (62, 101) decreased only in station 130, and ciliates species showed various specific responses. Ciliates were the only group (apart from one fungal sequence) in which some representatives relatively increased at higher As concentrations. However, responses were highly OTU-specific. One *Colpodea* representative was quite resistant to As contamination; *Karyorelictea* and an unclassified ciliate were sensitive; *Nassophorea*, *Litostomatea*, *Spirotrichea* and *Phyllopharyngea* showed various responses, often similar between both stations, and sometimes different (e.g. 36, 108).

Discussion

We studied the effect of As contamination on marine benthic microeukaryotic communities in two subtidal sediment types in the Belgian Continental Zone, a silty contaminated (130) and a sandy non-contaminated (230) station. Sediment-water microcosms were spiked with a series of arsenic (0, 60, 120, 240, 480, 960 $\mu g\ L^{-1}$).

Description of the active microeukaryotic communities in the sediments

The active microeukaryotic communities in these subtidal stations were dominated by ciliates (Fig. 5A). During this study, we detected 34 different ciliate sequences, representing 7 different classes. Phyllopharyngea and Spirotrichea were the dominant classes, followed by Litostomatea, Nassophorea, Colpodea, Prostomatea (fish parasite Cryptocaryon irritans; Montero, *et al.*, 2007) and Karyorelictea (Fig. 5B), all of which –except the parasite- are common in marine sediments (Patterson, *et al.*, 1989). Most of these classes were also observed in ciliate-specific clone libraries by Shimeta, *et al.* (2007) and Pede, *et al.* (chapter 2) from silty subtidal sediments. Fungi contributed 13.6% and 10.5%, and stramenopiles 11.4% and 8.8% to total diversity in silty and sandy sediments respectively. Fungi often represent a significant fraction of 18S rDNA sequences in surveys of (especially oxygen-depleted) marine environments (Stoeck & Epstein, 2003, Luo, *et al.*, 2005, Takishita, *et al.*, 2007, Edgcomb, *et al.*, 2011), where they play an important role as saprobes and symbionts, but also as pathogens in algae and animals (Hyde, *et al.*, 1998). The stramenopiles were mainly related to diatoms (e.g. *Odontella* ssp., *Cyclotella* spp., *Skeletonema* ssp., *Thalassiossira* ssp, *Minidiscus* ssp., etc.; see Table 3); representatives of the phytoplankton in these coastal waters (M'Harzi, *et al.*, 1998, Croot, *et al.*, 2002), which can be found as resting

stages in the sediments (McQuoid, 2002, Harnstrom, *et al.*, 2011). Less abundant groups (1.8-5.3%) included Rhizaria (cercozoans), Amoebozoa, dinophytes, Metazoa (2 nematodes) and Euglenozoa.

When comparing higher-level taxonomic diversity (i.e. presence/absence of ciliates, Fungi, Amoeba, etc.) in both sediments, there was little difference (Fig. 6A), and 76% of the OTUs was shared between both stations. A higher total diversity (# OTUs) was observed in station 230, especially for ciliates (Fig. 7); e.g. Karyorelictea were only found in sandy sediments (Fenchel 1987, Hirt, *et al.*, 1995, Shimeta, *et al.*, 2007), and Litostomatea, Spirotrichea and Phyllopharyngea were more diverse in sandy sediments compared to silty sediments. However, as the average diversity per sample from station 230 was equal or lower than in sediments of station 130 (Fig. 3), the higher total diversity is most probably due to the greater spatial heterogeneity (replicates) within the sandy sediments (Figs. 2, 4; especially replicate a was different). Community structure in the silty and sandy sediments were significantly different (see also Pede, *et al.*, chapter 2), and these differences in community composition (Fig. 4) were related to several OTUs, such as the higher abundances of cercozoans (nrs. 18, 26) and metazoans (49, 105) in sandy sediments and the higher abundance of one Amoeba (62) in silty sediments (Figs. 4, 7). Moreover, except from the difference in sediment type, it cannot be excluded that the difference in contamination history between the sandy and the silty sediment plays a role (cf. Chariton, *et al.*, 2010).

Effect of As treatment on microeukaryotic diversity and community composition

The addition of arsenic in our study caused a significant reduction in number of active microeukaryotic OTUs after 48 hours in sediments that received $\geq$ 480 µg As L^{-1}. A similar effect was observed in response to acute and periodic contamination by Pb (1 mg Pb L-1; Fernandez-Leborans & Novillo, 1994) and Cd (1000 mg Cd dm-3; Fernandez-Leborans, *et al.*, 2007). The decrease observed in our study was higher in the sandy sediment (43%) with no contamination history, than in the silty sediment (32%) with a history of As contamination. Furthermore, the toxic effect of the lowest concentration (60 µg As L^{-1}) seemed to be higher in the sandy station with the disappearance of some species, while in station 130 the first species disappeared at 120 µg L^{-1}, and most only at 480 µg L^{-1} (Fig. 7). This indicates a higher As sensitivity of many taxa in the sandy sediment compared with the taxa in the silty sediment which may be acclimatized (if the same species as in the sandy sediment) or selected (different species) to live at higher As concentrations. Even though diversity (SR)

decreased, general higher-level taxonomic diversity (based on presence/absence) remained relatively stable throughout the different treatments, except for a steady decline of Fungi in both sediments (Fig. 6A), suggesting that species losses occurred in most groups.

The actual structure of the active communities (based on diversity and relative abundance) showed pronounced changes with increasing As concentrations (Fig. 5). Change was most distinct at As concentrations ≥ 480 µg L^{-1} in both sediment types. In station 130, the effect of As contamination was significant, and mainly caused by the decrease of several OTUs e.g. amoebae, ciliates and Fungi (indicated in green and red in Fig. 7, but see also Fig. 4B) and the increase of three ciliates and one euglenozoan (indicated in blue in Fig. 7) from the lowest to the highest As contamination level. The change in community composition in this silty sediment was gradual, with significant change already occurring at concentrations of 120 µg L^{-1} (Fig. 4, Table 2). However, no OTUs were specific for these communities at intermediate As concentrations (see Fig. 4 - no arrows pointing in this direction). In station 230, the shift in community composition only occurred at As concentrations > 480 µg L^{-1} and was mainly caused by the decrease of a number of Fungi and ciliate OTUs, while no OTUs showed a pronounced increase with increasing As concentrations (no arrows pointing in the direction of the highest concentration; Fig. 4). However, the change in community composition in this sediment type was not significant, which could be related to the large differences between the replicates. Fig. 7 shows that some OTUs actually do show an increase with increasing As concentrations, but these concern mainly less important/abundant OTUs. Most of the dominant bands varied less (Fig. 7). Moreover, the patterns observed in station 230 are generally less consistent (see Fig. 7; e.g. 16, 89, 77, 44, etc.), probably again related to the variation between replicates. At first sight, it seems surprising that the change in community composition in response to As contamination is more pronounced and significant in the silty sediment (which is presumed to harbor more metal-tolerant organisms), especially at lower As concentrations. While we have no obvious explanation for this observation, we believe it may be related to the fate of the As after addition to the microcosms. It is not unlikely that physical and chemical factors related to sediment composition may influence its speciation and hence bioavailability. More information is needed on the exact speciation and toxicity of As in the different sediment types.

The response to As contamination was most pronounced in Fungi and ciliates. Fungi decreased as a whole and many OTUs disappeared in both sediments what clearly indicates that Fungi in our sediments were sensitive to As (Figs. 6B, 7). This contrasts with previous

studies which show that Fungi are quite tolerant to metal contamination (e.g. Cernansky, *et al.*, 2009, Vala, 2010). Moreover, Fungi are used as biosorbents for the removal of metal-contaminated industrial effluents (Das, *et al.*, 2008), and also appear a promising candidate for As remediation (Vala, 2010, Srivastava, *et al.*, 2011) due to their high cell wall binding capacity and high intracellular metal uptake capacity (Kapoor & Viraraghavan, 1997, Gadd, 2000). It should be noted however that disappearance from the DGGE gels does not necessarily mean that the organisms disappeared as a consequence of contamination; it is also possible that they became inactive, or that their activity (~rRNA content) dropped below the detection limit of the technique we used. Many ciliates decreased especially in station 230, but in general ciliates were the only group whose total relative abundance increased (Fig. 6B), which was especially due to members of the classes Spirotrichea, Phyllopharyngea, Litostomatea and Colpodea, especially in station 130 (Fig. 7). For example a Colpodea OTU appeared to be a tolerant opportunistic ciliate (Fig. 7), which is in accordance with other reports for soil Colpoda strains showing high tolerance to Cu, Zn and Cd (Diaz, *et al.*, 2006). Total ciliate relative abundance increased from 53% to 68% at higher arsenic concentrations in station 130 (while diversity decreased with nearly 2%). Likewise, Fernandez-Leborans, et al. (2007) found that after 48h of treatment with Cd, ciliates became the dominant members in the protist community. Moreover, it is generally observed that ciliates can adapt to a wide range of metal contamination (Diaz, *et al.*, 2006, Rehman, *et al.*, 2008, 2010a), and other polluted (Lara, *et al.*, 2007a) or extreme environments (e.g. hypersaline deep-sea basin; Alexander, *et al.*, 2009). This could be related to the fact that they possess specific resistance/adaptation mechanisms; bioaccumulation (by arsenate reduction and methylation) is the most common trace metal resistance mechanism among ciliates (Yin, *et al.*, 2011), and generally among eukaryotic aquatic microorganisms (Zhou, *et al.*, 2008). A similar experiment, recently performed by Yin *et al.* (2011), studied the arsenic metabolism in the freshwater ciliate *Tetrahymena thermophyla* after the addition of different doses of arsenic. They concluded that As methylation and then efflux of the methylated species may be the key pathways for As detoxification in *T. thermophila*. This metal resistance and bioaccumulation might be related to the biosynthesis of ciliate metallothioneins (Diaz, *et al.*, 2006), which have unique features compared to metallothioneins from other organisms (Gutierrez, *et al.*, 2009). Ciliate metallothioneins (MTs) are unusually long proteins and have more cysteine residues with regard to standard MT; therefore each molecule might immobilize more metallic atoms than standard ones. The bioaccumulation is metal-species dependent however, and this process might not be the main mechanism involved in Cu resistance in ciliates (Diaz, *et al.*,

2006, Martin-Gonzalez, *et al.*, 2006), because the Cu-MTs are shorter (more similar to the standard MTs) (Gutierrez, *et al.*, 2009). Another metal-resistance mechanisms is by ATPase pumps (Nies, 2003, Diaz, *et al.*, 2006). Due to their high bioaccumulation capacity and metal tolerance, ciliates can also (cf. Fungi) be used for bioremediation events (Rehman, *et al.*, 2010b). The metal-tolerance however is not general for all ciliate taxa; e.g. Madoni & Romeo (2006) tested trace metal tolerance in four ciliates, and reported large differences between the different species, as we observed in our study. A single Amoeba species also appeared to be sensitive (mainly in station 130). Cercozoa, Bacillariophyta, Euglenozoa and Metazoa seemed less affected as a group (however only few representatives), though some species-specific responses were observed; e.g. for Metazoa and Bacillariophyta (*Astomonema* sp. 49 and the stramenopile 22 seemed sensitive; Fig. 7). Interestingly, many OTUs (e.g. 3 Phyllopharyngea, 2 Litostomatea and 1 Karyorelictea) which were absent from station 130, showed a sensitive response (decreased or disappeared in the profiles) in station 230 (Fig. 7). These taxa may be specific for sandy sediments, but it is also possible that they represent metal-sensitive taxa, which for this reason are not present and/or active in the contaminated silty sediment. Most OTUs generally showed no differential behaviour in both sediment, i.e. sensitive OTUs in silty sediment never showed a distinct increase in sandy sediments and vice versa. However, a few OTUs present in both sediment types showed contrasting responses to As depending on the sediment type [for example the relative abundance of *Acineta* sp. (82) decreased in station 230 while it is stable in the contaminated sediments of station 130]. Keeping in mind that we are dealing with relative abundance values (and therefore absolute changes in abundance could be different), it is also possible that we are dealing with two different but closely related taxa, as we only targeted approximately 200bp of the ribosomal RNA. Differential responses among strains or even individuals and clones within a species to pollutants have been reported before (Forbes, 1998).

It is not clear whether the decreases observed in specific taxa are direct consequences of the toxic effect of the trace metal, or whether they represent indirect responses e.g. caused by lower food availability to protozoan grazers due to toxic effects on their prey organisms. It has been shown (in soils) that bacteria for example can show sensitive responses to metals, including As (Wang, *et al.*, 2010), resulting in sharp decreases in bacterial numbers. By analogy, an increase in some OTUs may be the result of an increase in the availability of specific food items or a decrease in predation [e.g. by carnivores such as *Acineta* ssp. (102), *Trachelocerca* ssp. (44), *Litonotus* ssp. (3); Fig. 7], and/or competitors.

Finally, based on these results, we can conclude that high concentrations of As have a toxic effect on active microeukaryotic communities. They cause a reduction in species richness and changes in community composition, and especially Fungi and several ciliate groups are affected, either negatively or positively. The hypothesis that communities from sediments with an As contamination history (station 130) would be more resistant to the toxic effects of the As compared with communities from non-contaminated sediments (station 230), was only valid for the impact on species richness.

Acknowledgments

This research was supported by a Belgian Federal research program (Science for a Sustainable Development, SSD, contract MICROMET n° SD/NS/04A & 04B) and BOF-GOA projects 01GZ0705 and 01G01911 of Ghent University (Belgium). Many thanks to Andre Catrijsse and the crew on the R.V. Zeeleeuw.

7

General Discussion

The aim of this thesis was to gain a better insight in the relationships between microbial communities, mineralisation of algae-derived phytodetritus and trace metal contaminants in subtidal marine sediments. More specifically, we wanted to assess to what degree the composition and structure of microeukaryotic (protist) communities is related to trace metal contamination, how the deposition of phytoplankton influences the activity of benthic microbes (both bacteria and microeukaryotes) and trace metal mobility. To realize these aims, we performed two field campaigns to study the diversity and distribution of subtidal benthic protist communities in relation to physical, chemical (incl. trace metals) and microbiological parameters (chapters 2 and 3), and two microcosm experiments (chapters 4-6). The first one was aimed at studying the effect of phytodetritus deposition on protist community structure and trace metal mobilization, and their interaction (chapters 4-5), the second one at assessing the impact of different degrees of As contamination on protist community structure in these marine sediments (chapter 6).

We focused on subtidal sediments of the Belgian Coastal Zone (BCZ), situated in the Southern Bight of the North Sea because they are heavily contaminated by trace metals that pose a potential threat to the marine ecosystem in the area (OSPAR, 2000, Danis, *et al.*, 2004). Moreover, the BCZ is characterized by extensive, annual spring phytoplankton blooms, which are deposited on the sediments (Lancelot, *et al.*, 2005). Remineralisation of this phytodetritus has been shown to lead to effluxes of trace metals (Eggleton & Thomas, 2004, Gao, *et al.*, 2009), which can affect the composition, structure and activity of micro-, meio- and macrobenthic communities, and can bioaccumulate in higher trophic levels in both the sediment and water column (Fratini, *et al.*, 2008, Joksimovic, *et al.*, 2011).

In order to predict/understand the response of marine ecosystems to metal contamination and algal bloom deposition, a good baseline knowledge of the inhabitants of this environment is required. Benthic communities are composed of complex and highly diverse assemblages of prokaryotic and eukaryotic organisms, often in very high densities (Tian, *et al.*, 2009, Chariton, *et al.*, 2010, First & Hollibaugh, 2010). While studies on benthic marine environments have to date mainly focused on bacterial, meio- and macrobenthic communities (e.g. Steyaert, *et al.*, 1999, Vanaverbeke, *et al.*, 2000, Gillan & Pernet, 2007, Franco, *et al.*,

2008), very little is known about the diversity and ecology of protist communities, despite their important role in the benthic food web, the functioning of the microbial loop and benthic-planktonic coupling of cycles of matter and energy (Fenchel, 1969, Patterson, *et al.*, 1989). To date however, data on benthic microeukaryotic communities were completely lacking for the BCZ.

Below, the results of the field campaigns and the microcosm experiments are integrated and discussed. First, given the overall lack of data on subtidal benthic microeukaryotes, we discuss the general biodiversity and community composition of these organisms in BCZ subtidal sediments. Then, we discuss the importance of spatial and seasonal variation in various environmental factors for shaping microeukaryote community structure and diversity, with special emphasis on the effect of phytoplankton bloom deposition (and concomitant metal fluxes) on the activity and composition of the communities. Finally, we combine results from all chapters to assess to what degree and how subtidal benthic communities are affected by trace metal contamination.

Benthic microeukaryotic diversity and community composition in the BCZ

Benthic microeukaryotic community composition was studied using Denaturant Gradient Gel Electrophoresis (DGGE) and group-specific (ciliate and cercozoan) clone libraries. In total, 163 (DGGE) and 20 (clone library) unique (99% sequence similarity) sequences (OTUs) were observed when compiling all data from the field studies and microcosm experiments. These numbers agree with those reported in similar studies based on SSU rDNA/RNA-based fingerprinting and clone libraries of comparable sampling effort (e.g. Shimeta et al. 2007), but are much lower then what is found in recent massively parallel sequencing based studies of benthic microeukaryote communities from marine sediments based on the same gene. For example, Pawlowski *et al.* (2011b) found 942 to 1756 microeukaryote OTUs within single samples from deep sea sediments, while Chariton et al. (2010) reported about 2500 microeukaryote OTUs from intertidal sediments in an Australian estuary. While Pawlowski *et al.* (2011) argue that a significant fraction of their OTUs may belong to free or extracellular DNA, or resting stages or sedimented cells of planktonic organisms, the total number of OTUs found is still much higher than what we recover using DGGE and clone libraries. This corroborates the findings by Stoeck, *et al.* (2009) who, in a comparison of a clone library and

massively parallel tag sequencing study of the same marine pelagic sampling site, showed that clone library-based diversity estimates were not only severely underestimated diversity, but in particular missed the so-called 'rare biosphere', (Nolte, *et al.*, 2010, Scheckenbach, *et al.*, 2010).

In general, Stramenopila, Alveolata, Fungi, Rhizaria, and Amoebozoa were the dominant groups in our DGGE data (Fig. 1). We also found several metazoan sequences, but these were not the focus of our study and are therefore not further discussed. The main taxonomic groups present (DNA) in the sediments were also active (RNA), but their relative importance in the active community was often clearly different than in the total community (Fig. 1), especially for the Stramenopila and the ciliates.

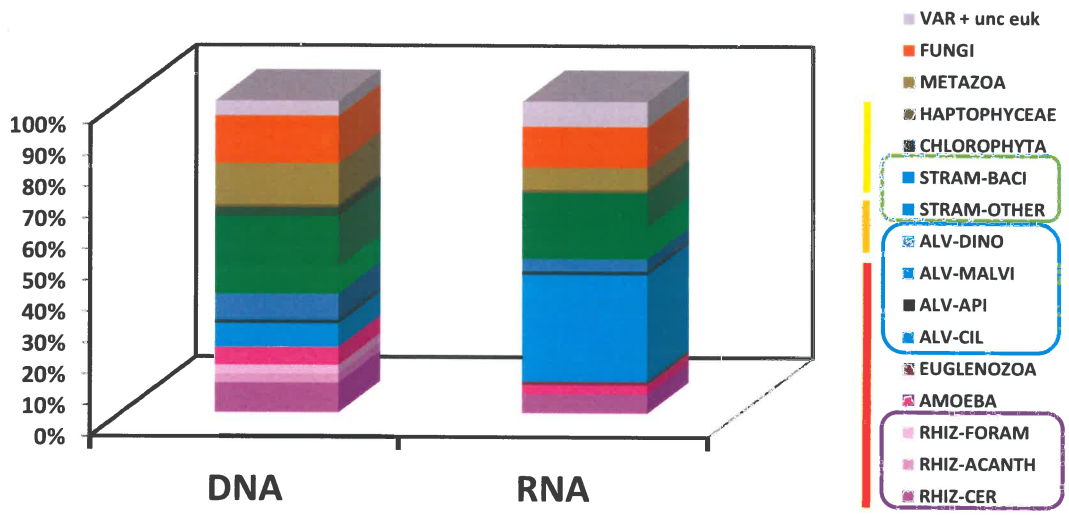

Figure 1: Microeukaryotic community composition in the subtidal sediments from the BCZ based on the number of OTUs per group for all sequences retrieved from all DGGE bands (ciliate- and cercozoan clone libraries are not included!) during the different studies in this thesis. A comparison between the total (DNA) and the active community (RNA) is given. RHIZ, Rhizaria (purple); CER, Cercozoa; ACANTH, Acantharea; FORAM, Forminifera; AMOEBA; ALV, Alveolata (blue); CIL, ciliates; API, Apicomplexa; MALVI, Marine Alveolates Group I; DINO, Dinophyceae; STRAM, Stramenopila (green); BACI, Bacillariophyceae; OTHER include *Pirsonia*, Oomycetes, Bicosoecida, Labyrinthulidae, Chrysophyceae and Pelagophyceae; VAR, various eukaryotes; unc euk, uncultured eukaryote. Red line, heterotrophs; orange; heterotrophs/phototrophs; yellow, phototrophs.

Interestingly, the number of *identical* DGGE-derived sequences shared between the total and active community was much more limited (26). This agrees with observations by Stoeck, *et al.* (2007b) for plankton samples from an anoxic Danish fjord, while Not, *et al.* (2009) and Takishita, *et al.* (2010) found an even lower similarity between DNA and RNA-based microeukaryotic clone libraries from the Mediterranean Sea and microbial mats of deep-sea cold-seep sediments respectively. These observations suggest that even within the taxonomic groups observed, the active species can be quite different from those that dominate the total (DNA) pool. Whether these non-active taxa mainly concern allochtoneous taxa (e.g. from the plankton) or passive stages of benthic organisms is hard to assess as very little information is available on the specific ecological preferences of many planktonic and benthic protists. In addition, we have to keep in mind that this observation only concerns *sequenced* bands and the information from which community the sequence was obtained. Indeed, in chapter 5 we showed that the total number of OTUs (band classes) shared between the DNA- and RNA-based DGGE profiles (so both excised/sequenced and non-excised bands) amounted to 61% of all OTUs present in both communities. This shows that comparisons based on bulk sequence data alone are probably strongly biased towards the most dominant components in a particular community.

The relative contribution of **phototrophic organisms** (e.g. Stramenopila-Bacillariophyta and several Dinophyta) in these (dark) sediments was relatively high, as was previously observed in other coastal marine sediments (Shimeta, *et al.*, 2007, Park, *et al.*, 2008) and even deep sea sediments (Pawlowski *et al.* 2011b). Most sequences however belonged to phytoplankton taxa (e.g. *Thalassiossira* and *Skeletonema*) which, together with the fact that they were more numerous in the total than the active communities, indicates that they most probably represent dead and/or decaying cells, or resting spores or cells (Boon & Duineveld, 1998, M'Harzi, *et al.*, 1998, McQuoid & Nordberg, 2006).

Ciliates were relatively rare in the total but dominant in the active microeukaryote community (Fig. 1). This finding appears to be in contrast with the more equal contribution of ciliates in the DNA and RNA fractions in chapter 5 (Fig. 2), and therefore is probably mainly caused by the high numbers of unique ciliate OTUs in the microcosm communities in chapter 6. Ciliates are a typical and often dominant component of many marine benthic microeukaryote communities, both in shallow (Garstecki, *et al.*, 2000) and deep-sea (Takishita, *et al.*, 2010) sediments. Surprisingly, in the field studies from chapters 2 and 3,

only three ciliates were detected using DGGE. The fact however that ciliate-specific clone libraries revealed fifteen different ciliate OTUs in the 2007 field study (for which DGGE recovered none) confirms an earlier report that DNA-based DGGE analysis often fails to recover a large fraction of protozoan diversity, possibly due to their lower abundance (Shimeta, *et al.*, 2007). It is unclear why ciliates are more easily detected in the RNA fraction. Shimeta et al. (2007) found no ciliates in a rDNA-based DGGE study of a subtidal coastal sediment, but did observe ciliates in microscopic counts, and attributed the discrepancy to the low number of ciliate species in relation to other protists (mainly diatoms). Possibly, the rRNA content per cell is much higher for ciliates than for other protists, or alternatively, the presence of inactive diatoms hid the DNA signal from the ciliates. Representatives of eight classes (Litostomatea, Oligohymenophorea, Phyllopharyngea, Spirotrichea, Nassophorea, Colpodea, Prostomatea and Karyorelictea) were found (clone library, RNA- and DNA DGGE bands), most of which have been reported from coastal subtidal and deep-sea sediments (Shimeta, *et al.*, 2007, Takishita, *et al.*, 2010 respectively). Difference in dominance of the groups exists depending on the sediment type (chapter 6).

For **Cercozoa**, the number of OTUs in the DGGE and clone library was comparably low. Three (chapter 2) respectively six (chapter 3) OTUs were observed using DGGE, and these belonged to three different orders (Cryomonadida, Thaumatomonadida, and Aconchulinida). The five cercozoan OTUs found in the clone library however were all members of the Cryomonadida (Cavalier-Smith & Chao, 2003, but see Hoppenrath & Leander (2006) for uncertainties about Protaspis ssp.), a group commonly found in marine environments (cf. chapter 2), suggesting that different primer sets in this case were biased against certain classes within higher-order taxonomic groups. In a similar habitat (shallow subtidal coastal sediments, Buzzards Bay, USA), general eukaryotic primer sets failed to recover Cercozoa (Shimeta, *et al.*, 2007). Moreover, the low contribution of Cercozoa was also evident from the RNA analyses, suggesting that cercozoans were actually not a major component of the active communities (Fig. 1). These observations are surprising, as generally a high global cercozoan biodiversity is suggested, and cercozoans have been reported to constitute a significant portion of protist communities in other marine sediments (Bass & Cavalier-Smith, 2004) including anoxic sediments around fumaroles (Takishita, *et al.*, 2005), and deep sea sediments (Pawlowski, *et al.*, 2011b), where they were even more dominant than ciliates. Cryomonadida and Thaumatomonadida are important groups of bacterivore flagellates (Bass & Cavalier-Smith, 2004), while Aconchulinida are a group of amoeboid bacterivores but also

parasites (Bass, *et al.*, 2009b). More data from various subtidal sediment types are needed to assess whether and how the importance of Cercozoa differs between different sediment habitats.

Fungi are an important component in both the total and active communities, confirming the results of other studies (cf. Stoeck & Epstein, 2003, Edgcomb, *et al.*, 2011). We observed representatives of the Blastocladiomycota, Ascomycota, Chytridiomycota and Basidiomycota. Fungi play an important role in the utilization and recycling of nutrients, and especially Basidiomycota can be very abundant in anoxic sulphide-rich environments (Luo, *et al.*, 2005, Edgcomb, *et al.*, 2011). Chytridiomycota on the other hand are known as parasites (Rasconi, *et al.*, 2011) (see below).

Several **pathogens-parasites** were observed during this study with representatives from different groups. These include a.o. the Marine Alveolates Group I *Duboscquella* ssp. (a parasite of other protists, mainly ciliates - Harada, *et al.*, 2007), the rhizarian *Cryothecomonas* ssp., the heterotrophic stramenopile *Pirsonia* spp. and Chytridyomycota (phytoplankton parasites - Tillmann, *et al.*, 1999, Kuhn, *et al.*, 2000, Rasconi, *et al.*, 2011), the cercozoan Vampyrellidae ssp. (parasite of algae and Fungi - Bass, *et al.*, 2009b), the ciliate *Cryptocaryon irritans* and the dinoflagellate *Pfiesteria shumwayae* (fish parasites - Colorni & Diamant, 1993, Vogelbein, *et al.*, 2002, Shimizu, 2003). Our study thus underscores the importance of eukaryotic parasites in marine benthic ecosystems, confirming previous observations (Kagami, *et al.*, 2007, Gachon, *et al.*, 2009, Scheckenbach, *et al.*, 2010, Mangot, *et al.*, 2011, Rasconi, *et al.*, 2011).

Very little data are available on the general composition of subtidal benthic microeukaryote communities, so comparison with other subtidal sediments is not straightforward. However, differences between sediment habitats are probably pronounced, witness the large differences in overall composition between our communities and those from various deep sea sediments (Pawlowski *et al.* 2011b). Dominant groups in their study included dinoflagellates, Cercozoa, ciliates and Euglenozoa, followed by Metazoa, Bacillariophyta, other Stramenopiles and other Rhizaria; Fungi and Amoebozoa were very rare. In contrast, we found only one euglenozoan and no Radiolaria (Rhiziaria), and dinoflagellates were rare. Euglenozoa and Radiolaria were also found in deep-sea pelagic samples (Sauvadet, *et al.*, 2010), showing that they may be important components of deep-sea environments in general (Pawlowski *et al.* 2011b). The observed differences may be related to the different habitat characteristics; deep-sea

sediments for example have a lower input of fresh algae-derived detritus compared to the more productive coastal area (like the BCZ).

Microeukaryotic distribution patterns in relation to physical and chemical variables, with special attention for the impact of phytoplankton bloom deposition

Microeukaryotic communities were strongly different between different sediment types (sandy vs. silty), both in their total community (chapter 2) and active community (chapter 6) structure. This is most probably related to pronounced differences in physical and chemical characteristics of these different sediments. Both grain size and flow regime (hydrodynamics) were related to microeukaryote community structure in a subtidal marine sediment studied by Shimeta *et al.* (2007). It is known that silty sediments have smaller interstitial spaces, and therefore probably select for smaller organisms (Patterson, *et al.*, 1989). This may explain why we found a higher diversity of ciliates (Litostomatea, Spirotrichea and Phyllopharyngea) in the sandy sediments, despite the fact that total numbers of active ciliates were relatively similar in both sediments (chapter 6, Fig. 6, 7). Differences in grain size are also coupled with different sediment permeability, oxygen levels, organic matter content, redox potential, sulphide content and pH, which have all been invoked to explain differences in protist community structure in marine sediments (see below, and also Patterson, *et al.*, 1989, Fenchel & Bernard, 1996, Fenchel & Finlay, 2008) but also higher nematode diversity in sandy than in silty sediments (Vanaverbeke, *et al.*, 2011).

Surprisingly, season and depth were not significantly related to variation in protist community structure in the 2007 field data. However, when focusing on a single, silty metal-contaminated sediment (chapter 3), microeukaryotic (and protozoan) community structure did significantly change with depth-related and seasonal variation in redox potential, pH and sulphides. The latter was probably mainly related to the deposition of phytoplankton-derived detritus, especially in late spring (see below). Interestingly, also an independent effect of metals was observed (see below). Fenchel *et al.* (1969) argued that the response to prevailing redox potentials may account for the vertical zonation that characterizes much of the distribution of marine benthic ciliates, with many species of ciliates only being found within a limited range of redox potentials. Some OTUs in our study were clearly restricted to the deeper anoxic reduced sediments, while others occurred across the whole depth gradient. For example, the

vertical and seasonal distribution pattern of an *Acineta* sp. (chapter 3) clearly shows that this species is restricted to reduced, low pH sediments (Fig. 2). Besides grain size, pH and Eh, the biomass and diversity of bacterial communities (available food), oxygen and the concentrations of dissolved sulphides also significantly affected microeukaryotic community structure , both in the field (chapter 3) and microcosm (chapter 5) data (Patterson, *et al.*, 1989, Epstein, 1997, Fenchel & Finlay, 2008).

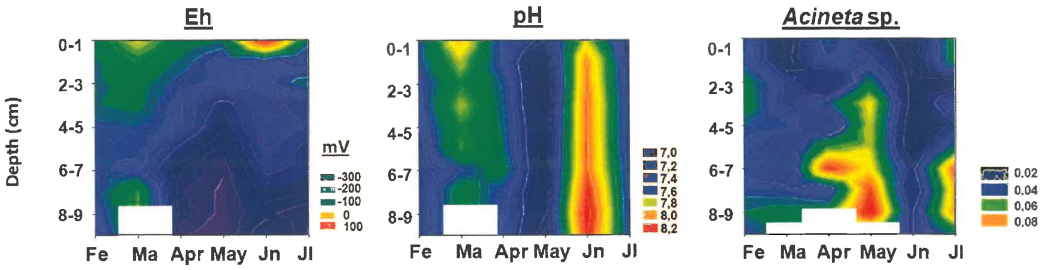

Fig 2. Vertical variation (0-10 cm) in redox potential (Eh) and pH, and vertical distribution of the ciliate *Acineta* sp. (CIL85), based on relative abundances DGGE profiles of DNA in the period February-July 2008 in station 130 (based on data from chapter 3). White = missing values.

The deposition of the spring phytoplankton bloom was clearly visible as high concentrations of chlorophyll *a* in the upper sediment layer (chapter 3). This event stimulated bacterial activity and mineralization and initiated a cascade of redox reactions, with concomitant changes in pH (Fig. 2), dissolved sulphides and metal speciation (chapter 3) (Middelburg & Levin, 2009), and initiated and activated the development of the microbial loop (chapter 5; see also van Hannen, *et al.*, 1999a). Composition of both the total and active bacteria and protozoan communities changed significantly. Bacterial production increased first (2h-d2), followed by heterotrophic nanoflagellate (HNF) biomass and the relative importance of several HNF (d2-d7) and ciliates (d7). The fact that bacterial biomass did not significantly increase suggests that biomass development in this group was controlled by grazing, most probably by HNF (d2) and ciliates (d7). HNF as well did not show a biomass increase, which may be related to enhanced ciliate grazing and/or competition on day 7 (cf. Wey, *et al.*, 2008). Other studies have shown that increased microbial activity and biomass also results in higher densities and diversity of nematodes (Vanaverbeke, *et al.*, 2004). Bak & Nieuwland (1989) studied seasonal fluctuations in benthic protozoan communities in marine sediments, and also

measured a positive relation between protist numbers and bacterial productivity (see also Hondeveld, *et al.*, 1994). In contrast with our findings however, (Bak & Nieuwland, 1989) found that under conditions of high organic input only an insignificant fraction of the bacterial flora was consumed.

Phytoplankton deposition resulted in increased mobilisation and upward fluxes of metals (chapter 4, Gao, *et al.*, in press), probably as a consequence of changes in the redox environment or degradation of organic matter caused by microbial activity (Eggleton & Thomas, 2004). A positive link between the activity of microbial (bacterial and protist) communities and metal remobilization events was suggested (chapter 4), confirming previous findings (Eggleton & Thomas, 2004)

Microeukaryotic community diversity and structure are affected by trace metals – evidence from a field and experimental data.

In the 2007 field data set (chapter 2), we found that communities were significantly different between sandy and silty sediments, which strongly differed in their degree of metal contamination. However, no significant independent effect of the trace metals on protist community structure was observed, which was most probably due to the strong intercorrelation between metals and other variables (such as grain size and chlorophyll *a* content). Likewise, in the microcosm experiment with phytodetritus deposition (chapter 5), we observed strong correlations between metals and community composition in the upper sediment layers of the sediment. However, here as well, metals strongly covaried with other variables such as chlorophyll *a*, pH and salinity. We did not check for a possible independent effect of the metals in this experiment. Microeukaryotic diversity, like bacterial diversity (cf. also Gillan, *et al.*, 2005), was never affected by high metal concentrations (chapters 2, 3 & 5, cf. also Chariton, *et al.*, 2010). In contrast, significant, independent effects of various bioavailable trace metals on protist community structure were observed in the 2008 field data set (chapter 3). After partialling the effect of other significant environmental factors, including some which are known to strongly affect metal bioavailability (redox potential, chlorophyll *a*, pH, dissolved sulphides and bacterial biomass, (Calmano, *et al.*, 1993, Scoullos & Pavlidou, 2000, Eggleton & Thomas, 2004), we still found that an additional 14-19% of the variation in microeukaryotic community structure could be significantly related to metal

concentrations. Of course, we cannot completely rule out that other, unmeasured factors, which correlate with the metals, actually caused the structural changes observed. For example, metal concentrations could have affected the distribution of prey items, competitors or predators of the protist, thus indirectly affecting protist community structure. Our results from the As contamination experiment (chapter 6), however, do show that high concentrations of trace metals can indeed directly affect protist communities and their activity.

Acute intoxication by high As concentrations (added as arsenate (AsO_4^{3-}), a highly toxic inorganic form of As had a significant impact on the structure and diversity of the active microeukaryotic community in both a silty and sandy sediment (chapter 6). Acute intoxication with high metal concentrations can also result in a decrease in protist densities (Leborans, *et al.*, 1998, Fernandez-Leborans & Herrero, 2000, tested for Pb and Zn), but this was not measured in our study. Arsenic is a notoriously toxic metal and As contamination in the BCZ is high (chapter 2).

High As (> 480 µg L^{-1}) concentrations significantly decreased the diversity of the active microeukaryotic communities. This decrease was more pronounced in sandy than in silty sediments, suggesting that the communities from the silty sediments were comprised less metal-intolerant species at the onset of the experiment (as these were already contaminated by As). While in both sediment types a change in community structure was observed, the observed shift was not significant in the sandy sediment, and also occurred at lower As concentrations in the silty sediment. We have no explanation for this phenomenon. Indeed, we would have expected the silt-inhabiting community to be more tolerant to As contamination. A possible explanation could be found in the different behaviour of the As compound in the silty vs the sandy sediment (different speciation and hence different toxicity). However, little is known about As speciation in sediments.

We observed distinct species-specific differences in the responses of protists to As contamination. While some ciliate OTUs disappeared at higher As concentrations, others actually increased in relative abundance, even at the highest (480-960 µg As L^{-1}) concentrations. Ciliates were the only protists that increased in relative importance, resulting in an overall increase in total relative contribution of ciliates to the active community. Ciliates are known to be able to accumulate high amount of metals. Bioaccumulation (by arsenate reduction and methylation) is the most common trace metal resistance mechanism among ciliates (Yin, *et al.*, 2011), and in general among eukaryotic aquatic microorganisms (Zhou, *et*

al., 2008). This ciliate metal resistance and bioaccumulation process might be related to the biosynthesis of ciliate metallothioneins (Diaz, *et al.,* 2006), which have unique features compared to metallothioneins from other organisms (Gutierrez, *et al.*, 2009). Ciliates are an important food source for higher trophic levels, and thus form a potential source of metal pollution to higher trophic levels due to their capacity for metal accumulation (Langston, *et al.*, 1999, Twining & Fisher, 2004).

Cercozoa seemed relative unaffected by high As concentrations (chapter 6), which corroborates our observations in chapter 5, where we observed higher abundances of *Protaspis* spp. (see Fig. 4; CerPro44) during periods of high As concentrations, and our observations in chapter 3, where significant positive correlations were found between the cercozoan OTUs and As. On the other hand, negative correlations were found with Pb, Cr, Fe, Mn, and Ni, suggesting that the observed relationship with As cannot be extrapolated to other metals.

Fungi appeared to be rather sensitive to the As contamination, and all (except 1one) members of the fungal community disappeared (or became inactive) as a consequence of acute As contamination. In chapter 3, a decrease of Fungi was also observed in the upper sediment layer during periods of increased metal effluxes, including As (compare Figs. 3 and 5 – chapter 3). This is surprising, since previous studies indicated that Fungi are quite resistant to metal contamination (e.g. Cernansky, *et al.*, 2009, Vala, 2010). Moreover, Fungi are used as biosorbents for the removal of metal-contaminated industrial effluents (Das, *et al.*, 2008), and also appear a promising candidate for As remediation (Vala, 2010, Srivastava, *et al.*, 2011) due to their high cell wall binding capacity and high intracellular metal uptake capacity (Kapoor & Viraraghavan, 1997, Gadd, 2000).

Future perspectives

Our knowledge on the role of microbial eukaryotes in highly complex marine benthic ecosystems is still seriously hampered by a general lack of data on their biodiversity and their ecology. In recent years, significant progress has been made with respect to the inventarization of protist diversity in marine ecosystems, through the use of high-throughput molecular techniques (such as massively parallel tag sequencing and other metagenomic and metatranscriptomic approaches, cf. Amaral-Zettler, *et al.*, 2009, Stoeck, *et al.*, 2009) and

ongoing projects will result in a more complete and detailed picture of protist diversity in these ecosystems (e.g. the TARA Oceans project, cf. http://oceans.taraexpeditions.org/and the Earth Microbiome project, http://www.earthmicrobiome.org/). However, many marine sediment habitat types remain undersampled and understudied (witness the general lack of data on shallow subtidal coastal sediments), and extreme benthic environments are at the moment probably better characterized than globally common ones. In addition, extremely little is as yet known about the precise functional role of most benthic protists in their habitats. Combined experimental and molecular approaches (e.g. RT-qPCR on functional genes`, metagenome/transcriptome-based molecular trait-based ecology`, cf. Raes, *et al.* 2011) will undoubtedly further advance of understanding of these ecosystems in the near future.

Summary

The overall objective of this thesis was to obtain a better insight in the interactions between microbial communities, metal contaminants and algae-derived organic matter in subtidal, metal-contaminated sediments in the Belgian Coastal Zone (BCZ). The BCZ is characterized by extensive, annual spring phytoplankton blooms, and it has been estimated that 24% of the phytoplankton production is deposited onto the sediments. Remineralisation of this phytodetritus has been shown to lead to effluxes and hence bioavailability of trace metals (TM). The activity of benthic microbial organisms (pro- and eukaryotes) has been pointed out as one potential factor acting upon the release of TM into the water column. It remains unclear however, how microbial communities, phytodetritus deposition and TM behaviour interact. In order to predict/understand the response of marine ecosystems to metal contamination and algal bloom deposition, good baseline knowledge of the inhabitants of this environment is required. During this study, we focussed on the protist (~unicellular eukaryotes) communities, as these are largely understudied compared to bacterial, meio- and macrobenthic communities, despite their important role in the benthic food web, the functioning of the microbial loop and benthic-planktonic coupling of cycles of matter and energy.

During two field campaigns (2007-2008), we studied the diversity and spatio-temporal variation in diversity and community structure in the subtidal sediments of the BCZ in relation to a suite of physical, chemical (incl. TM) and microbiological parameters. The *in situ* studies were complemented with laboratory experiments in which sediment cores were incubated under various environmental conditions, viz. with and without phytodetritus deposition, and with different arsenic (As) concentrations. This not only allowed giving a more detailed picture about the effect of phytodetritus deposition on protist community structure and trace metal mobilization, and their interaction, but also to assess the impact of different degrees of As contamination on protist community structure in these marine sediments (chapter 6).

In **Chapter 2,** we described microeukaryotic community composition in 9 BCZ stations with different granulometries and TM loads, before and after the spring phytoplankton bloom and compared the upper sediment layer (0-1) and deeper (9-10cm) layers. Variation in community structure was studied using 18S rDNA-based DGGE fingerprint analyses of microeukaryotic

communities, complemented with the construction of group-specific (ciliates and cercozoans) clone libraries. Our results showed that microeukaryotic diversity was dominated by Stramenopila (mainly diatoms), Metazoa and Fungi. Protozoan diversity was underestimated based on DGGE analyses with general eukaryotic primers, but the clone libraries using group-specific primers showed that especially ciliates were much more diverse. Our data revealed that sediment type was the prime variable determining microeukaryotic community structure, and its overriding influence probably masked temporal and depth-related variability. Metals were strongly correlated to the sediment characteristics (grain size, CHL *a*, silt content); the effect of the trace metals on community composition could not be distinguished from the differences in sediment type.

In **Chapter 3,** we performed a more detailed, monthly analysis of protist community variation with depth (0-10 cm) in one silty, metal-contaminated station, for the period February to July 2008 (including periods of intense algae blooms). Microeukaryote and protozoan community composition changed with depth (~ redox, sulphides and pH) and with time, from February to July (~phytoplankton bloom deposition), with especially May and July being distinct. Increased microbial mineralization caused pronounced changes in the redox environment and the bioavailable metal concentrations in the sediment, which correlated with the observed seasonal and vertical variation patterns in community structure. Eh and pH were the dominant factors structuring the communities, but trace metals as well had a significant, independent impact (14-19 %) on the variation in microbial community structure.

The effects of phytoplankton bloom deposition and TMs on the protist communities were analyzed in more detail in two microcosm experiment.

In the first experiment (Chapters 4 and 5), the deposition of a phytoplankton bloom was simulated in metal-contaminated sediment cores, and sampling was performed immediately (2h), 2 days and 7 days after the start of the experiment. Chapter 4 focussed on the effect of bacterial mineralization of the phytoplankton-derived detritus on the release of metals while in Chapter 5 we studied the effect of the phytodetritus deposition on the structure of the total and active bacterial and microeukaryotic communities (with focus on Protozoa), and assessed how this related to metal mobilization. This allowed giving a more detailed picture about the short-time response of benthic microbial communities to organic matter enrichment and metal contamination, as well as the potential role of microbial communities in metal mobilization.

In **Chapter 4**, we observed that the onset of mineralization (as revealed by CLPP analysis) was very fast and started within 2h after phytodetritus deposition. Increased bacterial production was observed after two days, while bacterial biomass was stable and probably controlled by heterotrophic nanoflagellates (HNF). A clear link was established between heterotrophic microbial activity and effluxes of the TMs As, Co and Mn. In **Chapter 5,** DNA- and RNA-based fingerprints of bacteria and Protozoa showed distinct changes in the total and active community structure as a consequence of the algal enrichment, and with time. The enrichment effect was most pronounced after 2 and 7 days for bacteria and Protozoa respectively. Our results suggest that phytodetritus deposition activates and stimulates the microbial loop, via changes in bacterial activity, biomass and community composition, together with subsequent changes in numbers and relative abundance of heterotrophic nanoflagellates and ciliates, and composition and activity of protozoan communities. No effect of the metal fluxes was observed for bacterial and microeukaryotic diversity (~ species richness). Calculations based on our results suggest that during phytoplankton blooms the microbial activity alone may induce the release of substantial amounts of dissolved As in areas of the BCZ covered by muddy sediments.

In the second microcosm experiment (**Chapter** 6) we studied the effect of As, a notoriously toxic TM, on active protist communities (based on 18S rRNA-DGGE analyses). Sediments from a metal-contaminated silty station and an unpolluted sandy sediment were spiked with a range of As concentrations (0-960 $\mu g\ L^{-1}$) and incubated in the dark for 2 days. Diversity (~number of DGGE bands) significantly decreased at contamination levels $\geq 480\ \mu g\ As\ L^{-1}$ in both sediment types, but the decrease was more pronounced in the sandy (43%) than in the silty sediment (32%), suggesting higher tolerance to As contamination in the silty sediment. In addition, a significant shift in community composition occurred at contamination levels $\geq 120\ \mu g\ As\ L^{-1}$ and again at $\geq 480\ \mu g\ As\ L^{-1}$ in silty sediment. Surprisingly, the effect of As on protist community composition was not significant in the sandy sediment. Fungi responded most sensitively to high As concentrations, while only some ciliates increased in relative abundance with higher As levels. These included representatives from various classes such as the *Phyllopharyngea, Spirotrichea, Litostomatea* and *Colpodea.* The observed responses contributed to the interpretation of OTU-specific positive and negative correlations with several metals that had been found in chapter 3 and 5, as in natural environments, it was not possible to isolate the effect of the metals from that of the environmental variability. Indeed, trace metals often strongly co-vary with many physico and- biogeochemical parameters.

In **Chapter 7**, the results of the field campaigns and the microcosm experiments were integrated and discussed. An overview was given of the overall composition of the microeukaryotic communities in the subtidal sediments of the BCZ. Generally, Stramenopila, Alveolata, Fungi, Rhizaria, and Amoebozoa were the dominant groups, ecologically important as primary producers (mainly diatoms), grazers (Rhizaria, Alveolata, Amoebozoa, heterotrophic stramenopiles), saprobes (Fungi) or pathogen-parasites (e.g. Marine Alveolates Group I, several heterotrophic Stramenopila, e.g. *Pirsonia* sp.) in these sediments. The importance of spatial and seasonal variation in various environmental factors was demonstrated for shaping microeukaryote community structure and diversity, with a pronounced impact of sediment parameters and phytoplankton bloom deposition on the activity and composition of the communities. Finally, we can conclude that microeukaryotic communities in the sediments are affected by trace metals, as evidenced by both the field and experimental data.

Samenvatting

De algemene doelstelling van dit proefschrift was om een beter inzicht te krijgen in de interacties tussen microbiële gemeenschappen, metaalverontreinigingen en organisch materiaal afkomstig van algen in sublitorale, met metalen verontreinigde sedimenten in het Belgische kustgebied (BCZ). De BCZ wordt gekenmerkt door uitgebreide, jaarlijkse lente fytoplanktonbloeien, en er wordt geschat dat 24% van de fytoplanktonproductie wordt afgezet op de sedimenten. Het is aangetoond dat remineralisatie van dit phytodetritus kan leiden tot effluxes van metalen en daarmee de biobeschikbaarheid van deze elementen verandert. De activiteit van benthische micro-organismen (pro- en eukaryoten) wordt beschouwd als een potentieel belangrijke invloed op de efflux van metalen naar de waterkolom. Het is echter onduidelijk hoe microbiële gemeenschappen, phytodetritus afzetting en metalen op elkaar inwerken. Om beter de reactie te begrijpen van mariene ecosystemen op de metaalvervuiling en de depositie van algenbloeien, is een goede basiskennis van de bewoners van deze omgeving vereist. Tijdens deze studie hebben we ons gericht op protistengemeenschappen (~ eencellige eukaryoten), omdat deze groep van micro-organismen weinig bestudeerd is ten opzichte van bacteriële, meio- en macrobenthische gemeenschappen, ondanks hun belangrijke rol in het benthische voedselweb, het functioneren van de 'microbiële lus' en de benthische-planktonische koppeling van cycli van materie en energie.

Gedurende twee veldcampagnes (2007-2008) bestudeerden we de diversiteit en de ruimtelijke en temporele variatie in diversiteit en gemeenschapsstructuur in sublitorale sedimenten van de BCZ met betrekking tot een reeks van fysische, chemische (incl. metalen) en microbiële parameters. De veldstudies werden aangevuld met laboratorium-experimenten waarin sedimentstalen werden geïncubeerd onder verschillende milieuomstandigheden, namelijk met en zonder phytodetritus depositie, en met verschillende arseenconcentraties (As). Dit liet niet alleen toe een meer gedetailleerd beeld te geven van de directe reactie van benthische microbiële gemeenschappen op de verrijking met organisch materiaal en metaalvervuiling, en hoe deze factoren op elkaar inwerken, maar ook om het effect van As contaminatie op de eukaryote microbiële gemeenschappen te beoordelen.

In **hoofdstuk 2** beschreven we de samenstelling van de microeukaryotische gemeenschap in 9 BCZ stations met verschillende korrelgroottes en TM ladingen, voor en na de lente algenbloei en vergeleken we de bovenste sedimentlaag (0-1) met diepergelegen (9-10cm) lagen. Variatie

in de gemeenschapsstructuur werd bestudeerd met behulp van 18S rDNA-gebaseerde DGGE fingerprint analyses van microeukaryotische gemeenschappen, aangevuld met de aanmaak van groep-specifieke (ciliaten en cercozoa) clone libraries. Onze resultaten toonden aan dat de microeukaryotische diversiteit werd gedomineerd door Stramenopila (voornamelijk diatomeeën), Metazoa en Fungi. Protozoa diversiteit is onderschat op basis van DGGE analyses met algemene eukaryote primers, maar uit de clone libraries met behulp van de groep-specifieke primers bleek dat vooral ciliaten veel soortenrijker waren. Sediment type bleek de belangrijkste variabele te zijn in het bepalen van de microeukaryotische gemeenschapsstructuur, en dat net door deze grote variatie tussen de verschillende sedimenttypes de temporele en diepte-gerelateerde variabiliteit gemaskeerd werd. Metalen waren sterk gecorreleerd met de sediment eigenschappen (korrelgrootte, CHL *a*, slibgehalte) en het effect van de metalen op de gemeenschapssamenstelling kon niet worden onderscheiden van de verschillen in sediment type.

In **hoofdstuk 3** hebben we een meer gedetailleerde, maandelijkse analyse van protistengemeenschap variatie met diepte (0-10 cm) in één slibrijk, metaal-gecontamineerd station, voor de periode februari tot juli 2008 (inclusief perioden van intense algenbloei). De microeukaryotische (en protozoa in het bijzonder) gemeenschapsstructuur varieerde significant met de diepte (~ redoxpotentiaal en pH) en het seizoen, gerelateerd aan de inbreng van fytoplankton. Seizoensgebonden opwaartse metaalfluxen werden gemeten tijdens periodes van verhoogde phytodetritus sedimentatie, waarschijnlijk als gevolg van de verhoogde microbiële activiteit, gestimuleerd door de verhoogde voedselbeschikbaarheid. We vonden aanwijzingen dat de mobilisatie van deze metalen (~ verhoogde biologische beschikbaarheid) in de sedimenten een invloed konden hebben op de gemeenschappen. Meer specifiek vonden we dat na het uitsluiten van omgevingsfactoren, met inbegrip van enkele belangrijke factoren die de biobeschikbaarheid van metalen bepalen, zoals redoxpotentiaal, chlorofyl *a*, pH, opgeloste sulfiden en bacteriële biomassa (Calmano, et al., 1993, Eggleton & Thomas, 2004), een bijkomende belangrijke fractie van 14-19% van de variatie in de microeukaryotische / protisten gemeenschapsstructuur was gerelateerd aan de biobeschikbare metalen.

De effecten van fytoplankton bloei depositie en metalen werden in meer detail onderzocht in twee microcosmos experimenten.

In een eerste experiment (hoofdstukken 4 en 5) werd de afzetting van een algenbloei gesimuleerd in metaal-verontreinigde sediment cores; bemonstering werd onmiddellijk uitgevoerd (2u), 2 en 7 dagen na de start van het experiment. Hoofdstuk 4 richt zich op het effect van bacteriële mineralisatie van het fytoplankton detritus op het vrijkomen van metalen, terwijl we in hoofdstuk 5 het effect van de phytodetritus depositie bestudeerden op de structuur van de totale en actieve bacteriële en microeukaryotische gemeenschappen (met focus op Protozoa) in dit experiment, en beoordelen we hoe dit zich verhoudt tot metaal mobilisatie. Hierdoor kon een meer gedetailleerd beeld gegeven worden over de korte-tijd respons van benthische microbiële gemeenschappen op aanrijking met organisch materiaal en metaalvervuiling, evenals de potentiële rol van microbiële gemeenschappen op metaalmobilisatie.

In **hoofdstuk 4** hebben we geconstateerd dat mineralisatie erg snel van start ging (zoals blijkt uit CLPP analyse) en begon binnen 2 uur na phytodetritus depositie. Een verhoogde bacteriële productie werd waargenomen na twee dagen, terwijl de bacteriële biomassa stabiel was en waarschijnlijk gecontroleerd werd door heterotrofe nanoflagellaten (HNF). Een duidelijk verband werd gelegd tussen heterotrofe microbiële activiteit en effluxen van de metalen As, Co en Mn. In **hoofdstuk 5** werd gezien dat ook totale (gebaseerd op de SSU rDNA) en actieve (op basis van SSU rRNA) microbiële gemeenschappen snel reageerden (binnen 2 uur na de afzetting) op de toename van voedselbeschikbaarheid. Het verrijkingseffect was het meest uitgesproken na 2 en 7 dagen voor respectievelijk bacteriën en Protozoa. Onze resultaten suggereren een detritus-afhankelijke ontwikkeling van de microbiële lus, via veranderingen in de bacteriële biomassa, samen met de nakomende wijzigingen in de aantallen en de abundantie van heterotrofe nanoflagellates en ciliaten. Geen effect van de metaalfluxen werd waargenomen voor bacteriële en microeukaryotische diversiteit (~ soortenrijkdom). Berekeningen op basis van onze resultaten suggereren dat tijdens fytoplanktonbloei alleen de microbiële activiteit aanzienlijke hoeveelheden opgeloste As kan vrijmaken in gebieden van de BCZ bedekt door slibrijke sedimenten.

In een tweede microcosmos experiment (**hoofdstuk 6**) bestudeerde we het effect van arseen (As), een zeer giftig metaal, op de actieve microeukaryotische gemeenschappen (gebaseerd op de SSU rRNA-DGGE analyses). Sedimenten uit een metaalverontreinigd slibrijk station en een niet verontreinigd zandig station werden verrijkt met een reeks van As-concentraties (0-960 microgram L^{-1}) en geïncubeerd in het donker voor **2** dagen. We hebben duidelijke negatieve effecten geconstateerd van As-contaminatie op de diversiteit en de samenstelling

Chantangsi C & Leander BS (2010) An SSU rDNA barcoding approach to the diversity of marine interstitial cercozoans, including descriptions of four novel genera and nine novel species. International Journal of Systematic and Evolutionary Microbiology 60: 1962-1977.

Chapman PM, Wang FY, Janssen C, Persoone G & Allen HE (1998) Ecotoxicology of metals in aquatic sediments: binding and release, bioavailability, risk assessment, and remediation. Canadian Journal of Fisheries and Aquatic Sciences 55: 2221-2243.

Chariton AA, Court LN, Hartley DM, Colloff MJ & Hardy CM (2010) Ecological assessment of estuarine sediments by pyrosequencing eukaryotic ribosomal DNA. Frontiers in Ecology and the Environment 8: 233-238.

Chen CP, Sun L, Gao YH, *et al.* (2009) Seasonal changes of viable diatom resting stages in bottom sediments of Xiamen Bay, China. Journal of Sea Research 61: 125-132.

Cheung YH, Neller A, Chu KH, Tam NFY, Wong CK, Wong YS & Wong MH (1997) Assessment of sediment toxicity using different trophic organisms. Archives of Environmental Contamination and Toxicology 32: 260-267.

Ciceri G, Maran S, Martinotti W, Queirazza G (1992) Geochemical cycling of heavy metals in a marine coastal area: benthic flux determination from pore water profiles and in situ measurements using benthic chambers. Hydrobiologia 235/236:501–517.

Clarke K & Warwick R (2001) Change in Marine Communities: An Approach to Statistical Analysis and Interpretation. 2nd edition: PRIMER-E, Plymouth, UK. 172pp.

Clarke K & Gorley R (2006) PRIMER v6: User Manual / tutorial. PRIMER-E Ltd., Plymouth UK 192pp.

Colorni A & Diamant A (1993) Ultrastructural features of *Cryptocaryon irritans*, a ciliate parasite of marine fish. European Journal of Protistology 29: 425-434.

Coolen MJL & Shtereva G (2009) Vertical distribution of metabolically active eukaryotes in the water column and sediments of the Black Sea. Fems Microbiology Ecology 70: 525-539.

Corinaldesi C, Danovaro R & Dell'Anno A (2005) Simultaneous recovery of extracellular and intracellular DNA suitable for molecular studies from marine sediments. Applied and Environmental Microbiology 71: 46-50.

Croot PL, Karlson B, Wulff A, Linares F & Andersson K (2002) Trace metal/phytoplankton interactions in the Skagerrak. Journal of Marine Systems 35: 39-60.

Danis B, Wantier P, Dutrieux S, Flammang R, Dubois P & Warnau M (2004) Contaminant levels in sediments and asteroids (*Asterias rubens* L., Echinodermata) from the Belgian coast and Scheldt estuary: polychlorinated biphenyls and heavy metals. Science of the Total Environment 333: 149-165.

Das N, Vimala R & Karthika P (2008) Biosorption of heavy metals - An overview. Indian Journal of Biotechnology 7: 159-169.

Dauwe B, Middelburg JJ & Herman PMJ (2001) Effect of oxygen on the degradability of organic matter in subtidal and intertidal sediments of the North Sea area. Marine Ecology-Progress Series 215: 13-22.

Davison W & Zhang H (1994) In-situ speciation measurements of trace components in natural-waters using thin-film gels. Nature 367: 546-548.

Davison W (1991) The solubility of iron sulfides in synthetic and natural-waters at ambient-temperature. Aquatic Sciences 53: 309-329.

Dawson SC & Pace NR (2002) Novel kingdom-level eukaryotic diversity in anoxic environments. Proceedings of the National Academy of Sciences of the United States of America 99: 8324-8329.

de Mora S, Fowler SW, Wyse E & Azemard S (2004) Distribution of heavy metals in marine bivalves, fish and coastal sediments in the Gulf and Gulf of Oman. Marine Pollution Bulletin 49: 410-424.

Debelius B, Forja JM, DelValls A & Lubian LM (2009) Toxicity and bioaccumulation of copper and lead in five marine microalgae. Ecotoxicology and Environmental Safety 72: 1503-1513.

Dell'Anno A, Fabiano M, Duineveld GCA, Kok A & Danovaro R (1998) Nucleic acid (DNA, RNA) quantification and RNA/DNA ratio determination in marine sediments: Comparison of spectrophotometric, fluorometric, and high-performance liquid chromatography methods and estimation of detrital DNA. Applied and Environmental Microbiology 64: 3238-3245.

Denis L, Desroy N (2008) Consequences of spring phytodetritus sedimentation on the benthic compartment along a depth gradient in the Eastern English Channel. Mar Pollut Bull 56:1844–1854.

Desroy N, Denis L (2004) Influence of spring phytodetritus sedimentation on intertidal macrozoobenthos in the eastern English Channel. Mar Ecol Prog Ser 270:41–53.

Diaz S, Martin-Gonzalez A & Gutierrez JC (2006) Evaluation of heavy metal acute toxicity and bioaccumulation in soil ciliated protozoa. Environment International 32: 711-717.

DiazRavina M & Baath E (1996) Development of metal tolerance in soil bacterial communities exposed to experimentally increased metal levels. Applied and Environmental Microbiology 62: 2970-2977.

Diggles BK (2001) A mycosis of juvenile spiny rock lobster, *Jasus edwardsii* (Hutton, 1875) caused by *Haliphthoros* sp., and possible methods of chemical control. Journal of Fish Diseases 24: 99-110.

Doherty M, Tamura M, Vriezen JAC, McManus GB & Katz LA (2010) Diversity of Oligotrichia and Choreotrichia Ciliates in Coastal Marine Sediments and in Overlying Plankton. Applied and Environmental Microbiology 76: 3924-3935.

Dopheide A, Lear G, Stott R & Lewis G (2008) Molecular characterization of ciliate diversity in stream biofilms. Applied and Environmental Microbiology 74: 1740-1747.

Edgcomb V, Orsi W, Leslin C, *et al.* (2009) Protistan community patterns within the brine and halocline of deep hypersaline anoxic basins in the eastern Mediterranean Sea. Extremophiles 13: 151-167.

Edgcomb VP, Kysela DT, Teske A, Gomez AD & Sogin ML (2002) Benthic eukaryotic diversity in the Guaymas Basin hydrothermal vent environment. Proceedings of the National Academy of Sciences of the United States of America 99: 7658-7662.

Edgcomb VP, Beaudoin D, Gast R, Biddle JF & Teske A (2011) Marine subsurface eukaryotes: the fungal majority. Environmental Microbiology 13: 172-183.

Fukunaga A, Anderson MJ, Webster-Brown JG & Ford RB (2010) Individual and combined effects of heavy metals on estuarine infaunal communities. Marine Ecology-Progress Series 402: 123-136.

Gachon CMM, Strittmatter M, Muller DG, Kleinteich J & Kupper FC (2009) Detection of Differential Host Susceptibility to the Marine Oomycete Pathogen *Eurychasma dicksonii* by Real-Time PCR: Not All Algae Are Equal. Applied and Environmental Microbiology 75: 322-328.

Gadd GM (2000) Bioremedial potential of microbial mechanisms of metal mobilization and immobilization. Current Opinion in Biotechnology 11: 271-279.

Gadd GM (2004) Microbial influence on metal mobility and application for bioremediation. Geoderma 122: 109-119.

Gao Y, Leermakers M, Gabelle C, *et al.* (2006) High-resolution profiles of trace metals in the pore waters of riverine sediment assessed by DET and DGT. Science of the Total Environment 362: 266-277.

Gao Y (2009) Trace metal behavior in sedimentary environments. VUB, Brussels, Belgium 310 pp.

Gao Y, Lesven L, Gillan D, *et al.* (2009) Geochemical behavior of trace elements in sub-tidal marine sediments of the Belgian coast. Marine Chemistry 117: 88-96.

Gao Y, Leermakers M, Pede A, *et al.* (in press) Benthic fluxes of trace metals caused by phytodetritus in muddy sedimens of the Belgian Coastal Zone. Environmental Chemistry.

Garland JL, Mills AL (1991) Classification and characterization of heterotrophic microbial communities on the basis of patterns of community-level sole-carbon-source utilization. Appl Environ Microbiol 57:2351–2359.

Garstecki T, Verhoeven R, Wickham SA & Arndt H (2000) Benthic-pelagic coupling: a comparison of the community structure of benthic and planktonic heterotrophic protists in shallow inlets of the southern Baltic. Freshwater Biology 45: 147-167.

Gillan DC (2004) The effect of an acute copper exposure on the diversity of a microbial community in North Sea sediments as revealed by DGGE analysis - the importance of the protocol. Marine Pollution Bulletin 49: 504-513.

Gillan DC, Danis B, Pernet P, Joly G & Dubois P (2005) Structure of sediment-associated microbial communities along a heavy-metal contamination gradient in the marine environment. Applied and Environmental Microbiology 71: 679-690.

Gillan DC & Pernet P (2007) Adherent bacteria in heavy metal contaminated marine sediments. Biofouling 23: 1-13.

Gillan D, Pede A, Sabbe K, *et al.* (subm., chapter 4) Effect of bacterial mineralisation of phytoplankton-derived phytodetritus on the release of arsenic, cobalt and manganese from muddy sediments in the Southern North Sea: A microcosm study.

Gillan DC, Baeyens W, Bechara R, *et al.* (subm.) Links between bacterial communities in marine sediments and trace metal geochemistry as measured by *in situ* DET/DGT approaches.

Glud RN (2008) Oxygen dynamics of marine sediments. Marine Biology Research 4: 243-289.

Goedkoop W, Gullberg KR, Johnson RK & Ahlgren I (1997) Microbial response of a freshwater benthic community to a simulated diatom sedimentation event: Interactive effects of benthic fauna. Microbial Ecology 34: 131-143.

Gohin F, Lampert L, Guillaud JF, Herbland A, Nézan E (2003) Satellite and in situ observations of a late winter phytoplankton bloom, in the northern Bay of Biscay. Cont Shelf Res 23:1117–1141.

Graf G (1992) Benthic-pelagic coupling - a benthic view. Oceanography and Marine Biology 30: 149-190.

Gutierrez JC, Martin-Gonzalez A, Diaz S & Ortega R (2003) Ciliates as a potential source of cellular and molecular biomarkers/biosensors for heavy metal pollution. European Journal of Protistology 39: 461-467.

Gutierrez JC, Amaro F & Martin-Gonzalez A (2009) From heavy metal-binders to biosensors: Ciliate metallothioneins discussed. Bioessays 31: 805-816.

Gypens N, Lacroix G, Lancelot C (2007) Causes of variability in diatom and *Phaeocystis* blooms in Belgian coastal waters between 1989 and 2003: A model study. J Sea Res 57:19–35.

Hamels I, Moens T, Mutylaert K & Vyverman W (2001) Trophic interactions between ciliates and nematodes from an intertidal flat. Aquatic Microbial Ecology 26: 61-72.

Hamels I, Sabbe K, Muylaert K & Vyverman W (2004) Quantitative importance, composition, and seasonal dynamics of protozoan communities in polyhaline versus freshwater intertidal sediments. Microbial Ecology 47: 18-29.

Hamels I, Muylaert K, Sabbe K & Vyverman W (2005) Contrasting dynamics of ciliate communities in sandy and silty sediments of an estuarine intertidal flat. European Journal of Protistology 41: 241-250.

Harada A, Ohtsuka S & Horiguchi T (2007) Species of the parasitic genus *Duboscquella* are members of the enigmatic Marine Alveolate Group I. Protist 158: 337-347.

Harnstrom K, Ellegaard M, Andersen TJ & Godhe A (2011) Hundred years of genetic structure in a sediment revived diatom population. Proceedings of the National Academy of Sciences of the United States of America 108: 4252-4257.

Hayward BH, Droste R & Epstein SS (2003) Interstitial ciliates: Benthic microaerophiles or planktonic anaerobes? Journal of Eukaryotic Microbiology 50: 356-359.

Hermi M, Mahmoudi E, Beyrem H, Aissa P & Essid N (2009) Responses of a Free-Living Marine Nematode Community to Mercury Contamination: Results from Microcosm Experiments. Archives of Environmental Contamination and Toxicology 56: 426-433.

Hirt RP, Dyal PL, Wilkinson M, Finlay BJ, Roberts DM & Embley TM (1995) Phylogenetic Relationships among Karyorelictids and Heterotrichs Inferred from Small Subunit rRNA Sequences: Resolution at the Base of the Ciliate Tree. Molecular Phylogenetics and Evolution 4: 77-87.

Hitzl W, Rangger A, Sharma S, Insam H (1997) Separation power of the 95 substrates of the BIOLOG system determined in various soils. FEMS Microbiol Ecol 22:167–174.

Hondeveld BJM, Nieuwland G, Vanduyl FC & Bak RPM (1994) Temporal and spatial variations in heterotrophic nanoflagellate abundance in North-Sea sediments. Marine Ecology-Progress Series 109: 235-243.

Hondeveld BJM, Nieuwland G, VanDuyl FC & Bak RPM (1995) Impact of nanoflagellate bacterivory on benthic bacterial production in the North Sea. Netherlands Journal of Sea Research 34: 275-287.

Hong YS, Kinney KA & Reible DD (2011) Effects of cyclic changes in pH and salinity on metals release from sediments. Environmental Toxicology and Chemistry 30: 1775-1784.

Hoppenrath M & Leander BS (2006) Dinoflagellate, euglenid, or cercomonad? The ultrastructure and molecular phylogenetic position of *Protaspis grandis* n. Sp. Journal of Eukaryotic Microbiology 53: 327-342.

Hoshino YT & Matsumoto N (2007) DNA- versus RNA-based denaturing gradient gel electrophoresis profiles of a bacterial community during replenishment after soil fumigation. Soil Biology & Biochemistry 39: 434-444.

Howe AT, Bass D, Scoble JM, Lewis R, Vickerman K, Arndt H & Cavalier-Smith T (2011) Novel Cultured Protists Identify Deep-branching Environmental DNA Clades of Cercozoa: New Genera *Tremula, Micrometopion, Minimassisteria, Nudifila, Peregrinia*. Protist 162: 332-372.

Huettel M, Ziebis W, Forster S & Luther GW (1998) Advective transport affecting metal and nutrient distributions and interfacial fluxes in permeable sediments. Geochimica Et Cosmochimica Acta 62: 613-631.

Hunt CD (1983) Variability in the benthic Mn flux in coastal marine ecosystems resulting from temperature and primary production. Limnol Oceanogr 28:913–923.

Hyde KD, Jones EBG, Leano E, Pointing SB, Poonyth AD & Vrijmoed LLP (1998) Role of fungi in marine ecosystems. Biodiversity and Conservation 7: 1147-1161.

Irvin TR & Irgolic KJ (1995) In-vitro prenatal toxicity of trimethylarsine, trimethylarsine oxide and trimethylarsine sulfide. Applied Organometallic Chemistry 9: 315-321.

Iskrenova-Tchoukova E, Kalinichev AG, Kirkpatrick RJ (2010) Metal cation complexation with natural organic matter in aqueous solutions: molecular dynamics simulations and potentials of mean force. Langmuir 26:15909–15919.

Jayaraju N, Reddy B & Reddy KR (2008) The response of benthic foraminifera to various pollution sources: A study from Nellore Coast, East Coast of India. Environmental Monitoring and Assessment 142: 319-323.

Jayaraju N, Reddy B & Reddy KR (2011) Anthropogenic impact on Andaman coast monitoring with benthic foraminifera, Andaman Sea, India. Environmental Earth Sciences 62: 821-829.

Jeon S, Bunge J, Leslin C, Stoeck T, Hong SH & Epstein SS (2008) Environmental rRNA inventories miss over half of protistan diversity. Bmc Microbiology 8: 13.

Joksimovic D, Tomic I, Stankovic AR, Jovic M & Stankovic S (2011) Trace metal concentrations in Mediterranean blue mussel and surface sediments and evaluation of the mussels quality and possible risks of high human consumption. Food Chemistry 127: 632-637.

Jørgensen B (1982) Mineralization of organic matter in the sea bed-the role of sulphate reduction. Nature 296: 643-645.

Jørgensen BB, Revsbech NP (1985) Diffusive boundary layers and the oxygen uptake of sediments and detritus. Limnol Oceanogr 30:111–122.

Jørgensen B, Schulz HD & Zabel M (2006) Bacteria and Marine Biogeochemistry. Marine Geochemistry), 169-206. Springer Berlin Heidelberg.

Kagami M, de Bruin A, Ibelings BW & Van Donk E (2007) Parasitic chytrids: their effects on phytoplankton communities and food-web dynamics. Hydrobiologia 578: 113-129.

Kandeler E, Kampichler C & Horak O (1996) Influence of heavy metals on the functional diversity of soil microbial communities. Biology and Fertility of Soils 23: 299-306.

Kapoor A & Viraraghavan T (1997) Heavy metal biosorption sites in *Aspergillus niger*. Bioresource Technology 61: 221-227.

Kathol M, Fischer H & Weitere M (2011) Contribution of biofilm-dwelling consumers to pelagic-benthic coupling in a large river. Freshwater Biology 56: 1160-1172.

Kerkhof L & Ward BB (1993) Comparison of nucleic-acid hybridization and fluorometry for measurement of the relationship between rna/dna ratio and growth-rate in a marine bacterium. Applied and Environmental Microbiology 59: 1303-1309.

Kirchman D, Sigda J, Kapuscinski R, Mitchell R (1982) Statistical analysis of the direct count method for enumerating bacteria. Appl Environ Microbiol 44:376 – 382.

Knowles FC, Benson AA (1983) The biochemistry of arsenic. Trends Biochem Sci 8:178–180.

Kohlmeyer J (1979) Marine fungal pathogens among Ascomycetes and Deuteromycetes. Experientia 35: 437-439.

Kowalchuk GA, Os GJ, Aartrijk J & Veen JA (2003) Microbial community responses to disease management soil treatments used in flower bulb cultivation. Biology and Fertility of Soils 37: 55-63.

Kristensen E, Ahmed SI & Devol AH (1995) Aerobic and anaerobic decomposition of organic matter in marine sediment: Which is fastest? Limnology and Oceanography 40: 1430-1437.

Kuhn S, Lange M & Medlin LK (2000) Phylogenetic position of *Cryothecomonas* inferred from nuclear-encoded small subunit ribosomal RNA. Protist 151: 337-345.

Lacroix G, Ruddick K, Gypens N & Lancelot C (2007a) Modelling the relative impact of rivers (Scheldt/Rhine/Seine) and Western Channel waters on the nutrient and diatoms/*Phaeocystis* distributions in Belgian waters (Southern North Sea). Continental Shelf Research 27: 1422-1446.

Lacroix G, Ruddick K, Park Y, Gypens N & Lancelot C (2007b) Validation of the 3D biogeochemical model MIRO&CO with field nutrient and phytoplankton data and MERIS-derived surface chlorophyll *a* images. Journal of Marine Systems 64: 66-88.

Lancelot C, Billen G, Sournia A, *et al.* (1987) *Phaeocystis* blooms and nutrient enrichment in the continental coastal zones of the North-Sea. Ambio 16: 38-46.

Lancelot C, Spitz Y, Gypens N, *et al.* (2005) Modelling diatom and *Phaeocystis* blooms and nutrient cycles in the Southern Bight of the North Sea: the MIRO model. Marine Ecology-Progress Series 289: 63-78.

Lancelot C, Gypens N, Billen G, Garnier J, Roubeix V (2007) Testing an integrated river–ocean mathematical tool for linking marine eutrophication to land use: The *Phaeocystis*-dominated Belgian coastal zone (Southern North Sea) over the past 50 years. J Mar Syst 64:216–228.

Langston WJ, Burt GR & Pope ND (1999) Bioavailability of metals in sediments of the Dogger Bank (central North Sea): A mesocosm study. Estuarine Coastal and Shelf Science 48: 519-540.

Lanzen A, Jorgensen SL, Bengtsson MM, Jonassen I, Ovreas L & Urich T (2011) Exploring the composition and diversity of microbial communities at the Jan Mayen hydrothermal vent field using RNA and DNA. Fems Microbiology Ecology 77: 577-589.

Lara E, Berney C, Harms H & Chatzinotas A (2007a) Cultivation-independent analysis reveals a shift in ciliate 18S rRNA gene diversity in a polycyclic aromatic hydrocarbon-polluted soil. Fems Microbiology Ecology 62: 365-373.

Lara E, Berney C, Ekelund F, Harms H & Chatzinotas A (2007b) Molecular comparison of cultivable protozoa from a pristine and a polycyclic aromatic hydrocarbon polluted site. Soil Biology & Biochemistry 39: 139-148.

Leborans GF, Herrero YO & Novillo A (1998) Toxicity and bioaccumulation of lead in marine protozoa communities. Ecotoxicology and Environmental Safety 39: 172-178.

Lee JY, Moon SH & Yun ST (2010a) Contamination of groundwater by arsenic and other constituents in an industrial complex. Environmental Earth Sciences 60: 65-79.

Lee KY, Kim KW & Kim SO (2010b) Geochemical and microbial effects on the mobilization of arsenic in mine tailing soils. Environmental Geochemistry and Health 32: 31-44.

Lee WJ & Patterson DJ (2002) Abundance and biomass of heterotrophic flagellates, and factors controlling their abundance and distribution in sediments of Botany Bay. Microbial Ecology 43: 467-481.

Levin LA, Ekau W, Gooday AJ, *et al.* (2009) Effects of natural and human-induced hypoxia on coastal benthos. Biogeosciences 6: 2063-2098.

Li XD, Shen ZG, Wai OWH & Li YS (2000a) Chemical partitioning of heavy metal contaminants in sediments of the Pearl River Estuary. Chemical Speciation and Bioavailability 12: 17-25.

Li XD, Wai OWH, Li YS, Coles BJ, Ramsey MH & Thornton I (2000b) Heavy metal distribution in sediment profiles of the Pearl River estuary, South China. Applied Geochemistry 15: 567-581.

Lillis L, Doyle E & Clipson N (2009) Comparison of DNA- and RNA-based bacterial community structures in soil exposed to 2,4-dichlorophenol. Journal of Applied Microbiology 107: 1883-1893.

Liu G, Cai Y (2010) Complexation of arsenite with dissolved organic matter: conditional distribution coefficients and apparent stability constants. Chemosphere 81:890–896.

Liu L, Zhu W, Xiao L & Yang LY (2010) Effect of decabromodiphenyl ether (BDE 209) and dibromodiphenyl ether (BDE 15) on soil microbial activity and bacterial community composition. Journal of Hazardous Materials 186: 883-890.

Lopez-Garcia P, Philippe H, Gail F & Moreira D (2003) Autochthonous eukaryotic diversity in hydrothermal sediment and experimental microcolonizers at the Mid-Atlantic Ridge. Proceedings of the National Academy of Sciences of the United States of America 100: 697-702.

Luo QW, Krumholz LR, Najar FZ, Peacock AD, Roe BA, White DC & Elshahed MS (2005) Diversity of the microeukaryotic community in sulfide-rich zodletone spring (Oklahoma). Applied and Environmental Microbiology 71: 6175-6184.

Luo W, Li HR, Cai MH & He JF (2009) Diversity of microbial eukaryotes in Kongsfjorden, Svalbard. Hydrobiologia 636: 233-248.

Madoni P & Romeo MG (2006) Acute toxicity of heavy metals towards freshwater ciliated protists. Environmental Pollution 141: 1-7.

Mangot JF, Debroas D & Domaizon I (2011) Perkinsozoa, a well-known marine protozoan flagellate parasite group, newly identified in lacustrine systems: a review. Hydrobiologia 659: 37-48.

Manini E, Fiordelmondo C, Gambi C, Pusceddu A & Danovaro R (2003) Benthic microbial loop functioning in coastal lagoons: a comparative approach. Oceanologica Acta 26: 27-38.

Martin-Gonzalez A, Diaz S, Borniquel S, Gallego A & Gutierrez JC (2006) Cytotoxicity and bioaccumulation of heavy metals by ciliated protozoa isolated from urban wastewater treatment plants. Research in Microbiology 157: 108-118.

Matthai C & Birch G (2001) Detection of anthropogenic Cu, Pb and Zn in continental shelf sediments off Sydney, Australia - A new approach using normalization with cobalt. Marine Pollution Bulletin 42: 1055-1063.

McArdle BH & Anderson MJ (2001) Fitting multivariate models to community data: A comment on distance-based redundancy analysis. Ecology 82: 290-297.

McKinley AC, Miskiewicz A, Taylor MD & Johnston EL (2011) Strong links between metal contamination, habitat modification and estuarine larval fish distributions. Environmental Pollution 159: 1499-1509.

McQuoid MR (2002) Pelagic and benthic environmental controls on the spatial distribution of a viable diatom propagule bank on the Swedish west coast. Journal of Phycology 38: 881-893.

McQuoid MR & Nordberg K (2006) Composition and origin of benthic flocculent layers in Swedish fjords following the spring bloom - contribution of diatom frustules and resting stages. Nova Hedwigia 83: 1-16.

Meyer-Reil LA, Köster M (1992) Microbial life in pelagic sediments: the impact of environmental parameters on enzymatic degradation of organic material. Mar Ecol Prog Ser 81:65–72.

Meysman FJR, Galaktionov OS, Gribsholt B & Middelburg JJ (2006) Bio-irrigation in permeable sediments: An assessment of model complexity. Journal of Marine Research 64: 589-627.

Meysman FJR, Malyuga VS, Boudreau BP & Middelburg JJ (2008) Quantifying particle dispersal in aquatic sediments at short time scales: model selection. Aquatic Biology 2: 239-254.

M'Harzi A, Tackx M, Daro MH, Kesaulia I, Caturao R & Podoor N (1998) Winter distribution of phytoplankton and zooplankton around some sandbanks of the Belgian coastal zone. Journal of Plankton Research 20: 2031-2052.

Middelburg JJ & Levin LA (2009) Coastal hypoxia and sediment biogeochemistry. Biogeosciences 6: 1273-1293.

Mills HJ, Martinez RJ, Story S & Sobecky PA (2005) Characterization of microbial community structure in Gulf of Mexico gas hydrates: Comparative analysis of DNA- and RNA-derived clone libraries. Applied and Environmental Microbiology 71: 3235-3247.

Milner MG, Saunders JR & McCarthy AJ (2001) Relationship between nucleic acid ratios and growth in Listeria monocytogenes. Microbiology-Sgm 147: 2689-2696.

Montagna PA (1982) Sampling design and enumeration statistics for bacteria extracted from marine sediments. Appl Environ Microbiol 43:1366–1372.

Montero FE, Cuadrado M, Crespo FP & Raga JA (2007) *Cryptocaryon irritans* and *Enteromyxum leei*, two threats for the culture of *Diplodus puntazzo* in the Mediterranean. Bulletin of the European Association of Fish Pathologists 27: 242-249.

Moodley L, Middelburg JJ, Herman PMJ, Soetaert K & de Lange GJ (2005) Oxygenation and organic-matter preservation in marine sediments: Direct experimental evidence from ancient organic carbon-rich deposits. Geology 33: 889-892.

Moriarty DJW, Pollard PC, Hunt WG, Moriarty CM, Wassenburg TJ (1985) Productivity of bacteria and microalgae and the effect of grazing by holothurians in sediments on a coral reef flat. Mar Biol 85:293–300.

Mukhopadhyay R, Rosen BP, Phung LT, Silver S (2002) Microbial arsenic: from geocycles to genes and enzymes. FEMS Microbiol Rev 26:311–325.

Musslewhite CL, McInerney MJ, Dong HL, *et al.* (2003) The factors controlling microbial distribution and activity in the shallow subsurface. Geomicrobiology Journal 20: 245-261.

Muyzer G, Dewaal EC & Uitterlinden AG (1993) Profiling of complex microbial-populations by Denaturing Gradient Gel-Electrophoresis analysis of Polymerase Chain Reaction-amplified genes-coding for 16S ribosomal-RNA. Applied and Environmental Microbiology 59: 695-700.

Muyzer G & Smalla K (1998) Application of denaturing gradient gel electrophoresis (DGGE) and temperature gradient gel electrophoresis (TGGE) in microbial ecology. Antonie Van Leeuwenhoek International Journal of General and Molecular Microbiology 73: 127-141.

Nicol GW, Glover LA & Prosser JI (2003) Spatial analysis of archaeal community structure in grassland soil. Applied and Environmental Microbiology 69: 7420-7429.

Niegel C & Matysik FM (2010) Analytical methods for the determination of arsenosugars-A review of recent trends and developments. Analytica Chimica Acta 657: 83-99.

Nies DH (2003) Efflux-mediated heavy metal resistance in prokaryotes. Fems Microbiology Reviews 27: 313-339.

Nogales B, Lanfranconi MP, Pina-Villalonga JM & Bosch R (2011) Anthropogenic perturbations in marine microbial communities. Fems Microbiology Reviews 35: 275-298.

Noll M, Matthies D, Frenzel P, Derakshani M & Liesack W (2005) Succession of bacterial community structure and diversity in a paddy soil oxygen gradient. Environmental Microbiology 7: 382-395.

Nolte V, Pandey RV, Jost S, Medinger R, Ottenwalder B, Boenigk J & Schlotterer C (2010) Contrasting seasonal niche separation between rare and abundant taxa conceals the extent of protist diversity. Molecular Ecology 19: 2908-2915.

Not F, del Campo J, Balague V, de Vargas C & Massana R (2009) New Insights into the Diversity of Marine Picoeukaryotes. Plos One 4: 7.

Nriagu JO (Ed.). Arsenic in the Environment: Human Health and Ecosystem E¡ects. Advances in Environmental Science and Technology, 1994, Vol. 27. John Wiley and Sons, New York.

Ogilvie LA & Grant A (2008) Linking pollution induced community tolerance (PICT) and microbial community structure in chronically metal polluted estuarine sediments. Marine Environmental Research 65: 187-198.

Orcutt BN, Sylvan JB, Knab NJ & Edwards KJ (2011) Microbial Ecology of the Dark Ocean above, at, and below the Seafloor. Microbiology and Molecular Biology Reviews 75: 361-+.

OSPAR (2000) Quality Status Report 2000, Region II-Greater North Sea. OSPAR Commission, London 136pp.

Pakhomova SV, Hall POJ, Kononets MY, Rozanov AG, Tengberg A, Vershinin AV (2007) Fluxes of iron and manganese across the sediment–water interface under various redox conditions. Mar Chem 107:319–331.

Park SJ, Park BJ, Pham VH, Yoon DN, Kim SK & Rhee SK (2008) Microeukaryotic diversity in marine environments, an analysis of surface layer sediments from the East Sea. Journal of Microbiology 46: 244-249.

Patterson DJ, Larsen J & Corliss JO (1989) The Ecology of Heterotrophic Flagellates and Ciliates Living in Marine Sediments. Progress in Protistology 3: 185-277.

Pawlowski J, Christen R, Lecroq B, Bachar D, Shahbazkia HR, Amaral-Zettler L & Guillou L (2011a) Eukaryotic Richness in the Abyss: Insights from Pyrotag Sequencing. Plos One 6: 10.

Pawlowski JPJ, Christen R, Lecroq B, Bachar D, Shahbazkia HR, Amaral-Zettler L & Guillou L (2011b) Eukaryotic Richness in the Abyss: Insights from Pyrotag Sequencing. Plos One 6: 10.

Pawlowski JPJ, Christen R, Lecroq B, Bachar D, Shahbazkia HR, Amaral-Zettler L & Guillou L (2011c) Eukaryotic Richness in the Abyss: Insights from Pyrotag Sequencing. Plos One 6.

Penna A, Fraga S, Battocchi C, Casabianca S, Giacobbe MG, Riobo P & Vernesi C (2010) A phylogeographical study of the toxic benthic dinoflagellate genus Ostreopsis Schmidt. Journal of Biogeography 37: 830-841.

Pershagen G (1985) Lung cancer mortality among men living near arsenic-emitting smelters. Am J Epidemiol 122:684–694.

Petersen W, Wallmann K, Li P, Schroeder F, Knauth HD (1996) The influence of diagenetic processes on the exchange of trace contaminants at the sediment-water interface. In: Calmano W, Förstner U (eds) Sediments and toxic substances. Springer, Berlin, 37–50.

Petersen W, Willer E & Willamowski C (1997) Remobilization of trace elements from polluted anoxic sediments after resuspension in oxic water. Water Air and Soil Pollution 99: 515-522.

Phipps DA (1981) Chemistry and Biochemistry of Trace Metals in Biological Systems In: Effect of Heavy Metal Pollution on Plants. Lepp N.W. (eds.). Applied Science Publishers, Barking.

Piola RF & Johnston EL (2008) Pollution reduces native diversity and increases invader dominance in marine hard-substrate communities. Diversity and Distributions 14: 329-342.

Potvin M & Lovejoy C (2009) PCR-Based Diversity Estimates of Artificial and Environmental 18S rRNA Gene Libraries. Journal of Eukaryotic Microbiology 56: 174-181.

Pringault O, Viret H & Duran R (2010) Influence of microorganisms on the removal of nickel in tropical marine sediments (New Caledonia). Marine Pollution Bulletin 61: 530-541.

Raes J, Letunic I, Yamada T, Jensen LJ & Bork P (2011) Toward molecular trait-based ecology through integration of biogeochemical, geographical and metagenomic data. Molecular Systems Biology 7.

Rasconi S, Jobard M & Sime-Ngando T (2011) Parasitic fungi of phytoplankton: ecological roles and implications for microbial food webs. Aquatic Microbial Ecology 62: 123-137.

Rauch M & Denis L (2008) Spatio-temporal variability in benthic mineralization processes in the eastern English Channel. Biogeochemistry 89: 163-180.

Rauch M, Denis L & Dauvin JC (2008) The effects of *Phaeocystis globosa* bloom on the dynamics of the mineralization processes in intertidal permeable sediment in the Eastern English Channel (Wimereux, France). Marine Pollution Bulletin 56: 1284-1293.

Rehman A, Shakoori FR & Shakoori AR (2008) Uptake of heavy metals by *Stylonychia mytilus* and its possible use in decontamination of industrial wastewater. World Journal of Microbiology & Biotechnology 24: 47-53.

Rehman A, Shakoori FR & Shakoori AR (2010a) Resistance and Uptake of Heavy Metals by *Vorticella microstoma* and Its Potential Use in Industrial Wastewater Treatment. Environmental Progress & Sustainable Energy 29: 481-486.

Rehman A, Shakoori FR & Shakoori AR (2010b) Multiple Heavy Metal Tolerant Ciliates, *Oxytricha fallax* and *Paramecium caudatum*, Isolated From Industrial Effluents and Their Potential Use in Wastewater Treatment. Pakistan Journal of Zoology 42: 301-309.

Reilly C (2004) *The nutritional trace metals*. Blackwell Publishing, Oxford, UK.

Reimann C, Matschullat J, Birke M & Salminen R (2009) Arsenic distribution in the environment: The effects of scale. Applied Geochemistry 24: 1147-1167.

Rico D, Martin-Gonzalez A, Diaz S, de Lucas P & Gutierrez JC (2009) Heavy metals generate reactive oxygen species in terrestrial and aquatic ciliated protozoa. Comparative Biochemistry and Physiology C-Toxicology & Pharmacology 149: 90-96.

Riedel GF, Sanders JG, Osman RW (1987) The effect of biological and physical disturbances on the transport of arsenic from contaminated estuarine sediments. Est Coast Shelf Sci 25:693–706.

Rivaro P, Cullaj A, Frache R, Lagomarsino C, Massolo S, De Mattia MC & Ungaro N (2011) Heavy Metals Distribution in Suspended Particulate Matter and Sediment Collected from Vlora Bay (Albania): A Methodological Approach for Metal Pollution Evaluation. Journal of Coastal Research 54-66.

Rousseau V, Becquevort S, Parent JY, Gasparini S, Daro MH, Tackx M & Lancelot C (2000) Trophic efficiency of the planktonic food web in a coastal ecosystem dominated by Phaeocystis colonies. Journal of Sea Research 43: 357-372.

Rousseau V, Leynaert A, Daoud N & Lancelot C (2002) Diatom succession, silicification and silicic acid availability in Belgian coastal waters (Southern North Sea). Marine Ecology-Progress Series 236: 61-73.

Rousseau V, Park Y, Ruddick K, Vyverman W, Parent JY, Lancelot C (2008) Phytoplankton blooms in response to nutrient enrichment. In: Current status of eutrophication in the Belgian coastal zone. V. Rousseau, C. Lancelot and D. Cox (Eds). Presses Universitaires de Bruxelles, Bruxelles, 45–59.

Ruddick K & Lacroix G (2006) Hydrodynamics and meteorology of the Belgian Coastal Zone; *in* Rousseau, V. *et al.* (Ed.) (2006). Current status of eutrophication in the Belgian Coastal Zone. pp. 1-15.

Sapp M, Parker ER, Teal LR & Schratzberger M (2010) Advancing the understanding of biogeography-diversity relationships of benthic microorganisms in the North Sea. Fems Microbiology Ecology 74: 410-429.

Satta CT, Angles S, Garces E, Luglie A, Padedda BM & Sechi N (2010) Dinoflagellate cysts in recent sediments from two semi-enclosed areas of the Western Mediterranean Sea subject to high human impact. Deep-Sea Research Part Ii-Topical Studies in Oceanography 57: 256-267.

Sauvadet A-L, Gobet A & Guillou L (2010) Comparative analysis between protist communities from the deep-sea pelagic ecosystem and specific deep hydrothermal habitats. Environmental Microbiology 12: 2946-2964.

Sauvant MP, Pepin D & Piccinni E (1999) *Tetrahymena pyriformis*: A tool for toxicological studies. A review. Chemosphere 38: 1631-1669.

Savin MC, Martin JL, LeGresley M, Giewat M & Rooney-Varga J (2004) Plankton diversity in the Bay of Fundy as measured by morphological and molecular methods. Microbial Ecology 48: 51-65.

Scheckenbach F, Hausmann K, Wylezich C, Weitere M & Arndt H (2010) Large-scale patterns in biodiversity of microbial eukaryotes from the abyssal sea floor. Proceedings of the National Academy of Sciences of the United States of America 107: 115-120.

Schoemann V, Becquevort S, Stefels J, Rousseau V, Lancelot C (2005) Phaeocystis blooms in the global ocean and their controlling mechanisms: a review. J Sea Res 53:43–66.

Scoullos M & Pavlidou AS (2000) Metal speciation studies in a brakish / marine interface system. Global Nest: The International Journal 2: 255-264.

Sekimoto S, Hatai K & Honda D (2007) Molecular phylogeny of an unidentified *Haliphthoros* -like marine oomycete and *Haliphthoros milfordensis* inferred from nuclear-encoded small- and large-subunit rRNA genes and mitochondrial-encoded cox2 gene. Mycoscience 48: 212-221.

Servais P (1990) Estimation de la production bactérienne en milieu marin par mesure du taux de synthèse protéique. Oceanol Acta 13:229–235.

Sherr EB & Sherr BF (2002) Significance of predation by protists in aquatic microbial food webs. Antonie Van Leeuwenhoek International Journal of General and Molecular Microbiology 81: 293-308.

Shimeta J, Amos CL, Beaulieu SE & Ashiru OM (2002) Sequential resuspension of protists by accelerating tidal flow: Implications for community structure in the benthic boundary layer. Limnology and Oceanography 47: 1152-1164.

Shimeta J, Amos CL, Beaulieu SE & Katz SL (2003) Resuspension of benthic protists at subtidal coastal sites with differing sediment composition. Marine Ecology-Progress Series 259: 103-115.

Shimeta J, Gast RJ & Rose JM (2007) Community structure of marine sedimentary protists in relation to flow and grain size. Aquatic Microbial Ecology 48: 91-104.

Shimizu Y (2003) Microalgal metabolites. Current Opinion in Microbiology 6: 236-243.

Sime-Ngando T & Niquil N (2011) Editorial: 'Disregarded' microbial diversity and ecological potentials in aquatic systems: a new paradigm shift ahead. Hydrobiologia 659: 1-4.

Sirjacobs D, Alvera-Azcárate A, Barth A, Lacroix G, Park Y, Nechad B, Ruddick K, Beckers JM 2011) Cloud filling of ocean colour and sea surface temperature remote sensing products over the Southern North Sea by the Data Interpolating Empirical Orthogonal Functions methodology. J Sea Res 65:114–130.

Skrabal SA, Donat JR, Burdige DJ (1997) Fluxes of copper-complexing ligands from estuarine sediments. Limnol Oceanogr 42:992–996.

Skrabal SA, Donat JR, Burdige DJ (2000) Pore water distributions of dissolved copper and copper-complexing ligands in estuarine and coastal marine sediments. Geochim Cosmochim Acta 64:1843–1857.

Speir TW, Kettles HA, Parshotam A, Searle PL & Vlaar LNC (1999) Simple kinetic approach to determine the toxicity of As[V] to soil biological properties. Soil Biology & Biochemistry 31: 705-713.

Spencer KL (2002) Spatial variability of metals in the inter-tidal sediments of the Medway Estuary, Kent, UK. Marine Pollution Bulletin 44: 933-944.

Spokes LJ & Jickells TD (1995) Factors controlling the solubility of aerosol trace metals in the atmosphere and on mixing into seawater. Aquatic Geochemistry 1: 355-374.

Srivastava PK, Vaish A, Dwivedi S, Chakrabarty D, Singh N & Tripathi RD (2011) Biological removal of arsenic pollution by soil fungi. Science of the Total Environment 409: 2430-2442.

Starink M, Krylova IN, Bär-Gilissen MJ, Bak RPM, Cappenberg TE (1994) Rates of benthic protozoan grazing on free and attached sediment bacteria measured with fluorescently stained sediment. Appl Environ Microbiol 60:2259–2264.

Stefanowicz A (2006) The Biolog Plates Technique as a Tool in Ecological Studies of Microbial Communities. Polish J Environ Stud 15:669–676.

Steyaert M, Garner N, van Gansbeke D & Vincx M (1999) Nematode communities from the North Sea: environmental controls on species diversity and vertical distribution within the sediment. Journal of the Marine Biological Association of the United Kingdom 79: 253-264.

Steyaert M, Vanaverbeke J, Vanreusel A, Barranguet C, Lucas C & Vincx M (2003) The importance of fine-scale, vertical profiles in characterising nematode community structure. Estuarine Coastal and Shelf Science 58: 353-366.

Stoeck T & Epstein S (2003) Novel eukaryotic lineages inferred from small-subunit rRNA analyses of oxygen-depleted marine environments. Applied and Environmental Microbiology 69: 2657-2663.

Stoeck T, Hayward B, Taylor GT, Varela R & Epstein SS (2006) A multiple PCR-primer approach to access the microeukaryotic diversity in environmental samples. Protist 157: 31-43.

Stoeck T, Bruemmer F & Foissner W (2007a) Evidence for local ciliate endemism in an Alpine Anoxic lake. Microbial Ecology 54: 478-486.

Stoeck T, Zuendorf A, Breiner HW & Behnke A (2007b) A molecular approach to identify active microbes in environmental eukaryote clone libraries. Microbial Ecology 53: 328-339.

Stoeck T, Behnke A, Christen R, *et al.* (2009) Massively parallel tag sequencing reveals the complexity of anaerobic marine protistan communities. Bmc Biology 7.

Stoeck T & Stock A (2010) The protistan gap in th eukaryotic tree of life 1. Palaeodiversity 3: 151-154

Sugie K & Kuma K (2008) Resting spore formation in the marine diatom Thalassiosira nordenskioeldii under iron- and nitrogen-limited conditions. Journal of Plankton Research 30: 1245-1255.

Sullivan KA, Aller RC (1996) Diagenetic cycling of arsenic in Amazon shelf sediments. Geochim Cosmochim Acta 60:1465–1477.

Sundby B, Anderson LG, Hall POJ, Iverfeldt A, Rutgers van der Loeff MM, Westerlund SFG (1986) The effect of oxygen on release and uptake of cobalt, manganese, iron and phosphate at the sediment -water interface. Geochim Cosmochim Acta 50:1281–1288.

Takishita K, Miyake H, Kawato M & Maruyama T (2005) Genetic diversity of microbial eukaryotes in anoxic sediment around fumaroles on a submarine caldera floor based on the small-subunit rDNA phylogeny. Extremophiles 9: 185-196.

Takishita K, Yubuki N, Kakizoe N, Inagaki Y & Maruyama T (2007) Diversity of microbial eukaryotes in sediment at a deep-sea methane cold seep: surveys of ribosomal DNA libraries from raw sediment samples and two enrichment cultures. Extremophiles 11: 563-576.

Takishita K, Kakizoe N, Yoshida T & Maruyama T (2010) Molecular Evidence that Phylogenetically Diverged Ciliates Are Active in Microbial Mats of Deep-Sea Cold-Seep Sediment. Journal of Eukaryotic Microbiology 57: 76-86.

Tao SF & Taghon GL (1997) Enumeration of protozoa and bacteria in muddy sediment. Microbial Ecology 33: 144-148.

Taylor GT, Iturriaga R & Sullivan CW (1985) Interactions of bactivorous grazers and heterotrophic bacteria with dissolved organic-matter. Marine Ecology-Progress Series 23: 129-141.

Taylor W & Sanders R (1991) Protozoa. Ecology and Classification of North American Freshwater Invertebrates 37-94.

Ter Braak CJF & Smilauer P (2002) CANOCO Reference Manual and CanoDraw for Windows User's Guide: Software for Canonical Community Ordination (version 4.5). www.canoco.com, Ithaca NY, USA.

Thamdrup B, Fossing H, Jørgensen BB (1994) Manganese, iron, and sulfur cycling in a coastal marine sediment, Aarhus Bay, Denmark. Geochim Cosmochim Acta 58:5115–5129.

Thiyagarajan V, Tsoi MMY, Zhang W & Qian PY (2010) Temporal variation of coastal surface sediment bacterial communities along an environmental pollution gradient. Marine Environmental Research 70: 56-64.

Thomas PM (1999) Toxic Metals. In: Tietz textbook of Clinical Chemistry. Burtis C.A., Ashwood E.R. (eds). W.B. Saunders Company, 982-998.

Thomsen HA, Buck KR, Bolt PA & Garrison DL (1991) Fine-structure and biology of *Cryothecomonas* gen-nov (Protista Incertae Sedis) from the ice biota. Canadian Journal of Zoology-Revue Canadienne De Zoologie 69: 1048-1070.

Tian F, Yu Y, Chen B, Li HR, Yao YF & Guo XK (2009) Bacterial, archaeal and eukaryotic diversity in Arctic sediment as revealed by 16S rRNA and 18S rRNA gene clone libraries analysis. Polar Biology 32: 93-103.

Tillmann U, Hesse KJ & Tillmann A (1999) Large-scale parasitic infection of diatoms in the Northfrisian Wadden Sea. Journal of Sea Research 42: 255-261.

Toes ACM, Finke N, Kuenen JG & Muyzer G (2008) Effects of deposition of heavy-metal-polluted harbor mud on microbial diversity and metal resistance in sandy marine sediments. Archives of Environmental Contamination and Toxicology 55: 372-385.

Turley CM, Lochte K (1990) Microbial response to the input of fresh detritus to the deep-sea bed. Paleogeog. Palaeoclim Palaeoecol 89:3–23.

Twining BS & Fisher NS (2004) Trophic transfer of trace metals from protozoa to mesozooplankton. Limnology and Oceanography 49: 28-39.

Vala AK (2010) Tolerance and removal of arsenic by a facultative marine fungus Aspergillus candidus. Bioresource Technology 101: 2565-2567.

Van den Brink PJ & Ter Braak CJF (1999) Principal response curves: Analysis of time-dependent multivariate responses of biological community to stress. Environmental Toxicology and Chemistry 18: 138-148.

Van den Eynde D (2004) Interpretation of tracer experiments with fine-grained dredging material at the Belgian continental shelf by the use of numerical models. J Mar Systems 48:171–189.

Van der Zee C, van Raaphorst W (2004) Manganese oxide reactivity in North Sea sediments. J Sea Res 52:73–85.

Van Duyl FC, Bak RPM, Kop AJ, Nieuwland G, Berghuis EM & Kok A (1992) Mesocosm experiments: mimicking seasonal developments of microbial variables in North Sea sediments. Hydrobiologia 235: 267-281.

van Hannen EJ, van Agterveld MP, Gons HJ & Laanbroek HJ (1998) Revealing genetic diversity of eukaryotic microorganisms in aquatic environments by denaturing gradient gel electrophoresis. Journal of Phycology 34: 206-213.

van Hannen EJ, Mooij WM, van Agterveld MP, Gons HJ & Laanbroek HJ (1999a) Detritus-dependent development of the microbial community in an experimental system: Qualitative analysis by denaturing gradient gel electrophoresis. Applied and Environmental Microbiology 65: 2478-2484.

van Hannen EJ, Veninga M, Bloem J, Gons HJ & Laanbroek HJ (1999b) Genetic changes in the bacterial community structure associated with protistan grazers. Archiv Fur Hydrobiologie 145: 25-38.

van Nugteren P, Moodley L, Brummer GJ, Heip CHR, Herman PMJ & Middelburg JJ (2009) Seafloor ecosystem functioning: the importance of organic matter priming. Marine Biology 156: 2277-2287.

Vanaverbeke J, Franco M, van Oevelen D, Moodley L, Provoost P, Steyaert M, Soetaert K, Vincx M. (2008) Benthic responses to sedimentation of phytoplankton on the Belgian Continental Shelf. In: Current status of eutrophication in the Belgian coastal zone. V. Rousseau, C. Lancelot and D. Cox (Eds). Presses Universitaires de Bruxelles, Bruxelles, 73–90.

Vanaverbeke J, Gheskiere T & Vincx M (2000) The meiobenthos of subtidal sandbanks on the Belgian Continental Shelf (Southern Bight of the North Sea). Estuarine Coastal and Shelf Science 51: 637-649.

Vanaverbeke J, Gheskiere T, Steyaert M & Vincx M (2002) Nematode assemblages from subtidal sandbanks in the Southern Bight of the North Sea: effect of small sedimentological differences. Journal of Sea Research 48: 197-207.

Vanaverbeke J, Merckx B, Degraer S & Vincx M (2011) Sediment-related distribution patterns of nematodes and macrofauna: Two sides of the benthic coin? Marine Environmental Research 71: 31-40.

Vanaverbeke J, Steyaert M, Soetaert K, Rousseau V, Van Gansbeke D, Parent JY & Vincx M (2004) Changes in structural and functional diversity of nematode communities during a spring phytoplankton bloom in the southern North Sea. Journal of Sea Research 52: 281-292.

Vanduyl FC, Bak RPM, Kop AJ, Nieuwland G, Berghuis EM & Kok A (1992) Mesocosm experiments - mimicking seasonal developments of microbial variables in North-Sea sediments. Hydrobiologia 235: 267-281.

Vannerum K, Huysman M, De Rycke R, *et al.* (2011) Transcriptional analysis of cell growth and morphogenesis in the unicellular green alga *Micrasterias* (Streptophyta), with emphasis on the role of expansin. BMC Plant Biology 11: 128.

Vashchenko MA, Zhadan PM, Almyashova TN, Kovalyova AL & Slinko EN (2010) Assessment of the contamination level of bottom sediments of Amursky Bay (Sea of Japan) and their potential toxicity. Russian Journal of Marine Biology 36: 359-366.

Veldhuis MJW & Admiraal W (1987) Influence of phosphate depletion on the growth and colony formation of *Phaeocystis pouchetii*. Marine Biology 95: 47-54.

Veuger B & van Oevelen D (2011) Long-term pigment dynamics and diatom survival in dark sediment. Limnology and Oceanography 56: 1065-1074.

Vogelbein WK, Lovko VJ, Shields JD, Reece KS, Mason PL, Haas LW & Walker CC (2002) *Pfiesteria shumwayae* kills fish by micropredation not exotoxin secretion. Nature 418: 967-970.

Wang F, Yao J, Si Y, *et al.* (2010) Short-time effect of heavy metals upon microbial community activity. Journal of Hazardous Materials 173: 510-516.

Wang Q, Garrity GM, Tiedje JM & Cole JR (2007) Naive Bayesian classifier for rapid assignment of rRNA sequences into the new bacterial taxonomy. Applied and Environmental Microbiology 73: 5261-5267.

Wang QS, He MC & Wang Y (2011) Influence of combined pollution of antimony and arsenic on culturable soil microbial populations and enzyme activities. Ecotoxicology 20: 9-19.

Warnken KW, Gill GA, Griffin LL, Santschi PH (2001) Sediment-water exchange of Mn, Fe, Ni and Zn in Galveston Bay, Texas. Mar Chem 73:215–231.

Wells ML, Kozelka PB, Bruland KW (1998) The complexation of 'dissolved' Cu, Zn, Cd and Pb by soluble and colloidal organic matter in Narragansett Bay, RI. Mar Chem 62:203–217.

Westerlund SFG, Anderson LG, Hall POJ, Iverfeldt A, Rutgers van der Loeff MM, Sundby B (1986) Benthic fluxes of cadmium, copper, nickel, zinc, and lead in the coastal environment. Geochim Cosmochim Acta 50:1289–1296.

Wey JK, Scherwass A, Norf H, Arndt H & Weitere M (2008) Effects of protozoan grazing within river biofilms under semi-natural conditions. Aquatic Microbial Ecology 52: 283-296.

Wilms R, Sass H, Kopke B, Koster H, Cypionka H & Engelen B (2006) Specific bacterial, archaeal, and eukaryotic communities in tidal-flat sediments along a vertical profile of several meters. Applied and Environmental Microbiology 72: 2756-2764.

Wright SW, Jeffrey SW, Mantoura RFC, Llewellyn CA, Bjornland T, Repeta D & Welschmeyer N (1991) Improved HPLC method for the analysis of chlorophylls and carotenoids from marine-phytoplankton. Marine Ecology-Progress Series 77: 183-196.

Yin XX, Zhang YY, Yang J & Zhu YG (2011) Rapid biotransformation of arsenic by a model protozoan *Tetrahymena thermophila.* Environmental Pollution 159: 837-840.

Zhang W, Ki JS & Qian PY (2008) Microbial diversity in polluted harbor sediments I: Bacterial community assessment based on four clone libraries of 16S rDNA. Estuarine Coastal and Shelf Science 76: 668-681.

Zhou QF, Zhang JB, Fu JJ, Shi JB & Jiang GB (2008) Biomonitoring: An appealing tool for assessment of metal pollution in the aquatic ecosystem. Analytica Chimica Acta 606: 135-150.

Zwart G, Huismans R, van Agterveld MP, *et al.* (1998) Divergent members of the bacterial division Verrucomicrobiales in a temperate freshwater lake. Fems Microbiology Ecology 25: 159-169.